



UNIVERSITAT_{DE}
BARCELONA

Spatial and Temporal Characteristics of Precipitation Variability and Drought Patterns in the Eastern Mediterranean

Shifa Mathbout

ADVERTIMENT. La consulta d'aquesta tesi queda condicionada a l'acceptació de les següents condicions d'ús: La difusió d'aquesta tesi per mitjà del servei TDX (www.tdx.cat) i a través del Dipòsit Digital de la UB (diposit.ub.edu) ha estat autoritzada pels titulars dels drets de propietat intel·lectual únicament per a usos privats emmarcats en activitats d'investigació i docència. No s'autoritza la seva reproducció amb finalitats de lucre ni la seva difusió i posada a disposició des d'un lloc aliè al servei TDX ni al Dipòsit Digital de la UB. No s'autoritza la presentació del seu contingut en una finestra o marc aliè a TDX o al Dipòsit Digital de la UB (framing). Aquesta reserva de drets afecta tant al resum de presentació de la tesi com als seus continguts. En la utilització o cita de parts de la tesi és obligat indicar el nom de la persona autora.

ADVERTENCIA. La consulta de esta tesis queda condicionada a la aceptación de las siguientes condiciones de uso: La difusión de esta tesis por medio del servicio TDR (www.tdx.cat) y a través del Repositorio Digital de la UB (diposit.ub.edu) ha sido autorizada por los titulares de los derechos de propiedad intelectual únicamente para usos privados enmarcados en actividades de investigación y docencia. No se autoriza su reproducción con finalidades de lucro ni su difusión y puesta a disposición desde un sitio ajeno al servicio TDR o al Repositorio Digital de la UB. No se autoriza la presentación de su contenido en una ventana o marco ajeno a TDR o al Repositorio Digital de la UB (framing). Esta reserva de derechos afecta tanto al resumen de presentación de la tesis como a sus contenidos. En la utilización o cita de partes de la tesis es obligado indicar el nombre de la persona autora.

WARNING. On having consulted this thesis you're accepting the following use conditions: Spreading this thesis by the TDX (www.tdx.cat) service and by the UB Digital Repository (diposit.ub.edu) has been authorized by the titular of the intellectual property rights only for private uses placed in investigation and teaching activities. Reproduction with lucrative aims is not authorized nor its spreading and availability from a site foreign to the TDX service or to the UB Digital Repository. Introducing its content in a window or frame foreign to the TDX service or to the UB Digital Repository is not authorized (framing). Those rights affect to the presentation summary of the thesis as well as to its contents. In the using or citation of parts of the thesis it's obliged to indicate the name of the author.



Programa de Doctorat
Geografia, Planificació Territorial i Gestió Ambiental

**Spatial and Temporal Characteristics of Precipitation Variability
and Drought Patterns in the Eastern Mediterranean**

PhD Thesis Presented by

Shifa Mathbout

PhD Directors

Prof. Dr. Javier Martín Vide

Dr. Joan Albert López Bustins

Barcelona, 2015

**The thesis is submitted in fulfilment of the requirements for the degree of
Doctor of Geography at University of Barcelona.**

November-2015

*Depending on where you live in the world and what you do for a living,
You will have a very different opinion on rain from others.
In some countries, rain is the great facilitator of life.
Not just for drinking water for people and the wildlife,
But for farmers who need rain to grow their crops.
Rain is vital for the cycle of life.
However, in other countries where there is no shortage of rainfall,
It is seen as nothing more than an inconvenience.
Even worse, recent heavy rainfall has resulted in severe flooding and deaths.
In this way, rain can be seen as both the giver and the taker of life.*



*I dedicate this thesis to my family
To the whole people who have been oppressed in my home country” Syria”.*

Summary

As precipitation is a very important parameter of climate and hydrology, exploring spatial and temporal distribution and variation of this variable can give an idea about climate conditions and water resources in the future. Therefore accurate mapping of the temporal and spatial distributions of precipitation is important for many applications in hydrology, climatology, agronomy, ecology and other environmental sciences. In this thesis, spatiotemporal distributions and variations of total annual, seasonal and monthly precipitation of the Eastern Mediterranean (EM) are analysed. The Eastern Mediterranean is one of the most prominent hot spot of climate change in the world further; extreme climatic events such as drought are expected to become more frequent and intense in this region.

Main data source is instrumental data of monthly and daily precipitation at 103 and 70 meteorological stations, respectively.

Spatial coherence analysis, coefficient of variation (CV), rainfall seasonality index (SI), incomplete gamma distribution and precipitation concentration index (PCI) are applied to evaluate the seasonality and variability of annual, seasonal and monthly precipitation amounts and their distribution. Daily precipitation concentration index (CI) is used as an important index for specifying daily rainfall characteristics. Additionally, rainfall entropy is also calculated for monthly and daily data for finding the most suitable probability distribution under the available information. High to moderate irregularity and rainfall concentration are the two very characteristic features of rainfall in the EM. Highest values of daily CI are detected in the southern parts of the EM. Distribution of annual precipitation CI trends indicate a statistically significant increase in the northern and northwestern regions of the EM.

Four meteorological drought indices (DIs) are calculated at monthly time scale, the Standardized Precipitation Index (SPI), the Modified China Z Index (MCZI), the Statistical Z -scores and the Rainfall Decile based Drought Index (DI) while the Effective Drought Index (EDI) is calculated at daily time scale. All

selected DIs with multiple time steps are applied to compute the severity for five time steps of 3, 6, 9, 12 and 24-month, and compared with each other and EDI. The most significant factor affecting the spatial accuracy of drought indices is seasonality. Study of DIs shows that the DIs are highly correlated at same time steps and can alternatively be used and the DIs computed for 6 and 9-month time step are best correlated with each other. SPI and MCZI are more consistent in detecting droughts for different time steps. EDI is found to be best correlated with other DIs when considering all time steps. The investigation shows that the use of an appropriate time step is as important as the type of DI used to identify drought severities.

Principal Component Analysis (PCA) is employed and reveals the main modes and spatiotemporal variability of seasonal and annual precipitation and droughts over the EM. The preliminary analysis indicated tendencies towards a drier climate due to a statistically significant decrease in annual precipitation over the EM.

The analysis of indicators of extreme events reveals a much more complex transformation of the climatic pattern with strong regional and seasonal variation.

The results demonstrated that an extreme wet spells in the EM will shorten in all seasons, except autumn. Precipitation extremes are projected to become more pronounced in the northern parts of the EM than in southern ones and tend to be more significant during autumn. Extreme and heavy precipitation events showed a statistically significant decrease in whole parts of the EM and in the southern ones, respectively with a significant decreasing in total precipitation amount. A significant increase in daily intense precipitation events in the northern parts of the EM. In addition, climate extreme indices recommended by the joint World Meteorological Organization (CCL/CLIVAR/JCOMM) Expert Team on Climate Change Detection and Indices (ETCCDI) are also calculated for daily precipitation data.

Finally, Mann- Kendall test, cumulative sum chart (CUSUM), regime shift index (RSI) calculated by a sequential algorithm are applied for detecting the shifts in the means of seasonal and annual precipitations. Mann-Kendall test and the

linear slopes of trends are calculated using Sen's slope estimator to determine the trend magnitude for SPI, CI, extreme precipitation indices, dry and drought periods. The highest decreasing of rainfall amounts is found in spring and winter and these seasons are the overall driving factor of trends in annual precipitation. Overall results of the trend analysis on the reconstructed shows that over last 52 years the drought events are more sever and frequent after 1990s over the EM which reflects negative effects on socio- economic sectors as well as water resources in this region. The findings of this study could be used or extended in further studies in the future to gain insights regarding the precipitation variability, drought patterns and extreme events over the domain of the EM.

Key words: Eastern Mediterranean, Precipitation variability, Climate regionalization, Temporal trends, Drought indices, Climate extremes.

Acknowledgements

I would like to thank many people without whose influences, help and great guidance and invaluable supports based on their abundant knowledge, experience and the greatest patients, I could not have finished my Ph.D.

Firstly, I would like to thank Prof. Javier Martin-Vide for agreeing to be my academic advisor and providing me the opportunity to work on a research project that enhanced my knowledge and gave me the skills and expertise to conduct an independent study. His encouragement, mentoring and advice have been an influencing factor throughout my graduate study.

I gratefully acknowledge my second supervisor, Dr. Joan Albert López Bustins who provided me with a lot of guidance to achieve insight into the data by concentrating on the most appropriate analyses in the large analysis of data. His suggestions, opinions and corrections have been very important in making this thesis. I would like to sincerely thank him for all his effort and time that gave me during last three years.

A special thanks to Prof. Jürg Luterbacher, who have generously shared his knowledge and experiences both in research and life. He provided me with a lot of important feedback and suggestions especially related to the extreme events and was my supervisor in the international stay at Justus Liebig University Giessen in Germany. I would like to thank him for his patience and time as well and I am also grateful to all those friends I met in the University of Giessen.

I wish to express my gratitude to all the people at the Department of Physical Geography and Regional Geographical Analysis, Faculty of Geography and History, University of Barcelona. As a member of Climatology Group (2014 SGR 300, Catalonia Regional Govt), (<http://www.ub.edu/gc/menu.htm>) at University of Barcelona and the two supported research projects financed by the Spanish Ministry of Economy and Competitiveness: PRECABAL (CGL2011-29263-C02-01) and WEMOTOR (CSO2014-55799-C2-1-R).

I would like to thank all the past and present colleagues in the group for the fruitful discussion and pleasant cooperation.

Above all, I want to send warm thanks to the team of ERASMUS MUNDUS (AVEMPACE mobility scheme II) project at University of Barcelona (Marta Arias Tiell and David Ibarra Rubio) and Dr. Saleh AL Jaffout from Jordan for all facilities and supports they gave during my study.

Many thanks for my ex-supervisor Dr. Michael Skaf who was a source of inspiration and guidance to me in a country away from my home and will always be so for a long time. I want to express my great appreciation and special thanks to Dr. Akram Shalghin and Dr. Frank Shotkoski who helped me in correcting the grammatical errors too.

I would like to show my deep gratitude to my spiritual father in Spain, Ceferino Alejandro Monge, who stood beside me in all difficult moments and supported me to continue and complete. His support and sensibility gave me extra strength to overcome the obstacles which I faced during my study and stay here.

Last but not the least I would like to thank my family and all my friends whose belief in my pursuits enabled me to undertake the endeavour of higher education and their moral support has always been and will be necessary throughout my life.

Finally, this thesis is dedicated to my great and lovely mother, father, my dear brother and his family and to the whole Syrian who have been oppressed.

I dedicate this work to all who work and hurt them the works of others.

List of tables

Table 2.1	List of stations used in Precipitation Analysis.	29
Table 3.1	Rainfall variability index classes based on Australian Bureau of ...	41
Table 3.2	Seasonality index (SI) classes and the associated different rainfall regime.	43
Table 3.3	Drought classification by SPI value and corresponding event probabilities.	58
Table 3.4	Category and values of drought for CZI -MCZI index.	60
Table 3.5	Classification of Z- Score index (Standard Distribution Index).	61
Table 3.6	Classification of drought conditions by using Decile Index.	63
Table 3.7	New definition for dry and drought duration.	65
Table 3.8	Drought severity classification by the EDI index.	65
Table 3.9	Definition of extreme precipitation indices used in this study.	76
Table 4.1	Percentage explained variance and percentage of cumulative variance...	83
Table 4.2	Statistical characteristics of the precipitation in the identified sub-regions...	90
Table 4.3	P values calculated by Anderson-Darling (A-D) test applied to the...	97
Table 4.4	Values for constant a and b of exponential curves, the daily concentration...	113
Table 4.5	The values of parameters α and $1/\beta$ for each station during two periods...	134
Table 4.6	Monthly, seasonal and annual results of Mann–Kendall and Sen’s slope...	155
Table 4.7	Results obtained from PCA analyses for SPI at different time scales	160
Table 4.8	Significant abrupt changes in the annual SPI values during 1961-2012...	174
Table 4.9	Frequency distribution (in percent) of the annual SPI values in seven...	180
Table 4.10	Top 10 drought cases based on the AEDI values for 52 years in three...	209
Table 4.11	Pearson correlation coefficients of indices with same time scales for...	229

Table 4.12	Summary of the commonly used DIs and their strong and weak points.	232
Table 4.13	Percentages (%) of the 70 precipitation stations with linear positive (+)...	239
Table 4.14	Correlation coefficients between precipitation extremes indices over...	255

List of figures

Figure 1.1	The global annual mean Earth's water cycle for the 1990s...	1
Figure 1.2	Seasonal distribution of precipitation over the Mediterranean according to...	4
Figure 1.3	CMIP5 multi-model mean results of projected average percent change in...	11
Figure 1.4	The sequence of drought impacts associated with meteorological...	15
Figure 2.1	1 Location map of stations with continuous daily and monthly records of...	33
Figure 3.1	Exponential curve of accumulated number of precipitation days...	48
Figure 3.2	Probability Density Function (PDF) for different values of shapes and scales.	52
Figure 3.3	Schematic diagram of an equiprobability transformation from a fitted...	56
Figure 3.4	Trend analyses framework.	69
Figure 3.5	Example of daily precipitation successful quality control procedures using...	74
Figure 4.1	Spatial distribution of mean annual precipitation in the Mediterranean...	81
Figure 4.2	Spatial distribution of PCs loadings (Empirical Orthogonal Functions...	84
Figure 4.3	Spatial distribution of mean annual rainfall CVs values over 1961-2012.	87
Figure 4.4	CV of the autumn "a", winter "b" and spring "c" precipitation over the ...	88
Figure 4.5	Box-Whisker diagram of statistical characteristics of the mean.	89
Figure 4.6	The relationship between latitude and annual CVs calculated for each...	91
Figure 4.7	The relationship between altitude and annual CVs calculated for each...	91
Figure 4.8	Spatial distribution of mean annual rainfall variability index during...	93
Figure 4.9	Scatterplots of latitude and annual rainfall variability index computed...	94
Figure 4.10	Spatial distribution of mean seasonal rainfall variability index during...	95
Figure 4.11	The annual and multiseasonal correlation coefficients between rainfall...	96

Figure 4.12	Rainfall Seasonality Index \overline{SI} in the whole stations over 1961-2012.	98
Figure 4.13	Box-whisker diagram of Seasonality Index (SI) over 1961-2012.	99
Figure 4.14	Mean \overline{SI}_t values distribution in whole stations over 1961-2012.	100
Figure 4.15	Scatter diagram and linear regression line of seasonality index \overline{SI} ...	101
Figure 4.16	Box-whisker diagram of the ratio $\overline{SI} / \overline{SI}_t$ in all districts over 1961-2012.	102
Figure 4.17	Histogram plots for frequency distribution of monthly rainfall amounts for.	103
Figure 4.18	Scatter diagram and linear regression line of seasonality index \overline{SI} ...	104
Figure 4.19	Observed trend in \overline{SI} values during 1961-2012 over the EM.	105
Figure 4.20	Regime shifts in Mean Individual Seasonality Index from selected stations...	107
Figure 4.21	Summary of all regime shift index (RSIs) in mean estimated by STARS...	108
Figure 4.22	Spatial distribution of temporal irregularity index S_1 over the EM during...	109
Figure 4.23	Scatter diagrams and linear regressions of annual rainfall S_1 and CV...	110
Figure 4.24	Concentration or Lorenz curves of some meteorological stations over the...	112
Figure 4.25	Spatial distribution of annual concentration index (CI) in 70 daily rainfall...	113
Figure 4.26	Observed trends of annual precipitation CI (1961-2012). Positive trends ...	116
Figure 4.27	Annual precipitation CI trends at various significance levels as determined...	117
Figure 4.28	Temporal changes in the annual precipitation CI between 1961 and 2012...	118
Figure 4.29	precipitation time series data (left) and their abrupt changes (right) ...	122
Figure 4.30	Mean value of the Precipitation Concentration Index (annual scale)...	124
Figure 4.31	Relationship between annual PCI values and latitude.	125
Figure 4.32	Spatial distribution of the rotated PC loadings (EOFs) across...	126
Figure 4.33	Temporal patterns of corresponding EOF1 and EOF2 scores derived...	127

Figure 4.34	Spatial distribution for the entropy of monthly (a) and daily (b) rainfall...	129
Figure 4.35	Relationship between monthly entropies and both longitude and latitude...	130
Figure 4.36	Relationship of daily entropies and latitude over 1961-2012	131
Figure 4.37	Relationship between entropies and CV in autumn “a” , spring ”b” ...	133
Figure 4.38	Scatter plot diagram of pairs of shape (α) and size parameters ($1/\beta$) for...	138
Figure 4.39	Scatter plot diagram of pairs of latitude and shape parameters for all...	139
Figure 4.40	Shape parameter distribution for rainfall stations during the two 26-yr...	140
Figure 4.41	Spatial distribution of the shape parameter for (a) the first period...	142
Figure 4.42	Probability density function (PDF) fitted to the annual rainfall in some...	144
Figure 4.43	Trends in seasonal and annual rainfall over the EM in during 1961–2012...	147
Figure 4.44	Annual rainfall linear trends for different periods in some selected stations...	149
Figure 4.45	Scores time series of the PCs of annual precipitation. Bluee lines denote...	151
Figure 4.46	Time scores series of the significant PCs of seasonal precipitation. Blue...	152
Figure 4.47	Abrupt changes in annual precipitation between 1961 and 2012, as...	153
Figure 4.48	Trend in precipitation over the EM with altitude over the EM.	158
Figure 4.49	Spatial distribution of the first sixth PCs loadings (EOFs) for SPI series...	162
Figure 4.50	Evolution of the 12- and 24-month SPI from the scores series representing...	166
Figure 4.51	Observed trend of SPI at different time scales. Positive trends are in blue...	169
Figure 4.52	Temporal evolution of the averaged SPI over the wet period...	170
Figure 4.53	Evolution of the SPI index of observed rainfall records in some...	171
Figure 4.54	Abrupt changes in annual SPI values between 1961 and 2012as...	177
Figure 4.55	Spatial distribution of the frequency (in per cent) of the SPI values falling...	182

Figure 4.56	Temporal evolution of the averaged MCZI over the wet period...	185
Figure 4.57	Percentage of years affected by various drought severity levels according...	187
Figure 4.58	Spatial distribution of the PCs loadings for MCZI series in wet period...	188
Figure 4.59	59 Frequency distribution of the MCZI values in the wet period for each...	189
Figure 4.60	Observed trend of seasonal MCZI. Positive trends are in blue and negative...	190
Figure 4.61	Scatter diagram for the SPI-3 and MCZI for the selected stations for ...	192
Figure 4.62	Histogram plot of the SPI and MCZI distribution in winter for some ...	194
Figure 4.63	Comparisons of the SPI-9 and MCZI-9 in the wet period for 1961–2012...	195
Figure 4.64	Histogram plot of the SPI-9 and Z-Score-9 (wet period) distribution for...	196
Figure 4.65	Time series of drought indices and rainfall at two Stations (Palmyra)...	197
Figure 4.66	Monthly drought risk occurrences (%) according to Z-score and MCZI...	199
Figure 4.67	Annual rainfall variability in five stations representing five regions...	201
Figure 4.68	Box-Whisker diagram of DI values in five regions over...	202
Figure 4.69	Histograms of the drought frequency classes of the SPI, MCZI, Z score...	203
Figure 4.70	Evolution of the EDI index of observed rainfall records in some stations...	205
Figure 4.71	Comparison between frequency distributions of EDI values in two periods...	212
Figure 4.72	Frequency distribution of the daily EDI values in some selected stations...	213
Figure 4.73	Histograms of the drought duration frequency corresponding to $EDI < 0$...	214
Figure 4.74	Observed frequency of long term drought durations (a) and monthly...	216
Figure 4.75	Observed trend of total dry days $EDI < 0$ “a” and severe dry days $EDI < -1$...	217
Figure 4.76	Time series of daily precipitation and EDIs calculated for the same period...	219
Figure 4.77	Scatter plot of the date of annual minimum, 12-month SPI and AWRI...	221

Figure 4.78	Drought class percentages by EDI and SPI time scales as an average of ...	222
Figure 4.79	Scatter diagram for the SPI and EDI for some selected stations for 12 ...	223
Figure 4.80	Histograms of the drought frequency classes of the SPI and EDI for...	225
Figure 4.81	Time series of drought indices (DIs) and rainfall in Raqa (Syria)...	227
Figure 4.82	Correlation of drought indices for five time scales. Each time scale ...	230
Figure 4.83	Spatial patterns trend in the annual indices of precipitation...	237
Figure 4.84	Frequency of the 10 extreme precipitation indices trends shown....	238
Figure 4.85	Spatial patterns trend in the seasonal R1Xday and R5Xdayindices for...	242
Figure 4.86	Frequency of seasonalRX1 day and RX5day trends type in the EM over...	243
Figure 4.87	Mean correlations between the RX1day and RX5day indices and total...	244
Figure 4.88	Interannual variability of CDD in some selected stations over 1961-2012...	246
Figure 4.89	Annual anomalies for CWD index (right) and trend lines (left) calculated...	247
Figure 4.90	Histograms of the R10 frequency values in different periods for the 70...	248
Figure 4.91	The average contribution of extreme and heavy wet days to total...	252
Figure 4.92	Interannual variability of SDII in some selected stations over 1961-2012.	254
Figure 4.93	Spatial distribution of Pearson correlation coefficients between both...	258

List of software, macros and packages.

Name of tool	Description
AnClim	Software for time series analysis and homogenization.
EasyFit 5.5	Distribution Fitting Software.
STATISTICA 7	Software for data analysis, data management, data visualization, and data mining procedures.
SPSS. 17.0	Statistical Package for the Social Sciences (Software package used for statistical analysis.
Change-Point Analysis CPA	A Powerful New software for detecting changes.
Surfer 13	Powerful Contouring, Gridding, and 3D Surface Mapping Software for Scientists and Engineers.
DrinC 1.5	Software for drought analysis based on drought indices.
Minitab 17	A statistical software to improve quality and the confidence to know you've done it right.
RSI, Sequential Regime Shift Detection Software.	A software designed to automatically detect statistically significant shifts in the mean level and the magnitude of fluctuations in time series.
Precintcon package	A corresponding R package "precintcon" was deposited in the R archive CRAN and is accessible at the URL: https://github.com/lucasvenez/precintcon under the GPL General Public License.
Entropy package	A corresponding R package "entropy" was deposited in the R archive CRAN and is accessible at the URL: http://cran.r-project.org/web/packages/entropy/ under the GPL General Public License.
Standardized Precipitation Index SPI package	SPI" was deposited in the R archive CRAN, version 1.1, and license: GPL-2 which published by Neves (2012) and accessible at the URL: http://cran.r-project.org/web/packages/spi/index.html

RClimdex 1.3	R based program. A software developed by Zhang and Yang (2004) at the Canadian Meteorological Service was used to obtain the climatic extremes indices.
RHtestsV3	RHtest software package detects multiple step change points that might exist in data series, and it can be used as a reference set of homogenous time series well correlated with a base series (Wang and Fing 2010).

Table of Contents

Summary.....	i
Acknowledgements	iv
List of tables	vi
List of figures.....	viii
List of software, macros and packages.....	xiii
1.1 Introduction of topic	1
1.2 The climate of the Mediterranean region	3
1.3 Precipitation variability and change in the Mediterranean.....	8
1.4 Extreme precipitation	12
1.5 Drought, and drought in the Eastern Mediterranean	14
1.6 Literature review on precipitation trends in the Mediterranean.	18
1.7 Objectives of Thesis	22
1.8 Thesis Outline and structure.....	23
2.1 Daily and Monthly data:	27
2.2 Data Quality and Homogeneity Test	34
3.1 Rainfall spatiotemporal, frequency and variability analyses.....	39
3.1.1 Spatial coherence analysis and coefficient of variation (CV).....	39
3.1.2 Rainfall seasonality index (SI).....	41
3.1.3 Temporal irregularity index (S_I)	43
3.1.4 Concentration index	44
3.1.4.1 Precipitation Concentration index (PCI).....	45
3.1.4.2 Daily concentration index (CI)	46
3.1.5 Entropy of rainfall (H).....	48
3.1.6 Spatial and temporal changes in rainfall frequency distribution patterns	50
3.2 Meteorological drought indices (DIs)	53
3.2.1 Standardized Precipitation Index (SPI).....	55
3.2.2 China Z Index (CZI), and Modified China Z Index (MCZI)	59
3.2.3 Statistical Z -scores (Standard Distribution Index).....	61
3.2.4 Rainfall decile based drought index (The Decile Index, DI)	62
3.2.5 Effective Drought Index (EDI)	63
3.3 Spatial patterns by means of Principal Component Analysis (PCA)	67

3.4 Monotonic trends and abrupt change detection.....	69
3.5 Assessment of precipitation extreme.....	71
3.5.1 Monitoring changes in extreme precipitation.	72
4.1 Spatial and temporal analysis of precipitation variability and frequency.	81
4.1.1 Spatial variability of annual and seasonal precipitation	81
4.1.2 Intra-annual and seasonal precipitation variability	82
4.1.3 Spatial coherence analysis and coefficient of variation (CV).....	86
4.1.4 Characteristics of the identified subregions	97
4.2 Changes in seasonality precipitation.	98
4. 2.1 Seasonality and individual seasonality indices of rainfall regimes	98
4. 2.2 Spatio and temporal changes in seasonality index SI	105
4.2.3 Detection of regime shifts by STARS.....	106
4.3.3 Precipitation irregularity over the EM	109
4.4 Spatial and temporal variability of daily concentration index (CI) over the EM	111
4.4.1 Spatial distribution of average precipitation CI	111
4.4.2 Spatial and temporal distribution of annual precipitation CI.....	115
4.5 Spatial and temporal distribution of the annual Precipitation Concentration Index PCI.	124
4.6 The spatial distribution features of entropy over the EM.....	128
4.6.1 The relationship between entropies, longitude, latitude and CV.	130
4.7 Spatial and temporal changes in rainfall frequency distribution patterns	134
4.8 Long term precipitation trends and variability.	146
4.9 Meteorological drought analysis using several drought indices	159
4.9.1 Study of observed spatial characteristics of meteorological drought using the Standardized Precipitation Index (SPI)	159
4.9.1.1 Temporal variability of meteorological drought using the Standardized Precipitation Index (SPI)	164
4.9.1.2 Drought frequency distribution using SPI	179
4.9.2 Drought analysis using the Modified China Z Index (MCZI) and Statistical Z –scores and Deciles.....	185
4.9.3 Assessment drought severity using daily Effective Drought Index (EDI).	204

4.9.3.1 Analysis of EDI values.	204
4.4.3.2 Drought event and its return period	218
4.9.3.3 Comparison between the SPI and EDI.	222
4.10 Observed changes in daily precipitation extremes.	237
4.10.1 Trends in seasonal precipitation indices	241
4.10.2 Indices of maximum length of dry and wet periods.....	244
4.10.3 Daily precipitation absolute threshold indices	248
4.10.4 Indices of extreme precipitation events of 1- and 5-day durations	249
4.10.5 Daily precipitation percentile threshold indices and simple daily precipitation intensity (SDII)	250
4.10.6 Correlations between extreme and mean precipitation indices.....	254
Main conclusions	263
Limitations of the study and recommendations for further works:.....	267

Chapter One

Introduction

1.1 Introduction of topic

Precipitation varies substantially from year to year and over decades. Not only the amount but also the intensity, frequency, duration or timing of rainfall can change and affect the environment and society (Trenberth, 2011).

Precipitation over land may be stored temporarily as snow or soil moisture, while excess rainfall runs off and forms streams and rivers, which discharge the freshwater into the oceans, thereby completing the global water cycle (Fig 1.1). The global warming refers to an unequivocal and continuing rise in the average temperature of earth surface. This is being caused by the increasing of greenhouse gases concentrations produced by human activities with an associated impacts vary from region to region around the globe and contribute significantly to recent drying in some areas by driving warming over land and ocean (Dai, 2011). It is predict that the subtropics will dry and expand poleward in the current century as a consequence of greenhouse gas-driven climate change (IPCC, 2007, 2013).

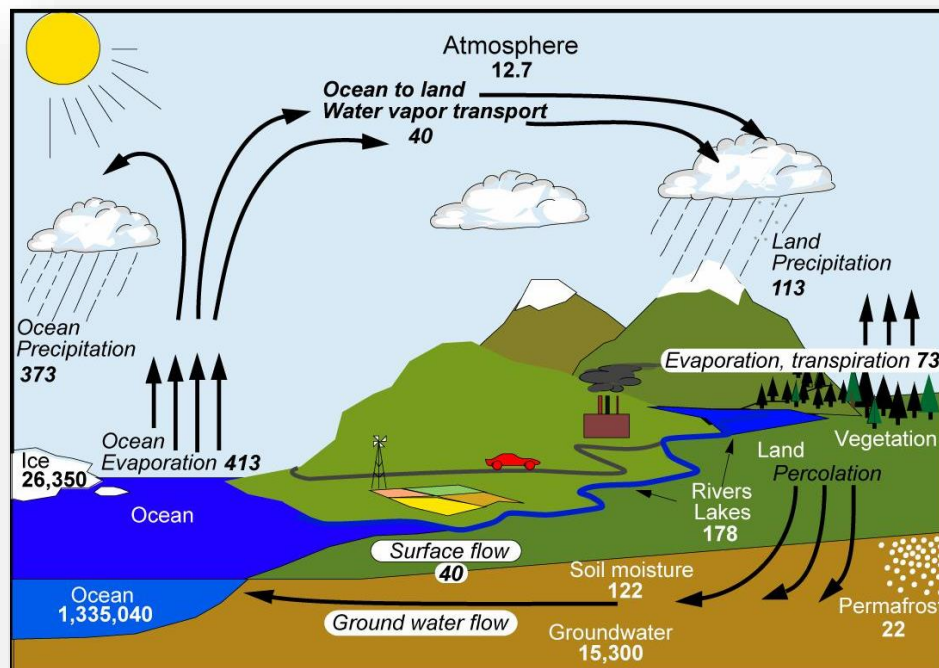


Figure 1.1 The global annual mean Earth's water cycle for the 1990s.

Units: Thousand km³ for storage, and thousand km³/yr for exchanges.

From Trenberth *et al.* (2007).

Under global warming, the water holding capacity of air increases by about 7% per 1°C warming, which leads to increased water vapour and the moisture content in the atmosphere, which in turn may lead to increase in total precipitation amount and heavy precipitation events (Hense *et al.*, 1998; Trenberth, 1999; Trenberth *et al.*, 2003; Allan and Soden, 2008).

In the sub-tropics, where evaporation is primarily controlled, increased heating causes a greater evaporation which increases the surface drying, thereby increasing the intensity and duration of drought (Trenberth, 2011; Dai, 2011). Based on observed precipitation data, the changes of total precipitation in many countries and regions have been detected (Dai *et al.*, 1997; Zhai *et al.*, 2005; Longobardi and Villani, 2009) which proved that there were an increasing trend in land precipitation at higher latitudes since the beginning of the twentieth century, and a decreasing tendency at the subtropics and tropics outside of the monsoon trough after about 1970 (Trenberth and Jones 2007; Trenberth, 2011). These decreases are more evident in the Mediterranean, southern Asia, and throughout Africa.

Precipitation over the USA, Canada, and Northern Europe increased significantly in the twentieth century (Karl and Knight 1998; Zhang *et al.*, 2000; Trenberth and Jones., 2007). In contrast, precipitation in the Mediterranean, including the eastern, central-western Mediterranean basin, Italy, and Spain, decreased in latter half of the twentieth century (Piervitali *et al.*; 1998; Trenberth and Jones, 2007) associated with deep changes in its spatiotemporal variability (Piervitali *et al.*, 1997; Millan *et al.*, 2005; Mehta and Yang., 2008). The implications of these changes are particularly significant for these areas, stressed by the combination of a dry climate and an excessive water demand. Changes in the precipitation characteristics are very important for agriculture, hydrology and water resources.

Climate change can significantly impact the hydrological cycle of the Mediterranean region. Increased evaporation has been detected, whereas regional precipitation has decreased during recent decades (Mariotti, 2010; Allan and

Zveryaev, 2011) resulted in significant increases in the loss of fresh water from the Mediterranean Sea into the atmosphere.

Increased heavy rains are detected in most regions even when mean precipitation is not increasing (Easterling *et al.*, 2000; Groisman *et al.*, 2004, 2005, Alexander *et al.*, 2006; Groisman and Knight, 2008). Much of this increase occurred during the last three decades of the 20th century and expected to be increased in the 21st century over many areas of the globe (IPCC, 2013).

1.2 The climate of the Mediterranean region

The Mediterranean region extends over three continents namely Europe, Africa and Asia and covers an area of about 1.35 million km² landmasses and 2.5 million km² sea surface (without the Black Sea).

The Mediterranean region can be viewed as transitional zone located between moderate climate of European mid latitudes and semiarid and arid climate of northern Africa and the Middle East. This area is influenced by subtropical and mid-latitude climate dynamics being directly affected by continental and maritime air masses with significant origin differences (Barry and Chorley, 2003), which in turn considered as the main causes of its phenomena complexity and richness (Lionello *et al.*, 2012). This location produces a high rates of evapotranspiration, a large climate variability at multiple timescales and a very strong seasonal variability in precipitation in many areas (Lionello *et al.*, 2006; Lionello *et al.*, 2012). All these factors make the Mediterranean to be among the “Hot-Spots” in the future climate change projections (Giorgi, 2006, Diffenbaugh and Giorgi 2012) and hypothesized that climatic change may have the greatest effects (Lavorel *et al.*, 1998). Mountains play a major role in maintaining the water supply in the region, as they are the main contributor to runoff (Beniston, 2003; De Jong *et al.*, 2009).

The Mediterranean climate is overall defined as a mid-latitude temperate climate with a warm or hot dry summer season (Köppen, 1990). Major climate type of the Köppen classification for the Mediterranean climate is characterized by hot, dry summers and cool, wet winters and located between

about 30° and 45° latitude north and south of the Equator and on the western sides of the continents. Depending on the summer temperature, the climate is divided into the Csa and Csb subtypes. However winter and summer temperatures can vary greatly between different regions with a Mediterranean climate. Most of the Mediterranean precipitation above all in the eastern basin occurs from October to March reaching its peak during the winter months (Xoplaki, 2002). Spring and autumn also contribute to a significant amount of precipitation. The Mediterranean area is characterized by strong spatiotemporal contrast in precipitation patterns related to its geographical position, changes in the large-scale atmospheric circulation and also the orographic features differences. (Xoplaki *et al.*, 2004; Lionello *et al.*, 2006; Brunetti *et al.*, 2011) (Fig 1.2). A high heterogeneity of seasonal precipitation regimes can be observed in some Mediterranean areas (Martin-Vide and Olcina Cantos, 2001).

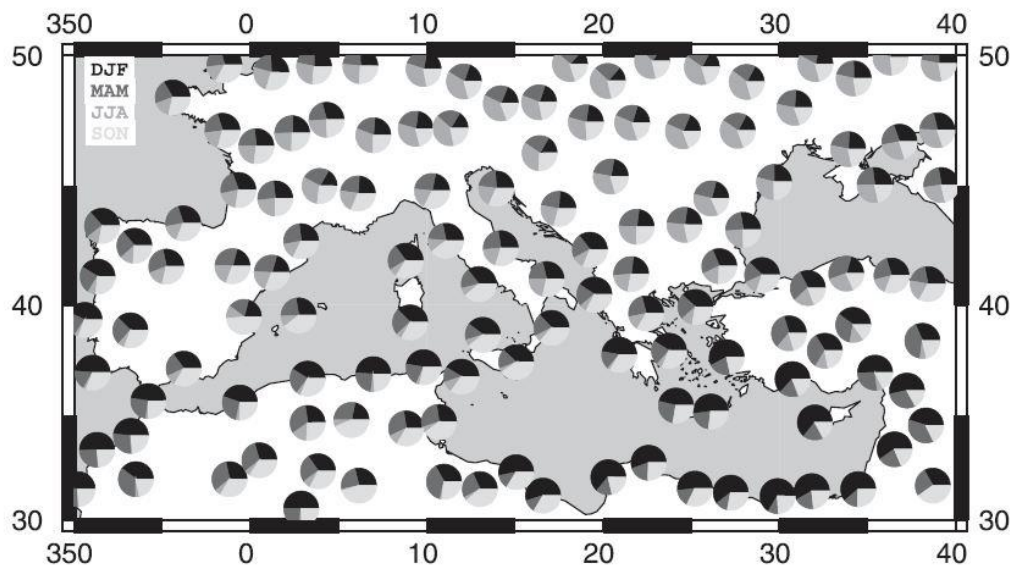


Figure 1.2 Seasonal distribution of precipitation over the Mediterranean according to the monthly database from the Global Historical Climatology Network (GHCN) over 1948–1990 (Adapted from Fernández *et al.*, 2003).

Summer conditions over the eastern Mediterranean are highly persistent, particularly during the July–August period. The lower levels of the atmosphere are dominated by the Persian trough (Alpert *et al.*, 1990; Bitan Saaroni *et al.*, 2003;

Ziv *et al.*, 2004), a surface low-pressure trough extending from the Asian monsoon through the Persian Gulf, and along southern Turkey to the Aegean Sea.

The seasonal cycle of precipitation in the Mediterranean Basin is manifested through warm and dry conditions in summer and rainy conditions from October to April, mainly associated with cyclonic disturbances that also exhibit a significant intermonthly variability (Alpert *et al.*, 1990; Trigo *et al.*, 1999; Trigo, 2006; Flocas *et al.*, 2010). Precipitation, evaporation and atmospheric moisture transport are the key elements of the regional atmospheric hydrological cycle. Evaporation is the major part of Mediterranean water budget, while annual precipitation constitutes half the amount of evaporation rate (Mariotti *et al.*, 2002). It is now well known that there are many mechanisms driving precipitation variability in different parts of the Mediterranean region and these large-scale atmospheric circulation patterns explain much of the variability and trends in precipitation and temperature at the regional scale (Trigo and Palutikof, 2001; Brunetti *et al.*, 2002; López-Bustins *et al.*, 2008; Vicente-Serrano *et al.*, 2009).

The main patterns found to be important for the Mediterranean Region are the North Atlantic Oscillation (NAO) which is the major driver for precipitation variability in the Euro–Mediterranean region both in winter (Hurrell 1995; Dunkeloh and Jacobeit 2003, Martin *et al.*, 2004) and summer (Zveryaev, 2004; Zveryaev and Allan, 2010). The NAO has been shown to impact both marine and terrestrial ecosystems (Fromentin and Planque, 1996; Alheit and Hagen, 1997; Beniston, 1997). The NAO is seen to markedly affect snowpack variability and water resource availability in many mountain areas (López-Moreno *et al.*, 2011).

Dunkeloh and Jacobeit (2003) emphasize the important role of the East Atlantic Jet pattern (ET) (Barnston and Livezey 1987) for summer and the Mediterranean meridional circulation pattern for winter and spring precipitation variability in Mediterranean region. The ET is responsible for the modulation of precipitation in the EM (Krichak *et al.*, 2002) and can explain much of precipitation anomalies in the Mediterranean which cannot be ascribed to the NAO (Quadrelli *et al.*, 2001). There is also indication of the East Atlantic/Western Russia pattern (EA/WR) (Barnston and Livezey 1987) influence on the Eastern

Mediterranean precipitation (Hurrell *et al.*, 2001; Krichak and Alpert, 2005). Price *et al.* (1998) indicated a possible role of the El Niño Southern Oscillation (ENSO) associated effects. A number of other studies have indicated that ENSO related to rainfall anomalies are found at a nation wide-scale in Mediterranean and in Middle East regions in spring and winter and other periods of the year (Rodó *et al.*, 1997; Türkeş, 1998; Arpe *et al.*, 2000). Strong negative stresses in the precipitation of the west and central Mediterranean were caused by persisting positive trends in NAO phase after the 1970s while, in the Eastern Mediterranean, positive phases of EA/WR in the same period further enhanced precipitation deficits. For example, Krichak *et al.* (2002) observed reduction of the north Israel precipitation by the EA/WR positive trend.

The Mediterranean Oscillation MO has been considered as the most important regional low-frequency pattern influencing rainfall in the Mediterranean basin (Corte-Real *et al.*, 1995; Kutiel *et al.*, 1996; Maheras *et al.*, 1999; Dunkeloh and Jacobeit, 2003; Baldi *et al.*, 2004). The Western Mediterranean Oscillation (WeMO) have been highlighted as the most important for explaining the climate variability of different sectors of the Mediterranean region (Martin-Vide and Lopez Bustins, 2006; Lopez-Bustins *et al.*, 2008; Lana *et al.*, 2015) and could also explain the non-stationary nature of the link between NAO and climate in eastern Iberia (Beranova and Huth, 2007; Vicente- Serrano and López-Moreno, 2008).

It is foreseen that recent climatic changes will negatively affect vegetation water availability due to variation in rainfall amounts, changes in dry spells frequency and intensity, and expected decrease in rainfall infiltration (Pereira, 2011). These quantitative or qualitative changes can irreversibly damage the human communities and natural ecosystems (Luterbacher *et al.*, 2006) by affecting causing significant impacts on natural, social and economic sectors, water resources, agriculture, ecosystems, forestry, health, insurance and industry (Parry, 2000; Huang *et al.*, 2014). Thus, the Mediterranean climate shows a complex pattern of spatial and seasonal variability, the matter makes the prediction of rainfall variability from year to year, within the year and spatially during the single rainy event is so difficult. Therefore, the tendencies of rainfall distribution patterns

in Mediterranean are difficult to assess due to the inter-annual variability of its climate (Ramos *et al.*, 2006).

The Eastern Mediterranean (EM) region is located in the area where both mid-latitude and sub-tropical atmospheric processes play significant roles during the rainy season, (Petterssen, 1956; Shay-El and Alpert, 1991; Krichak and Alpert, 1998; Shay-El *et al.*, 2000). Climate of the EM and especially that located in the Eastern Coastal Mediterranean zone is characterized by changeable rainy weather with moderate temperatures during the cool seasons, and dry and hot weather in summer. The conditions fit the “Mediterranean” type of the Köppen and Geiger’s (1936) classification. They are significantly determined by the location of the region in the zone dominated by polar front activity in winter, and by a subtropical high-pressure system during summer. The EM region is a part of a continental system extending from south-western to south-eastern Europe (in its northern part) to central Asia and north-eastern Africa (in its eastern and southern parts). It is also characterized by substantial differences in the amounts of solar radiation between northern and southern parts. A large part of the EM air moisture originates from the North Atlantic and Arabian Sea areas (Lionello *et al.*, 2006).

The most prominent influence of independent large scale circulation mode is the NAO in the EM (Dunkeloh and Jacobeit, 2003; Martin *et al.*, 2004). Other teleconnection patterns such as North Caspian Sea Pattern (NCP) (Kutiel *et al.*, 2002) and the EA/WR (Krichak and Alpert, 2005) have been demonstrated to play an important role too in the study area. A teleconnection pattern between the EM and northeastern Atlantic was identified at 500 and 300 hPa in winter, which will be referred to as the Eastern Mediterranean Pattern (EMP), appearing as an independent mode of the upper circulation. A positive phase of EMP is associated with a decrease in temperatures and an increase in precipitation, while the opposite occurs during the negative phase of EMP. It was found that the EMP continues to influence the regional climate of the Eastern Mediterranean in the future under warmer global conditions with inverse impact between the two phases (Hatzaki *et al.*, 2007). The negative phase of the EMP prevails throughout the year with the maximum frequency at wintertime (Hatzaki *et al.*, 2007). The higher composite

anomalies of precipitation reduction during the negative phase are consistent with the overall predicted decreasing in the future winter precipitation (Raisanen *et al.*, 2004) and the decrease of cyclone frequency over the Eastern Mediterranean (Lionello *et al.*, 2002; Anagnostopoulou *et al.*, 2006). Moreover, winters in the EM are characterized by passing disturbances known as Cyprus cyclones and, during periods without them, intrusions of high pressure systems and polar air masses (Alpert *et al.*, 1990; Saaroni *et al.*, 1996; Levin and Saaroni, 1999). During summer, the EM is influenced by the quasi-stationary Persian Gulf trough system.

The Eastern Mediterranean and the Middle East (EMME) are an extremely sensitive area to climatic changes which are associated with increases in the frequency and intensity of droughts and hot weather conditions (Lelieveld *et al.*, 2012). Precipitation patterns in the EMME do not only depend upon the synoptic weather conditions but also on the pronounced topography, for instance, the Taurus and Zagros Mountains through which the Euphrates and Tigris rivers supply the much needed water downstream (Barth and Steinkohl, 2004; Evans *et al.*, 2004). Rainfall seasonality is a very important issue in the EMME and a strong northwest-southeast gradient of the contribution of winter precipitation to the annual totals is detected (Lelieveld *et al.*, 2012). From southern Greece and Libya towards the Middle East, the winter precipitation contributes more than 50% of the annual totals, even other parts in Egypt, Jordan, Israel, Lebanon, southern Turkey and Cyprus, it reaches 60–80% (Xoplaki, 2002).

It has been demonstrated that local or regional changes of meteorological parameters in mid-latitudes, including rainfall, are mainly controlled by the atmospheric circulation (Steinberger and Gazit-Yaari, 1996). Nevertheless, not all observed changes in rainfall can be explained by changes in atmospheric circulation (Goodess and Jones, 2002).

1.3 Precipitation variability and change in the Mediterranean.

Rainfall variability in space and time is one of the most relevant characteristics of Mediterranean (Sumner *et al.*, 1993; Romero *et al.*, 1998). Precipitation variability occurs over a wide range of temporal and spatial scales,

i.e. at global (New *et al.*, 2001), regional (Lawrimore *et al.*, 2001) and subregional scales (Gonzalez- Hidalgo *et al.*, 2011). Mediterranean region is characterized by complex pattern of inter-annual as well as intra-annual rainfall variability.

Since 1970s, the changes in rainfall patterns in the Mediterranean region has been evidently detected (Maheras, 1988; Maheras and Kolyva-Machera, 1990; Wheeler and Martín-Vide, 1992). Climatic conditions in the Mediterranean Basin have become drier and warmer in the recent decades (Kafle and Bruins, 2009), and climate change models predict a decrease of up to 20% in total annual rainfall by the year 2050 (UKMO, 1995; Evans, 2009, 2010; Black, 2010) with an increase of the frequency of heavy/intense rainfall events in autumn and winter seasons, particularly in the winter (Brunetti *et al.*, 2001; Kostopoulou and Jones, 2005). An increase in inter annual rainfall variation in the EM was also predicted (Evans, 2009; Black, 2010). Giorgi and Lionello (2008) projected a pronounced drying (–25% to –30%) in the current century for the Mediterranean region, most markedly in summer.

These decreased rainfall regions include the Middle and Eastern Mediterranean, and the western and southern margins of Turkey (ECSN, 1995). Changes in rainfall (rather than temperature or CO₂) is the most important component of climate change in the Mediterranean Basin, where water is the primary limiting resource (Fay *et al.*, 2000; Miranda *et al.*, 2011; Shafran-Nathan *et al.*, 2012). Many regions have already observed negative trends in precipitation over the Mediterranean land during the last decades (Steinberger and Gazit-Yaari, 1996; Piervitali *et al.*, 1998; New *et al.*, 2001; Giorgi, 2002; Xoplaki *et al.*, 2004; Longobardi and Villani, 2009; Toreti *et al.*, 2010; Ziv *et al.*, 2013; IPCC, 2013; Coric *et al.*, 2015; Pérez-Palazón *et al.*, 2015), although annual precipitation may vary strongly from region to another depending on local topography. Arnell (2004) showed that most countries in the EMME are prone to increasing water stress. Precipitation in the Mediterranean is scarce and irregular and there is a significant risk of much drier future climate conditions (Lionello *et al.*, 2012). Current climate models predict an increase tendency in the Mediterranean mean surface pressure in the future, an increase in the frequency of anticyclonic circulation, and a

weakening of the local Mediterranean storm track (Lionello and Giorgi 2007; Rojas *et al.*, 2013; Seager *et al.*, 2014; Zappa *et al.*, 2015). Under climate change scenarios the precipitation in the Mediterranean is projected to decline in all parts and all seasons (Giorgi and Lionello 2008; IPCC, 2013; Dubrovsky *et al.*, 2014; Seager *et al.*, 2014) leading to increasing aridification, reduction in fresh water supplies and decrease in river runoff in the region (Evans, 2008; Lelieveld *et al.*, 2012) (Fig 1.3). It has been noticed that the change in the number of dry days, rather than in the mean precipitation per rainy day contributes to the precipitation reduction in the subtropics, including most of the Mediterranean area (Polade *et al.*, 2014)

The work by Mariotti *et al.* (2008) using CMIP3 multi-model simulations showed that the average model prediction had a 20% decrease water availability and 24% increase in freshwater losing over the Mediterranean basin due to a progressive decrease in rainfall during the 20th century (in average -0.007 mm/day per decade) and enhanced evaporation which would accelerate in the 21st century, followed by rapid drying from 2020 and onwards (-0.02 mm/day per decade).

Shaltout and Omstedt (2012) demonstrated that the EM experienced a drying trend of 0.06 mm /month/year over the 1958–2009 period. It is also expected that the drying trends in the Mediterranean are not uniformly distributed (Giorgi and Lionello, 2008).

Projections in anthropogenic scenarios also show that this decrease of annual rainfall is associated with an increase of heat-waves and droughts and expected to start earlier in the year and last longer (Giorgi, 2006; Beniston *et al.*, 2007; Giorgi and Lionello, 2007).

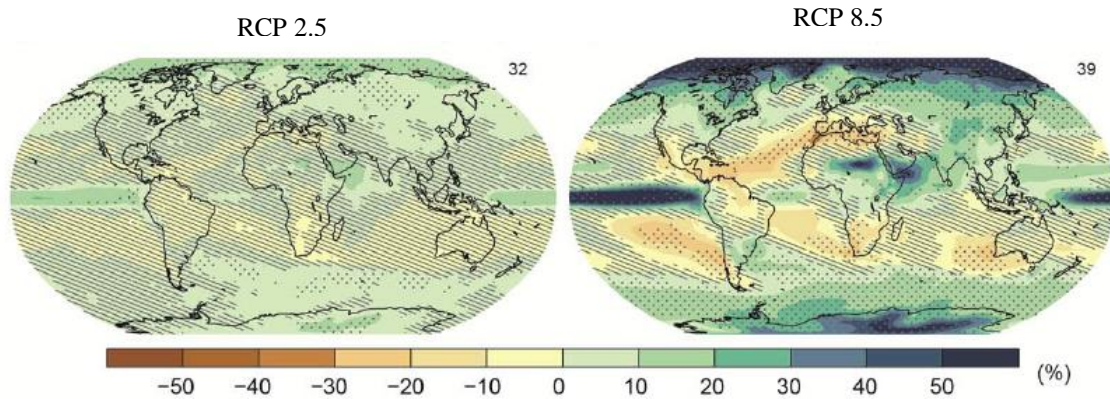


Figure 1.3 CMIP5 multi-model mean results of projected average percent change in annual mean precipitation for (2081-2100) relative to (1986-2005).

(Source: IPCC, 2013, Summary for policymakers)

The total annual rainfall will decrease, while seasonal and inter-annual variation in rainfall will increase (Golodets *et al.*, 2013) with very wet years alternating with drought ones. This water demand is associated with extreme population growth which exacerbates the risk in this region (Chenoweth *et al.*, 2011). Under these conditions, drying became more evident in parts of central and the EM and in particular in the Italy–Greece region (Xoplaki 2002; Feidas *et al.*, 2007; Nastos and Zerefos 2009).

According to the recent IPCC (2013) assessment, the Mediterranean region is projected to experience a significant drying trend associated with increasing sea surface temperature until 2100. Across the Mediterranean, studies about rainfall concentration showed more irregular values in daily rainfall concentration under Mediterranean climate types (Cortesi *et al.*, 2012). According to the European trend atlas based on weather station data (Schonwiese *et al.*, 1994; Schonwiese and Rapp, 1997) and on trend analyses applied to gridded rainfall data (Jacobeit, 2000), the majority of the Mediterranean regions, however, have tended toward decreasing winter precipitation during the last few decades, mostly starting in the 1970s and proceeding to an accumulation of dry years in the 1980s and 1990s. Recent downscaling results (Lionello *et al.*, 2008; Evans, 2009; Jin *et al.*, 2010; Dai, 2011) suggest that the EM will experience a decrease in precipitation during the rainy season due to a northward displacement of the storm tracks.

Higher precipitation concentration, represented by higher percentages of the yearly total precipitation in a few very rainy days was detected in many parts of Western Mediterranean (Brunetti *et al.*, 2000, 2001, 2004; Costa and Soares, 2009; Brunetti *et al.*, 2012; Brugnara *et al.*, 2012), whereas no statistically significant trend has been detected in the number of intense or extreme events (Kioutsioukis *et al.*, 2010). Finally, the expected drying trends in the Mediterranean Sea are not uniformly distributed, as there are sub-areas where wetting trends are also expected as the Alps region especially in winter (Giorgi and Lionello, 2008) and some sub-regions in the south and east (Jacobeit *et al.*, 2007).

1.4 Extreme precipitation

Under the background of global warming, frequencies and intensities of extreme climate events may either increase or decrease, with obvious regional differences (IPCC 2007, 2013). In recent years, there is an increasing concern in weather and climate extremes, since they may cause serious disasters to human society and nature and seem to be more sensitive to climate change than mean values (Karl and Easterling 1999; Trigo *et al.*, 2006; Aguilar *et al.*, 2009).

Extreme weather and related societal impacts are becoming an increasingly interesting area and also has received much more attention in many regions around the world, including Southeast Asia (Endo *et al.*, 2009), North America (Kunkel, 2003), Central America and northern South America (Aguilar *et al.*, 2005), India (Pal and Al-Tabbaa, 2011), Middle East (Zhang *et al.*, 2005a), Greece (Kioutsioukis *et al.*, 2010), South Portugal (Durao *et al.*, 2010), Southern and West Africa (New *et al.*, 2006) and Germany (Zolina *et al.*, 2008). On the global scale, daily climate extremes also have been analyzed (Alexander *et al.*, 2006), indicating that the changes in precipitation extremes present a complicated pattern and have apparent regional characteristics.

Many results have shown that the increases in economic losses, coupled with a rise in deaths, may be caused due to the facts that climate extremes are increasing in frequency and intensity. Climate extremes can also affect energy consumption, human comfort and tourism (Henderson and Muller, 1997; Subak *et*

al., 2000). The Intergovernmental Panel on Climate Change (IPCC) concluded in its Fourth Assessment Report (IPCC, 2007) that climate change has begun to affect the frequency, intensity and duration of extreme events such as very high temperatures, extreme precipitation, droughts, etc. Some of the changes in weather and climate extremes observed in the late 20th century are projected to continue into the future. Extreme events comprise a facet of climate variability under stable or changing climate conditions. The extremes are related to several environmental factors which increase their frequency and intensity such as: Ocean-atmospheric variables relationships, air temperature (Blain, 2011), precipitation (Grimm and Tedeschi, 2009), wind speed (Friederichs *et al.*, 2009) and sea surface temperature (SST) (Silva and Mendes, 2013), regional micro-climate changes (Willems *et al.*, 2012) and orographic effects (Houze *et al.*, 2012). Both frequencies and intensities of extreme precipitation over mid- and high-latitude land regions of the North Hemisphere have increased in recent decades (Alexander *et al.*, 2006) and might be a response to the anthropogenic global warming (IPCC 2007, Zhang *et al.*, 2007). Global warming was suggested to be linked with an increase in heavy rainfall due to an increase in atmospheric vapour and the warmer air (IPCC, 2001).

Xoplaki *et al.* (2012) and Ulbrich *et al.* (2012) demonstrated different types of extremes occur in the Mediterranean region: warm summers, explosive cyclones, extreme dust events and stormy wind-wave heights.

Precipitation extremes in the EM are more complicated as compared to other Mediterranean areas, due to their complex topographical features. Kostopoulou and Jones (2005) assessed the annual maximum number of consecutive dry days in the EM, indicating an increase of the maximum length of dry spells during the last decades. The EM especially, showed a tendency towards drier conditions (Kutiel *et al.*, 1996; Türkeş, 1998), while the western and central areas indicated a negative trends in the number of wet days and mean annual precipitation over the period 1951–1996 (Brunetti *et al.*, 2001; Alpert *et al.*, 2002). Mediterranean precipitation extremes make an important contribution to the seasonal totals. Approximately 60% of annual mean is attributed to precipitation extremes (Toreti *et al.*, 2010).

1.5 Drought, and drought in the Eastern Mediterranean

Drought are recognized as an environmental disaster and has attracted the attention of environmentalists, ecologists, hydrologists, meteorologists, geologists and agricultural scientists (Wilby and Wigley, 2000; Paulo *et al.*, 2012). Approximately 85% of the natural disasters are related to extreme meteorological events (Obasi, 1994) with drought being the one that causes most damages (CRDE, 2003).

It occurs in virtually all climatic zones, such as high as well as low rainfall areas, and are mostly related to the reduction in the amount of precipitation received over an extended period of time, such as a season or a year. It is a recurring phenomenon that affected all this area with different intensities, durations and spatial extents which is often stated that drought is one of the most complex natural hazards, and that it affects more people than any other hazard (Wilhite *et al.*, 2007). The definition and identification of drought events have long been objectives of many research efforts (Lloyd-Hughes and Saunders, 2002; Mishra and Singh, 2011). It has been defined by the international meteorological community in general terms as a “prolonged absence or marked deficiency of precipitation which results in water shortage for some activity or causes a serious hydrological imbalance (WMO, 1992; AMS, 1997). Other researchers defined drought as a natural recurrent feature of the climate cycle occurs in different climatic zones which is generally perceived to be a prolonged period with significantly lower precipitation relative to normal levels or increased evaporative demand or a combination of both of them resulting in diminished water resources availability and reduced carrying capacity of the ecosystems (Pereira *et al.*, 2002). According to Salinger (1995), drought-like conditions occur when the supply of moisture from precipitation or stored in the soil or hydrological reservoir is insufficient to fulfil the optimum water requirements of plants, water supply for urban dwellers, and inflows into hydro-power lakes. The start of a drought is not easy to ascertain, although its end may be. Droughts appear suddenly, spread in an unstructured manner, and can end in various ways (Wilhite, 2000).

Drought is generally classified into four categories (Dracup *et al.*, 1980; Wilhite and Glantz; AMS, 1997, 2004; Mishra and Singh, 2010): (1) meteorological drought which is an indicator of other drought types with below normal precipitation, and usually occurs first before other types of drought (Olukayode –Oladipo,1985;WMO,2012; Zhao *et al.*, 2013) and determined by the difference in precipitation from the normal average in a region over a certain period of time; (2) hydrological drought, occurs when river streamflow and water storage in aquifers, lakes, or reservoirs fall below long-term mean levels and persist long after a meteorological drought has ended; (3) agricultural drought, it is a period with dry soils resulting from below normal precipitation, or increase evaporation which lead to reduced crop production and plant growth, this is influenced by multiple factors, such as soil moisture, crop type and irrigation; (4) socioeconomic drought which relates the supply and demand of various commodities to drought. The relationship between the different types and categories of drought is complex and can be illustrated as in Fig 1.4.

Common to all types of drought is the fact that they originate from a deficiency of precipitation that results in water shortage and availability for some activity or for some group (Wilhite and Glantz 1985).

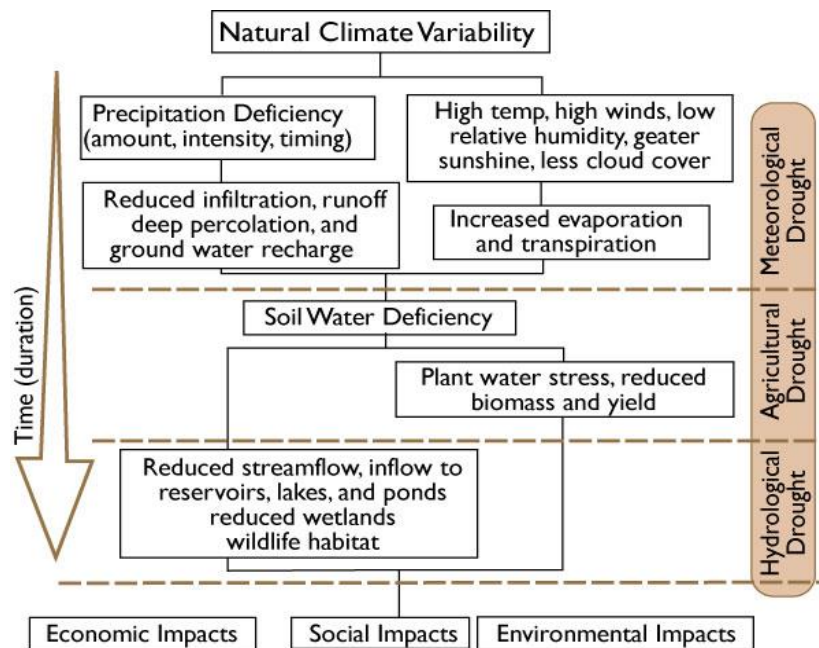


Figure 1.4 The sequence of drought impacts associated with meteorological, agricultural and hydrological droughts (National Droughts Mitigation Centre, USA).

Drought severity, duration, frequency and spatial extent are the most useful indicators for assessing the spatiotemporal characteristics of droughts in a given region (Zhai and Feng, 2008; Burke and Brown, 2010; Nandintsetseg and Shinoda, 2012), which in turn considered as one of the most important aspects of drought disaster mitigation (Wan *et al.*, 2014). These characteristics are increasing, the percentage of the world subjected to extreme drought will expand from 1% to 30% in the 21st century (Burke *et al.*, 2006), and the number of severe drought events and drought duration are likely to increase (Blunden *et al.*, 2011). Severe drought can adversely affect crop yield, increase risk of forest fires, exacerbate and intensify land degradation and desertification, and increase competition for resources and the social violence (Pausas, 2004; MacDonald, 2007). However, temperature has a very important role in the moisture availability and various empirical studies have demonstrated that an increase in temperature affects the severity and duration of droughts (IPCC, 2007) and the response of a specific system to drought can be very complex (Vicente-Serrano *et al.*, 2011).

The seasonality and climatological conditions vary by location. Drought severity may differ between regions under different climatic conditions. Semi-arid areas pose a challenge due to large contrasts between dry and wet conditions within a temporal cycle (Shahabfar and Eitzinger, 2013). Drought episodes evidently increased in Southern Europe and Mediterranean during the second half of the 20th century (Alpert *et al.*, 2002; Serra *et al.*, 2006; Kafle and Bruins 2009).

The increased drought frequency was observed over land areas surrounding the Mediterranean Sea in recent decades (Mariotti, 2010) which had serious consequences on ecosystem functions and services such as the water resources, vegetation diversity and productivity (Noy-Meir, 1973; Weltzin *et al.*, 2003; Goldest *et al.*, 2013) and food security (IFPRI, 2009). The land area surrounding the Mediterranean Sea has experienced ten of the twelve driest winters since 1902 in just the last 20 years (Hoerling *et al.*, 2012). Weiß *et al.* (2007) assess that 100-year droughts will occur more frequently in the future over large parts of the Mediterranean area. The wintertime Mediterranean precipitation over 1902-2010 has likely changed toward drier conditions and can be understood in a simple

framework of the region's sensitivity to a uniform global ocean warming and to modest changes in the ocean's zonal and meridional sea surface temperature gradients which likely played an important role in the observed Mediterranean drying (Hoerling *et al.*, 2012).

The AMS (1997) suggested that the time and space processes of supply and demand are the two basic and important processes which should be included in the drought definition for a good and correct derivation of a drought index. Drought is usually monitored and quantified by drought indices, and various indices have been developed to describe the drought in different applications (Dracup *et al.*, 1980; Wilhite and Glantz, 1985). Univariate indices are usually used to identify a drought when the variable exceeds a certain threshold value, such as precipitation (Blenkinsop and Fowler, 2007; Sylla *et al.*, 2010), runoff (Wang *et al.*, 2011) and soil moisture (Wang, 2005). Operationally, using an index for drought characterization serves the many purposes such as: (1) detecting of drought event and its real-time monitoring (Niemeyer, 2008), (2) describing the onset and the end of a drought period (Tsakiris *et al.*, 2007), (3) allowing drought managers and policymakers to identify the drought levels response (Zargar *et al.*, 2011), (4) evaluating the drought event (Niemeyer, 2008), and, (5) representing the concept of drought in a region (Tsakiris *et al.*, 2007).

Further, The Mediterranean region is affected by land degradation and desertification to a greater degree than most other regions in the world and is likely to continue to experience it to a greater degree in the future. Desertification is not only caused by climate but also by several decisions taken at all levels in society regarding land use (Xoplaki, 2004). The situation is approaching critical levels in Morocco, Lebanon, Syria, Israel and Turkey, while the northern parts of the Mediterranean are at a lower risk of desertification than the eastern and southern ones. Moreover, water availability already falls below, or approaches 1,000 m³ per capita per year in all southern parts of the EM (ARLEM report, 2011).

Several reports in the last few years have suggested that climate change and natural resource scarcity contributed to the events that have rocked the Middle East some Arab Countries such as Syria, Egypt and Libya since December 2010. They

have considered that the Arab Spring represents merely one example of what climate change may look like in the future. Climate change can explode into revolutions and tensions in these fragile social regions (Lagi *et al.*, 2012). For instance, in Syria, A UNDP report found that nearly 75% of farmers in northeast Syria experienced total crop failure and lost more than 85% of their livestock. Another United Nations report found that more than 800,000 Syrians have lost their entire livelihoods as a result of the droughts. These environmental challenges especially drastic changes in resource availability caused a violent unrest in these countries. It is increasingly clear that global and regional climatic changes have played a role in multiplying stress in this region, and that the impacts of climate change will have to be properly addressed by the affected governments and the international community (Femia and Werrell, 2012).

1.6 Literature review on precipitation trends in the Mediterranean.

The analysis of spatio and temporal precipitation variability has been of great concern during the past century by the increased attention to global climate change. Many previous studies have studied the climatic variations over the EM, particularly, the rainfall variability and its relation to large-scale atmospheric circulations (Stanhill and Rapaport, 1988; Ribera *et al.*, 2000; Maheras *et al.*, 2001; Kutiel *et al.*, 2002).

The relationship between large-scale atmospheric circulation and regional precipitation in Mediterranean has been also extensively studied and there are several studies which revealed the change in precipitation characteristics in different regions. For example, Krichak *et al.* (2002) found a combined effect of the NAO and the EA/WR on the rain regime in Israel. Maheras *et al.* (1999) investigated the role of large-scale circulation on wet and dry anomalies over the Mediterranean basin, emphasizing that dry seasons over the Mediterranean are influenced by a complex circulation over this region. For example, Espírito Santo *et al.* (2014) confirmed the role of NAO as a one of the most important teleconnection patterns in any season, and it has the greatest influence on precipitation extremes over mainland Portugal.

Several studies have considered the precipitation trend in various areas of the Mediterranean region. Most of these studies show a decreasing tendency of rainfall in the vast majority of the Mediterranean region (Amanatidis *et al.*, 1993; Karl, 1998; Alpert *et al.*, 2002; Xoplaki *et al.*, 2004; Kostopoulou and Jones, 2005; Lopez-Bustins *et al.*, 2008; Toreti *et al.*, 2010; Shaltout and Omstedt, 2014).

In spite of the decrease in the total rainfall over the Mediterranean, an increase in extreme daily rainfall was found for the period 1951–1995 (Alpert *et al.*, 2002). Morin (2011) found that the Mediterranean region is subjected to large inter-annual rainfall variability.

Palmieri *et al.* (1991), Brunetti *et al.* (2004) and Brunetti *et al.* (2006) confirm a strong decrease in precipitation trends over Italy, with a rainfall reduction of about 135 mm in the southern regions during the last 50 years.

Martín Vide (1987), Raso Nadal (1996), Montón and Quereda (1997) demonstrated a precipitation reductions in the southern parts of the Iberian Peninsula which become increasingly more pronounced southward and eastward. Another study by Lopez-Bustins *et al.* (2008) showed a significant decrease of winter rainfall in the western and central areas of Iberian Peninsula presents throughout the second half of the 20th century.

Cannarozzo *et al.* (2006) have also studied the spatial and temporal characteristics of annual and seasonal precipitation for 250 meteorological stations in Sicily, Italy over 1921-2000. Their results showed a significantly decreasing precipitation trend in annual and seasonal precipitation especially in winter. Shlomi and Ginat (2009) detected a decrease rainfall trends in the southernmost part of Israel between the years 1950 and 2008. Ziv *et al.* (2010) indicated the significant decrease trend over the majority of Israel only in the spring, reflecting a shortening of the rainy season associated with significant increase in dry spells. Kahya and Kalayci (2004), Partal and Kalayci (2006) and Önoğlu and Unal (2014) identified the regions of western and southeastern Turkey as areas of significant decreasing trends. Toros (1993) found a decreasing trend in the seasonal and annual rainfall after 1982 in the western part of Anatolia concluding that this decrease did not result from climatic change, but rather was only due to rainfall

fluctuations. In the context of climatic variability, Turkes (1996) analysed the spatial and temporal characteristics of Turkish annual mean rainfall and exhibited a significant downward direction in the mean annual precipitation for the majority parts of Turkey. Partal and Kalayci (2006) demonstrated a noticeable decrease in the annual mean precipitation in western and southern Turkey, as well as along the coasts of the Black Sea. Hatzianastassiou *et al.* (2008) showed the decreasing trend in mean annual precipitation due to the winter and spring decrease and the analysis indicated that the changing precipitation patterns in the region during winter are significantly non-correlated with the (NAO) in Greece. The same decrease was detected over most parts in Jordan, Syria and Lebanon too (Al-Mashagbah and Al-Farajat, 2013; Abou Zakhem and Hafez, 2007; Arkadan, 2008; Tarawneh and Kadiglou, 2002; Shehadeh and Ananbeh, 2013). In Cyprus, the period from the mid-1950s to the mid-1970s was at a low rainfall level compared with the first half of the 20th century (Kutiel *et al.*, 1996).

On the other hand, the evolution of changes in extreme climatic severity in the second half of the twentieth century has been studied. Several studies have detected at the global scale an increasing trends in extreme precipitation indices which also have been found in some studies in the Mediterranean region such as Xoplaki *et al.* (2004), Rodrigo (2010), Acero *et al.* (2012) and García-Barón *et al.* (2013). Sillmann and Roeckner (2008) detect significant increases of the consecutive dry day (CDD) index in regions over the Mediterranean especially along the African coast.

In the Eastern Mediterranean (EM), a significant decreasing trend affect the annual number of events with precipitation $\geq 10\text{mm}$, and the same tendency has been identified in winter for most areas in the EM too (Kostopoulou and Jones, 2005). For example, the number of events of extreme precipitation (90th and 95th) presented a statistically significant negative trend in Greece (Kostopoulou and Jones, 2005), whereas other studies (Alpert *et al.*, 2002; Tolika *et al.*, 2007) demonstrated also that in the EM, especially for stations over Cyprus and Israel, extreme precipitation does not present significant trends. Moreover, the results of Hertige *et al.* (2013) pointed to reductions of total and extreme precipitation

over the western and central-northern Mediterranean areas in summer and autumn and to increases in winter (Hertig *et al.*, 2012).

In contrast, over the EM area widespread precipitation increases are detected in summer and autumn, whereas reductions dominate in winter. It has been demonstrated that significant precipitation reductions up to -80 mm are assessed over the EM area in winter (Hertig *et al.*, 2013).

Many indices have been developed to estimate a variety of scales, types and impacts of drought and moisture deficiency (Byun and Wilhite, 1999; Heim, 2002) but few researchers have evaluated the relative performance of different drought indices to describe the different impacts of drought on several systems (Vicente-Serrano, 2012). Mavromatis (2007) compared different drought indices to evaluate the effects of drought on corn productivity. Vasiliades (2011) compared five drought indices to assess hydrological drought in Greece. Petros *et al.* (2011) tested and compared several empirical drought indices for evaluating the forestry and fire risk management under Mediterranean conditions. Paulo *et al.* (2012) also compared between four drought indices for the Mediterranean conditions. Lorenzo-Larcuz *et al.* (2010) compared the performance of two drought indices to determine the responses in river discharge and reservoir storage in central Spain. Morid *et al.* (2006) compared seven meteorological drought indices for drought monitoring in Iran. These indices are all rainfall-based ones and are able to quantify both dry and wet cycles.

Sims *et al.* (2002) compared between drought indices to evaluate the soil moisture variations in North Carolina. In China, Zhai *et al.* (2010) studied the relationship between two drought and streamflow data in ten regions. Mishra and Singh (2010) and White and Walcott (2009), among others, have pointed advantages and limitations of different indices.

1.7 Objectives of Thesis

The most important motivation of this thesis research is the requirement of an understanding of the spatio and temporal behavior of precipitation over the EM. Defining the variation of precipitation amount that occurs in time and through space can support the decision makers in water management, agriculture, urban planning, disaster management, energy and transportation. A specified probable trend existence over an area may point to future drought. Identifying space-time variation and distribution of precipitation may provide valuable information as it takes advantage of time variation by including it into interpolation.

Analysis of daily precipitation distribution and its effects on temporal concentration across this area is considered as one of the most important issues in climate research. Variation in the distribution of daily rainfall may lead to a higher precipitation concentration, generally resulting in an increase in yearly total precipitation over a limited number of rainy days. Consequently, changes in the temporal distribution of rainfall, and especially such a higher concentration, may severely affect water resources, groundwater recharge, water availability and hydroelectric production (Paredes *et al.*, 2006; Lopez-Moreno *et al.*, 2009). For these reasons, it is important to analyse the statistical structure of precipitation rates based on daily precipitation dataset.

This study overall aims to provide a better understanding of changes in precipitation characteristics in the Eastern Mediterranean (EM) for the second half of twentieth century and the main objectives of this thesis research work are:

1. To determine trends in precipitation at the annual and seasonal scale over the EM.
2. To identify abrupt changes in annual precipitation totals in the Eastern Mediterranean.
3. To investigate the spatiotemporal precipitation and variability throughout studying its seasonality, concentration and its irregularity.
4. To analyse the spatial and temporal changes in the frequency distribution of rainfall in the EM which will describe any climate changes in rainfall

distribution patterns, with due regard to extreme events at the lower and upper tails of the frequency distribution.

5. To improve our understanding of extreme precipitation events in the EM through different spatial scales observations, to assess recent changes in the tendency of extreme rainfall events.
6. To assess meteorological drought characteristics over whole area by evaluating the spatial and temporal performance of several drought indices.
7. To compare multi-monthly and daily drought indices to better identify a drought event and monitor its severity and frequency.

The statistical methods used to achieve these objectives are explained in the chapter 3.

1.8 Thesis Outline and structure.

Chapter 1 briefly discusses the climate in the Mediterranean and its general projected impacts on agriculture, water resources and hydrological variables. It then links climate change with observed and projected precipitation trends in several regions over Eastern Mediterranean. Chapter 1 also presents the problem statement of this thesis, which contains some reviews about issues that arise last two decades to assess trends in precipitation data. Finally, this chapter reviews the current literature on the range of topics covered in the thesis.

Chapter 2 gives a description of the study period and database used in this research and the source of this data. This chapter discusses the different types of precipitation data used, which totally cover 103 meteorological stations over the Eastern Mediterranean.

Chapter 3 summarizes the methods and materials used to achieve this research which contains all the ways and indices used to describe the precipitation variability and drought patterns.

Chapter 4 shows the whole results and findings of this study and presents some discussions of the main results.

Chapter 5 gives a general summary, conclusion, limitations of the study and recommendations for further research. It contains lists of the contributions to knowledge made by this present study.

Chapter Two

Study Period and Datasets

2.1 Daily and Monthly data:

This study overall aims to provide a better understanding of changes in precipitation characteristics in the Eastern Mediterranean for the second half of twentieth century. By analysing daily and monthly precipitation data, it is possible to detect, monitor and attribute changes in precipitation features and characteristics, and the extreme events. On regional scale and daily bases, some international climate databases available offering resolved data for achieving this research. For a better spatial coverage of the Mediterranean region, daily data of the European Climate Assessment & Dataset (ECA&D) (<http://eca.knmi.nl/>) has been used (Klein Tank *et al.*, 2002). Additionally, we used the daily Global Historical Climatology Network (GHCN-Daily) dataset (Gleason *et al.*, 2002) which developed to meet the needs of climate analysis and monitoring studies that require data at a daily time resolution.

The ECA&D database has both blended and non-blended series. Blended series are series which combined data of several neighbouring and surrounding stations to complete a candidate time series best. Non-blended series contain only data recorded by one candidate station. For our study, we used quality controlled non-blended series. The ECA&D has been started by the European Climate Support Network (ECSN) in 1998 and it is supported by the Network of European Meteorological Services (EUMETNET) and the European Commission.

Number of unpublished station time series were obtained by contacting the regional National Hydrological and Meteorological Services. The Syrian Meteorological Agency (<http://meteo.sy/index.php>), Lebanon weather Agency (<http://www.meteo-book-lebanon.com>), Jordan Weather Forecast (<http://www.jmd.gov.jo/>), Israel Government Portal, (The Governmental Database) (<http://data.gov.il/ims>) and Israel Meteorological Service (http://www.ims.gov.il/ims/all_tahazit/), Hellenic National Meteorological Service in Greece (<http://www.hnms.gr/hnms/english/index.html>), and Turkish State Meteorological Service (<http://www.mgm.gov.tr/index.aspx>).

Long records from three stations were also obtained directly from the meteorological agencies in each country: Limassol and Nicosia in Cyprus for the period 1887–2012, Beirut Airport in Lebanon, 1877-2012 and Jerusalem in Israel 1861-2012.

Unfortunately, daily data are comparatively less accessible than monthly values, in part because of the reluctance in many countries to release daily climate summaries for widespread public use (Alexander *et al.*, 2006) and for its high prices like Jordan and Turkey (in our study). Moreover, many data only exist in form of written information which has not been digitized yet (as the first part of dataset in Beirut and Jerusalem and some Syrian stations). To cover this problem the WMO-MEDARE on Mediterranean Climate Data Rescue was initiated in 2007 (Brunet and Kuglitsch, 2008), while in the frame of CIRCE efforts are continuously addressed to the collection of data from these areas.

Two different categorical dataset were used to achieve this research. Complete monthly data series for 103 spatially representative stations ranging between the year 1917 and 2012 were collected and analysed. Daily data for 67 stations of those stations was obtained and used in this research.

This station network, which is assumed to reflect regional hydroclimatic conditions, locates in 9 countries across the Eastern Mediterranean (Cyprus, Egypt, Greece, Israel, Jordan, Lebanon, Libya, Syria and Turkey). Functioning period was chosen that was common to all stations: 1961-2012.

Table 2.1 List of stations used in Precipitation Analysis.

Country	Station	Start Year		End Year	Log (°)	Lat (°)
		Monthl y	Daily			
Cyprus	Amiandos	1917	1917	2012	32.9	34.9
	Athalassa	1917	1917	2012	33.4	35.2
	Larnaca Airport	1917	1917	2012	33.6	34.9
	Limassol	1917	1917	2012	33.1	34.4
	Nicosia	1917	1917	2012	33.2	35.8
	Paphos Airort	1917	-	2012	32.5	34.7
	Polis	1917	1917	2012	32.4	35.0
Egypt	Alexandria	1901	-	2012	30.0	31.2
	Mersa - Matruh	1901	1959	2012	27.2	31.3
	Port Saied	1901	-	2012	32.3	31.3
Greece	Alexandroupoli Airport	1955	-	2012	25.9	40.9
	Hellinikon Airport	1955	1955	2012	23.7	37.9
	Herakilon Airport	1955	1955	2012	25.2	35.3
	Kithira Airport	1955	1955	2012	23.0	36.3
	Larissa Airport	1955	1955	2012	22.4	39.6
	Methoni	1955	1955	2012	21.7	36.8
	Milos	1955	-	2012	24.5	36.7
	Mytilene Airport	1955	1955	2012	26.6	39.1
	Naxos	1955	-	2012	25.4	37.1
	Souda Airport	1955	1955	2012	24.1	35.5
	Thessalonoki Airport	1955	1952	2012	23.0	40.5

	Tripolis Airport	1952	-	2012	22.4	37.5
Israel	Ashdod	1940	1940	2012	34.4	31.5
	Ashdot Ya'akov	1940	1940	2012	35.6	32.7
	Beer Sheva	1940	1940	2012	34.8	31.2
	Beer Tuvia	1940	-	2012	34.7	31.7
	Gazit	1940	1940	2012	35.3	32.8
	Har Kanaan	1940	1940	2012	35.2	31.5
	Jerusalem	1940	1940	2012	35.2	31.9
	Kfar Menachem	1940	1940	2012	34.5	31.4
	Lod Airport	1940	1940	2012	34.5	31.6
	Mitzpe Roman	1940	-	2012	34.8	30.6
	Tel Aviv	1940	1940	2012	32.0	32.0
Jordan	Amman Airport	1924	1961	2012	36.0	32.0
	H-4 Irwaidhed	1924	-	2012	38.2	32.5
	Irbid	1924	1961	2012	35.9	32.5
Lebanon	Beirut Airport	1877	1960	2012	35.5	33.8
	Trepoli	1931	1960	2012	35.8	34.5
Libya	Benina	1945	1945	2012	20.3	32.1
Syria	Abu Kamal	1958	1961	2012	40.9	34.4
	Aleppo	1946	1961	2012	37.2	36.2
	Athria	1958	1961	2012	37.5	35.2
	Damascus-Airport	1937	1961	2012	36.5	33.4
	Daraa	1958	1961	2012	36.1	32.6
	Deir Ezzour	1946	1961	2012	40.2	35.3

	Edleb	1961	1946	2012	36.6	35.9
	Hama	1958	1961	2012	36.8	35.1
	Hasakah	1958	1961	2012	40.8	36.5
	Hmemiem Airport	1958	1961	2012	35.9	35.4
	Izraa	1958	1961	2012	36.3	32.9
	Jarablous	1958	1961	2012	38.0	36.8
	Kamishli	1958	1961	2012	41.2	37.1
	Kharabo	1946	1961	2012	36.5	33.5
	Lattakia	1937	1961	2012	35.8	35.5
	Meslmia	1946	1961	2012	37.2	36.3
	Nabek	1946	1961	2012	36.7	34.0
	Palmyra	1946	1961	2012	38.3	34.6
	Raqa	1958	1961	2012	39.0	35.9
	Safita	1958	1961	2012	36.1	34.8
	Salamia	1946	1961	2012	37.0	35.0
	Swedaa	1958	1961	2012	36.6	32.7
	Tartous	1958	1961	2012	35.9	34.9
	Tl-Abiad	1958	1961	2012	39.0	36.7
Turkey	Adana Incirlik	1939	-	2012	35.4	37.0
	Afyon	1939	-	2012	30.5	38.8
	Akhisar	1939	-	2012	27.9	38.9
	Alanya	1940	-	2012	32.0	36.6
	Ankra Esenboga	1940	-	2012	33.0	40.1
	Antalya	1939	-	2012	30.7	36.9

Aydin	1961	-	2012	27.9	37.9
Balikesir	1938	-	2012	27.9	39.6
Bandirma	1961	-	2012	28.0	40.3
Bolu	1939	1961	2012	31.6	40.7
Bursa	1939	1961	2012	29.1	40.2
Canakkale	1938	-	2012	26.4	40.1
Corum	1939	1961	2012	35.0	40.6
Denizil	1961	1961	2012	29.1	37.8
Diyarbakir	1939	1961	2012	40.2	37.9
Edirne	1939	-	2012	26.6	41.7
Elazig	1939	-	2012	39.3	38.6
Eregli / Konya	1961	-	2012	34.1	37.5
Erzincan	1961	-	2012	39.5	39.7
Eskisehir	1939	-	2012	30.6	39.8
Finike	1961	1961	2012	30.2	36.3
Gazianteb	1939	-	2012	37.4	37.1
Iskenderun	1939	1961	2012	36.2	36.6
Isparta	1939	1961	2012	30.6	37.8
Istanbul-Ataturk	1939	1961	2012	28.8	41.0
Izmir/Cigli	1939	-	2012	27.0	38.5
Kastamonu	1939	1961	2012	33.8	41.4
Kayseri / Erkilet	1961	-	2012	35.4	38.8
Kirsehir	1939	-	2012	34.2	39.2
Konya	1939	1961	2012	32.5	38.0

Kutahya	1961	-	2012	30.0	39.4
Malatya/ Erhac	1939	-	2012	38.1	38.4
Mugla	1938	-	2012	28.4	37.2
Nigdi	1961	-	2012	34.7	38.0
Silifke	1961	-	2012	33.9	36.4
Sivas	1961	-	2012	37.0	39.8
Tokat	1961	1961	2012	36.6	40.3
Urfa	1961	-	2012	38.8	37.1
Usak	1939	-	2012	29.4	38.7
Uzgat	1961	-	2012	34.8	39.8

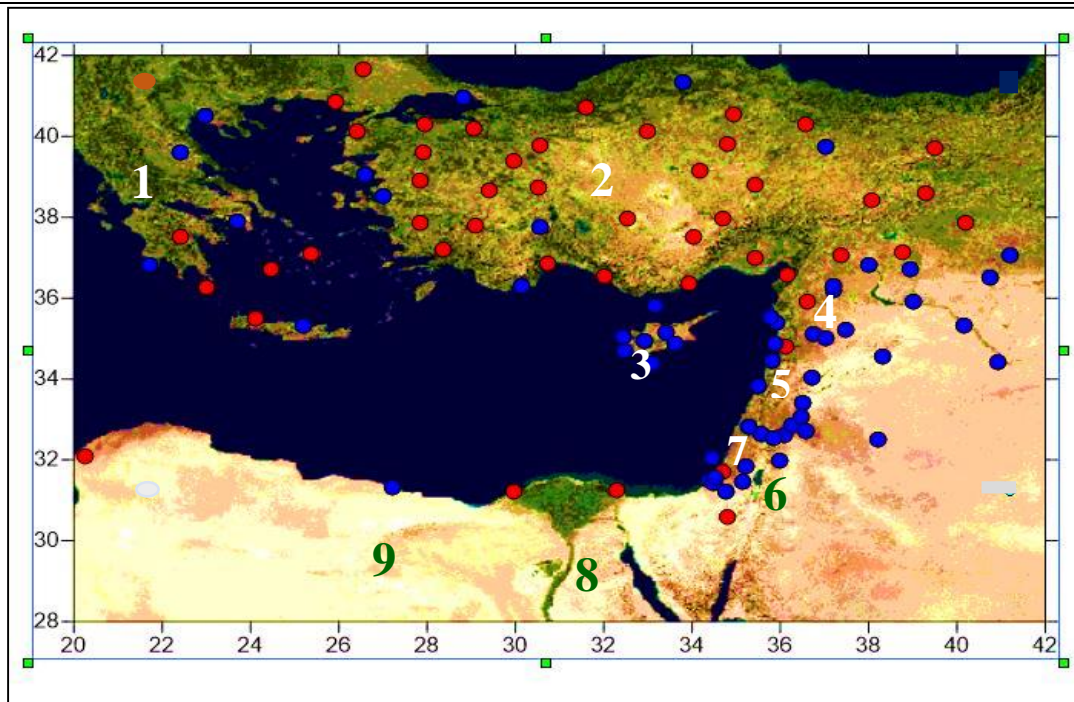


Figure 2.1 Location map of stations with continous daily and monthly records of precipitation for the period 1961-2012 (see also table 2).

- Stations with daily and monthly data (70)
- Stations with only monthly data (33) (1): Greece, (2): Turkey, (3): Cyprus, (4): Syria, (5): Lebanon (6): Jordan, (7): Israel, (8): Egypt, (9): Libya.

2.2 Data Quality and Homogeneity Test

The stations were selected based on the general criteria used by the ECA&D (Klein Tank *et al.*, 2002b): (1) data must be available for at least 40 years, (2) missing data must not be more than 10% of the total, (3) missing data from each year must not exceed 20%, (4) more than 3 months consecutive missing values are not allowed.

The quality of the data collected differs from country to country, but an effort was made to use the best possible data sources. Nevertheless to get nearly complete time series all stations were quality controlled. A common problem in climate data series is the presence of inhomogeneities. The majority of these appear as abrupt changes in the average values, but also appear as changes in the trend of the series (Alexandersson and Moberg, 1997).

Homogeneity is an important issue to detect the variability of the data. Climate data must be as homogenous as possible, especially for analysing extreme climate events (Aguilar *et al.*, 2003). In general when the data is homogeneous, it means that the measurements of the data are taken at a time with the same instruments and environments. The broader data quality control and homogenisation scheme used in this study has been applied by many investigators, including Vicente-Serrano *et al.* (2010) and Štěpánek, *et al* (2009).

SNHT developed by Alexandersson (1986) to detect a change in a series of rainfall data assumes a null hypothesis that the data values of testing variables are independent and identically distributed. Under the alternative hypothesis it assumes that a step-wise shift (a break) in the mean is present. SNHT reported by Alexandersson and Moberg (1997) proposed the construction of ratio (difference) reference series, which is generally used in precipitation and temperature studies. The most usual approach to obtain adjustment factors is to calculate separate averages on the difference or ratio series for two sections defined by a breakpoint (Aguilar *et al.*, 2003). When abrupt changes are identified in the time series, the obtained means are compared by calculating their ratio or difference and the

obtained factor is applied to the inhomogeneous part. Sometimes the changes or breakpoints may be gradual. In such a case the inhomogeneous section is detrended using the slope calculation on the difference or ratio time series.

In this research, the AnClim software (Štěpánek, 2007) was used in the application of the SNHT to each observatory. The test was applied for monthly data, it was also applied to seasonal and annual precipitation series, since this approach yields better results than using only monthly series. For each seasonal and annual series a T series was obtained using the SNHT. If the value of T in each month exceeded a certain threshold, the series was flagged as inhomogeneous. The threshold T value can be set to any given confidence level (α), and in this study a value of $\alpha = 0.05$ was used (refer values in Alexandersson and Moberg, 1997).

To ensure that only one inhomogeneity was present in series when using Alexanderson, a further modification was introduced into the AnClim software, which divides the series at the position of the found inhomogeneity and test the parts before and after the detected inhomogeneity separately. If no additional inhomogeneity was found in these two parts, we can rely upon the results of the given test for a whole length of the series (especially the significance of a test statistic).

A statistic $T(y)$ is used to compare the mean of the first y years with the last of $(n-y)$ years and can be written as below:

$$T_y = y\bar{Z}_1 + (n-y)\bar{Z}_2 \quad , y = 1, 2, \dots, n. \quad \text{where}$$

$$\bar{Z}_1 = \frac{1}{y} \sum_{i=1}^n \frac{(y_i - \bar{y})}{s} \quad \text{and} \quad \bar{Z}_2 = \frac{1}{n-y} \sum_{i=y+1}^n \frac{(y_i - \bar{y})}{s}$$

The year y consisted of break if value of T is maximum. To reject null hypothesis, the test statistic,

$$T_0 = \max_{1 \leq y \leq n} T_y$$

is greater than the critical value, which depends on the sample size.

The total amount of monthly precipitation series analysed is 1236. Based on the results of SNHT, some stations were not homogeneous since the null hypothesis for the SNHT are rejected at 0.05 level of significance. However, after applying the SNHT to 115 stations, there are 103 stations (89.56%) homogeneous and “useful”, 8 stations (6.95%) are inhomogeneous and “doubtful”, and 4 station (3.48%) is considered as “suspect”. Depending on these results we discarded 12 stations and completed this study with 103 stations. Most of the discarded stations are located in Lebanon and Jordan. Other stations in other countries have very good quality of time series data.

Chapter Three

Methodology

3.1 Rainfall spatiotemporal, frequency and variability analyses

The seasonal and annual spatial variability of the rainfall play an important role in many hydrological applications, such as evaluation of water balances, management of surface water resources, and forecasting the real- time of runoff occurrence. Precipitation can be regarded as a spatiotemporal variable. These analysis attempt to better describe the characteristics of the rainfall fields both on the temporal and spatial scales.

3.1.1 Spatial coherence analysis and coefficient of variation (CV)

Kraus (1977) proposed the Standardized Anomaly Index *SAI* which also called Precipitation Index (*PI*) (Delitala *et al.*, 2000) to measure the spatial coherence of interannual anomalies. This index has been widely used in studies on precipitation variations and has a number of important statistical properties (Katz and Glantz, 1986). The standardized anomaly index *SAI* (Henceforth precipitation index or *PI*) is defined as the average of the normalized station time series of seasonal averages over the M stations. It is constructed from the station average of the standardized rainfall anomalies (Katz and Glantz, 1986; Delitala *et al.*, 2000; Barbero and Moran, 2011).

$$SAI_i = \frac{1}{M} \sum_{j=1}^M \frac{x_{ji} - \bar{x}_j}{\sigma_j}$$

Where, $i = 1 \dots N$ denotes the year, $j = 1 \dots M$ denotes the station. x_{ji} is the precipitation at the station j at time i (usually a year, a season or a month), \bar{x}_j the long-term time mean and σ_j is the interannual standard deviation for the same station j . Normalization helps to compare intensity of dry and wet months in case of non-homogeneous annual distribution. However, this index still uses only one climatic variable. Because sites with higher mean rainfall tend to also have higher standard deviations, the *SAI* results in weighting the drier sites more than the wetter ones (Katz and Glantz, 1986).

The interannual variance of the SAI [$var(SAI)$] is a measure of the spatial coherence since it depends on the interstation correlations.

$$VAR(SAI_i) = VAR\left(\frac{1}{M} \sum_{j=1}^M \frac{x_{ji} - \bar{x}_j}{\sigma_j}\right)$$

Where \bar{x}_j the long-term time is mean over the M stations and σ_j is the interannual standard deviation for station j . The $VAR(SAI)$ is a maximum when all stations are perfectly correlated $VAR(SAI) = 1$ and a minimum when the stations are uncorrelated, resulting in a $VAR(SAI) = 1/M$ (Katz and Glantz, 1986). The regional annual SAI_i time series were also checked for normality, which is a prerequisite for the analysis, using the Anderson-Darling goodness of fit tests which gives more weight to tails than the Kolmogorov-Smirnov (K-S) goodness of fit.

Average annual precipitation maps, however, do not show the natural interannual variability of rainfall that occurs. For this reason the coefficient of variation CV, expressed as a percentage, was mapped. Higher values of CV indicate high variability of rainfall and vice versa.

The spatial variability of annual rainfall was expressed with the coefficient of variation (CV) using total annual rainfall data. The coefficient of variation of rainfall CV is defined as the standard deviation (σ) divided by the average annual rainfall (\bar{P}).

$$CV\% = \frac{\sigma}{\bar{P}} \times 100$$

According to Hare (1983), CV is used to classify the degree of variability of rainfall events as low, moderate and high. Areas with $CV > 30\%$ are highly vulnerable to drought (Hare, 1983). In this research, it is used to characterize the annual spatial variability of rainfall. High CV values (exceeding 35%) indicate a high degree of discrete temporal rainfall distribution. Those low CV values (under 20%) are referring to regular temporal rainfall.

Australian Bureau of Meteorology (2010) used a rainfall variability index for analysis of rainfall variability in Australia given as $(P_{90} - P_{10})/P_{50}$ and express

the variation in rainfall regimes, where, P_n is nth percentile of the data. Linacre and Hobbs (1977) found that the Mediterranean climate patterns produce high winter rainfall variability. The threshold value is given in the Table below (3.1).

Table3.1. Rainfall variability index classes based on Australian Bureau of Meteorology, (2010).

Class	Index
>1.5	Very high
1.25-1.5	High
1-1.25	Moderate to high
0.75-1	Moderate
0.50-0.75	Low to moderate
<0.50	Low

We have also calculated the skewness and kurtosis coefficients of rainfall data to detect the degree of asymmetry exhibited by the data and how the histogram peaks, respectively.

3.1.2 Rainfall seasonality index (SI)

The distribution of precipitation throughout the seasonal cycle is as important as the total annual amount of monthly or annual precipitation. The seasonal distribution of precipitation is the result of revolution of the earth resulting in the unequal heating of the earth's surface over the year. The distribution of rainfall through the season or year plays an important role in recharging the ground water.

Relative seasonality of rainfall refers to the degree of variability in monthly rainfall through the year (Walsh and Lawer, 1981). It assesses seasonal contrasts in rainfall amounts rather than whether months are “dry” or “wet” in absolute sense. Seasonality index helps in identifying the rainfall regimes based on the

monthly distribution of rainfall. In order to define these seasonal contrasts, the seasonality index \overline{SI} and \overline{SI}_i proposed by Walsh and Lawer (1981) and Kanellopoulou (2002), respectively were computed to quantify the annual rainfall regimes. These indices can show differences in relative seasonality even in areas with two or three rainfall peaks throughout the year.

The \overline{SI} is defined as the sum of the absolute deviation of mean monthly rainfall from the overall monthly mean divided by the mean annual rainfall. This is calculated by using the following formula which is a function of mean monthly and annual rainfall.

$$\overline{SI} = \frac{1}{R} \sum_{i=1}^{12} \left| X_n - \frac{R}{12} \right|$$

Where:

X_n Mean rainfall of month n .

R Mean annual rainfall.

Theoretically, the \overline{SI} can vary from zero (if all the months have equal rainfall) to 1.83 (if all the rainfall occurs in one month). The mean \overline{SI}_i is the average of \overline{SI} for each year i and it is defined as the sum of the absolute deviation of monthly rainfall from the mean monthly rainfall of year i divided by the annual rainfall (R_i) of year i .

Table 3.2 shows the different class limits of \overline{SI} and representative rainfall regimes (Kanellopoulou 2002; Guhathakurta and Sagi, 2013). Though the method uses the distribution of rainfall for all the 12 months, a seasonal pattern is detected when the \overline{SI} value is higher than 0.6.

Table 3.2. Seasonality index (SI) classes and the associated different rainfall regime (Kanellopoulou 2002; Guhathakurta and Sagi, 2013).

Rainfall Regime	Seasonality Index (SI)
Very equable	≤ 0.19
Equable but with a definite wetter season	0.20–0.39
Rather seasonal with a short drier season	0.40–0.59
Seasonal	0.60–0.79
Markedly seasonal with a long drier season	0.80–0.99
Most rain in 3 months or less	1.00–1.19
Extreme, almost all rain in 1–2 months	≥ 1.20

In order to evaluate the degree of variability in rainfall regimes the ratio of $\overline{SI} / \overline{SI}_t$ was also calculated.

\overline{SI} in all 103 series over 1961–2012 (52-yr) of the study area has been also computed in two different periods 1961–1986 (26-yr) and 1987–2012 (26-yr), and compared the values between these two periods to detect changes in rainfall pattern.

3.1.3 Temporal irregularity index (S_1)

The temporal irregularity of the pluviometric records can be measured by relating in some way consecutive monthly or annual amounts. Since some other indices like index of seasonality (SI) does not represent a sufficiently good estimation of the temporal irregularity, due to the use of monthly and annual means. Another possibility is to use some temporal irregularity indexes. In this research we have chosen one of these indices which previously used to characterize pluviometric regimes of Spain (Martín-Vide, 1987; Burgueño, 1993).

$$S_1 = \frac{1}{n-1} \sum_{i=1}^{n-1} \left| \ln - \frac{P_{i+1}}{P_i} \right|$$

P_i is annual or monthly amounts (in this study it refers to both). It is similar to a measure of entropy (to be presented in 3.1.5 section), due to the fact that very similar consecutive precipitation amounts give an index close to zero. At the other extreme, very different consecutive amounts correspond to high values of S (≥ 0.35). A minor shortcoming of this index is the fact that null amounts, which are common for summer months on the Mediterranean coast, cannot be used in the computation of last expression of S . In these cases, a smoothing of the amounts is considered, assigning totals of (1mm) to precipitations of less than this amount.

3.1.4 Concentration index

Spatial and temporal variability of rainfall is an important component of having knowledge of the water balance dynamics on different scales for water resources management and planning (De Luis *et al.*, 2011; Ezemonye and Emeribe, 2011), and they play an important role in agricultural planning, flood frequency, hydrological modelling, water resources assessments, evaluating the impacts of climatic and environmental factors (Michaelides *et al.*, 2009 as cited in Ngongondo *et al.*, 2011). Precipitation totals on annual, seasonal or monthly scales are key elements affecting water availability, but precipitation concentration in time also plays a decisive role.

Precipitation concentration is represented not only by the percentages of annual total precipitation on several rainy days but also by the time and degree of concentration of the total precipitation within a year. Higher precipitation concentration has the potential to cause floods and droughts, which is expected to have a considerable pressure on water resources. Different indices have been used for this purpose, and among these, two types of precipitation concentration index were widely applied. The first group of precipitation concentration index (Oliver, 1980) represents the degree to which annual or seasonal precipitation is distributed over 12 or 9 months, while the second type of precipitation concentration index (Martin- Vide, 2004) is used to evaluate the contribution of the days of greatest rainfall to the total amount (Apaydin *et al.*, 2006; Shi *et al.*, 2014).

In this study, the spatial and temporal patterns of precipitation concentration in EM were investigated using two indices: the precipitation concentration index (PCI) and the daily concentration index (CI) for measuring seasonality and daily heterogeneity using monthly and daily precipitation series, respectively. In particular, the trends of PCI and CI were tested by the Mann-Kendall method, and the relationship between PCI, CI and percentage of precipitation contributed by the rainiest days was analysed by the linear correlation analysis.

3.1.4.1 Precipitation Concentration index (PCI)

Monthly rainfall heterogeneity was investigated using the seasonal precipitation concentration index (PCI) series and its coefficient of variability originally defined by Oliver (1980) and modified by De Luis *et al.* (1997) to assess the temporal aspects of the rainfall distribution. The modified index is expressed as:

$$PCI_{Annual} = 100 \times \frac{\sum_{i=1}^{12} p_i^2}{(\sum_{i=1}^{12} p_i)^2}$$

Where P_i is the monthly precipitation in month i .

The PCI was also calculated on a seasonal scale for winter (Dec-Jan-Feb), spring (Mar-Apr-May) summer (Jun-Jul-Aug), autumn (Sep-Oct-Nov), and on supra-seasonal scales for wet (October to March) and dry (April to September) seasons in the EM according to the following equations:

$$PCI_{Seasonal} = 25 \times \frac{\sum_{i=1}^3 p_i^2}{(\sum_{i=1}^3 p_i)^2}$$

$$PCI_{supra-seasonal} = 50 \times \frac{\sum_{i=1}^6 p_i^2}{(\sum_{i=1}^6 p_i)^2}$$

According to the proposed formulae, on the annual, seasonal and supra-seasonal scale, the lowest theoretical value of PCI is 8.3, indicating the perfect

uniformity in precipitation distribution (i.e., that same amount of precipitation occurs in each month). Also, on all scales, a PCI value of 16.7 will indicate that the total precipitation was concentrated in 1/2 of the period and a PCI value of 25 will indicate that the total precipitation occurred in 1/3 of the period (i.e., total annual precipitation occurred in 4 months; total supra-seasonal precipitation occurred in 2 months and total seasonal precipitation occurred in 1 month).

According to this classification, Oliver (1980) suggested that PCI values of less than 10 represent a uniform precipitation distribution (i.e., low precipitation concentration); PCI values below 10 indicate a uniform monthly rainfall distribution in a year, whereas values ranging from 11 to 20 mean seasonality and values above 20 correspond to climates with substantial monthly variability.

3.1.4.2 Daily concentration index (CI)

Daily precipitation concentration index (CI) proposed by Martin-Vide (2004) is an important index for specifying daily rainfall characteristics. It measures the irregularity of the rainfall distribution by determining and quantifying the area of the concentration curve or Lorenz curve as the accumulation of rainy days number against the rainfall accumulated and equidistribution regression (Martin-Vide 2004; Zhang *et al.*, 2009; Li *et al.*, 2011; Ray *et al.*, 2012; Benhamrouche *et al.*, 2015). A large area represents a higher irregularity or a daily concentration. The CI is based on the fact that the contribution of daily rainfall events to total amount is generally well described by a negative exponential distribution (Brooks and Carruthers, 1953; Martin-Vide, 2004; Wang *et al.*, 2013), which means that few large daily amounts of precipitation occur in a given period and place. Actually, these few large daily amounts of precipitation can potentially affect hydrologic input (Martin- Vide, 2004).

The threshold 0.1 mm/day was used to separate wet and dry days and a 1 mm precipitation amount was used as the class interval (in an ascending order) to classify precipitation values. Irregularity of rainfall distribution was measured by determining percentage of rain contributed by days falling in each class. The

number of days with precipitation range falling into each class is counted and the associated amount of precipitation is computed, then the cumulative summation of that is calculated.

This approach for calculating cumulative precipitation is more reasonable than multiplying the midpoint of each class interval by the total number of rainy days (Martin- Vide, 2004). To assess both the impact of different daily precipitation values and the contribution of the largest precipitation value to the total precipitation value, the accumulated percentages of precipitation (Y) contributed by the accumulated percentages of days (X) during Y 's occurrence were analysed. From here, the cumulative summation of days and amounts can be calculated (Martin- Vide, 2004; Zhang *et al.*, 2009). Finally, cumulative frequency of rainy days (X) is plotted against associated precipitation amount (Y). This relationship exhibits a positive exponential distribution curve that could be described as (Olascoaga, 1950):

$$\hat{Y} = a\hat{X}.e^{b\hat{x}}$$

Where a and b are constants estimated by the least squares method. Generally, this curve is termed the concentration curve or Lorenz Curve (Shaw and Wheeler, 1994). Once both constants a and b have been determined, the normalized daily precipitation concentration index can be defined as follows:

$$CI = S/5000 \quad \text{Where,}$$

S is the area delimited by the exponential curve, and the line $Y = X$ is

$$S = (10000/2) - A,$$

With A being the definite integral of the exponential curve $= a\hat{X}.e^{b\hat{x}}$ between 0 and 100 (the range of allowed values for x), i.e. the area under the curve

$$A = \left[\frac{a}{b} e^{bx} \left(x - \frac{1}{b} \right) \right]_0^{100}$$

This method is used to reveal the structure of precipitation accumulation caused by the accumulated number of precipitation days at each station, which can then be used to determine the cause of the asymmetrical distribution of precipitation. The daily precipitation Concentration Index resembles the Gini

coefficient and is the ratio between S and the surface area of the lower triangle delimited by the equidistribution line (Martin-Vide, 2004) (Fig 3.1).

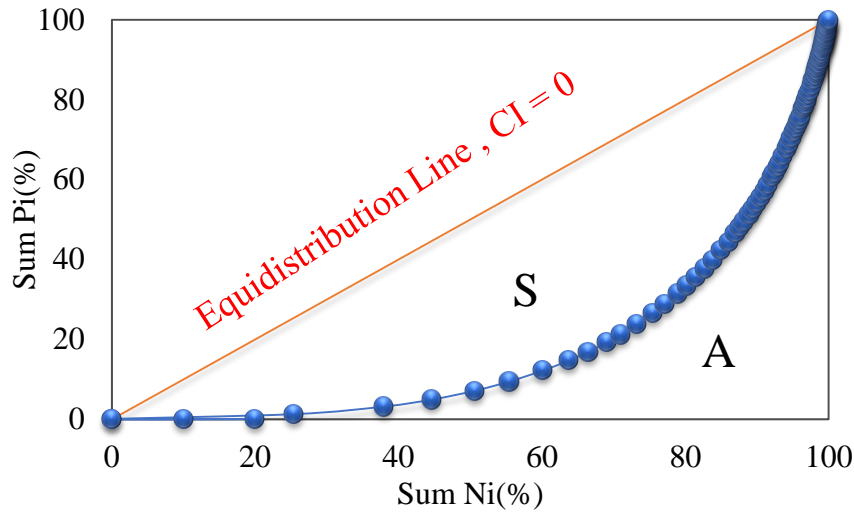


Figure 3.1 Exponential curve of accumulated number of precipitation days (Sum Ni) versus amount of accumulated precipitation (Sum Pi).

A high precipitation CI value (≥ 0.6) indicates that a high percentage of precipitation is concentrated into a few rainy days during the year for a given station. Consequently, the Gini coefficient as well as CI have been used as a measure of inequality in precipitation distributions.

This method was implemented on R software using the “precintcon” package developed by Lucas Venezian Povoia, 2015. A corresponding R package “precintcon” was deposited in the R archive CRAN and is accessible at the URL:

<https://github.com/lucasvenez/precintcon> under the GPL General Public License.

3.1.5 Entropy of rainfall (H)

Entropy is a basic concept in signal communicate on theory. It is a fundamental quantity in statistics and machine learning. It evaluates the amount of information contained in random signals and quantifies random signals based on their occurrence probability. It provides a measure of dispersion, uncertainty, disorder and diversification of precipitation intensity and/or precipitation amount

(Kawachi, 2001). In this study, it is used to investigate the spatial and temporal variability of precipitation

The concept of entropy was reintroduced in information theory by Shannon (Shannon, 1948), who showed that entropy is a purely probabilistic concept, a measure of the uncertainty related to a random variable.

The Shannon Entropy method could eliminate the randomness and establish the regularity of the time series. It is a measure of dispersion, uncertainty, disorder, diversification, spatial and temporal precipitation variability patterns, so it has been used to test the spatial structure and disorder of the precipitation (Chapman, 1986; Zhang and Liu, 2000). In order to obtain the entropy of the precipitation, the time series of the data for each station was regarded as a single observed event separately.

It has been used in applications assessing variability in the hydrological variables (Delsole and Tippet, 2007; Mishra *et al.*, 2009).

A discrete form of entropy $H(x)$ is given as (Shannon, 1948):

$$H(X) = H(p_1, p_2, \dots, p_n) = - \sum_{i=1}^n p_i \log p_i$$

Where X is a discrete random variable, P_i is the probability that X assumes a value $X = x_i$, and n is the number of values (sample size), and the value of $-\log p_i$ is an information of a random variable. Entropy is expressed in bits if the base of the logarithm is assumed to be equal to 2 and dit (or digit) for the base 10.

Thus H expresses our uncertainty or ignorance about the system's state, it reaches its maximum value if all states are equiprobable or there is more evenness in the probabilities of random values, that is, if we have no indication whatsoever to assume that one state is more probable than another state. Thus, it varies from zero to \log_n according to the shape of the distribution of probabilities p_i . The entropy value decreases with increasing number of constraints and increases with their decreasing number. Viewed in this manner, entropy can be regarded as a functional estimate of the uncertainty associated with the probability distribution (Kawachi *et al.*, 2001).

The different time series considered are: annual time series, which consists of all months for the entire length of study data; seasonal time series, which consist of individual seasons of each year for the entire length of data; and monthly time series, which consist of individual months of each year for the entire length of data.

The entropy would reach its maximum only when the monthly or seasonal rainfalls are equal at a given station.

This method was implemented on R software using the entropy package developed by Hausser and Strimmer (Hausser and Strimmer, 2009). A corresponding R package “entropy” was deposited in the R archive CRAN and is accessible at the URL:

<http://cran.r-project.org/web/packages/entropy/> under the GPL General Public License.

3.1.6 Spatial and temporal changes in rainfall frequency distribution patterns

Empirical histograms of rainfall totals over various time periods, and various climatic regions, may show a variety of shapes, from an exponential to a positively skewed, or close to normal distribution shape. In regions that have high amounts of rainfall, the mean has the highest frequency of rainfall and the distribution is close to normal (Vinnikov *et al.*, 1990; Juras, 1994). In arid regions, variability is high with low amounts of annual rainfall in some years and high amounts in others. The frequency distribution of annual rainfall in arid regions will thus present an asymmetric shape with a long tail to the right (positive skewness) (Hutchinson, 1990; Wilks, 1990; Yaakov, 2013). Climate change may involve a combination of two statistical outcomes: a shift in the location and a change in the scale of the distribution function, it is, a shift in the mean of the variable and an increase or decrease in the variance (Katz, 1991).

There are many probability distributions that could be successfully utilized to parameterize rainfall distributions. The critical component for these distributions is that they must be flexible enough to represent a variety of rainfall regimes (Husak *et al.*, 2007). Fitting a theoretical distribution to rainfall totals

makes it easy to estimate the frequency of rainfall amounts. Representative distribution parameters can be obtained from relatively short-term rainfall records, as short as 10 years in length (Revfeim, 1985).

The gamma distribution, being zero bounded provides a reasonably good fit to rainfall data, and has been widely used by many researchers (Mooley, 1973; Ropelewski *et al.*, 1985; Wilks, 1989; Ropelewski and Halpert, 1996; Husak *et al.*, 2007). Gamma distribution probability may be used to describe the precipitation probability and calculate cumulative frequency distribution (Zhai and Feng, 2008). It has, therefore, become a popular choice for fitting probability distributions to rainfall totals because its shape is similar to that of the histograms of rainfall data. According to Wilks (1990), it provides a flexible representation involving only two parameters. The probability density function (PDF) for the distribution can be presented by the following function:

$$f(x, \alpha, \beta) = \beta^\alpha \cdot x^{\alpha-1} e^{-\beta x} [\Gamma(\alpha)]^{-1} \quad \text{for } x \geq 0 \text{ and } \alpha, \beta > 0$$

Where: x is the random variable (rainfall total over the period of interest), α is the shape parameter of the distribution expressing the extent of the symmetry around the mode, β the empirical of the scale parameter of the distribution, scaling the rainfall amount at respective frequencies (Fig 3.2).

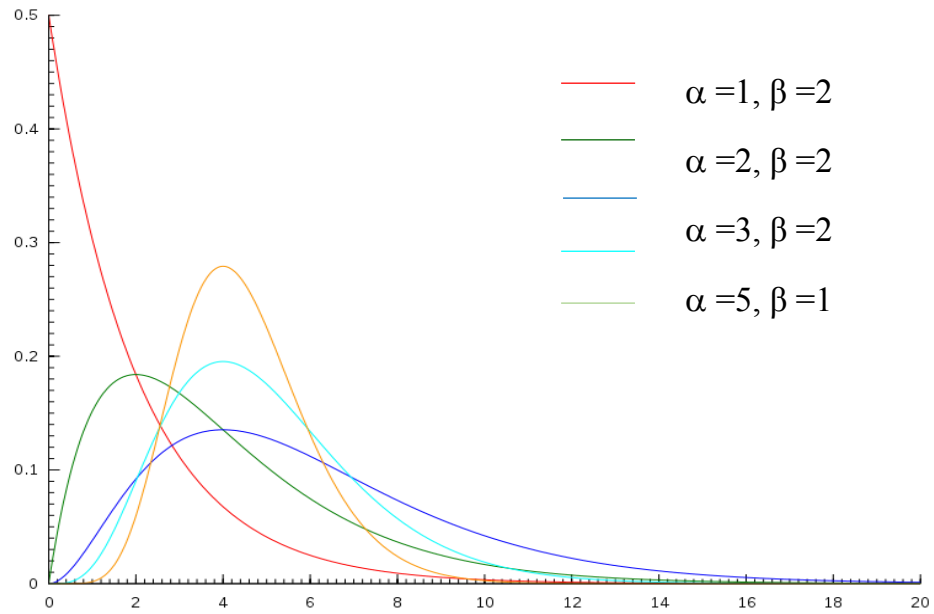


Figure 3.2 .Probability Density Function (PDF) of gamma distribution for different values of shapes and scales

In this thesis the parameters of the incomplete gamma distribution for the annual rainfall amounts at all stations and the goodness of fit are estimated by the use of the EasyFit statistical Software, version 5.5 (Math Wave Technologies, 2011). This is used to determine the best annual rainfall distribution, to calculate the distribution parameters α and β and to test the goodness of fit.

To reveal climatic changes in the temporal and spatial distribution patterns of annual rainfall, the 52-yr period was divided into two parts: 1961-1986 (26-yr) and 1987-2012 (26-yr). The gamma distribution was then fitted to the annual totals of rainfall at 103 rainfall stations possessing homogeneous long term records. The statistical significance of the changes in the distribution parameters between the two periods were checked by two sample t test at the significance level of 0.05. The spatial distribution of the shape parameters for the two periods, as well as the percent changes of the values of the second period with respect to the first one, were then plotted.

3.2 Meteorological drought indices (DIs)

Drought is often represented in terms of drought indices (DIs) which facilitate identification of drought intensity, duration, water deficiency and spatial extent (Mishra and Singh, 2010). Drought monitoring is an essential component of drought risk management. It is normally performed using various drought indices (DIs) that are calculated by integration of hydro-meteorological quantities such as precipitation, soil water content (moisture), stream flow, snowpack and groundwater over a given temporal-scale (Palmer, 1965; Türkes and Tatli, 2009).

The World Meteorological Organization (WMO) defines a drought index as “an index which is related to some of the cumulative effects of a prolonged and abnormal moisture deficiency” (WMO, 1992). DIs evaluate the departure of climate variables in a given time interval (month, season or year) from the “normal” conditions and are used as monitoring tools and operational indicators for water managers which provides a comprehensive picture for drought analysis and decision-making (Hayes *et al.*, 2011). Several drought indices have been developed, most of them based only on precipitation, some based on precipitation and potential evapotranspiration (PET), and others referring to runoff and vegetation conditions (Heim, 2002). Friedman (1957) identified four basic criteria that any drought index should meet: 1) the timescale should be appropriate to the problem at hand; 2) the index should be a quantitative measure of large-scale, long-continuing drought conditions; 3) the index should be applicable to the problem being studied; and 4) a long accurate past record of the index should be available or computable. A fifth criteria should be added for indices used in operational drought monitoring: 5) the index should be able to be computed on a near-real-time basis. Drought severity may differ from site to site under different climatic conditions, hence, as many as applications of DIs and their comparisons are beneficial for specific regions in the world.

Because of the complexity of drought, no single index has been able to adequately capture the intensity and severity of drought and its potential impacts (Heim, 2002). Several studies (Guttman, 1998; Morid *et al.*, 2006; Türkes and Tatli, 2010) have indicated that there is an advantage in considering more than one

DI for drought studies. According to Dogan *et al.*, (2012), comparing and combining different DIs may help:

- Characterize droughts.
- Examine the sensitivity and accuracy of DIs.
- Investigate the correlation between them.
- Explore how well they cohere with each other in the context of a specific objective.

A DI itself might be robust, but the incorporated time step is also important for sensitivity analysis. The uniformity of the required data for the computation of DIs provides a fair competition for comparison.

The choice of indices for drought monitoring in a specific area should eventually be based on the quantity of climate data available and on the ability of the index to consistently detect spatial and temporal variations during a drought event (Morid *et al.*, 2006). This thesis compares the performance of five indices for drought monitoring in the EM. These DIs are all rainfall-based indices and are able to quantify both dry and wet cycles.

The five DIs used include Deciles Index (Gibbs and Maher, 1967) and the Standardized Precipitation Index (SPI) (McKee *et al.*, 1993) which has gained world popularity and been applied worldwide because it is easily comparable. Furthermore, SPI has been recommended by the World Meteorological Organization (WMO, 2011). The Modified China Z Index (MCZI) which is used by the National Meteorological Centre of China (Wu *et al.*, 2001; Morid *et al.*, 2006) is also included and it monitors moisture conditions. Finally, the Z-Score and Effective Drought Index (EDI) are also used since they are considered as the best correlated index with other DIs when considering all time steps (Akhtari *et al.*, 2009; Park *et al.*, 2014).

A good understanding of drought statistics is therefore essential for planning and management of water resources. It can help water managers and planners answer questions about the expected frequency, duration and severity of droughts. It can also provide an additional information on precipitation and streamflow for

estimating changes in recharge and daily flows for the purposes of water resources modelling (Jones *et al.*, 2006).

3.2.1 Standardized Precipitation Index (SPI)

The SPI is described in detail by McKee *et al.* (1993), Guttman (1999) and Bordi *et al.* (2001). The calculation of the index realizes the fit of a gamma probability distribution function to long-term precipitation data for a given month. Based on the gamma parameters, the cumulative probability of precipitation for the given month can be derived.

SPI has been used along the last two decades extensively in Turkey (Sonmez *et al.*, 2005; Keskin *et al.*, 2009; Durdu, 2010), Mediterranean region (Lana *et al.*, 2001; Vicente-Serrano *et al.*, 2004 ; Salvati *et al.*, 2009; Lopez-Bustins *et al.*, 2013), United States (Guttman, 1999; Heim, 2002; Keyantash and Dracup, 2002; Budikova, 2008), and other parts of the world (Mishra and Singh, 2009; Edossa *et al.*, 2010; Roudier and Mahe, 2010; Stricevic *et al.*, 2011; Duan *et al.*, 2014; Qin *et al.*, 2014) .

The SPI allows the determination of duration, magnitude and intensity of droughts (Hayes *et al.*, 1999). It has become an important component in many drought monitoring efforts (National drought Mitigation Center (NDMC), North American Drought Monitor (NOAA) and European Drought Observatory (EDC).

As it is based on statistical probability and is designed to be a spatially and temporary invariant indicator capable of representing both drought and wet events in a similar probabilistic way, even when different precipitations regimes are being evaluated (Guttman, 1998; Hayes *et al.*, 1999; Wu *et al.*, 2007). The main advantage of the SPI is that it can be flexibly calculated at different temporal scales (1, 3, 6, 9, 12, 24 and 48 month intervals) according to user's interest for monitoring meteorological, agricultural or hydrological drought (Guttman, 1999). The short term durations of the order of months are important for vegetative cycle of some crops, while long term durations spanning seasons or years are important for water supply management, water resources planning and hydrological studies (Paulo *et al.*, 2003). According to SPI, the responsiveness to emerging

precipitation deficits of SPI was found more reliable for shorter timesteps (Edwards and McKee, 1997; Hayes *et al.*, 1999; Wu *et al.*, 2001).

Although SPI is more suitable for monitoring meteorological and hydrological droughts than agricultural ones, its flexibility in selecting time periods that correspond with growing seasons and crop times makes it useful to inform on some aspects of agricultural droughts (White and Walcott, 2009). McKee *et al.* (1993, 1995) originally used an incomplete gamma distribution to calculate the SPI. Efforts are now in progress to standardize the SPI computing procedure so that common temporal and spatial comparisons can be made worldwide by SPI users (Guttman, 1999).

Calculation of the SPI for a specific time period at any location requires a long-term monthly precipitation database with 30 year or more of data. The probability distribution function is determined from the long-term record by fitting a function to the data. The cumulative distribution is then transformed using equal probability to a normal distribution with a mean of zero and standard deviation of one so the values of the SPI are really in normalized values (Edwards and McKee, 1997). Various types of precipitation distributions have been used for different spatial regions and different time scales. The SPI is defined as the equivalent value of the accumulative probability in normal distribution (McKee *et al.*, 1993) (Fig 3.3).

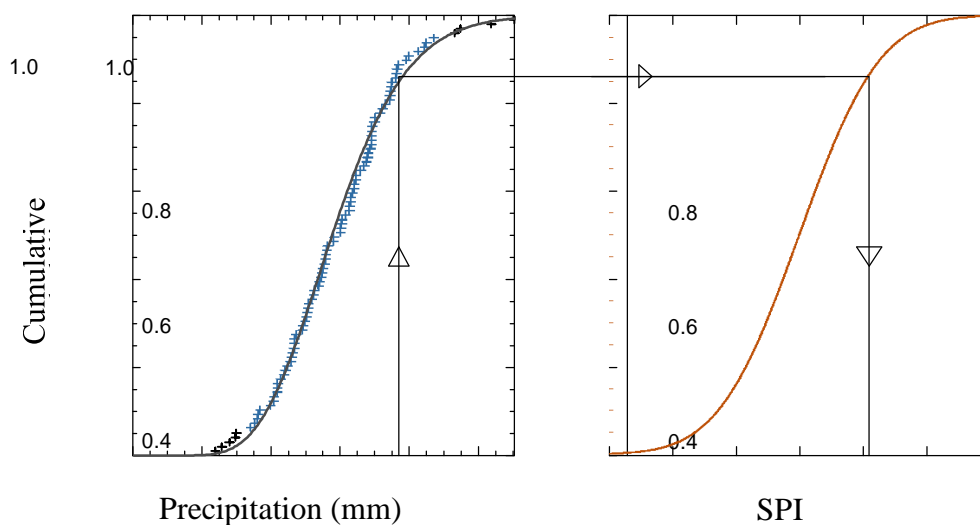


Figure 3.3 Schematic diagram of an equiprobability transformation from a fitted gamma distribution to the standard normal distribution (from Lloyd-Hughes and Saunder, 2002).

Lloyd-Hughes and Saunders (2002) described the detailed calculation of SPI. The most commonly used distribution for SPI calculation is the two-parameter gamma distribution with a shape and scale parameter, which is defined by its probability density function:

$$G(x) = \frac{1}{\beta^\alpha \Gamma(\alpha)} \int_0^x x^{\alpha-1} e^{-x/\beta} dx \quad \text{for } x > 0$$

Where α the shape parameter and β is the scale one. X is the precipitation value and $\Gamma(\alpha)$ is the gamma function.

The gamma distribution is undefined for $x = 0$, but the precipitation may have zero value, so the cumulative probability distribution given a zero value is derived as follows:

$$H(x) = q + (1-q) G(x)$$

Where q is the probability of the zero precipitation value. Fitting the distribution to the data requires α and β to be estimated. Edwards and McKee (1997) suggest estimating these parameters using the approximation of Thom (1958) for maximum likelihood as follows:

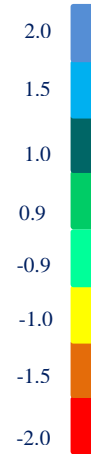
$$\alpha = \frac{1}{4A} \left(1 + \sqrt{1 + \frac{4A}{3}} \right), \quad \beta = \frac{\bar{x}}{\alpha}$$

$$A = \ln(\bar{x}) - \frac{\sum \ln(x)}{n}$$

The cumulative probability distribution is then transformed into the standard normal distribution to calculate SPI. The value of SPI indicates the strength of the anomaly. McKee *et al.* (1995) suggested a classification system to define the intensity of dry/wet phases (Table 3.3). SPI, in fact, is a standardized index that can be computed on different time scales, so as to allow monitoring most of drought types. For this reason SPI is a very useful drought index which can be used in risk assessment and decision-making (Guttman, 1999).

Table 3.3 Drought classification by SPI value and corresponding event probabilities.

SPI value Category	Category	Probability %
≥ 2	Extremely wet	2.3
1.50 to 1.99	Very wet	4.4
1.00 to 1.49	Moderately wet	9.2
0.01 to 0.99	Slightly wet	34.1
-0.99 to -0.00	Slightly dry	34.1
-1.49 to -1.00	Moderately dry	9.2
-1.99 to -1.50	Severely dry	4.4
≤ -2	Extremely dry	2.3



SPI has some limitations. This is calculated based on monthly precipitation (as are many other drought indices). Therefore, if a drought occurs, an index value is not available until the last day of the month or the subsequent month, when statistical analyses of precipitation for the particular month are completed. In addition, droughts can be relieved by a single day of heavy rainfall; however, this situation continues to be considered a drought until statistics on precipitation for the month are available. This factor hinders the accurate and suitable disaster prevention measures. Furthermore, SPI (as other monthly drought indices) cannot take into consideration the fact that substantial water resources generated by rainfall that occurred many months ago may have already been lost due to outflow and evaporation. Although the SPI can be calculated in all climatic regions (Heim, 2002), it is important to note that arid regions, those that experience many months with zero precipitation, may be problematic for the SPI depending on which PDF is used to normalize precipitation (Wu *et al.*, 2007). SPI also requires a long (and complete) precipitation record and strongly influenced by record length (Wu *et al.*,

2005). Therefore when comparing stations to each other, it is advised to use the same length of precipitation record and recommended to be more than 50 years (Wu *et al.*, 2005).

In order to identify the most appropriate SPI timescale, the drought index in this research was applied on short timescales (3 months), moderate timescales (6 and 9 months), as well as long timescales (12 and 24 months) using “SPI” R package.

A corresponding R package “SPI” was deposited in the R archive CRAN, version 1.1, and license: GPL-2 which published by Josemir Neves (2012) and accessible at the URL:

<http://cran.r-project.org/web/packages/spi/index.html>

Vicente-Serrano *et al* (2010) developed a new drought index, the Standardised Precipitation Evapotranspiration Index (SPEI) which is similar to SPI but incorporating estimates of moisture losses to the atmosphere due to evapotranspiration (PET). SPEI is also computed at different time scales based on the non-exceedance probability of precipitation and potential evapotranspiration (P-PET) differences (Vicente-Serrano *et al.*, 2010) and has the ability of depicting the multi-temporal nature of drought. Nevertheless, in this thesis, it is not carried out because we only have the rainfall data.

3.2.2 China Z Index (CZI), and Modified China Z Index (MCZI)

The China Z Index (CZI) is based on the Wilson–Hilferty cube-root transformation (Kendall and Stuart, 1977). Assuming that precipitation data follow the Pearson Type III distribution, the index is calculated as:

$$CZI_j = \frac{6}{C_s} \left(\frac{C_s}{2} \phi_j + 1 \right)^{1/3} - \frac{6}{C_s} + \frac{C_s}{6} \quad "a"$$

$$C_s = \frac{\sum_{j=1}^n (x_j - \bar{x})^3}{n \cdot \sigma^3} \quad "b"$$

$$\phi_j = \frac{x_j - \bar{x}}{\sigma} \quad "c"$$

Where j is the current month, C_s is coefficient of skewness, n is the total number of months in the record, ϕ_j is standard variable, also called the Z-Score,

and x_j is precipitation of month j and σ is the standard deviation. To compute the Modified China Z Index (MCZI), which is used in this research, the median of precipitation (Med) is used instead of the mean of precipitation in the calculation of the CZI (Med is substituted for mean precipitation (\bar{x}) in equations b and c) (Morid *et al.*, 2006).

Wu *et al.* (2001) attempted to reduce the differences between the SPI and the MCZI, but they concluded that the differences between these two indices did not reduce as significantly as they did between the SPI and the CZI. From this we can divide the drought in various areas in a year into four classes (Feng and Zhang, 2005) (Table 3.4).

Table 3.3 Category and values of drought for CZI -MCZI index.

CZI-MCZI Category	Category	CZI-MCZI values
7	Extremely dry	≤ -2.00
6	Severe drought	-1.5 to -1.99
5	Moderate drought	-1.00 to -1.49
4	Near normal	-0.99 to -0.99
3	Moderate wet	1.00 to 1.49
2	Very wet	1.50 to 1.99
1	Extremely wet	≥ 2.00

3.2.3 Statistical Z -scores (Standard Distribution Index)

The statistical Z-Score is the coefficient of variation of the precipitation anomaly. Z-Score indicates how many standard deviations a rainfall value is above or below the mean. It is not the same as SPI, because it does not require adjusting the data to fit gamma or Pearson type III distribution which causes the Z-Score not to represent short dry periods as SPI does (Edwards and McKee, 1997). Z-Score is frequently computed in drought studies (Komuscu, 1999; Tsakiris and Vangelis, 2004; Akhtari *et al.*, 2009).

The Z -Score is simply calculated as the difference between the precipitation during a selected time scale for each year of the series and the precipitation average, divided by the standard of the precipitation series deviation for the selected timescales.

$$Z = \frac{x_i - \bar{x}}{S}$$

Where x_i is the precipitation in month i . \bar{x} is the precipitation average of the study period and S is the precipitation standard deviation for the same period.

Considering the values resulting from this index, the intensity of drought is classified into the following (Table 3.5) (Wu *et al.*, 2001; Behzadi, 2013).

Table 3.5 Classification of Z- Score index (Standard Distribution index)

Z-Score	Intensity of drought
0 to -1.0	Slight Drought
-1.1 to -1.5	Medium Drought
-1.6 to -2.0	Severe Drought
< -2	Extreme Drought

Despite different underlying statistical distributions, the SPI, CZI and Z-Score have performed in a similar manner. This similarity may point to the

importance of utilizing long-term precipitation records for drought analyses (which can remove marginal differences between the indices).

Nevertheless, Z-Score differs from SPI because it does not require adjusting the data to any distribution of the previous indices. Z-Score is frequently computed in drought studies (Wu *et al.*, 2001; Morid *et al.*, 2006; Akhtari *et al.*, 2009). To differentiate it from SPI, Z-Score is sometimes called the Standardized Monthly Precipitation (SMP) (Sirdas and Sahin, 2008). Since the original SPI has been commonly used to fit a gamma distribution (McKee *et al.*, 1993), using Z-Score or SMP instead of SPI for further studies is better when the distribution type is normal.

The Z-Score Index can be used for measuring meteorological and agricultural drought since it only accounts for the moisture conditions during the current week or month (Quiring and Papakyriakou, 2003). It responds similarly to complex SPI and MCZI, but it is a little bit less consistent to its own time steps (Dogan *et al.*, 2012).

Both MCZI and Z-Score can be used as good drought predictors depending on the season, the length of drought and climatic conditions. They could be used instead of SPI when less data is available (Shahabfar and Eitzinger, 2013).

3.2.4 Rainfall decile based drought index (The Decile Index, DI)

Arranging monthly precipitation data into deciles is another drought-monitoring technique. It was developed by Gibbs and Maher (1967) and widely used in Australia (Coughlan, 1987) and commonly in drought studies (Keyantash and Dracup, 2002; Smakhtin and Hughes, 2007; Pandey *et al.*, 2008; Barua *et al.*, 2011). Monthly precipitation totals from a long-term record are first ranked from highest to lowest to construct a cumulative frequency distribution. The distribution is then split into 10 parts (tenths of distribution or deciles). The first decile is the precipitation value not exceeded by the lowest 10% of all precipitation values in a record. The second decile is between the lowest 10 and 20%, etc. Comparing the amount of precipitation in a month (or during a period of several months) with the long-term cumulative distribution of precipitation amounts in that period, the

severity of drought can be assessed. The deciles are grouped into five classes, two deciles per class as shown in Table 3.6. If precipitation falls into the lowest 20% (deciles 1 and 2), it is classified as much below normal. Deciles 3 to 4 (20 to 40%) indicate below normal precipitation, deciles 5 to 6 (40 to 60%) indicate near normal precipitation, 7 and 8 (60 to 80%) indicate above normal precipitation and 9 and 10 (80 to 100%) indicate much above normal precipitation. By definition, the fifth decile is the median, and it is the precipitation amount not exceeded by 50% of the occurrences over the period of record.

In the current study, monthly rainfall time series are arranged for calculating the decile index (DI) using DrinC software version 1.5 beta which was developed in the National Technical University of Athens by George Tsakiris *et al.* (2007).

Table 3.6 Classification of Drought Conditions by using DI

Deciles Classification	
Deciles 1 -2 (0- 20%)	Much below normal (MBN)
Deciles 3 -4 (20-40%)	Below normal (BN)
Deciles 5 -6 (40-60%)	Near normal (NN)
Deciles 7 -8 (60-80%)	Above normal (AN)
Deciles 9 -10 (80-100%)	Much above normal (MAN)

3.2.5 Effective Drought Index (EDI)

Byun and Wilhite (1999) developed the Effective Drought Index (EDI) to detect a drought and its beginning, end, and accumulation stress. It is an attempt to more accurately determine the exact start and end of a drought period and solve the common weaknesses of other previous DIs.

EDI is a standardized index that can be used to assess drought severity worldwide and it is a function of ‘precipitation needed for a return to normal’ conditions (or to recover from the accumulated deficit since the beginning of a

drought), which, in turn, is related to effective precipitation (EP). The EDI is the rainfall amount needed return to normal condition (or to recover from the accumulated deficit since the beginning of a drought).

EP is used to compute deficiency or surplus of water resources for a particular date and place. EP here refers to the summed value of daily precipitation with a time-dependent reduction function. EDI is a component measure that considers daily water accumulation with a weighting function for time passage. EDI in its original form is calculated with a daily timestep (Morid *et al.*, 2006; Akhtari *et al.*, 2009; Kim *et al.*, 2009; Kalamaras *et al.*, 2010; Roudier and Mahe, 2010; Pham *et al.*, 2013; Deo and Sahin, 2015), unlike many other DIs. EP for any day is a function of precipitation of the current day, as well as previous days but with lower weights

$$EP_i = \sum_{n=1}^i \left[\left(\sum_{m=1}^n p_m \right) / n \right]$$

Where i = duration of summation and P_m is the precipitation of $m-1$ days previously. The EP is the core of the EDI concept.

Then, mean (\overline{EP}) and standard deviation of the EP values for each month are calculated and the time series of EP values is converted to deviations from the mean (DEP):

$$DEP = \overline{EP} - EP$$

The PRN (precipitation of one day needed for a return to normal conditions) values are then calculated as:

$$PRN_j = DEP_j / \sum_{i=1}^n 1/N$$

The summation term is the sum of the reciprocals of all the months in the duration N . Finally EDI is calculated as:

$$EDI = PRN / s_{PRN}$$

Where s_{PRN} is the standard deviation of the PRN values of the relevant month.

Because negative values of DEP denote that precipitation is below normal, periods of consecutive negative values in DEP denote consecutive drier periods than normal. A dry duration then can be defined as the period of consecutive negative values of DEP and should be different from drought duration because drought means not only a “long-lasting” but also a “severe” water deficiency. Table 3.7 addresses this problem and presents some new definitions.

Table 3.7 New Definitions for dry and drought spells

Name	Definition
Dry spell	Period of consecutive negative values of DEP
Drought spell	Period that the EDI shows less than -1.0.

The EDI and the SPI have an almost similar range of numerical values as shown in Table 3.8.

Table 3.8 Drought severity classification by the EDI index (Morid *et al.*, 2006).

EDI value Category	Category
≥ 2.50	Extremely wet
1.50 to 2.49	Very wet
0.70 to 1.49	Moderately wet
-0.69 to 0.69	Normal
-0.70 to -1.49	Moderately dry
-1.50 to -2.49	Severely dry
≤ -2.50	Extremely dry

Compared to other DIs, the EDI has several advantages. First, it is the only index that was specifically designed to calculate daily drought severity. This enables rapid detection of drought and precise measurement of short-term drought. Second, by utilizing a calculation method that places greater emphasis on recent precipitation, it more accurately calculates the current level of available water resources. Finally, it calculates the total precipitation period, considering the continuity of the drought period during the entire calculation process, and provides the available water resources index (AWRI) as an auxiliary index (Byun and Lee, 2002). The EDI is distinguishable from existing DIs that only provide a calculation for a limited period (e.g., 12 months). Therefore, it becomes possible to diagnose prolonged droughts that continue for several years when using the EDI (Kim *et al.*, 2009).

The known advantages of SPI and EDI over other indices are that the computations only rely on widely measured precipitation data and they are sensitive to detect the onset of drought (Guttman 1999; Mishra and Singh 2010). One of the major weaknesses of the EDI is that it is relatively unknown so its ability to accurately monitor drought conditions remains largely untested (Morid *et al.*, 2006). Even though both the SPI and EDI only use precipitation data, the EDI is almost uncorrelated with the SPI. Another major disadvantage of using the EDI is that it lacks the nice statistical properties of some of the other precipitation-based indices (SPI, Deciles, etc.). For example, Morid *et al.* (2006) demonstrated that the EDI is not normally distributed. On the other hand, the EDI for drought assessment was considered to be more suitable than many other indices when predicting future droughts (Morid *et al.*, 2006; Kim *et al.*, 2009; Dogan *et al.*, 2012).

3.3 Spatial patterns by means of Principal Component Analysis (PCA)

Geostatistical and multivariate techniques are commonly used to analyse the spatial and temporal variability of precipitation, droughts and other variables of interest. Richman (1986) presented three types of eigentechniques which can be used in climatological studies, namely the Empirical Orthogonal function (EOF), principle component analysis (PCA) and Common Factor Analysis (CFA) mentioning in his study that the most researchers prefer to use a specific mode of PCA to study weather type classification. The Principle Component Analysis (PCA) is a convenient and useful method to reduce inter-correlated variables into a few linearly uncorrelated ones. PCA is a statistical technique applied to a single set of variables to determine which variable in this set form coherent, independent subsets. PCA is a widely used method to identify patterns in climatic data and to highlight their similarities and differences (Santos *et al.*, 2010). It is a standard statistical method, often used in climatological studies, to reduce the original intercorrelated variables in a small number of new linearly uncorrelated ones that explain most of the total variance.

The EOF technique developed by Pearson (1901) and Hotelling (1933) has become the most widely used way in extracting important patterns from measurements of climatic variables and identifying the anomalous patterns in the data. The original purpose of EOFs is reducing the large number of variables of the original data to a few variables, but without compromising much of the explained variance. It has been found that both PCA and EOF are slightly different and they can be considered the same for practical purposes, so many researchers used PCA, yet retain the term EOFs (Richman and Gong, 1999).

Precipitation and drought spatial variability analyses through the PCA have been undertaken by many authors as (Bonaccorso *et al.*, 2003; Cannarozzo *et al.*, 2006; Raziei *et al.*, 2008, 2009; Lopez-Bustins *et al.*, 2015). Some of them applied the PCA to the SPI for analysing the temporal and spatial variability of drought (Bordi and Sutera 2001; Bordi *et al.*, 2004; Vicente-Serrano *et al.*, 2004; Vicente-Serrano, 2006; Santos *et al.*, 2010).

The multivariate analysis in this study is carried out using the PCA. A set of new variables less than the number of the original variables have been specified and called Principle components (PCs). The first PCs account for a large proportion of variability and thus dimensional reduction of the original dataset can be achieved.

The PCA is used to capture the spatial patterns of co-variability of dryness/wetness according to SPI series at different stations. Rotated PCA is a powerful tool for objectively decomposing spatial arrays of climate data into natural regional clusters or patterns (Barnston and Livezey, 1987). For identifying drought modes in the EM, for a given time scale, the S-mode PCA (Rencher, 1998) is applied to the SPI-computed at 3-, 6-, 9-, 12- and 24 month time scales. The projection of the SPI fields onto the orthonormal eigen functions provides the principal components or PC score time series. Since the varimax rotation result in orthogonal components (uncorrelated and standardized factors) (Rencher 1998; Mestas-Nuñez, 2000), this method will be a good way in finding sub-regions within the area which have rather independent drought behaviours. The Varimax rotation, which is an orthogonal method used to maximize the variance between the weights of each principal component, was used to identify areas with independent drought variability (Raziei *et al.*, 2009). The loadings corresponding to each dataset were mapped to show the spatial patterns of drought variability across the EM; their associated PC scores were used for drought indices inter-comparison and trend analysis.

The temporal and spatial patterns of drought were analysed in this research to estimate the variability of precipitation and drought over the EM. These spatial statistical analyses were performed using SPSS version 17.0 software (SPSS Inc., Chicago, IL; www.spss.com).

3.4 Monotonic trends and abrupt change detection

It is very important to identify the historical changes in the mean annual precipitation (Pryor and Schoof, 2008). The variability and trends in rainfall and drought fluctuations have received a wide spread attention in climatological and hydrological studies. In the hypothesis testing for long-term trends, two types of trends are usually considered: one is the monotonic trend; the other is the step (shift) change (Hirsch *et al.*, 1991).

As many climatic time series, data in the EM are not normally distributed, non-parametric test were preferred over parametric ones, even though they do not quantify the magnitude of the trend identified (Hirsch and Slack, 1984). The trend analysis framework that was adopted in this research is outlined in Fig 3.4.

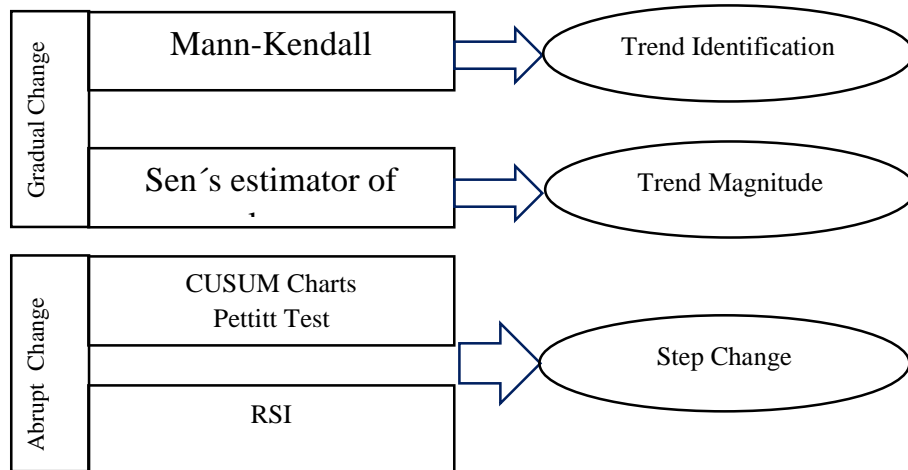


Figure 3.4 Trend analyses framework.

In order to detect trends and possible transitions, the non-parametric Mann-Kendall test (MK) or Kendall's Tau test (Mann, 1945; Kendall, 1975), the cumulative sum control chart (CUSUM) with bootstrap analysis (Taylor, 2000, 2006) and the regime shift index (RSI), calculated by a sequential algorithm of the partial CUSUM method combined with the t-test (Rodionov, 2004), were applied for detecting the shifts in the means of seasonal and annual precipitations, SPI, CI, extreme precipitation indices, dry and drought periods. The linear slopes of trends were calculated using Sen's slope estimator (Sen, 1968). These tests are widely

used to detect trends in climatology and hydrology because they are robust against no normal distributions and not sensitive to missing values.

Among the methods introduced above, MK test has been commonly used to test randomness against trend. It is robust to the influence of extremes and performs well with skewed variables due to its rank-based procedure; especially, when applied to annual total precipitation series, the MK test can result in more significant trends (Serrano *et al.*, 1999). Thus, it is highly recommended for general use by the World Meteorological Organization (WMO) (Mitchell *et al.*, 1966; Wang *et al.*, 2013) for evaluating a presence of a statistically significant trend in climatological and hydrological time series (Douglas *et al.*, 2000; Yue *et al.*, 2002; Birsan *et al.*, 2005). It does not assume any priority in the distribution of the data and allows the presence of a tendency over long period of rainfall data to be observed (Yavuz and Erdoğan, 2012). There are several studies (Tayanç *et al.*, 2009; Flocas *et al.*, 2008; Partal and Kahya, 2006) that analyse climatic trends for the EM mainly using the MK to identify trends and calculate their significance.

Abrupt change denotes a rupture in the established range of experience, that is, a surprisingly fast transition from one state to another (Berger and Labeyrie, 1985). Technically, an abrupt climate change occurs when the climate system is forced to cross a threshold, triggering a transition to a new state at a rate determined by the climate system itself, and faster than the cause (Matyasovszky, 2011; Bers *et al.*, 2013; Soulet *et al.*, 2013).

The multiple change points can be detected by CUSUM and RSI methods (Taylor, 2000 a, b; Rodinove, 2004; Abu-Taleb *et al.*, 2007). Trend analysis and change point detection in precipitation series have been investigated by many researchers worldwide (Karpouzou *et al.*, 2010; Sun *et al.*, 2010). The RSI point, a Sequential t-Test Analysis of Regime Shift (STARS), which is the most common type in detection means shifting (Rodinove, 2005), is identified when the means are statistically different and considered as a possible starting point of the new regime. Whereas the CUSUM charts are constructed by calculating and plotting a cumulative sum based on the data. CUSUM charts show the cumulative sum of differences between the values and the average. Then the average is subtracted

from each value and the cumulative therefor sum ends at zero (Taylor, 2000a, 2000b).

A change point is accepted only, if at least two methods detected the same point. Furthermore, in order to verify this change point, the Student t-test in difference in two means was used to ascertain that the mean in the sub-set before the change point and the mean in the sub-set after the change point are statistically and significantly different. To sum up, a change-point analysis is more powerful, better characterizes the changes, controls the overall error rate, is robust to outliers, is more flexible and is simpler to use.

Overall, change-point methodology has become along the last decades an important tool for identifying sustained changes in climatic variables (Jaruskova, 1996; Lund and Reeves, 2002; Lau and Wu, 2007; Briggs, 2008; Jandhyala *et al.*, 2009; Photopoulos *et al.*, 2010). Change-point methodology begins with the detection part where one applies change detection statistics to establish evidence for the presence of one or more changes in a given series.

To achieve these analyses the following software were used: AnClim (Štěpánek, 2007) for Pettitt test, SPSS Version 17 and MAKESENS (Salmi *et al.*, 2002) for Mann-Kendall test and Sen's slope estimator and Change Point Analyzer (Taylor, 2000a, 2000b) for CUSUM charts.

3.5 Assessment of precipitation extreme.

Within the context of global warming, extreme climate events have recently received much attention because they are more sensitive to climate change than mean values (Klein Tank and Konnen, 2003; Williams, *et al.*, 2010).

Extreme events are defined as the “occurrence of a value of a weather or climate variable above (or below) a threshold value near the upper (or lower) ends (‘tails’) of the range of observed values of the variable” (Lavell *et al.*, 2012). Extreme Value Theory is useful for extrapolation from limited data into areas where there are few or none. Extreme events are rare phenomena, which often lie outside the range of most measured or observed data. These events have very low probability, but are associated with high impacts and can lead to substantial

damage and losses due to their magnitude. These impacts may involve excessive loss of life, excessive economic or monetary losses, or both. Extreme precipitation is usually defined as the maximum daily precipitation within each year, so one will have as many extreme values as the total number of years. This has been the traditional method known as block-Maxima method for defining extreme value (Gumble, 1958). Establishing a probability distribution that provides a good fit to daily rainfall depth has long been a topic of interest in the fields of hydrology, climatology, and others. The investigations into the daily rainfall distribution are primarily spread over three main research areas, namely, stochastic precipitation models, frequency analysis of precipitation, and precipitation trends related to global climate change (Hanson *et al.*, 2008).

Statistical analyses in climate variability studies have often been concerned with averages of a random variable, such as mean precipitation or temperature. However, the studying of extreme events is recently considered as an important issue, and becomes increasingly studied these years (Brown and Katz, 1995; Zwiers and Kharin, 1998; Wettstein and Mearns, 2002; Fowler *et al.*, 2005; Katz, 2010). At least as early as Wigley (1985, 1988), it has been appreciated that the detected changes in both frequency and severity of extreme climate events are not closely match the detected ones in their corresponding averages (Katz, 2010).

3.5.1 Monitoring changes in extreme precipitation.

In order to elaborate the climatology of extreme indices of rainfall and to detect the changes in precipitation extremes, it was important to develop a set of indices that were statistically robust, covered a wide range of climates, and had a high signal-to-noise ratio. Climatic extreme indices recommended by the joint World Meteorological Organization (CCL/CLIVAR/JCOMM) Expert Team on Climate Change Detection and Indices (ETCCDI) (<http://www.clivar.org/organization/etccdi>), as well as from the European research project STARDEX (Statistical and Regional dynamical Downscaling of Extremes for European regions) were calculated to characterize the possible change in extreme of rainfall (floods, drought) over the EM, since these events have strong

impact on whole society. These indices have also been used in other studies for different regions around the world: Frich *et al.* (2002), Aguilar *et al.* (2005), Alexander *et al.* (2006), Herrera *et al.* (2010) and Jiang *et al.*, (2013), Buric *et al* (2015), and others.

In this study an R- based program RClimdex 1.3 software developed by Zhang and Yang (2004) at the Canadian Meteorological Service was used to obtain the climatic extremes indices following methodologies of Zhang *et al.* (2005) and Haylock *et al.* (2006). Data quality control was performed using RClimDex, developed and maintained by Xuebin Zhang and Feng Yang at the Climate Research Branch of the Meteorological Service of Canada. After data quality control and homogeneity assessment, the 70 stations have been selected, and the data for the period from 1 January 1961 to 31 December 2012 was analysed in this work. Data quality control is a necessary step prior to analysing the variations of precipitation and calculating extreme indices, since the erroneous outliers can seriously impact on their trends. RHTestsV3 software package was used to homogenize daily precipitation data. The RHtestsV3 package and its previous versions have been widely used along the last decade to homogenize climate data (Zhang *et al.*, 2005; Dai *et al.*, 2011; Vincent *et al.*, 2012; Wang *et al.*, 2013).

Figure 3.5 is an example of the plots used for quality control (QC) of precipitation data. It explains the data density in two different ways in some selected stations: a histogram (bars) to detect any problem in the precipitation data and a Kernel-filtered plot (line), a nonparametric test method to density fitting (Aguilar *et al.*, 2005). Both show that precipitation data from the station are fine. The precipitation data quality showed by this figure is good in these selected stations.

RClimdex provides 27 indices including temperature and precipitation indices. However, only 11 indices based on precipitation data were chosen for discussion here (Table 3.9) that better explain the climate behaviour of the EM. The resulting series were analysed through trends. The slopes of the annual trends and their statistical significance to climate indices were calculated based on non-

parametric Mann–Kendall test and least square method in order to detect trends within the time series.

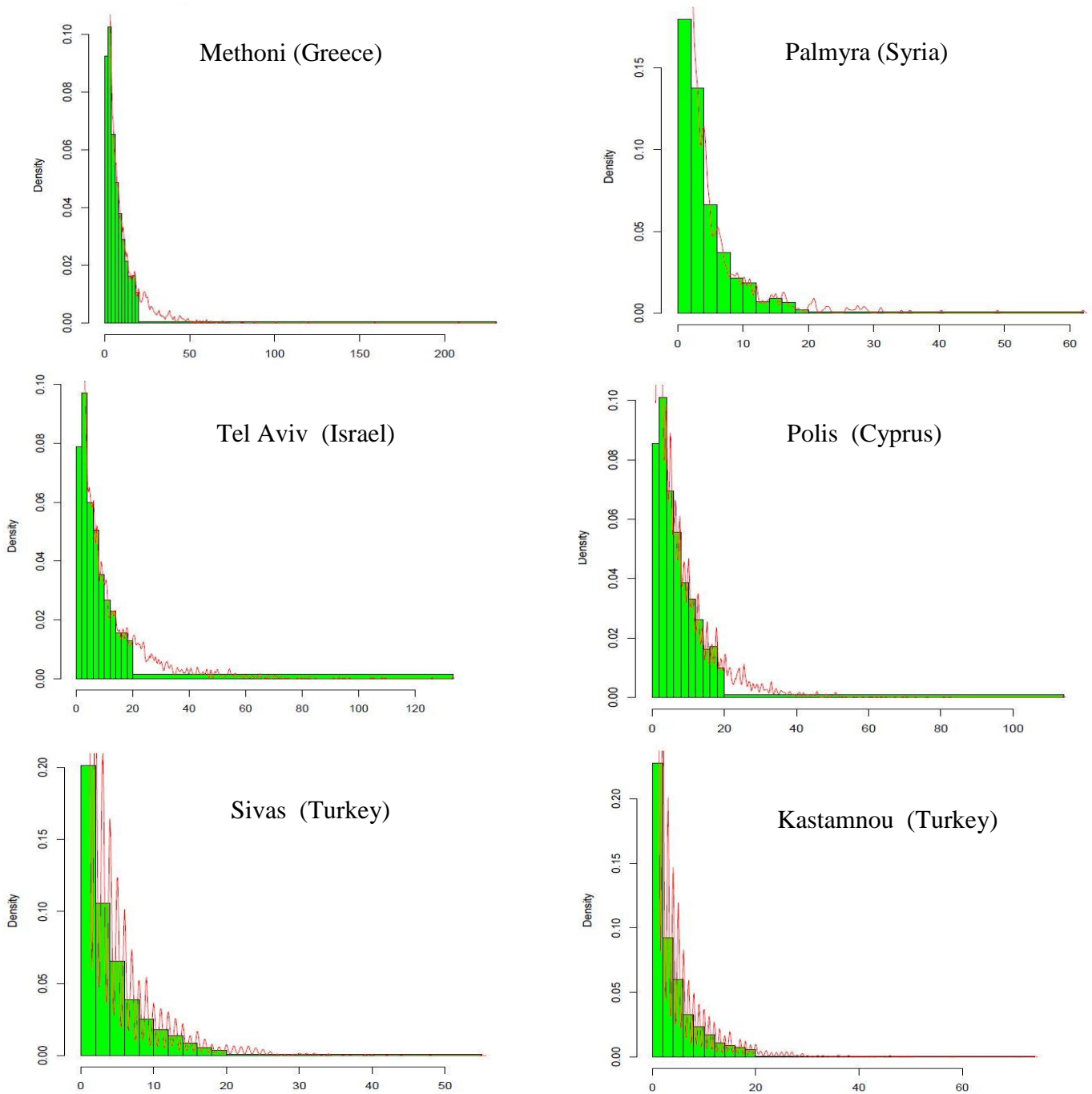


Figure 3.5 Example of daily precipitation successful quality control procedures using RClmDex (Histogram (vertical bars) and Kernel- filtered density (line) showing the high density)

The majority of previous indices provide information on the “wetness”, whereas the last index (Consecutive Dry Days, CDD) (Table 3.9) is a measure of “dryness” (Frich *et al.*, 2002). A dry day is defined when daily rainfall is less than 1 mm, while a wet day is a day with a precipitation amount greater than or equal to 1mm. CDD is the index that describes the lowest tail of the precipitation distribution, and is often referred to as a drought indicator. As drought is a complex phenomenon depending on various other factors besides of insufficient precipitation, CDD can be defined as a meteorological drought index which should be interpreted in combination with other precipitation indices (Tebaldi *et al.*, 2006; Orłowsky and Seneviratne, 2012) or DIs (Cardona *et al.*, 2012). Additionally, Consecutive Wet Days (CWD) and CDD are duration indices which calculate the maximum length of wet and dry spell, respectively. Analysis of CDD and CWD could be performed using different rainfall thresholds for a dry/wet day, such as less/more than or equal to 0.05 mm, 0.1 mm, 1.0 mm, 10 mm, etc. (Kutiel, 1985). In this study, CDD and CWD were evaluated using maximum consecutive dry or wet days (CDD/CWD) corresponding to precipitation $<1\text{mm/day}$ or $\geq 0\text{mm /day}$, respectively.

Table 3.9 Definition of extreme precipitation indices used in this study

ID	Indicator Name	Definition	Units
RX1day	Max 1-day precipitation amount	Monthly maximum 1-day precipitation	mm
Rx5day	Max 5-day precipitation amount	Monthly maximum consecutive 5-day precipitation	mm
SDII	Simple Daily Intensity Index	The ratio of annual total precipitation to the number of wet days (≥ 1 mm)	mm/day
R10	Number of heavy precipitation days	Number of days per year when precipitation ≥ 10 mm	Days
R20	Number of very heavy precipitation days	Number of days per year when precipitation ≥ 20 mm	Days
CDD	Consecutive dry days	Maximum number of consecutive days when precipitation < 1 mm	Days
CWD	Consecutive wet days	Maximum number of consecutive days when precipitation ≥ 1 mm	Days
R95p	Very wet days	Annual total precipitation from days $> 95^{\text{th}}$ percentile	mm
R99p	Extremely wet days	Annual total precipitation from days $> 99^{\text{th}}$ percentile	mm
PRCPTOT	Annual total wet-day precipitation	Annual total precipitation from days ≥ 1 mm.	mm

Dry days are those days when the amount recorded was < 1 mm.
Wet days are those days when the amount recorded was ≥ 1 mm.

Extreme dry spells are represented by the duration of the CDD index (Frich *et al.*, 2001), which is defined as the annual maximum number of consecutive dry days within a specific time period. The indices R10, R20 are based on absolute thresholds, i.e. they directly measure the number of very wet days and they are highly correlated with total, annual and seasonal precipitation in most climates. Similarly, the indices Rx1day (Max 1-day precipitation amount) and Rx5day (Max 5-day precipitation amount), the greatest 1 and 5 day total precipitation respectively, provide information about the most rain-intense periods of the year. The same applies to the 95th and 99th percentile of daily total precipitation (R95p and R99p, respectively). Rx5day is also known as a measure of short term precipitation intensity as well as an indicator for flood-producing events. PRCPTOT describes the total annual amount of precipitation on wet days defined as days with more than 1 mm of precipitation. SDII is a simple measure of precipitation intensity (Frich *et al.*, 2002) and describes the daily precipitation amount averaged over all wet days in a year. PRCPTOT and SDII are not necessarily associated with climate extremes but provide useful information about the relationship between changes in extreme conditions (e.g., RX5day or R95p) and other aspects of the distribution of daily precipitation (Donat *et al.*, 2012).

Chapter Four

Results and Discussion

4.1 Spatial and temporal analysis of precipitation variability and frequency.

4.1.1 Spatial variability of annual and seasonal precipitation

The spatial pattern of annual cumulated precipitation in the Mediterranean is shown in Fig 4.1. In the EM, our study region, it can be seen that the lowest annual precipitation, less than 100 mm, occurs in Jordan, Syria and Israel. The annual precipitation amounts range from 100 to 1,100 mm and the maximum values of annual precipitation occurs in northwestern parts which exceed 1,400 mm in coastal regions which are mainly controlled by the large-scale pressure systems and upper atmospheric circulation (Tatli *et al.*, 2004) and have a high internal variability in all seasons. Some of these variations are closely associated with the large-scale modes of circulation variability such as the NAO (Turkes and Erilat, 2006).

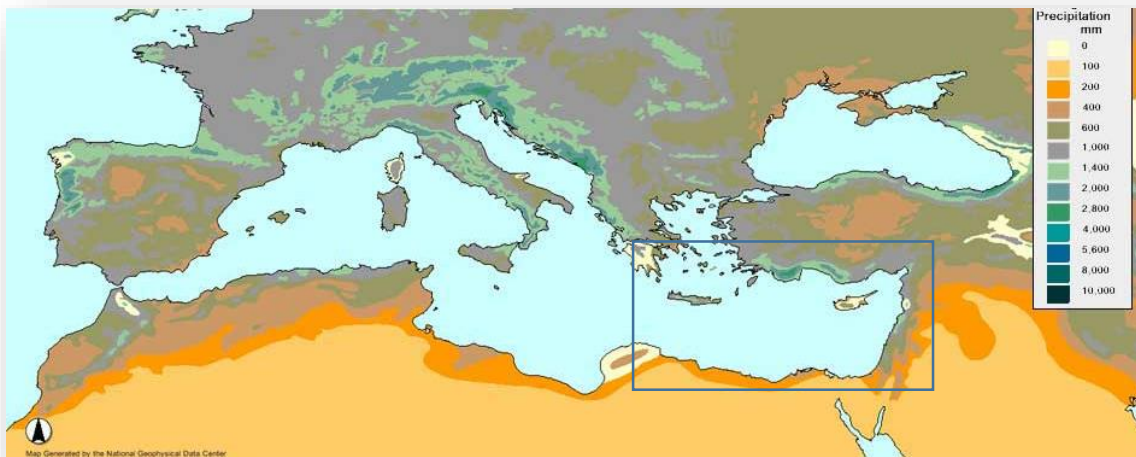


Figure 4.1. Spatial distribution of mean annual precipitation in the Mediterranean Basin over 1961-2010. (Source: NOAA).

The highest precipitation amounts are recorded in winter (400-800 mm) and spring (75-300 mm), respectively. The contribution of winter precipitation to the total annual precipitation decreases from 80% in the southeastern parts to 40-50% in the coastal regions in northwestern parts of Turkey (Fig. 1.2). In spring, the south and southeast areas receive almost the 20% of annual precipitation whereas

the northeastern parts receive between 20 and 30%. Therefore, the spatial pattern of this season is almost uniform across the study area which has a unimodal precipitation regime (winter, spring, autumn). The highest summer precipitation occurs in the northeastern parts of the EM, while most of other regions receive less than 5 mm during this season especially in Syria, Jordan and Israel because the EM is subjected to persistent air subsidence centred over Crete which makes this area under low humidity in the northern hemisphere between June and August at 300-500 hPa level preventing rain over this region during this season (Alpert *et al.*, 1990; Saaroni and Ziv, 2000; Ziv *et al.*, 2004).

Thus, in order to identify objectively the precipitation sub-regions, the annual precipitation amounts and the percentage of annual precipitation occurring in each season of the year appear to be suitable input variables for PCA applications.

4.1.2 Intra-annual and seasonal precipitation variability

Intra-annual and seasonal precipitation variability across the study area was assessed using the PCA which was applied to the variables computed for the whole stations. For studying precipitation variability, the S-mode PCA identifies the variability of annual precipitation time series at given stations across the study area. The rotated PC loadings and the explained and cumulative variances of the retained PCs are listed in Table 4.1.

Table 4.1 Percentage explained variance and percentage of cumulative variance of the rotated first five principal components (PCs) for the annual and seasonal (except summer) precipitation totals of the EM.

	Annual		Winter		Spring		Autumn	
C	Explained Variance (%)	Cumulative variance (%)	Explained Variance (%)	Cumulative variance (%)	Explained Variance (%)	Cumulative variance (%)	Explained Variance (%)	Cumulative variance (%)
1	27.63	27.63	31.45	31.45	30.71	30.71	21.10	21.10
2	15.80	43.43	18.58	50.04	11.47	42.71	13.83	34.93
3	6.32	49.75	5.38	55.42	6.81	48.99	6.54	41.47
4	6.13	55.83	4.77	60.19	5.70	54.68	5.75	47.22
5	5.10	60.98	4.19	64.38	4.35	59.02	5.45	52.67

These five loading PCs explain between the 50 and 65% of the total variances of annual and seasonal series. The extracted PCs should explain at least about 60% of total variance (Briffa *et al.*, 1994) and our set of PCs follows this recommendation. Their PC loadings are mapped in Fig 4.2 as Empirical Orthogonal Functions (EOFs), (summer is not analysed because it is very dry season in whole EM).

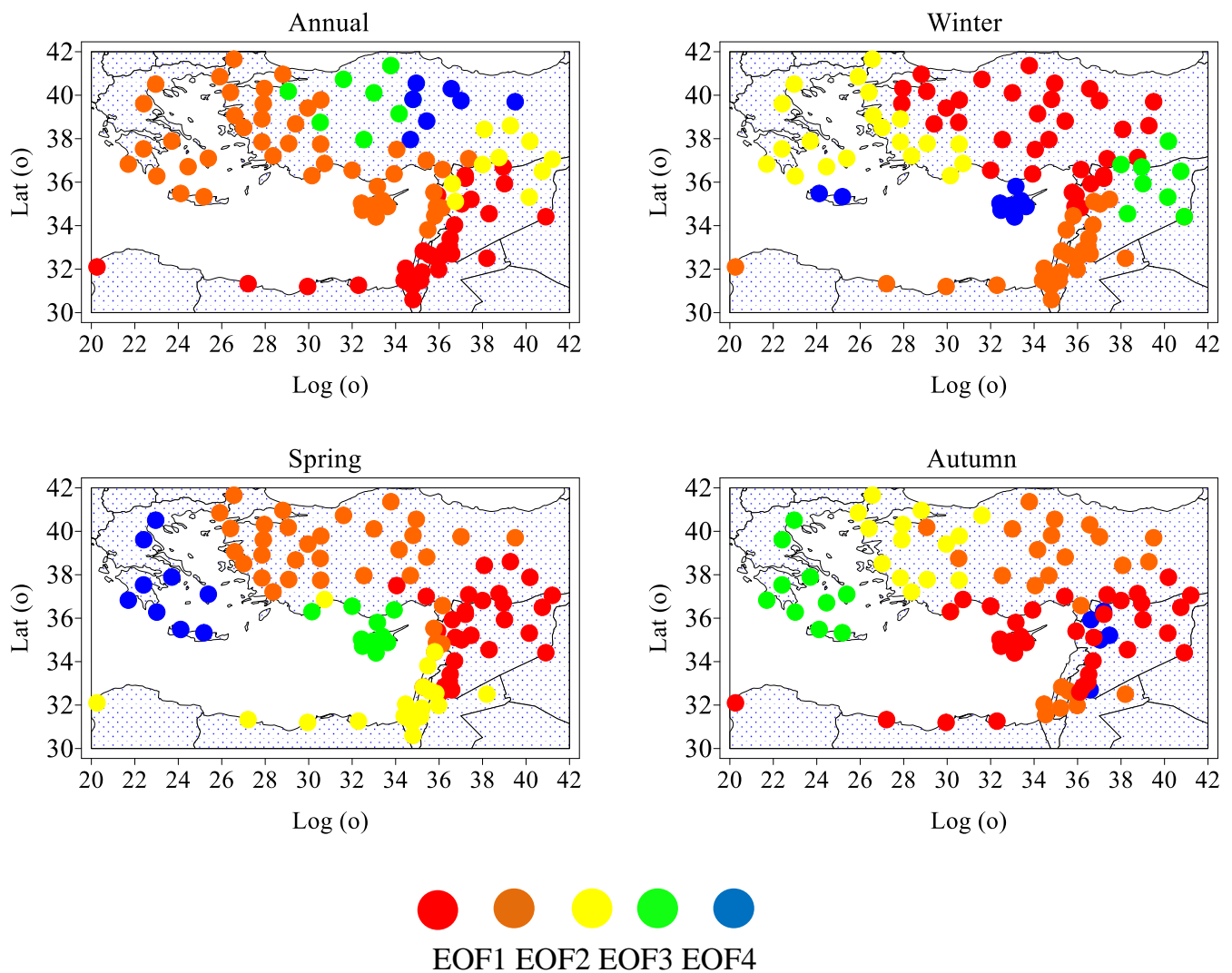


Figure 4.2 Spatial distribution of PCs loadings (Empirical Orthogonal Functions, EOFs) for annual and seasonal precipitation amounts during 1961-2012 over the EM.

High loadings (>0.5) indicate good correlations between the variables and the PCs scores. According to the PCA applied to the annual precipitation total series of 103 stations, the first PC (PC1) explains the variance in the spatial variability of annual rainfall series about 28% (Table 4.1). Greater positive PC1 loadings (>0.5) are found over Egypt, Israel, Jordan and south Syria; whereas the greater ones for PC2, which explains about 16% of total variance, are recorded in Cyprus, the coastal areas in Syria and Lebanon, western and the southwestern parts of Turkey which mainly have annual precipitation rates about 720 mm and more than 25% of its variability related to the NAO effects (Mann, 2002). The highest PC3 loadings cover the northeastern parts of Syria and southeastern parts of

Turkey (the closest parts to Syria) and explains about 6% of the total variance. The PC4 explains about 6 % of the total variance and has high positive loadings on annual precipitation in mid parts of Turkey at longitudes between 32° E and 34° E. Finally, the PC5 represents only 5% of total variance and its loadings are found over some parts of Turkey (mid and eastern parts) between 34° E and 40° E with mean annual precipitation about 550mm. Summing up, the precipitation regime in the EM exhibits large spatial variability.

In winter, the total mean precipitation corresponds to about 65% of the annual precipitation. The PC1 has high positive loadings on mean winter precipitation amounts and explains 31% of the total precipitation variance (Table 4.1). It shows positive loadings in northern parts (Turkey), which means that the Turkey has a considerable amount of winter precipitation. The observed patterns of winter precipitation are significant and spatially coherent over a large area in Turkey. High positive loadings values from the PC1 over Turkey relate to the influence of the precipitation regimes which are characterized with the macro Mediterranean climate and the Mediterranean transition to the continental Anatolia and indicate the influence of the large-scale atmospheric circulation and associated weather system patterns (Turkes *et al.*, 2009). Cullen and de Menocal (2000) found that 27% of the variance in winter precipitation in Turkey is related to the NAO. The PC2 explains about 19% of the variance in the winter precipitation totals (Table 4.1). Spatial variability of the PC2 loadings exhibits a spatially coherent correlation over south Syria, Israel and Jordan, north Egypt and north Libya. This spatial correlation pattern indicates the effects of cold fronts and the air masses that follow these fronts, which are associated with extra-tropical cyclones and caused more than 90% of the precipitation in Israel (Goldreich, 2003). On the other hand, in contrast to the PC1, the highest loadings of PC3 are found in Greece and in the western parts of Turkey.

In spring, the PC1, with 31% of explained variance, has high positive loadings on mean spring precipitation amounts in Syria and southern (Fig 4.2). The PC1 shows an existence of significant and apparent spatial autocorrelation pattern in Syria, which in turn indicates that this region is characterized by high amounts

of spring precipitation with very high variability. The PC2 and PC3 of the spring precipitation totals describe about 12% and 7%, respectively, of the variance in the spring precipitation variability. The loading patterns of the PC2 and PC3 do not prove the existence of any significant and apparent geographical autocorrelation pattern, with the exception of the spatial relationship patterns with the relatively positive values in Cyprus, which has a typical EM climate, and Israel, respectively.

In autumn, the PC1 loading pattern explains about 21% of the total variance and has high positive values on the mean amounts of autumn precipitation in the southern parts of Turkey, inland Syria, north Egypt and Libya. As shown in the figure above (Fig 4.2), the corresponding spatial pattern of PC1 indicates that all stations in Cyprus, the continental parts of Syria and southern parts of Turkey are characterized by a large percentage of autumnal precipitation and high rates of variability and an increasing trend (Giorgi, 2002; Turkes, 2008; Skaf and Mathbout, 2010; Altm *et al.*, 2012); thus indicating the importance and magnitude of autumnal precipitation in these regions. The PC2 of the autumn precipitation, which explains about 14% of total variance, has very high positive loadings (≥ 0.7), especially in northern parts of Israel. Kutiel (1991) related variations in the spatial and temporal properties of the rainfall regime in the Northern Israel to parallel changes in sea level pressure (SLP) in the Mediterranean. The PC3 for the autumn precipitation totals is related to only about 7% of the total variance. Spatial variability of the PC3 loadings exhibits a positively correlated distribution pattern in Turkey, with a maximum of 0.78 at the east of the country, namely on Mugla. Positive PC3 loadings at the east of Turkey mainly explain the influence of the frontal Mediterranean cyclones on the autumn precipitation coming directly through the Mediterranean basin (Turkes, 2008).

4.1.3 Spatial coherence analysis and coefficient of variation (CV).

To evaluate the spatial coherence of the mean annual precipitation in each subregion, the variance of Standardized Anomaly Index (SAI) ($\text{var} [\text{SAI}]$) (Katz and Glantz, 1986) was estimated. The ($\text{var} [\text{SAI}]$) varies between 0.47 in both subregions: PC4 and PC5 (Greece and Turkey),

and 0.65 in sub-regions PC1 and PC3 (southern Turkey, Syria, Israel and Jordan). The observed value of (var [SAI]) in PC2 (south Turkey) is 0.50. These results indicate a strong coherence in the first and third subregions and less inter/station noise, whereas the fourth and fifth ones reflect a moderate spatial coherence. The regional annual (var [SAI]) time series were also checked for normality, which is a prerequisite for the analysis, using the K-S and Anderson-Darling goodness of fit tests. Test results showed that the (var [SAI]) time series follow a normal distribution with 95% confidence level. Interannual variability of each station and each subregion was calculated through the coefficients of variation of annual precipitation (CV). It was employed as statistical measures of rainfall variability. As shown in Fig 4.3, CV values for annual rainfall range between 15% in Tokat (northern Turkey) in the subregion 5, reflecting less variability in interannual rainfall, and 83% in Kharabo (southern Syria) in the first subregion indicating that variability of rainfall across the years was extremely high.

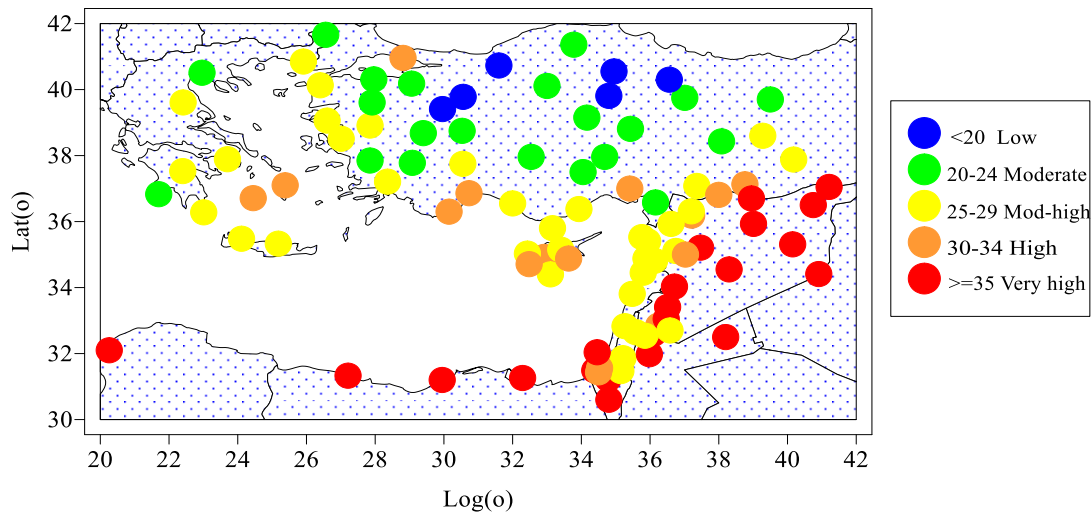


Figure 4.3 Spatial distribution of annual rainfall CVs values over 1961-2012.

It is observed that most stations in southern parts of the EM have high CVs values exceeding 30% which makes this area vulnerable to drought. The highest values of CV are detected in autumn, spring and winter, respectively. Summer is not considered because it is a very dry season in most stations and the precipitation amounts are very small, especially over Syria and Israel (Kutiel *et al.*, 1996; Xoplaki *et al.*, 2000; Tsvieli and Zangvil, 2005). The CV at seasonal scale shows

a high seasonal rainfall variability and its values varies between 30-163% in autumn, 25-92% in winter, and 28-127% in spring, which represents the degree of variability in monthly rainfall throughout the year. High values are detected in the southern parts of the EM in all seasons (Fig 4.4). The highest CV values can be found in areas with permanent conditions where rainfall appears erratic but might occur more or less throughout the year. For example, in Libya, winter rains (December and January) are the more probable and present, which contribute to more than 50% of total annual precipitation with very low amounts in autumns (Le Hou  rou, 1988)

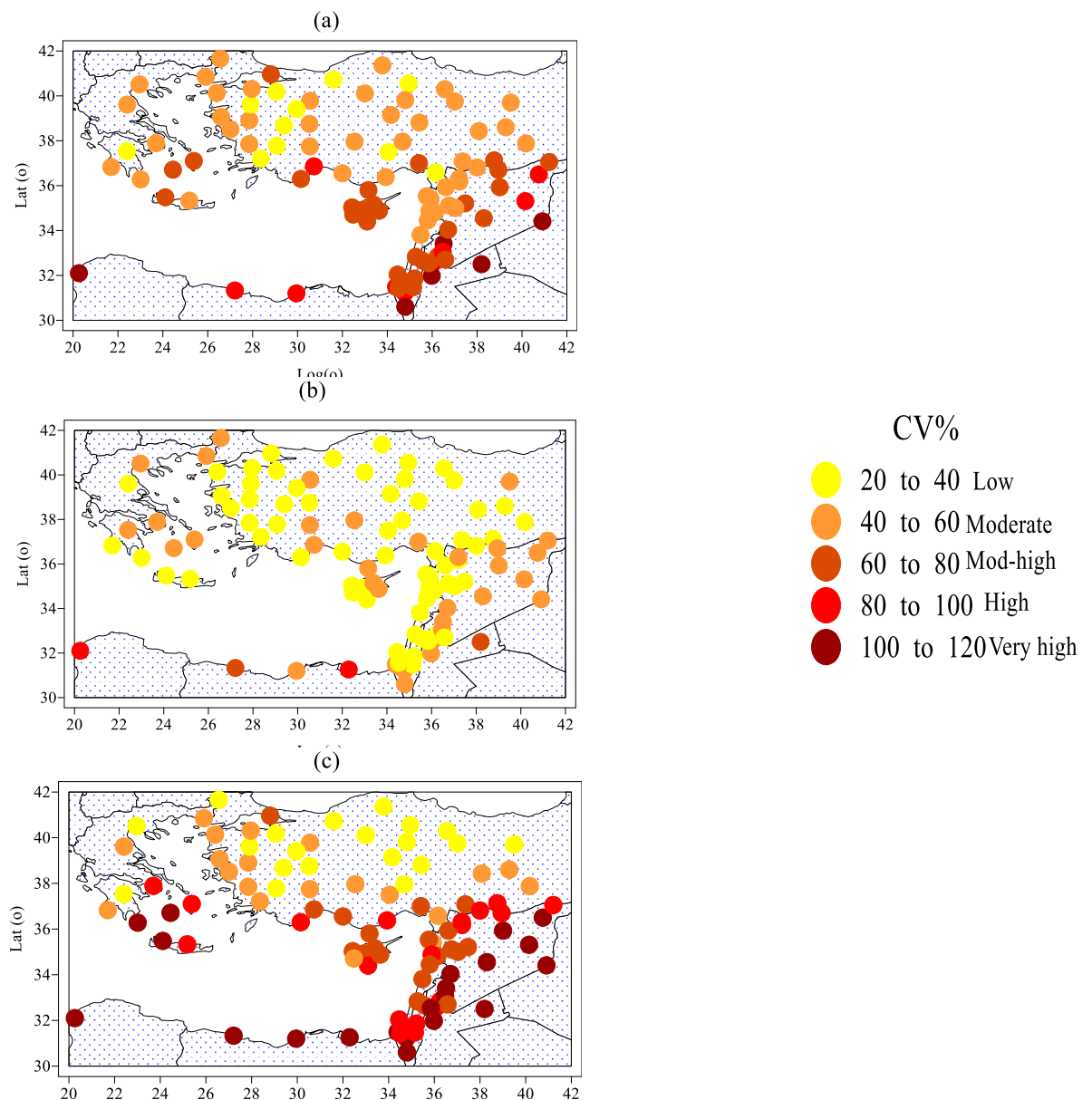


Figure 4.4 CV of the autumn “a”, winter “b” and spring “c” precipitation over the EM for 1961-2012.

It can be also observed that high values of CV are detected in the dry areas which have low rainfall amounts and vice versa. Similar results were obtained by other researchers in studies performed for Iran, which mean rainfall amounts are inversely proportional to the values of CV (Raziei *et al.*, 2014).

The CV map shows an irregular distribution of CV values, with high CVs mostly located in the eastern and southern parts of the EM. High CV values (exceeding 30%), as shown in Fig 4.5, indicate a high degree of discrete temporal rainfall distribution. The spatial distribution of CV alone can be used for simple rainfall zoning, the major shortage is that it cannot account for the changing tendency of time series. For example, the annual rainfall in Sivas and Kastamonu (Turkey) has quite different trends, even though both have the same CV and mean. Therefore, the CV values alone are not able to provide enough information for more accurate classification of the rainfall distribution zone, for this reason we have calculated the rainfall entropy (discussed later).

Regionally, Fig (4.5) and table 4.2 illustrate the CVs values and statistical characteristics of the precipitation across the identified sub-regions. (We remove the summer, which is almost dry in all regions).

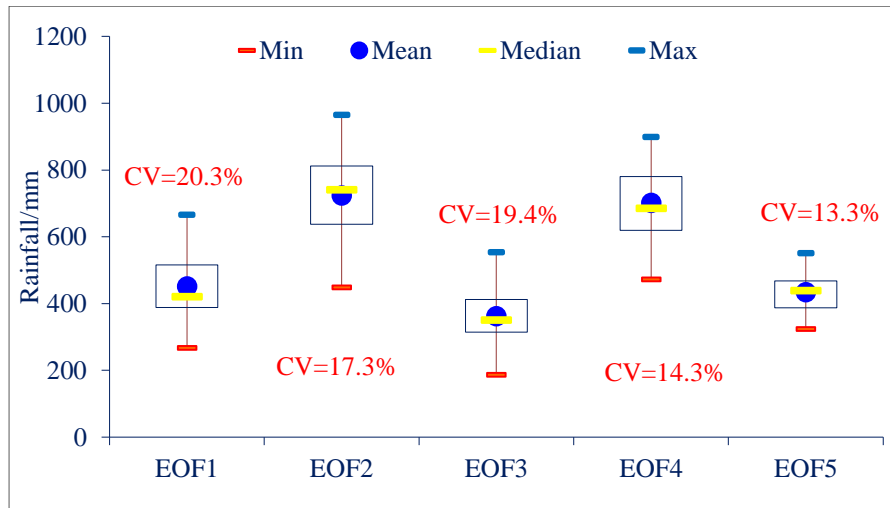


Figure 4.5 Box-Whisker diagram of statistical characteristics of the mean annual precipitation in the identified subregions.

Table 4.2 Statistical characteristics of the precipitation in the identified sub-regions (EOF1: Libya, Egypt, Israel, Jordan and south and mid Syria; EOF2: west and south Turkey, Cyprus, Greece, Lebanon and west Syria; EOF3 southeast Turkey and northeast Syria; EOF4: west Turkey; EOF5: centre and north Turkey)

Zone	Mean annual rainfall (mm)	Mean autumn rainfall (mm)	Mean winter rainfall (mm)	Mean spring rainfall (mm)	Autumn of the total rainfall (%)	Winter of the total rainfall (%)	Spring of the total rainfall (%)	Annual rainfall Skewness	Annual rainfall Kurtosis
EOF1	451.4	86.1	196.3	92.1	19.1	43.5	20.4	0.5	-0.1
EOF2	723.6	87.4	226.7	129.0	12.1	31.3	17.8	-0.2	-0.5
EOF3	362.4	87.3	294.7	86.5	24.1	81.3	23.9	0.2	-0.2
EOF4	701.7	132.8	171.6	146.5	18.9	24.5	20.9	0.1	-0.6
EOF5	434.6	65.8	330.3	150.7	15.1	76.0	34.7	0.2	-0.7

It can be seen that the EOF2 has the highest annual precipitation (732.6mm) with a maximum value occurs in winter (31.3%), spring (17.8%), while in autumn the share of precipitation is lower (12.1%). Negative values for the skewness in this region (-0.2) indicate that annual rainfall data are skewed to the left and there are few events of low precipitation and a large number of high ones and the value of median (740.8mm) is larger than the mean (723.6 mm). The EOF3 has detected the lowest total precipitation (434.6mm) with a positive skewness (0.2) and lowest negative kurtosis (-0.7). The winter and spring precipitation in EOF5 correspond to respectively 76 and 34.7% of total rainfall and are the main contributors to annual precipitation, while the percentage of autumn precipitation is small (15.1%). The skewness coefficient has detected the highest value (0.5) in EOF1 due the highest precipitation variability (CV=34.5%), while other regions show low skewness coefficient values ranging between 0.1 and 0.2 indicating a near normal distribution of annual rainfall in these regions. The negative values of kurtosis in all sub-regions indicate that the annual rainfall data tend to have a flat top near the mean rather than a sharp peak. In all regions, the precipitation is highly concentrated in the winter and spring months.

As shown, the highest values of CV 34.5% and 32.6 are detected in subregions 1 and 3 (southern Turkey, Syria, Israel and Jordan). Both subregions 4 and 5 (Greece and Turkey) have the smallest values (14.3% and 13.3%), respectively. The subregion 2 shows low variability in its annual rainfall (19.4%). The CVs values and latitude are negatively and statistically correlated ($r = -0.67$), at $p < 0.05$ they showed a strong negative correlation; such a correlation is clearly presented in Fig 4.6.

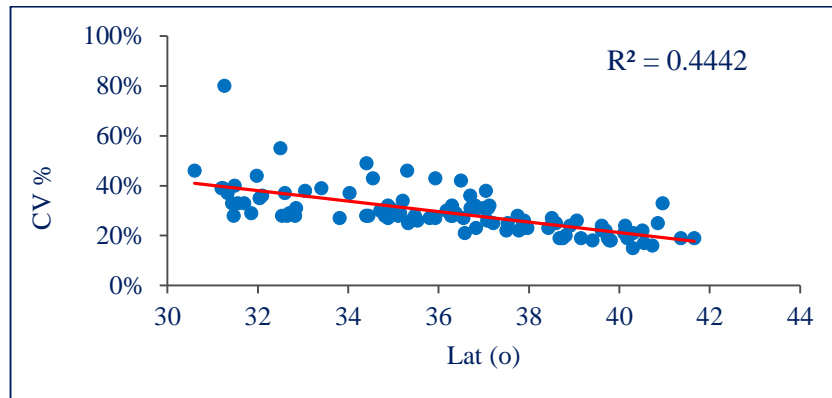


Figure 4.6 The relationship between latitude and annual CVs calculated for each station.

The data indicate non-statistically significant relationship between inter-annual rainfall variability and altitude ($r = 0.19$) at $P = 0.15$. Therefore, the altitude plays no significant role in affecting spatial trends of variability in the annual rainfall series (Fig 4.7).

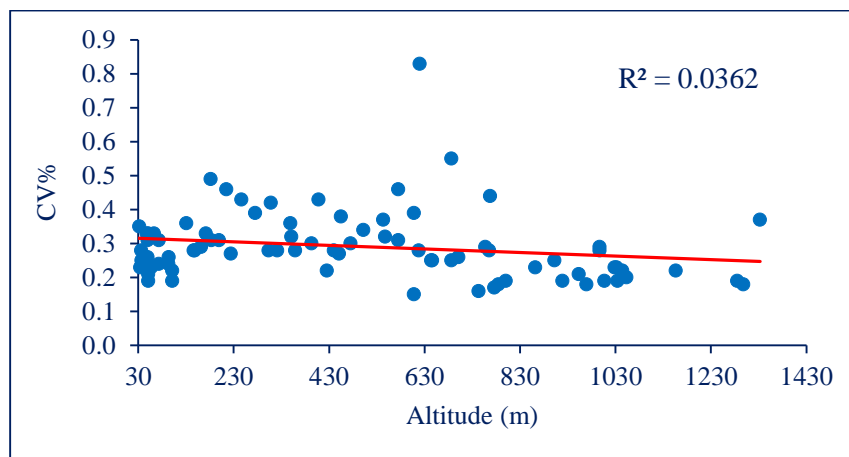


Figure 4.7 The relationship between altitude and annual CVs calculated for each station.

The influence of geographic features on the spatial distribution of mean annual precipitation has been long studied. Several studies announced the impacts of topographic factors including physiographic features (topography), altitude, slope and proximity to a ridge or crest of mountains on the annual and seasonal rainfalls variability and distribution. These studies found that the spatial variability of mean annual and mean monthly rainfall are best captured by such topographic variables (Al-Ahmadi and Al-Ahmadi, 2013) and we have found in our study that altitude is not well correlated with CV values in the EM, whereas high negative and significant correlation was detected between CVs and latitude. Whitmore (1968) showed that altitude, longitude and continentality may explain most of the spatial changes in mean annual precipitation in South Africa. Sevruck *et al* (1998) considered altitude as the best overall predictor of rainfall distribution. Nevertheless, the effect of altitude is not always positive; for instance, Lu *et al* (2008) discussed the negative correlation between summer precipitation and altitude in China and found that the correlation is becoming stronger with increased global warming. Rainfall index is also computed for the analysis of rainfall variability for all stations to identify the behaviour of the rainfall data. Ellis (1995) has also detected a negative correlation between interannual rainfall CV and latitude in Africa and dry ecosystems are more unstable than wet, because rainfall variability is inversely correlated with total rainfall and the lower annual rainfall is the greater the CV. The calculated variability using rainfall index showed good agreement in evaluating the variability and similar CVs results indicating high variation in annual rainfall and its values range between 0.39 in Tokat (Turkey) and 2.03 in Port Saied (Egypt) (Fig4.8).

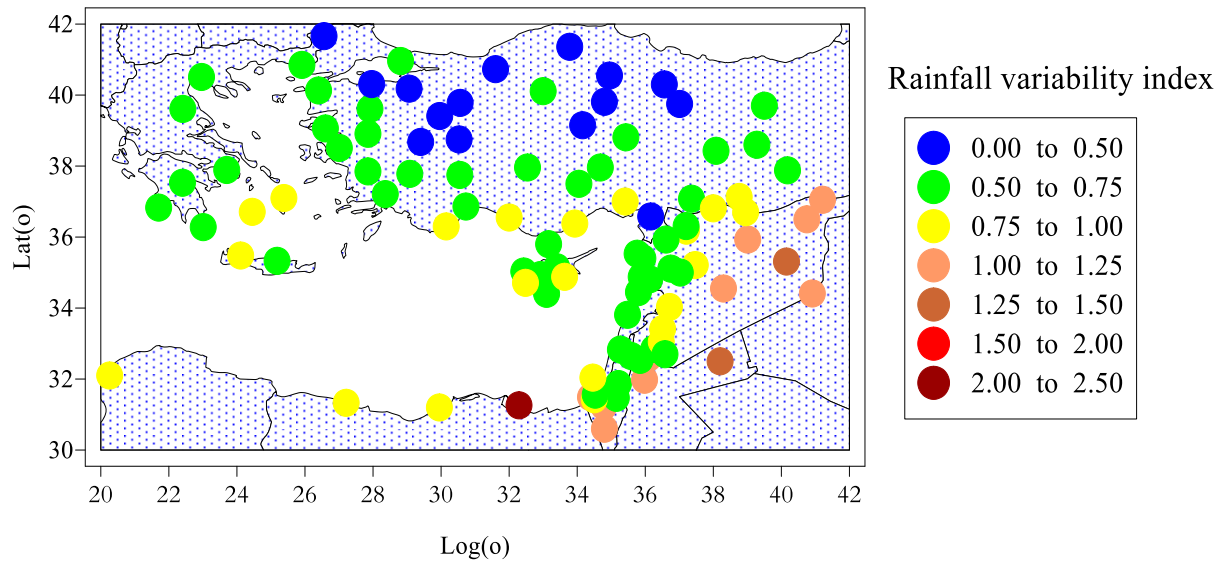


Figure 4.8 Spatial distribution of mean annual rainfall variability index during 1961-2012 over the EM.

This can be explained by the significant intermonthly variability due to the seasonal cycle of precipitation in this area which is mainly associated with cyclonic disturbances (Alpert *et al.*, 1990; Trigo, 2006; Flocas *et al.*, 2010). High values of rainfall variability index were detected in the southeastern parts of the EM and having the same behaviour of CVs values. Interannual rainfall variability expressed by the new rainfall index (Australian Bureau of Meteorology, 2010) indicated an inversely statistical significant relationship between latitude and interannual rainfall variability ($r = -0.65$) at ($p = 0.01$) (Fig 4.9). According to the variability index, the highest values were detected (0.7-0.6) in the third and first subregions (southern Turkey, Syria, Israel and Jordan), respectively, due to high interannual variability precipitation amounts in eastern and southeastern parts of the EM.

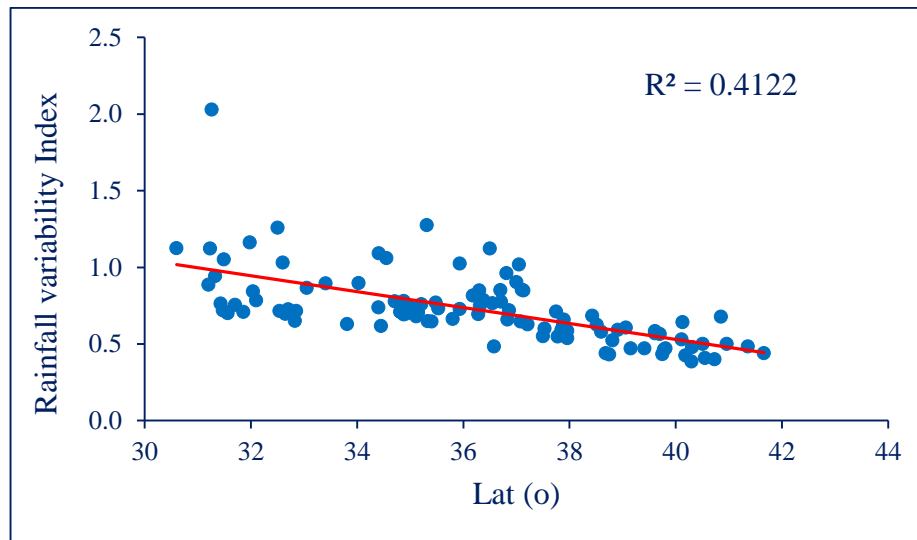


Figure 4.9 Scatterplots of latitude and annual rainfall variability index computed during 1961-2012 over the EM.

The precipitation regime presents highly irregular and variable behavior in winter and spring in both spatial and temporal and more evident in the spring. The nature of the rainy winter season and spatial variation is related to atmospheric circulation variability (Kutiel, 1991). In fact, the precipitation pattern over the EM shows a strong gradient between the northern parts and the other regions especially in the spring (Fig. 4.10). In winter, the precipitation variability index ranges between 0.63 in Bolu (Turkey) and 2.41 in Benina (Libya), whereas these values tend to be higher in spring and range between 0.61 in Yozgat (Turkey) and 3.0 in H-4 Irwaidhed (Jordan). It was observed that the Mediterranean coast of Turkey has a marked seasonal regime and a peak winter rainfall in most regions which agrees with other studies (Saris *et al.*, 2010). The seasonal precipitation regime in the southern parts of the EM present highest variability and irregularity comparing with other areas. It has been demonstrated that local or regional changes of meteorological parameters in mid-latitudes, including rainfall, are mainly controlled by the atmospheric circulation (Parker *et al.*, 1994; 1996; Türkes, 1998). Anomalies in the large-scale circulation patterns account for much of the precipitation variability in this area and the Mediterranean meridional circulation

pattern strongly affects the winter and spring precipitation variability (Barnston and Livezey 1987).

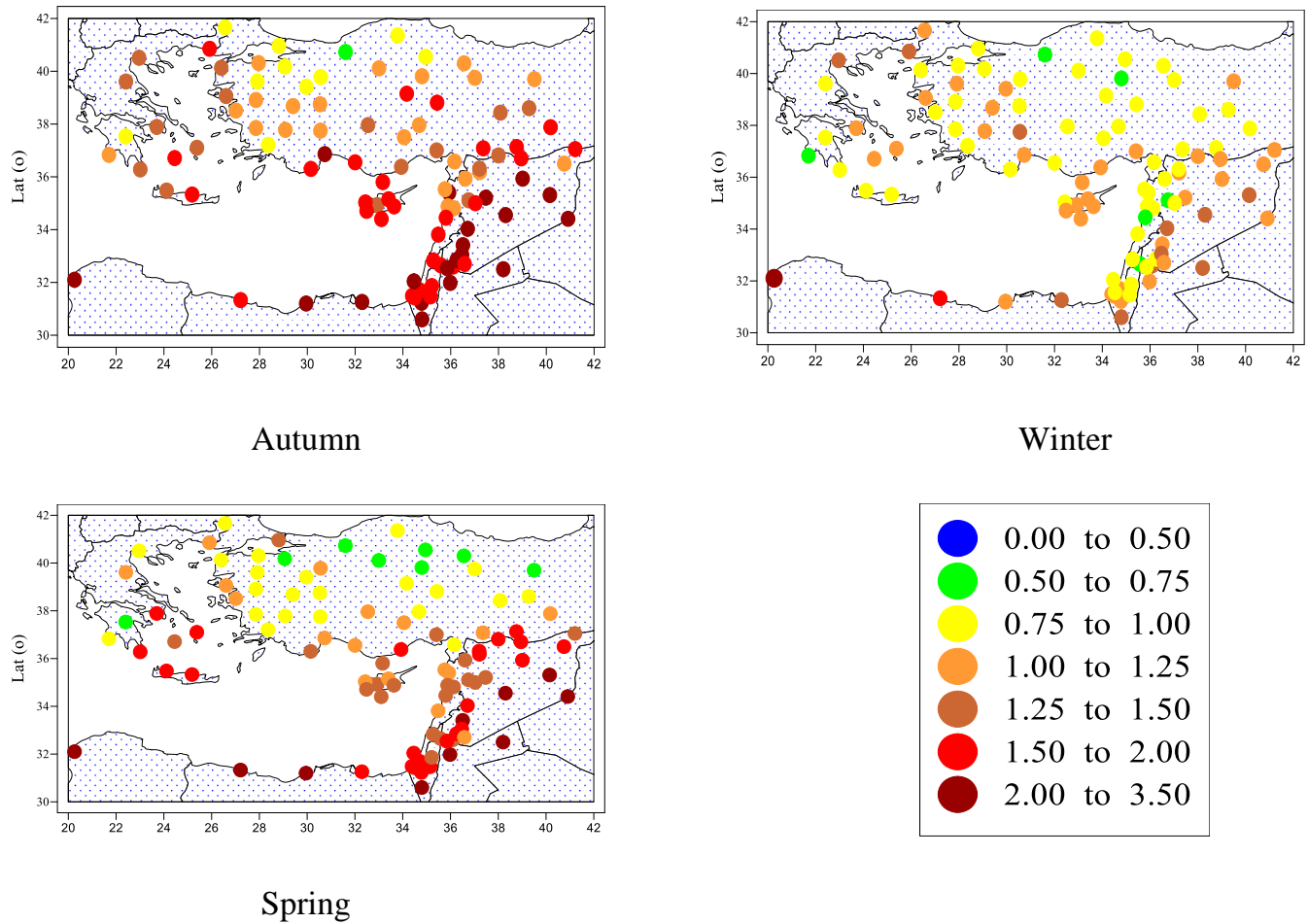


Figure 4.10 Spatial distribution of mean seasonal rainfall variability index during 1961-2012 over the EM

In summer, precipitation in some areas has an average amount ranges between (0-2 mm) such as the southern parts of the EM (Syria, Jordan, Lebanon and Israel) with high inter-annual variability in all regions. Precipitation variability index shows high values in summer exceeding 7 in Turkey and 30 in Syria and Israel. In comparison, the EM does not receive much autumn rain because the dominant atmospheric systems are located at northerly latitudes and the Mediterranean depression is relatively weak at this time, which means a particular ‘autumn type’ for the whole Mediterranean area does not occur on the monthly scale, since September and October still reflect a high rainfall variability.

High CV values and precipitation variability index were detected over the EM in whole regions and they had a negative and statistically significant correlation with latitude (Fig 4.6 and 4.11). As result, the rainfall variability index and latitude have revealed a strong correlation between them in all seasons (Fig. 4.11). At $p=0.01$, the correlation was high in spring ($r=-0.75$), in autumn and annually ($r=-0.65$), whereas it was moderate in winter ($r=-0.50$) (Fig 4.11).

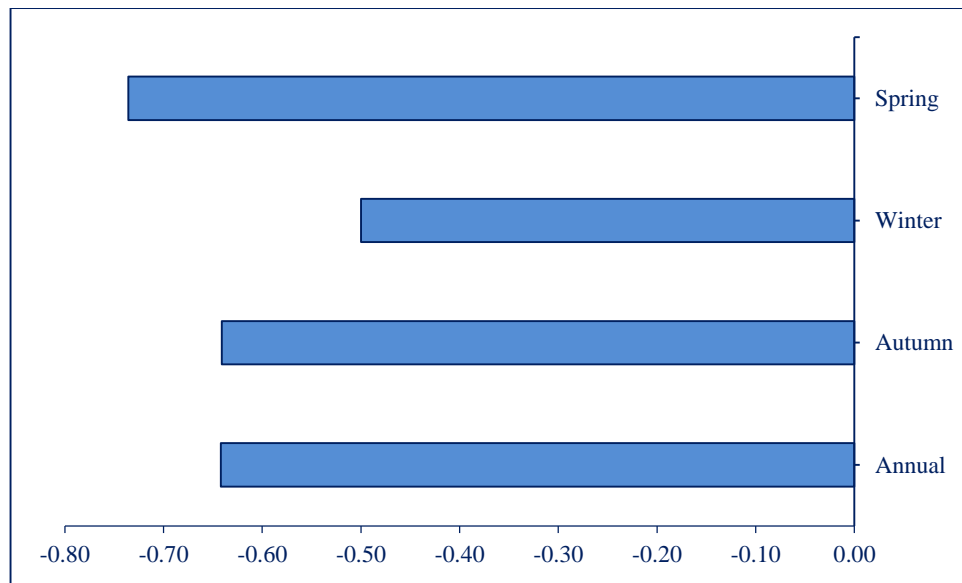


Figure 4.11 The annual and multiseasonal correlation coefficients between rainfall variability index and latitude

The EM rainfall anomalies are associated with large-scale, high-amplitude North Atlantic climate variability. Cyprus lows, a mid-latitude disturbances that tend to develop in this cyclogenetic area when upper troughs or cut-off lows penetrate the EM, are of major importance for rainfall over the EM. Sarroni *et al* (2010) and Ziv *et al* (2013) have showed that the interannual variations in the number of the Cyprus lows explain 50% of the variance in the interannual rainfall variation in EM especially in the southern part of the eastern coast of the Mediterranean, and Cyprus Lows contribute about 80% of the rainfall in Israel between November and March. This spatial variability of precipitation regimes has profound effects on water resources, aridity and desertification conditions (Xoplaki *et al.*, 2004).

4.1.4 Characteristics of the identified subregions

In order to verify that the identified sub-regions are really characterized by different seasonal precipitation regimes, we have considered for each season the distribution of the mean annual and seasonal precipitation at five subregions. (Table 4.3).

The Anderson-Darling (A-D) goodness of fit tests has been applied to check the null hypothesis that the distributions are the same (Table 4.3). It is the test to examine whether the sample data is drawn from a specific probability distribution.

Table 4.3 P values calculated by Anderson-Darling (A-D) test applied to the distributions of the annual and seasonal precipitation at the five regions.

	EOF1	EOF2	EOF3	EOF4	EOF5
Autumn	<0.05	<0.05	0.28	0.14	0.29
Winter	0.74	<0.05	0.88	0.68	0.06
Spring	0.07	0.39	0.22	0.52	0.49
Annual rainfall	0.07	0.85	0.45	0.55	0.62

According to Table 4.3, it seems that in autumn three subregions are characterized by independent precipitation regimes. The first (south Turkey, Cyprus, inland Syria and Egypt) and second (Lebanon, Israel and Jordan) subregions we cannot reject the hypothesis that the distributions are the same. The autumnal precipitation regime in both areas is highly variable and concentrated, and the CV values are exceeding 35% (46.6%, 54.9%) in PC1 and PC2, respectively. The same occurs in winter for PC2 due to the big irregularity in the rainfall seasonal patterns in Israel and long term variation in winter rainfall over Israel, which relates to the NAO behavior and to the GCMs greenhouse warming prediction (Zangvil *et al.*, 2003). In fact there are large variations from year to year in the seasonal rainfall, and particularly in its monthly distribution, so that it is difficult to find a season in which each of its months has even approximately

received its average amount. The distributions of spring and annual precipitation in all subregions can be considered different and independent.

4.2 Changes in seasonality precipitation.

4. 2.1 Seasonality and individual seasonality indices of rainfall regimes

There is insufficient information on how precipitation distribution has changed from one period to another. From the definition of seasonality index, it is clear that the lower is the value of seasonality index, the better is the distribution of monthly rainfall among the months of a year. From the \overline{SI} values of the period 1961-2012, the EM classified the region into five zones ranging from a rainfall regime which is “equable with a definite wetter season” (\overline{SI} ranges from 0.20 to 0.39) to the “most rain occurs in three months or less” (\overline{SI} ranges from 1.00 to 1.19) (Fig 4.12).

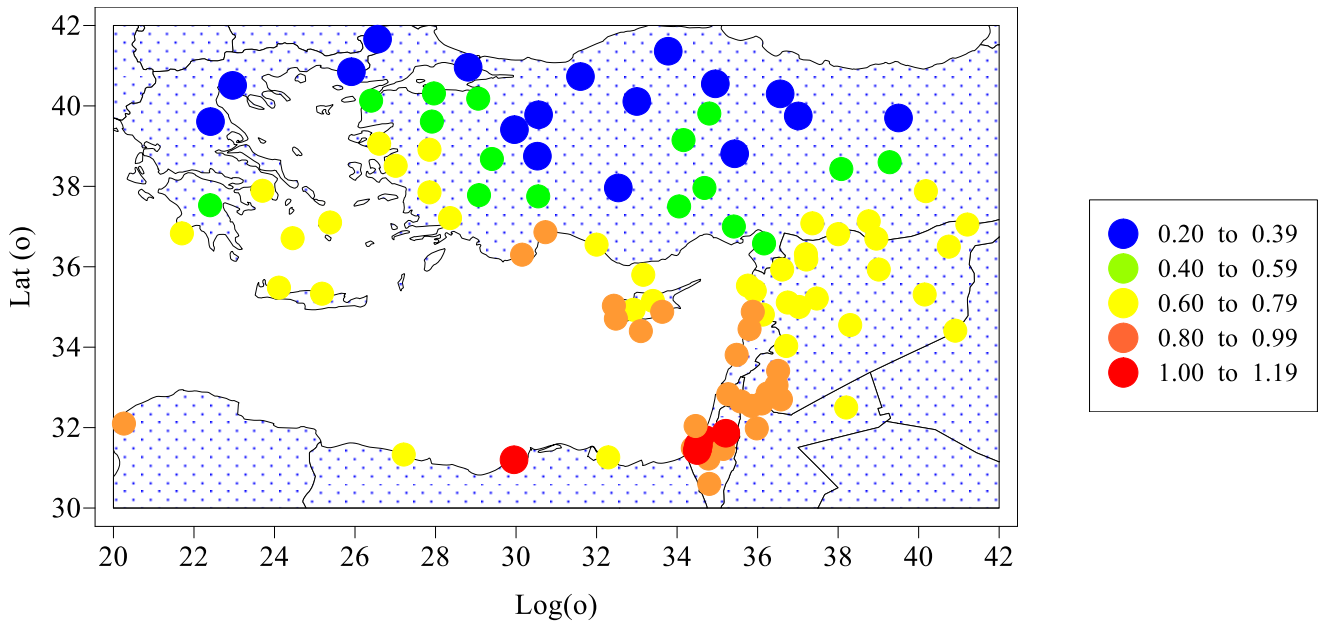


Figure 4.12 Rainfall Seasonality Index \overline{SI} in the whole stations over 1961-2012.

From \overline{SI} values of the period 1961-2012, it is observed that \overline{SI} varies between 0.22 and 1.02 (Fig 4.13), and the stations have seasonality index more than 1 and that the distribution of monthly rainfall in these areas is mostly attributed to 1 or 2 months do not exceed 5% of the regions studied and locate in Egypt (Alexandria) and in four other stations in Israel (Beer Tuvia, Jerusalem, Kfar

Menachem and Lod Airport), which has the highest values of \overline{SI} range between 0.83 and 1.02. The results show that the rainfall distribution in 23.3% of total stations is markedly seasonal and is distributed in 3-4 month period with a long dry season. 40% of stations have \overline{SI} values between 0.60 and 0.79, reflecting the rainfall in these stations is purely seasonal with rainfall occurring evenly in months. Zones have rather seasonal with a short dry season form 15.5% of the total area. The results indicate that all the stations fit the classification “Equable with a definite wetter season” locate at high latitudes and form 16.5% of the total number of stations.

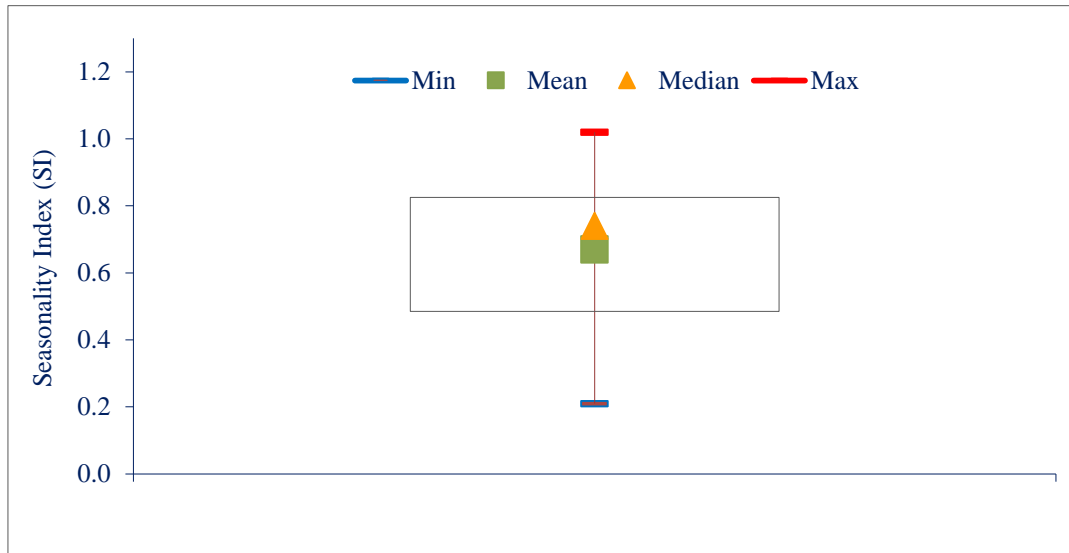


Figure 4.13 Box-whisker diagram of Seasonality Index (SI) over 1961-2012.

The \overline{SI}_i (sum of the absolute deviation of monthly rainfall from the mean monthly rainfall of year i divided by the annual rainfall (R_i) of year i) values are significantly higher than \overline{SI} ones (sum of the absolute deviation of mean monthly rainfall from the overall monthly mean divided by the mean annual rainfall) (Fig 4.14). This is in agreement with Walsh and Lawler (1981), whose results are based on similar studies in various regions of the world.

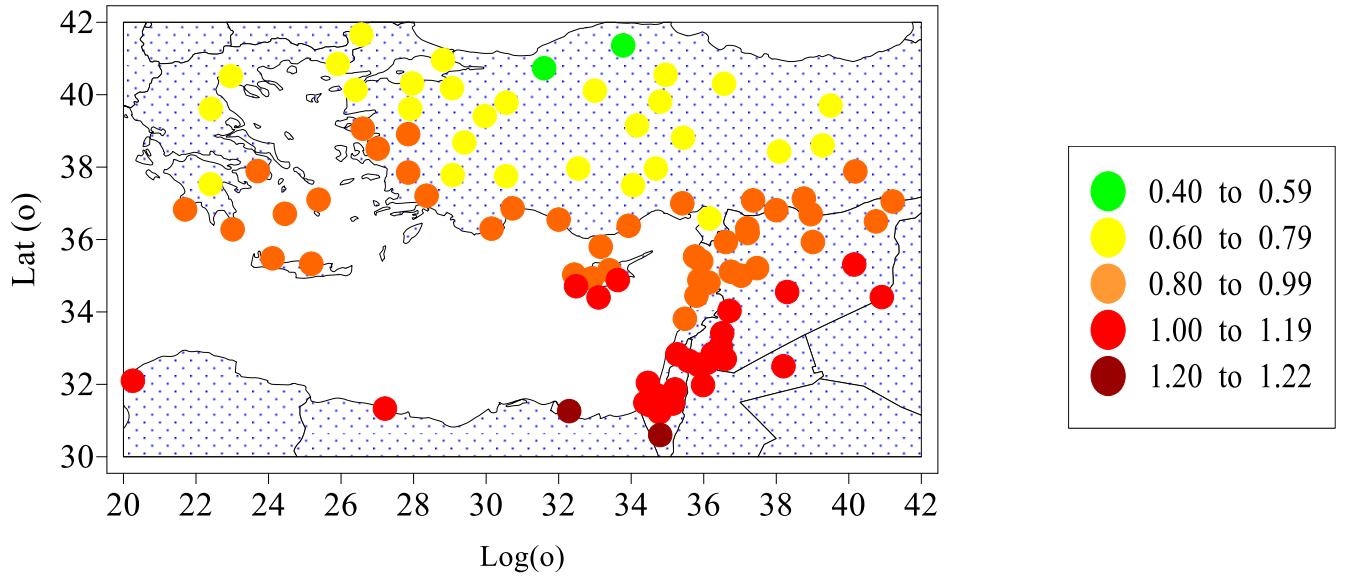


Figure 4.14 Mean \overline{SI}_t values distribution in whole stations over 1961-2012.

Fig. 4.14 shows that the classifications start from the third zone which fits “Rather seasonal with a short dry season” and indicates an existence of an additional one in which the rainfall occurs in one or two months. These results reflect a high degree of temporal variability in monthly rainfall through each year, which in turns gives a better understanding of how the rainfall in a particular district is varying.

Analysis of \overline{SI} gives an idea about the rainfall distribution among the months and separate the states in different rainfall regimes. In coastal areas, \overline{SI} values are greater than continental ones and range between 0.85 and 1 indicating seasonal regime with a long dry season and the extreme rainfall regime where almost all the rainfall occurs in one or two months. The results also allowed the definition of a statistically significant negative linear correlation ($r = -0.85$) between the \overline{SI} values and geographical latitude Φ (Fig.4.15). This result agrees with other previous studies on rainfall SI in Greece (Livada and Asimakopoulos, 2005).

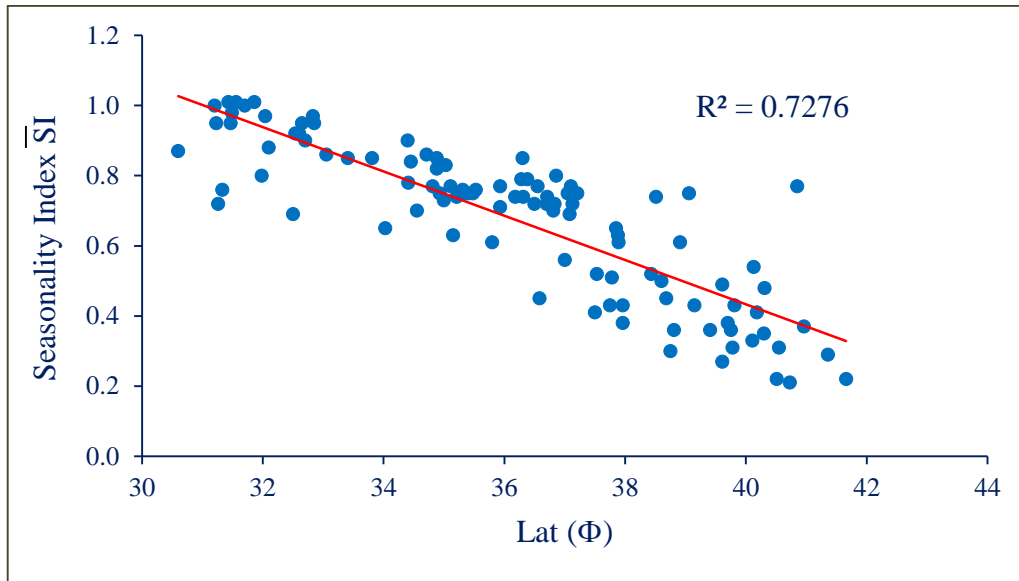


Figure 4.15 Scatter diagram and linear regression line of seasonality index \overline{SI} and latitude (ϕ)

$\overline{SI} / \overline{SI}_t$ “Replicability Index”

Walsh and Lawler (1981) used the ratio $\overline{SI} / \overline{SI}_t$ as a ‘replicability index’ (Bello, 1998) to indicate whether or not the wettest period occurs over a small range of months, or whether it may occur in any month during the year. Higher values of the ‘replicability index’ indicate that the wettest month of the year generally occurs in only the same few months every year, whereas the lower values refer that the wettest month of the year tends to be more evenly spread amongst a large number of different months.

Results from ‘replicability index’ illustrate a high degree of variability in the rainfall distribution regimes (Fig 4.16). The values range from 0.35 to 0.90. When this ratio is high, this means that the month of maximum rainfall occurs over a small spread of months and the range of \overline{SI}_t values is also small. This leads to a high repeatability of the mean rainfall regime and vice versa.

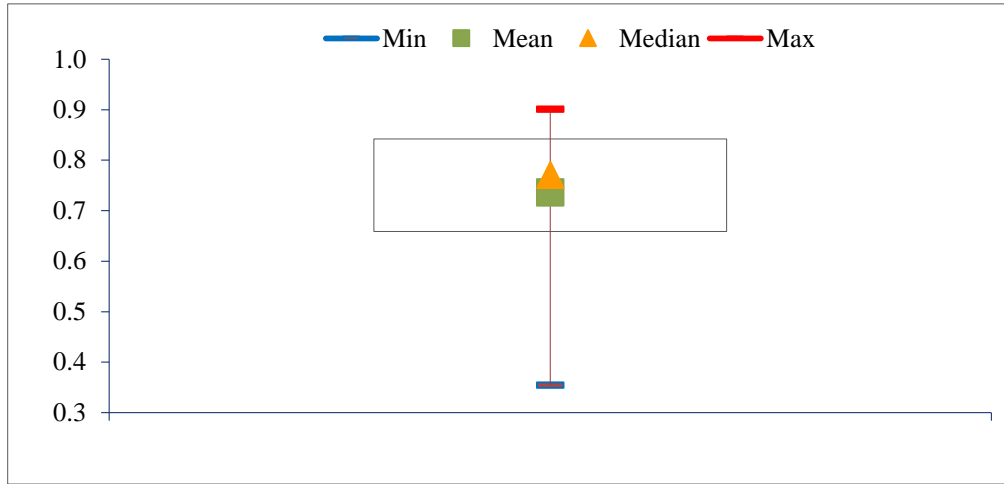


Figure 4.16 Box-whisker diagram of the ratio $\overline{SI} / \overline{SI}_t$ in all districts over 1961-2012.

The annual variation of rainfall for four stations was presented in Fig.4.17 to illustrate these points for three stations in four subregions with high and low $\overline{SI} / \overline{SI}_t$ values.

In Methoni and Tel Aviv, two coastal stations in Greece and Israel with an elevation of 55 and 32 m, respectively, the maximum rainfall occurs in a short time period (October to February) and the replicability index is estimated to be 0.85 and 0.87, respectively. In contrast, the replicability index ratio in Bolu and Eskisehir has the values 0.40 and 0.49, respectively, which reflects a wide variety of rainfall distribution over the months and shows a lack of reliability in rainfall and also in the appearance and amount of rainfall. Both of these stations are continental situated in the western and northwestern parts of Turkey with an elevation of 743 m and 785 m, respectively.

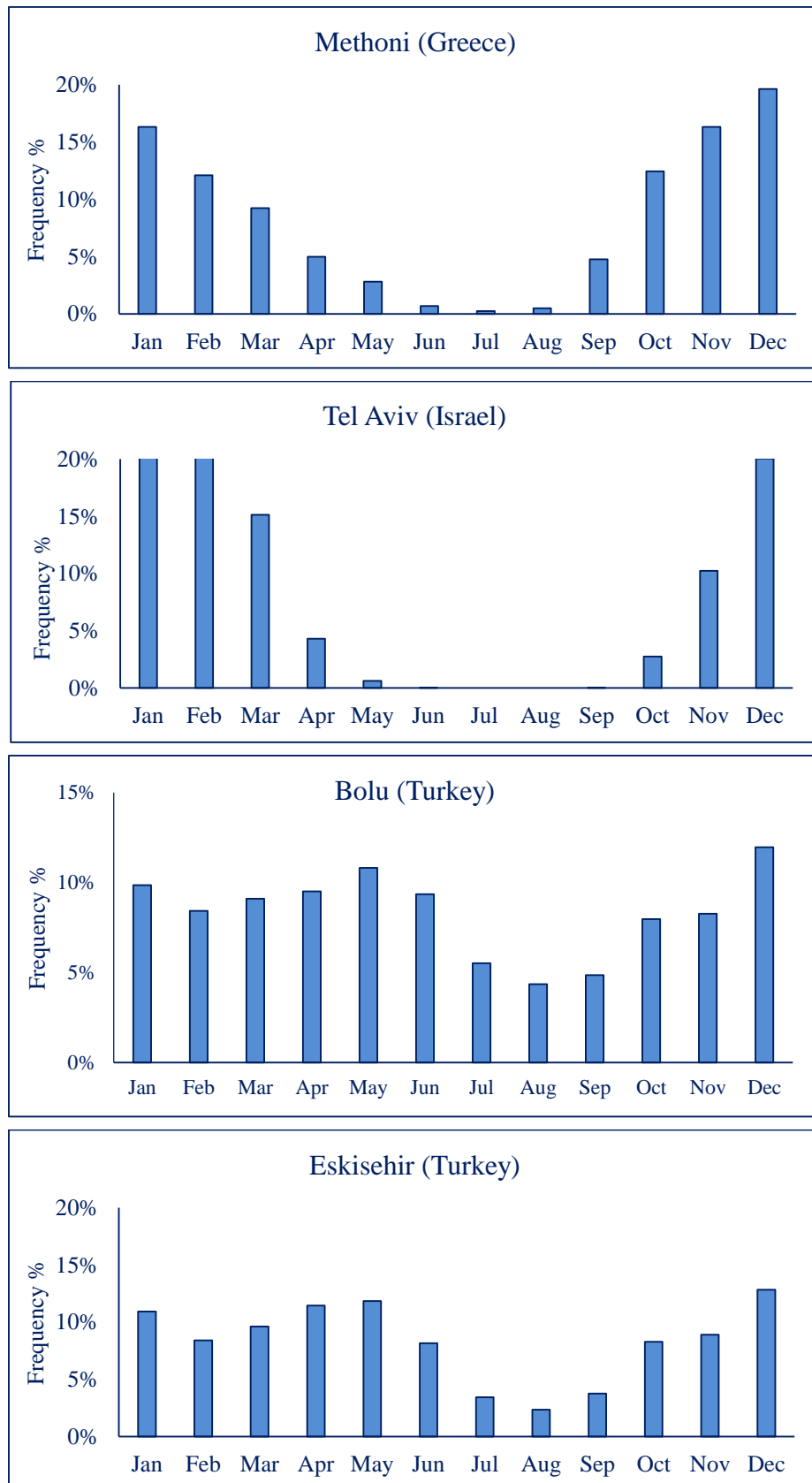


Figure 4.17 Histogram plots for frequency distribution of monthly rainfall amounts for selected stations of the subdivided regions.

Considering that the \overline{SI}_t gives more information about rainfall seasonality than the \overline{SI} index, the relationship between them has been evaluated. A statistically significant correlation ($r = 0.93$) between them was detected (Fig 4.18.).

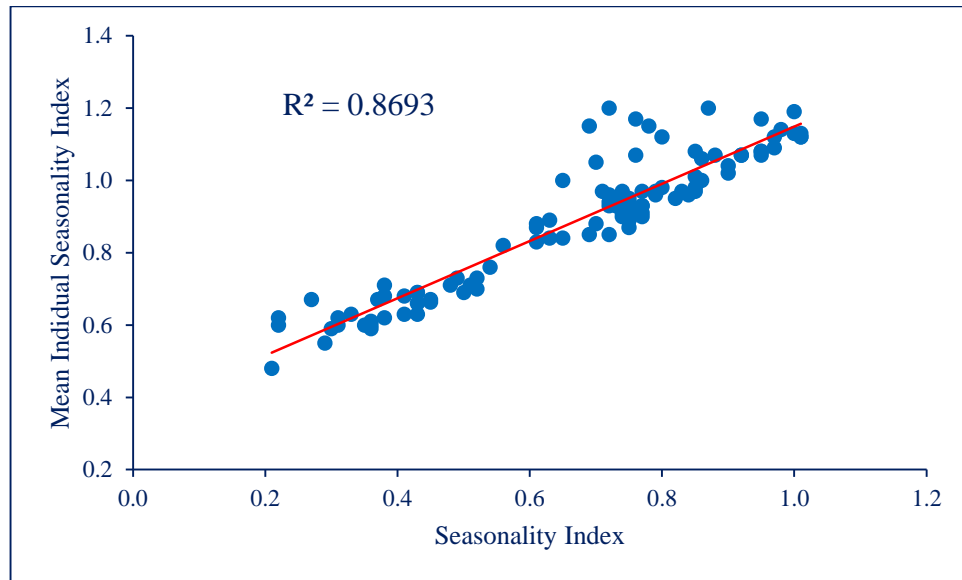


Figure 4.18 Scatter diagram and linear regression line of seasonality index \overline{SI} and mean individual seasonality index \overline{SI}_t

4. 2.2 Spatio and temporal changes in seasonality index \overline{SI}

Trend analysis has been done on the \overline{SI} for each series over (1961-2012). Fig 4.19 depicts the \overline{SI} trends for all stations over the EM. It is seen that the 56.3 % of total stations has an increasing trend and \overline{SI} index is increasing significantly at 95% confidence level over Afyon (Turkey), Thessaloniki Airport (Greece), Beer Tuvia, Jerusalem, Lod Airport, Tel Aviv and Gazit (Israel), Abu Kamal (Syria) and H-4 Irwaidhed (Jordan). The increased trend in \overline{SI} values reveals that the rainfall distribution in these stations has become asymmetric accompanied by changes in rainfall characteristics such as intensity and duration.

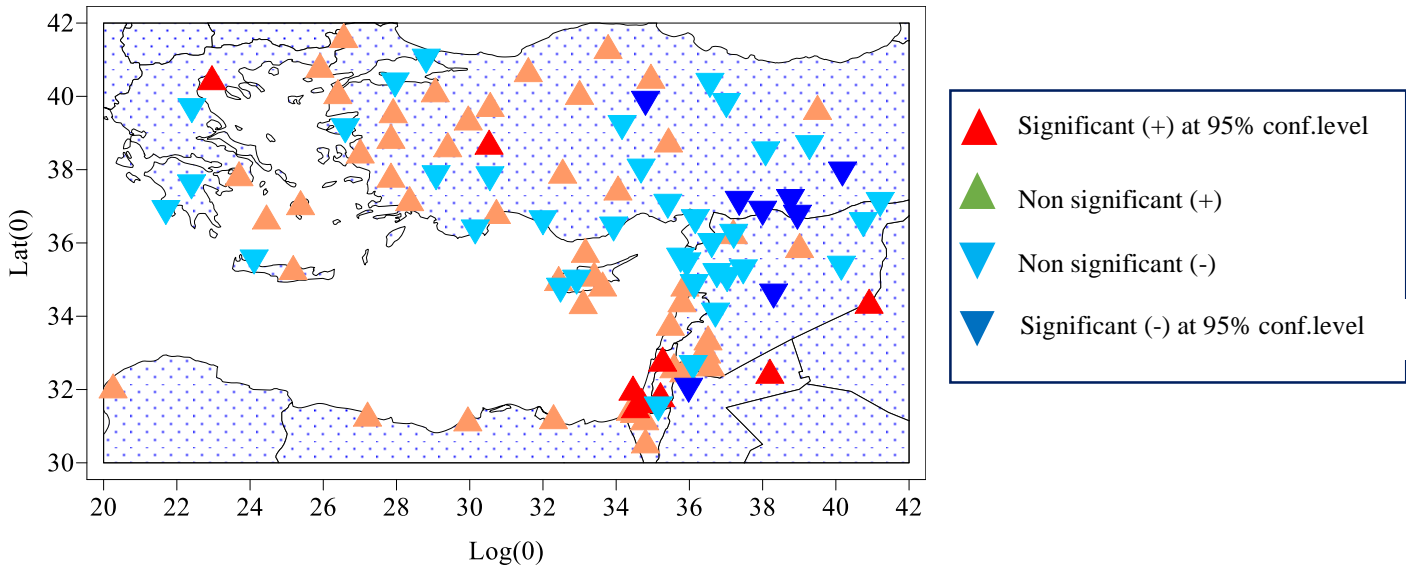


Figure 4.19 Observed trend in \overline{SI} values during 1961-2012 over the EM

A tendency towards increasing seasonality in Western Mediterranean is also indicated for much of Catalonia (northeastern Iberia) and in the most regions of Andalusia (southern Iberia) and seasonality index increased at a rate greater than 0.003 per year (Summer *et al.*, 2011).

\overline{SI} has showed a decreasing trend in other regions which is statistically significant in 8 weather stations at 95% confidence level: Diarbakir, Gazianteb, Yzgat and Urfa (Turkey), Palmyra, Jarablous and TL Abiad (Syria) and Amman Airport (Jordan).

4.2.3 Detection of regime shifts by STARS

Examining regime changes, in combination with precipitation seasonality trends gave a more complete understanding of how this seasonality is changing and confirmed the timing of major shifts.

The regime shift analysis using the STARS method reveals evident break points in mean individual \overline{SI}_t . STARS results determined by Cut-OFF length for proposed regimes (L=26) and the Huber Weight Parameters (H=1) indicated that abrupt change, mostly occurred in all weather stations in the late of 1970s to the end of 2012 (Fig 4.20). The sum of Regime Shift Index (RSI) calculated for each of the 103 single stations resulted in highest cumulative values in whole 1990s and peaked in the years 1989, 1995 and 2005. The highest RSI value for the \overline{SI}_t was obtained for the year 1998 in Israel (Gazit) and the second strongest shift occurred in 1995 in Jordan (H-4 Irwaished) (Fig 4.20).

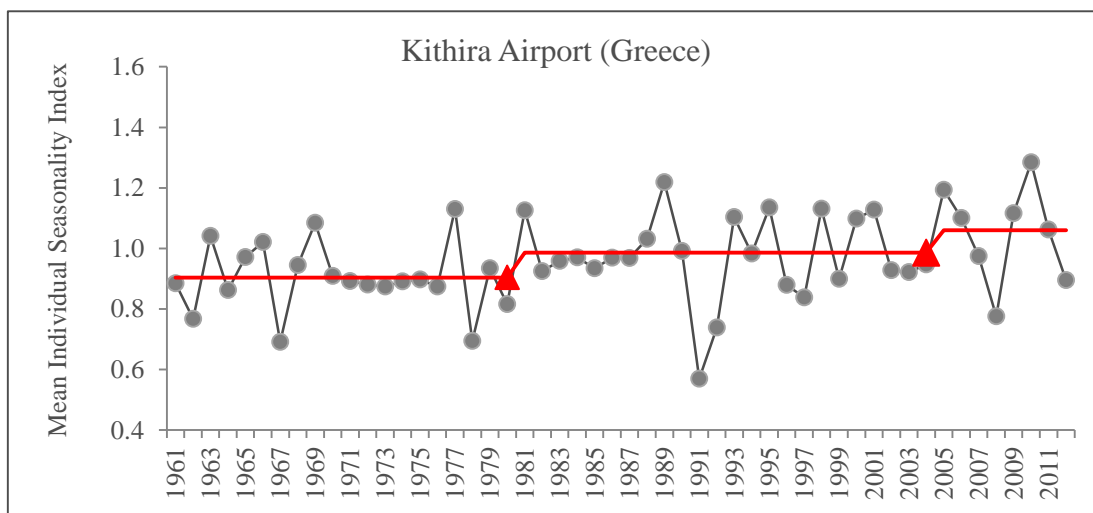
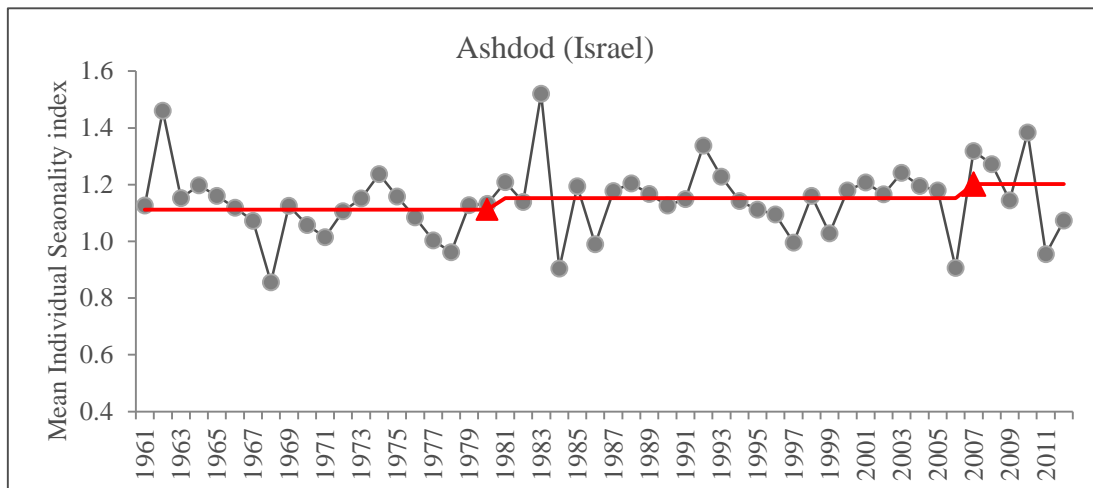
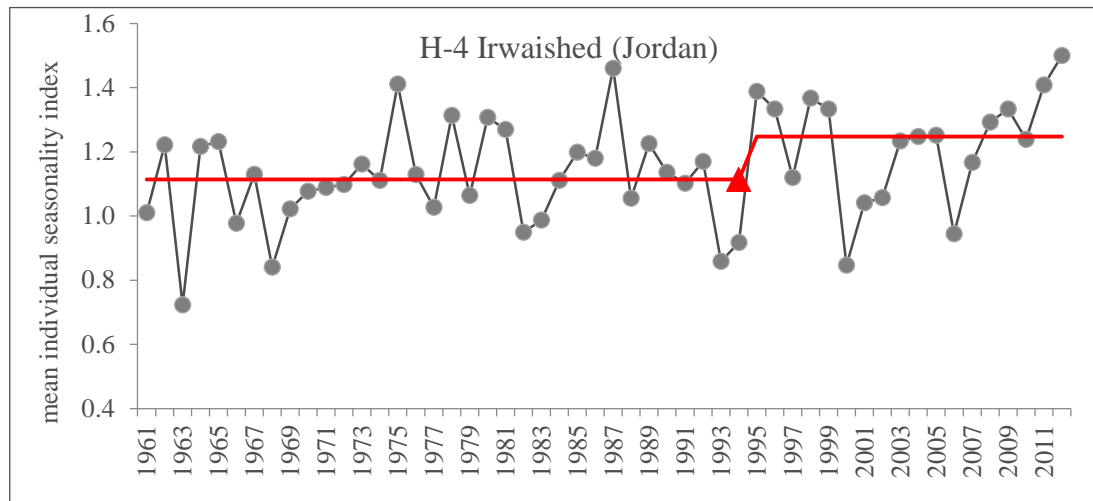


Figure 4.20 Regime shifts in Mean Individual Seasonality Index from selected stations over 1961 -2012 ($\alpha=0.05$; cut-off length= 26; Huber parameter = 1).

STARS analyses indicated step changes occurred during the period 1979-2004 in all stations from 2005 to 2012. It was also observed that not all stations show the same synchronous regime shifts due to high rate of interannual variability for each station and among all regions. The number of transitions per year ranged from 1 to 11, with high increased tendency after 1989 (Fig 4.21). Over the entire record, the mean number of transitions was “2.4” with a standard deviation (2.8) and detecting a high and the evident increase at last second part (from 1.5 to 4.1). Slight differences in the number of regimes between dry and wet years were found; with wet years tending to have slightly fewer regimes with a longer length than dry ones as shown in the figure above. This means that, in general, regimes are similar in length and at the first part and longer compared with the second part which tended to be shorter from the beginning of 1990s.

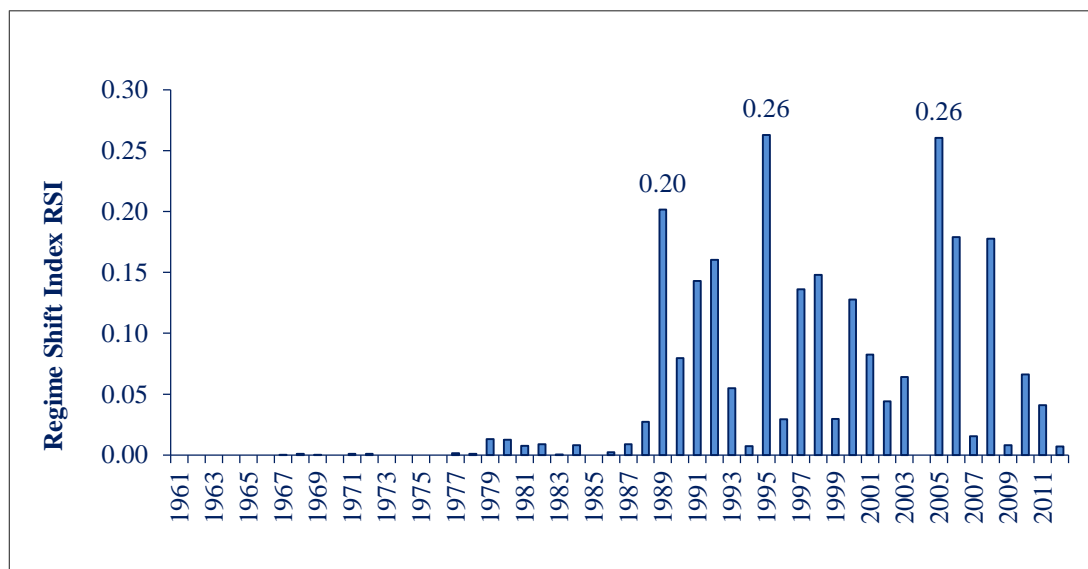


Figure 4.21 Summary of all regime shift index (RSIs) in mean estimated by STARS for 103 stations during 1961–2012 ($\alpha=0.05$; cut-off length= 26; Huber parameter = 1).

All these results indicate an increasing of interannual variability of seasonality over last several decades implying increasing uncertainty in the intensity, arrival and duration of seasonal rainfall in this period. We show that such increases in rainfall variability were accompanied by shifts in its seasonal magnitude, timing and duration, the matter which considered so important and

relevant to several ecological and social processes. The increasing tendency in precipitation concentration and seasonality is considered as an important factor in determining vegetation dynamics. Moreover, rainfall seasonality is directly related to disturbances like forest fires, which have a critical effect on soil erosion. Thus, the frequency and extent of forest fires in Mediterranean areas are directly related to summer water stress (Green *et al.*, 2007; Guan *et al.*, 2014). Thus, quantifying potential regimes, their shifts, and how they change through time will allow for a further understanding of the precipitation regime, which in turn will allow for observations of trends in its seasonality and variability in a changing climate.

4.3.3 Precipitation irregularity over the EM

The temporal irregularity index (S_1) was calculated for each station. The results showed a significant relationship with the entropy values (discussed later). As shown in Fig 4.22, the spatial distribution of the S_1 on an annual scale shows a clear growth of the irregularity from the north to the south which has an intensive interannual variability. The same results obtained in a previous study in the other Mediterranean region in Catalonia (north-eastern part of Spain) (Lana *et al.*, 2009).

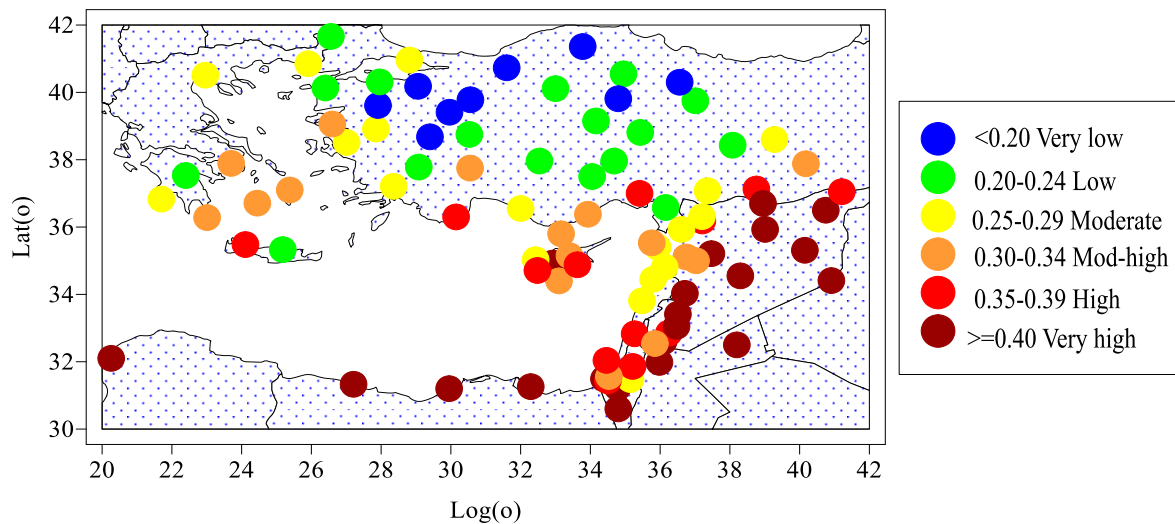


Figure 4.22 Spatial distribution of temporal irregularity index S_1 over the EM during 1961-2012.

The results showed high variation among the regions, ranged from 0.16 in Tokat (Turkey) to 0.74 in Port Saied (Egypt). Highest temporal irregularities are detected in the regions with high rainfall variability. The results point to a

correlation between variability of annual rainfall and its temporal irregularity. In West Mediterranean the coefficient of correlation between CV and S_1 for 35 annual precipitation series in peninsular Spain was +0.91 (p-value<0.000) (Martin-Vide, 2011). This relationship becomes stronger and more significant in the regions that located at the lower latitudes of the study area (30–33°N) and originally characterised by high rainfall variability (Fig 4.23, a). Thus, highly temporal irregular distribution and a high interannual variability characterize the mean annual rainfall in most regions of the EM. The results have also demonstrated an inverse and significant correlation between both annual and monthly rainfall entropy and their irregularities (Fig 4.23, b and c).

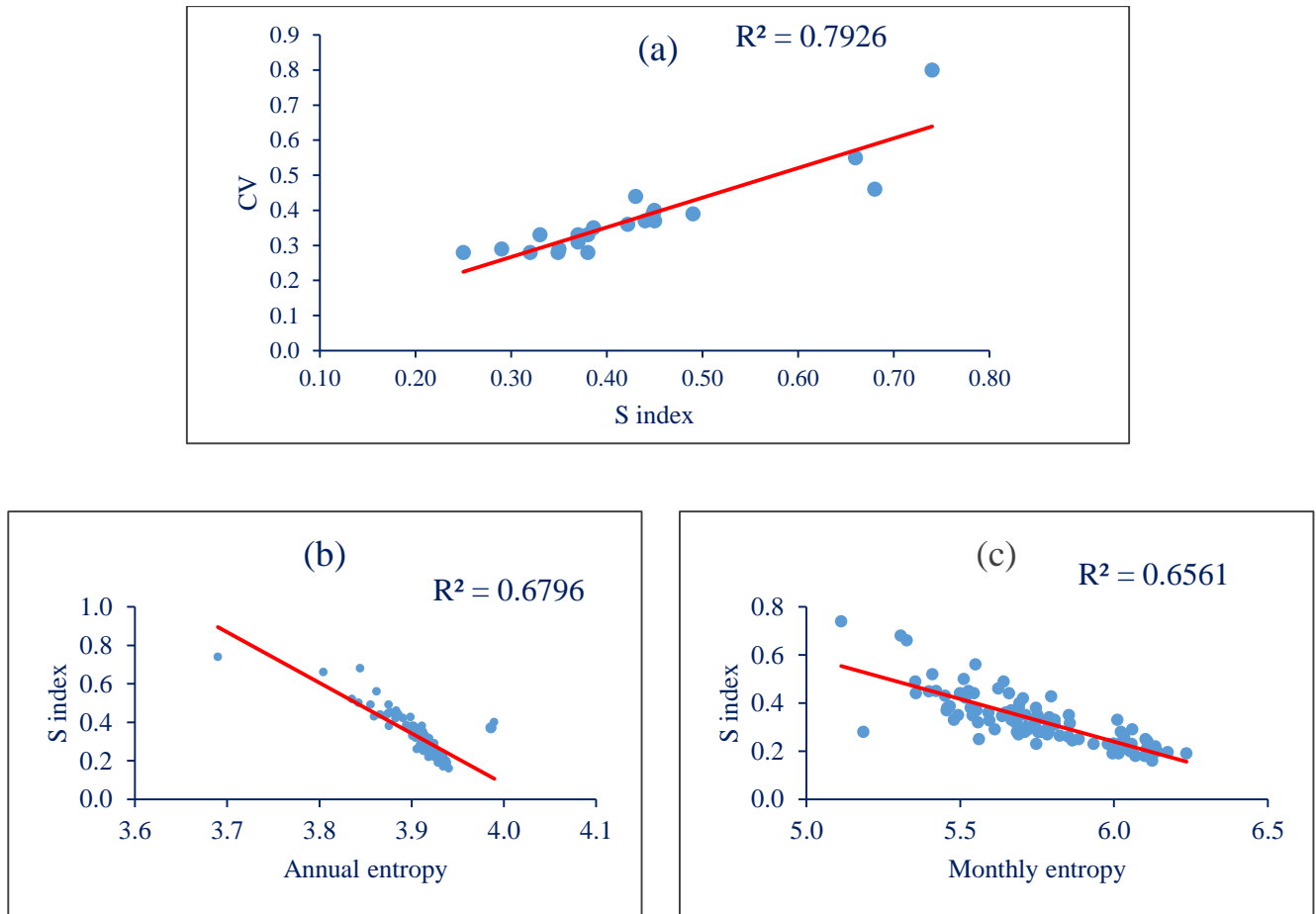


Figure 4.23 Scatter diagrams and linear regressions of annual rainfall S_1 and CV (a), annual rainfall S_1 and entropy (b) and annual rainfall S_1 and monthly rainfall entropy (c) over 1961-2012.

4.4 Spatial and temporal variability of daily concentration index (CI) over the EM

4.4.1 Spatial distribution of average precipitation CI

Precipitation CI values were estimated for 70 stations throughout the EM from 1961 to 2012. Table 4.4 shows the values of regression coefficients, a and b , which were estimated by the least squares method, CI values that calculated using the Lorenz Curve approach, the rainfall percentage contributed 25% of the rainy days and Z values which obtained through the Mann-Kendall test.

Study of daily CI index in the Mediterranean showed that 25% of the rainiest days represent at least 75% of the annual precipitation, and the highest values of CI (>0.61) which reveal high daily precipitation concentration were detected in the eastern part of the Iberian Peninsula (from Barcelona to Almeria) (Martin-Vide, 2004; Benhamrouche and Martin-Vide, 2011, 2012). CI values ranged between 0.50 in Sivas (Turkey) and 0.66 in Hellinikon Airport (Greece) with high variability interannual values. The highest values of CI were recorded at southern parts of the EM which also corresponded to the highest S_1 values with an average of (0.61). This threshold (0.61) defined by Martin-Vide (2004) to separate most Mediterranean parts of the Iberian Peninsula according to CI. This 0.61 threshold is clearly surpassed in most of these south EM areas which are featured by a lack of precipitation, especially in summer, which does not exceed (2 mm) as an average. In addition to measuring the overall precipitation distribution using Gini statistics or CI, analysis of Lorenz Curves may also contribute to an understanding of the precipitation distributions. Fig 4.24 presents calculated and observed cumulative precipitation percentages for some representative stations: Kastamonu and Finike (Turkey), Jerusalem and Tel Aviv (Israel), Limassol (Cyprus), Lattakia (Syria), Mytilene and Hellinikon Airports (Greece). The most intense areas of rainfall yielded a high precipitation CI values. In these regions, irregularity in daily rainfall amounts is mainly due to a high proportion of low rainfall amounts in which more than 70% of the total rain falls on 25% of the rainy days. It is clear that the extreme rainfall values can be found in Hellinikon Airport (Greece) with

75.7%, Har Kanaan (Israel) with 74.4%, Athalassa (Cyprus) with 73.4% and H-4 Irwaidhed (Jordan) with 73.1%.

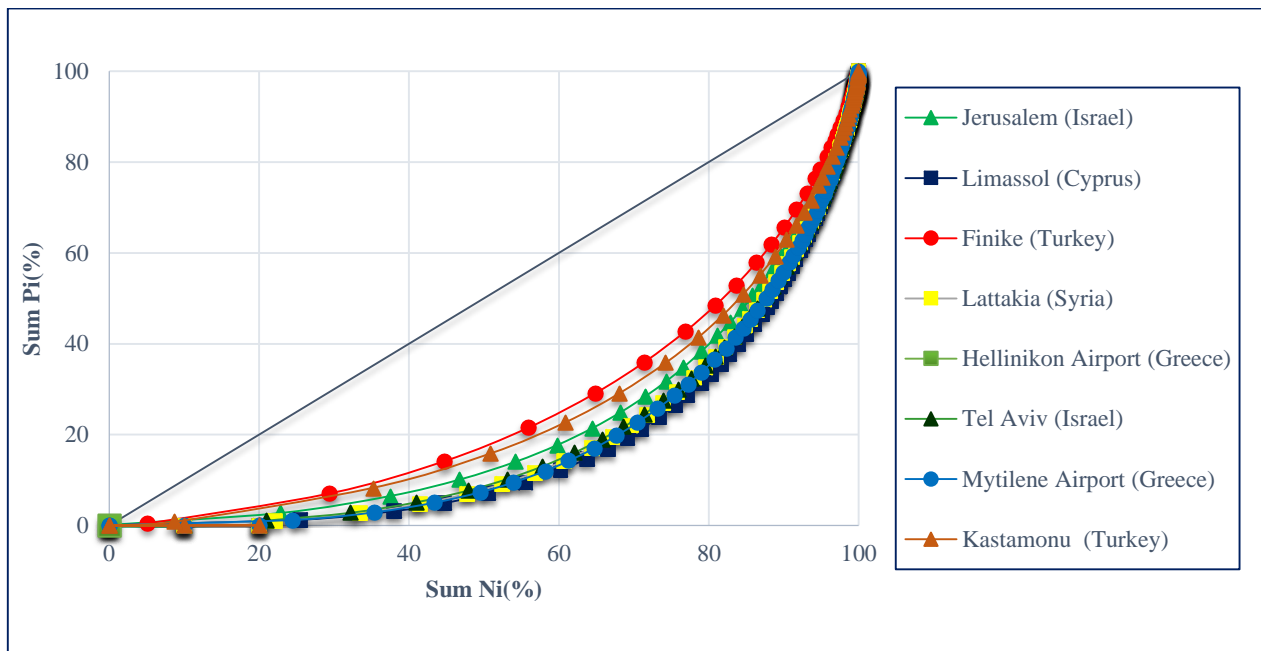


Figure 4.24 Concentration or Lorenz curves of some meteorological stations over the EM.

The maximum daily concentration values are located primarily in the southern parts of the EM across Syria, Lebanon, Jordan and Israel, and secondary maximum annual values are found in Greece, whereas the lowest values are detected in the northern parts of the EM in Turkey (Fig 4.25). The precipitation CI reflects different climate types and precipitation regimes, from lower values in the northern parts of the EM, to more irregular values (highly concentrated rainfall) under across the Mediterranean Sea in the southern and northwestern parts of the EM.

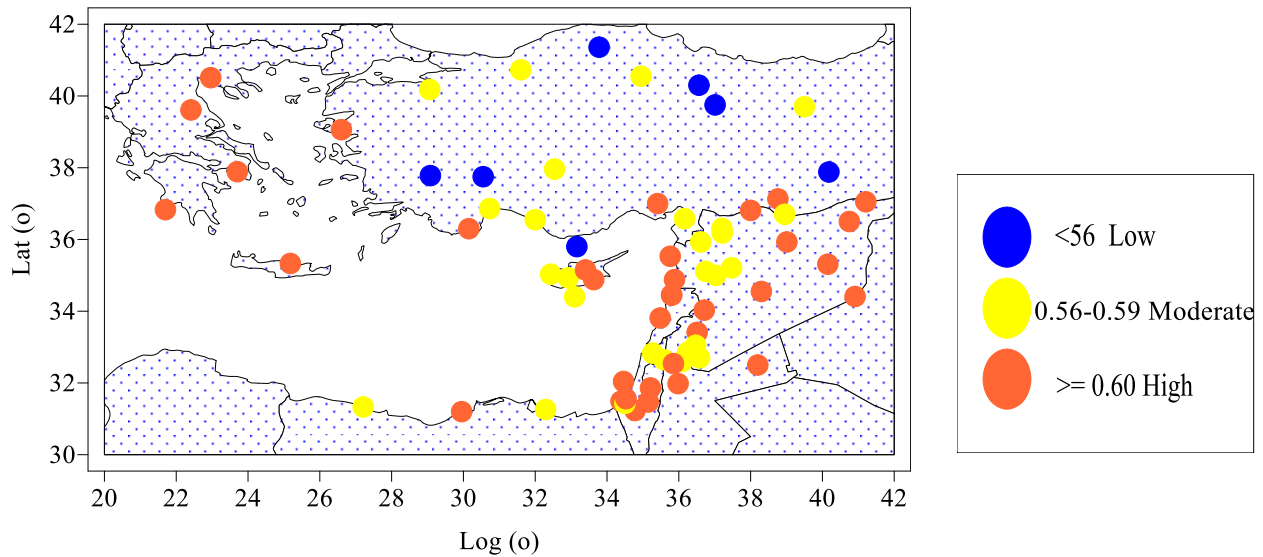


Figure 4.25 Spatial distribution of annual concentration index (CI) in 70 daily rainfall stations over 1961-2012.

Table 4.4 Values for constant a and b of exponential curves, the daily concentration index (CI), Z statistics and the rainfall percentage contributed by 25% of rainiest days for 70 stations across the EM (1960–2010).

Station	a	b	CI	Z	Rainfall %
Abu kamal (Syria)	0.024	0.036	0.63	-2.25*	72.7
Alanya (Turkey)	0.037	0.034	0.63	1.85*	73.1
Adana Incirlik (Turkey)	0.036	0.035	0.62	1.93*	73.1
Aleppo (Syria)	0.035	0.033	0.56	-2.11*	70.6
Alexandria (Egypt)	0.045	0.030	0.59	1.90*	71.2
Amiandos (Cyprus)	0.036	0.033	0.60	7.80***	70.9
Amman Airport (Jordan)	0.035	0.033	0.63	0.80	73.5
Antalya (Turkey)	0.039	0.034	0.56	1.45	68.9
Ashdod (Israel)	0.034	0.033	0.60	4.22***	70.1
Ashdot Ya'akov (Israel)	0.039	0.032	0.58	-3.54***	69.4
Athalassa (Cyprus)	0.037	0.031	0.62	0.08	73.4
Athria (Syria)	0.038	0.032	0.59	-2.08*	65.9
Beer Sheva (Israel)	0.027	0.035	0.62	2.16*	71.0
Beirut Airport (Lebanon)	0.023	0.036	0.61	-1.01	71.7
Benina (Libya)	0.038	0.034	0.67	-1.60*	70.1

Bolu (Turkey)	0.082	0.026	0.57	2.55*	66.9
Bursa (Turkey)	0.041	0.037	0.56	1.99*	66.7
Corum (Turkey)	0.091	0.018	0.56	2.25*	66.1
Damascus-Airport (Syria)	0.034	0.032	0.60	-0.67	71.7
Daraa (Syria)	0.037	0.032	0.59	-1.68*	70.0
Deir Ezzour (Syria)	0.031	0.034	0.61	0.54	68.8
Denizil (Turkey)	0.068	0.025	0.55	0.40	65.7
Diyarbakir (Turkey)	0.039	0.035	0.53	1.24*	63.2
Erzincan (Turkey)	0.094	0.021	0.56	2.42*	66.3
Edleb (Syria)	0.033	0.032	0.59	-1.97*	65.6
Finike (Turkey)	0.037	0.032	0.60	1.39	70.4
Gazit (Israel)	0.039	0.032	0.58	0.55	68.4
H-4 Irwaidhed (Jordan)	0.036	0.035	0.62	2.11*	73.1
Hama (Syria)	0.035	0.033	0.59	-0.90	69.9
Har Kanaan (Israel)	0.024	0.037	0.62	2.68***	74.4
Hasakah (Syria)	0.031	0.034	0.61	0.11	72.4
Hellinikon Airport (Greece)	0.016	0.040	0.66	1.44	75.7
Herakilon Airport (Greece)	0.025	0.036	0.62	1.57	72.8
Irbid (Jordan)	0.036	0.033	0.61	-1.30	72.8
Iskandarun (Turkey)	0.039	0.036	0.58	1.34*	67.9
Isparta (Turkey)	0.068	0.026	0.54	0.42	66.1
Izraa (Syria)	0.036	0.032	0.59	-1.69*	70.5
Jarablous (Syria)	0.034	0.033	0.60	0.10	70.6
Jerusalem (Israel)	0.018	0.040	0.64	3.94***	74.5
Kamishli (Syria)	0.031	0.034	0.60	-1.99*	70.4
Kastamonu (Turkey)	0.081	0.025	0.52	2.51*	62.3
Kfar Menachem (Israel)	0.047	0.030	0.56	1.20	68.0
Kharabo (Syria)	0.039	0.032	0.58	1.46*	67.0
Konya (Turkey)	0.061	0.023	0.57	0.22	67.4
Larissa Airport (Greece)	0.031	0.034	0.61	0.99	70.3
Larnaca Airport	0.031	0.034	0.60	6.14***	70.7
Lattakia (Syria)	0.024	0.037	0.62	-1.02	73.4
Limassol (Cyprus)	0.055	0.028	0.56	1.21*	68.2
Lod Airport (Israel)	0.026	0.036	0.62	1.70	72.4
Mersa – Matruh (Egypt)	0.047	0.030	0.58	3.90***	68.6

Meslmia (Syria)	0.037	0.032	0.59	0.76	65.8
Methoni (Greece)	0.029	0.035	0.61	0.61	71.2
Mytilene Airport (Greece)	0.022	0.038	0.63	0.84	71.6
Nabek (Syria)	0.036	0.032	0.62	2.09*	70.9
Nicosia (Cyprus)	0.063	0.027	0.54	4.28***	67.7
Palmyra (Syria)	0.032	0.033	0.61	-1.94	62.2
Polis (Cyprus)	0.055	0.028	0.56	6.43***	68.2
Port Saied (Egypt)	0.049	0.033	0.59	0.94	67.8
Raqa (Syria)	0.033	0.033	0.61	-1.30	72.3
Salamia (Syria)	0.044	0.031	0.58	-2.28*	65.4
Sivas (Turkey)	0.098	0.023	0.50	2.47*	57.5
Swedaa (Syria)	0.038	0.032	0.59	-2.67**	68.1
Tartous (Syria)	0.029	0.035	0.60	-0.29	70.1
Tel Aviv (Israel)	0.027	0.036	0.62	1.32	72.4
Thessaloniki Airport (Greece)	0.027	0.036	0.62	1.22	69.8
TL Abiad (Syria)	0.035	0.033	0.59	-1.22	68.3
Tokat (Turkey)	0.080	0.024	0.55	2.50*	67.4
Trepoli (Lebanon)	0.025	0.037	0.61	-1.03	72.8
Tripolis (Greece)	0.031	0.033	0.61	1.50	70.4
Urfa (Turkey)	0.038	0.038	0.62	1.66*	71.7

* Trends statistically significant at $\alpha = 0.05$

**Trends statistically significant at $\alpha = 0.01$

***Trends statistically significant at $\alpha = 0.001$

4.4.2 Spatial and temporal distribution of annual precipitation CI

Annual precipitation CI values exhibited varying temporal trends, which can be characterized as spatially heterogeneous among stations (Fig 4.26). The results show the number of rain gauges that present trends (positive and negative) for three different significance levels (Table 4.4). This table displays the regression slope estimates and Mann-Kendall (M-K) test statistics for the annual CI values for the entire period (1961-2012). 70% of the stations exhibited positive annual precipitation CI trends. About 11% of the stations showed significant positive changes at a $\alpha = 0.001$ significance level, which are located in

the southeastern parts of the EM especially in Israel, whereas 24% of total stations had a significant positive change at $\alpha=0.05$. Although the stations located in the northern parts of the EM have the lowest values of the annual CI, they obtained significant positive trends due to the significant decreasing in both annual rainfall amounts and number of rainy days. The annual precipitation CI exhibited a statistically significant decreasing trend at $\alpha=0.05$ at 10% of total stations. Significant decreasing trend at $\alpha=0.01$ and $\alpha=0.001$ was detected in Swedaa (south Syria) and Ashdot Ya'akov (Israel), respectively. The distribution of annual precipitation CI trends indicates that the significant increasing trend mainly occurs in the north, centre and northwestern parts of the EM (Turkey, Cyprus and Greece) and some parts of southeastern parts (mainly Israel) which are dominated by high precipitation CI values (Fig 4.26). These findings indicate that these areas are at risk for extreme precipitation events.

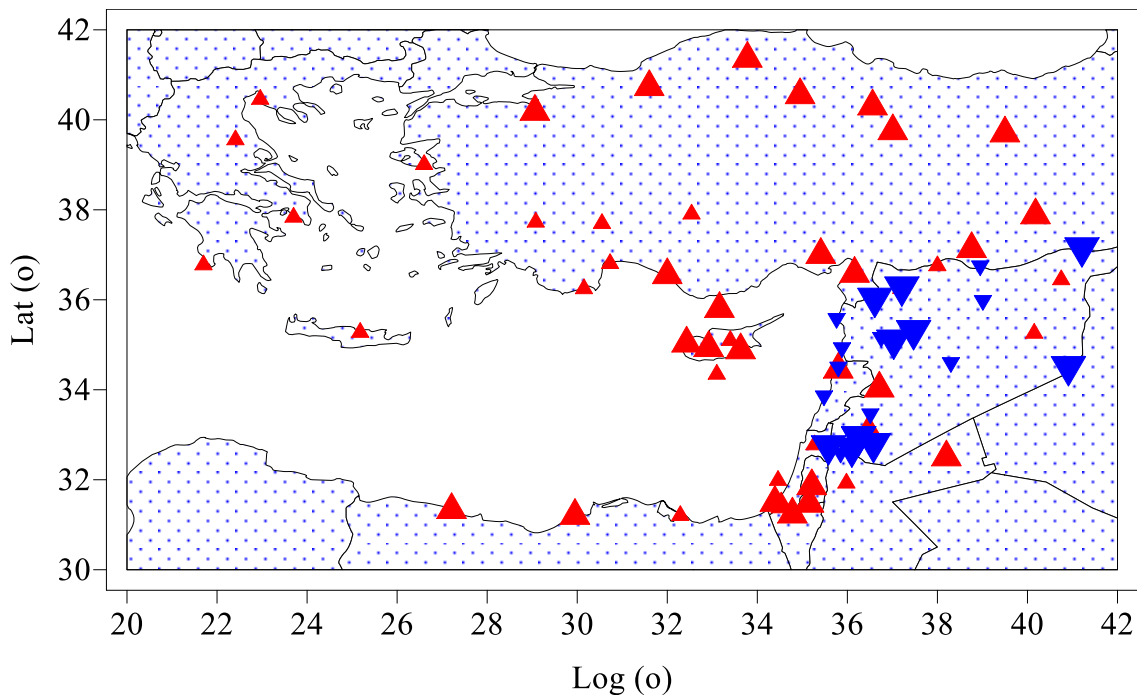


Figure 4.26 Observed trends of annual precipitation CI (1961-2012). Positive trends are in red and negative ones in blue. Large triangles represent significant trends, otherwise small triangles are shown.

Fig 4.27 shows the spatial distribution of the trend sign and summarizes the results showing the percentages of stations, which present trends (positive and negative) for three different values of significance level.

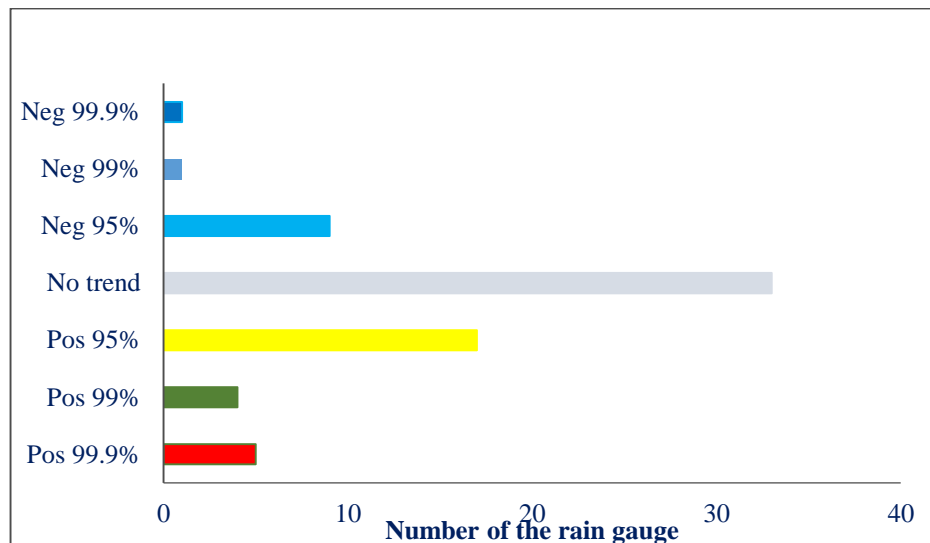


Figure 4.27 Annual precipitation CI trends at various significance levels as determined by the Mann–Kendall test.

A unique trend cannot be detected; however, there are more stations with a significant positive trend (37.1 %) of CI than those with a significant negative one (15.8%); 47.1% of the rainfall series reveals no significant trend. The spatial distribution of trends indicates homogeneity across the EM, with a clear global patterns on an annual scale. Generally, the eastern parts of the EM have an overall increasing trend of the daily CI; however, several stations located in the eastern parts, especially in Syria, showed a decreasing trend. Analysis of the precipitation CI demonstrated a widespread distribution of extreme events, and confirmed the irregularity and inequality of daily precipitation across this area. The northern and northwestern parts of the EM exhibited high levels of temporal variability in precipitation CI at the interannual level. Study results demonstrated that precipitation CI exceeded 0.70 at some stations for some years with high coefficient of variation (Fig 4.28). These areas exhibited inequalities in yearly precipitation due to a high percentage of days with low precipitation and a tendency toward non-uniform daily precipitation distribution which revealed at these stations.

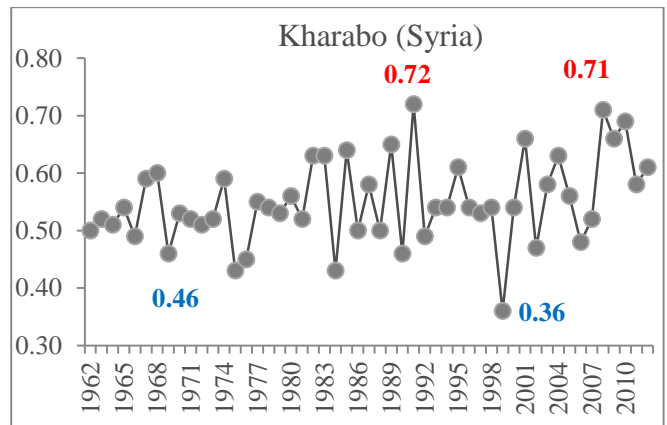
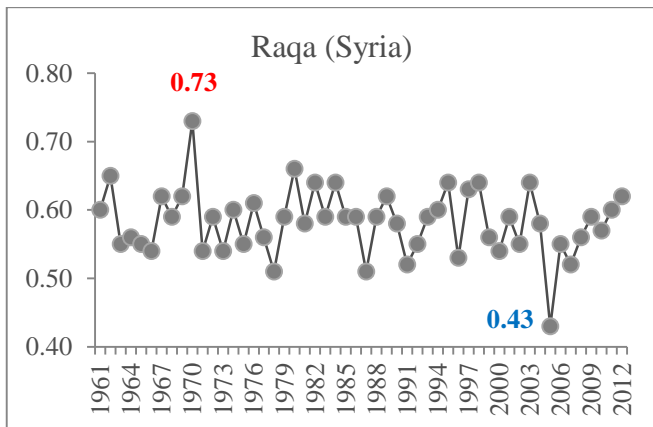
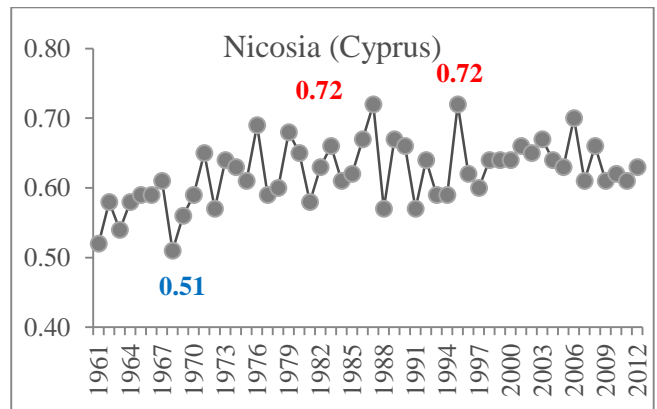
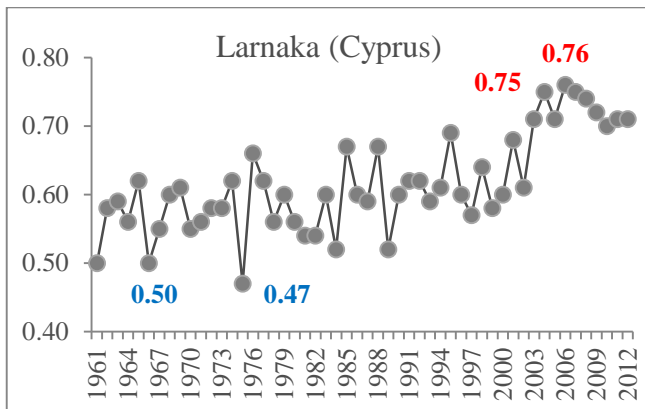
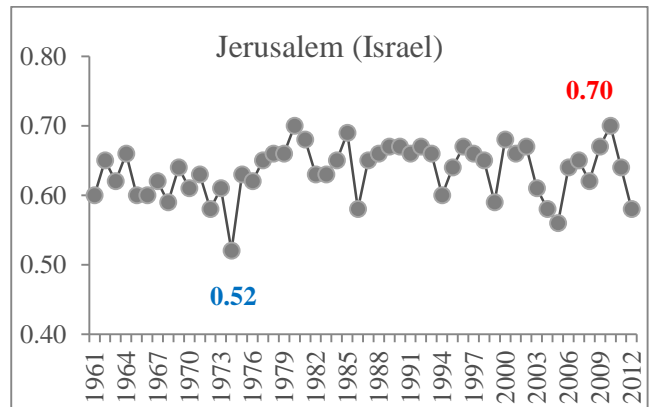
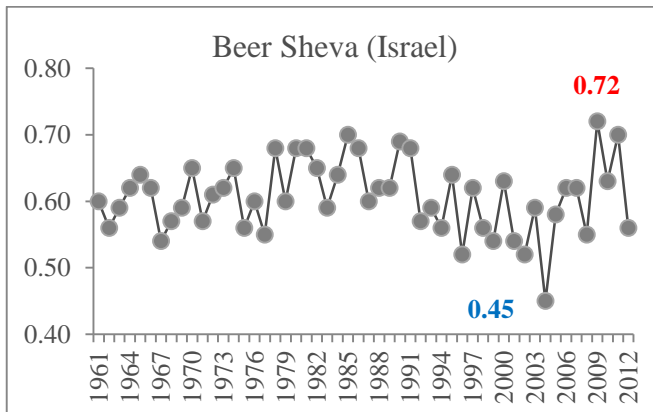
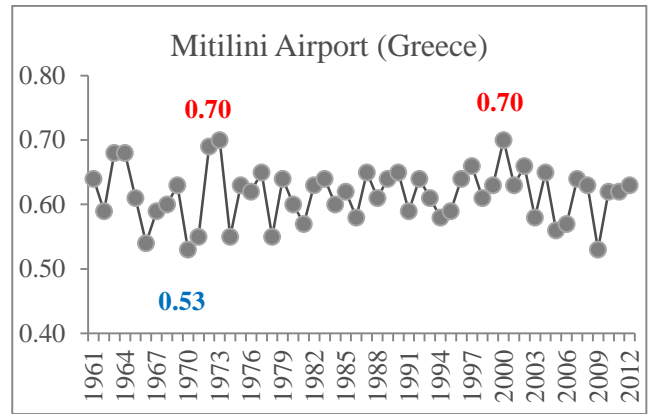
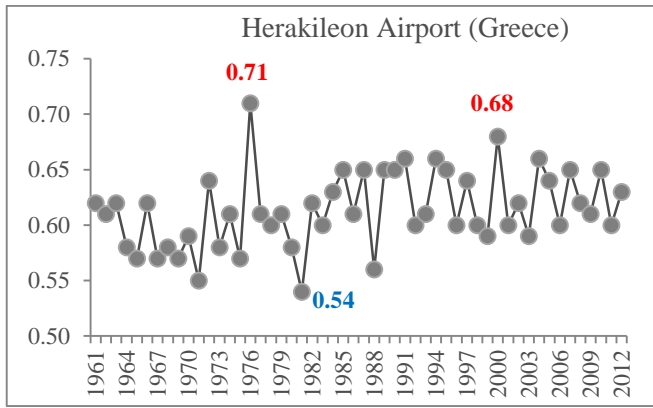
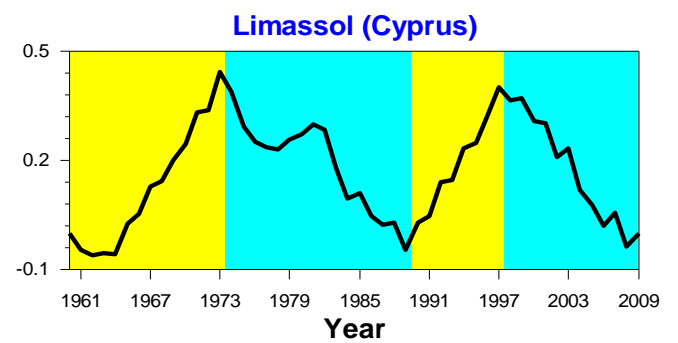
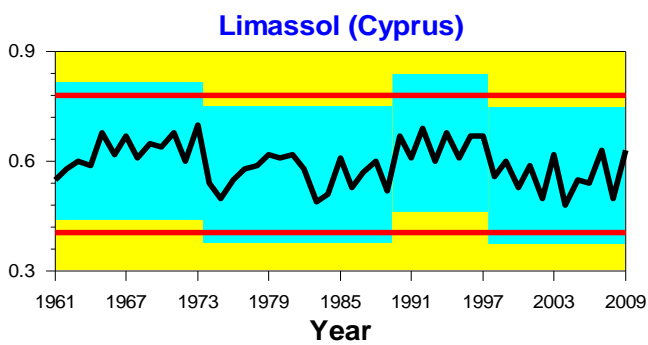
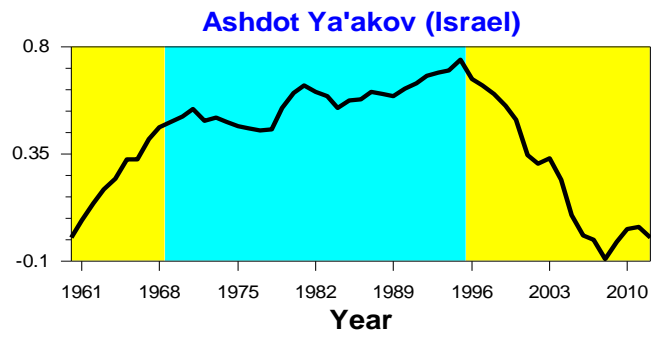
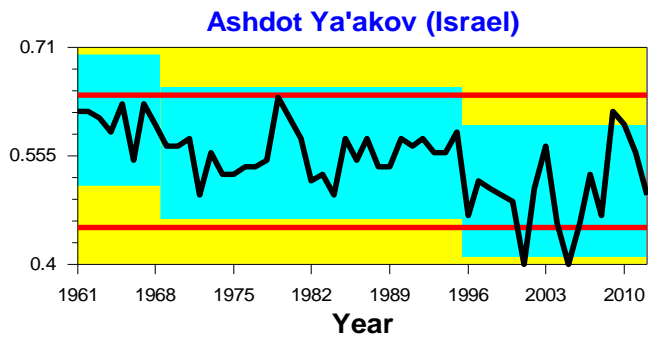
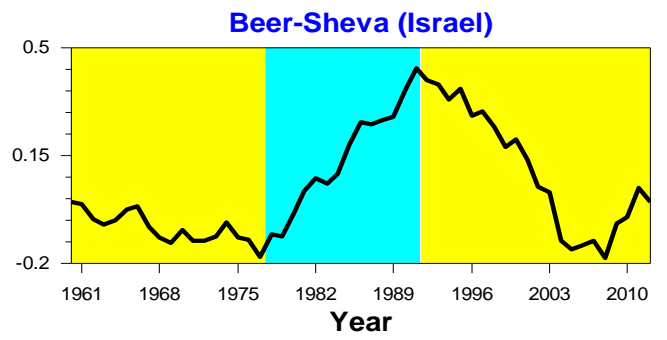
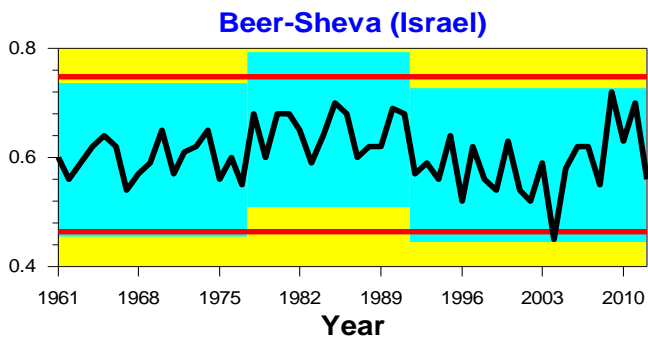
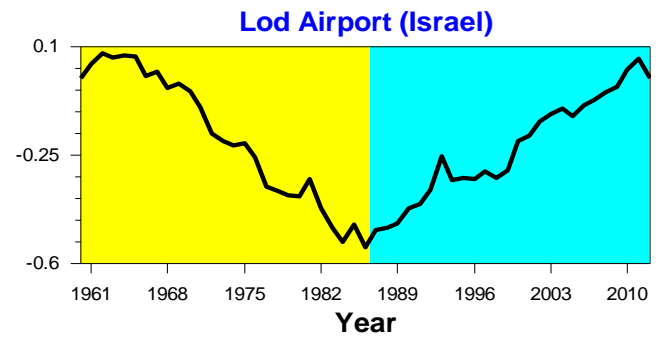
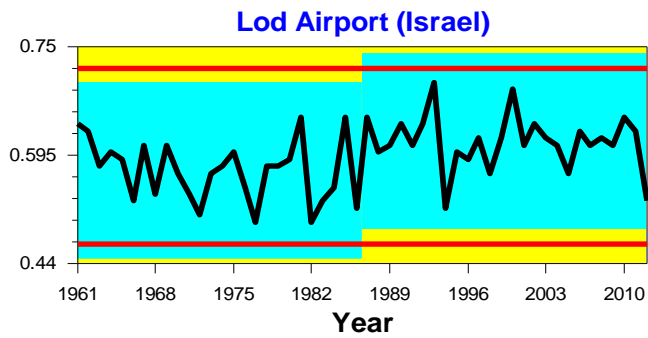
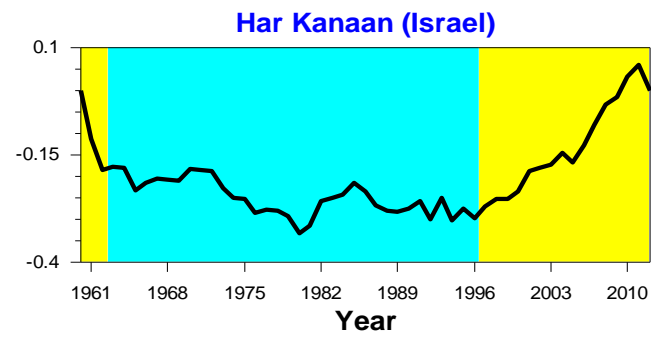
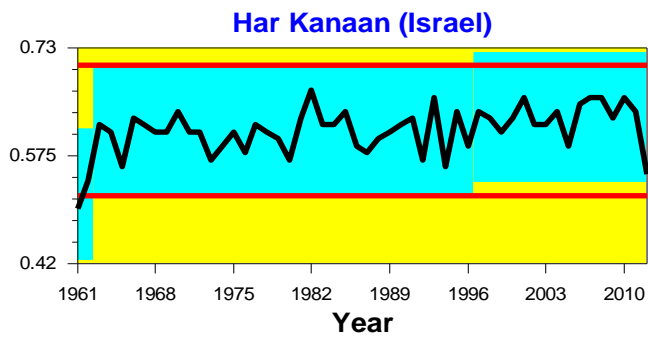


Figure 4.28 Temporal changes in the annual precipitation CI between 1961 and 2012 for some selected stations.

The results show that the annual precipitation CI values in the EM have a similar configuration to that of other Mediterranean areas with higher maximum CI values in the EM which exceed 0.75 in several years for many areas. For example, the annual precipitation CI values in Israel range between 0.50 and 0.77 (an average of 0.60 over the period 1961-2012), 0.47 and 0.77 (an average of 0.57 over the period 1941-2012). In Cyprus, these values vary between 0.41 and 0.76 (an average of 0.60 for the period 1961-2012), whereas these values become less for the period (1917-2012), and range between 0.36 and 0.76 with an average of 0.58. In Syria, the CI values vary between 0.47 and 0.73 and average of 0.60 over 1961-2012. The mean annual precipitation CI values in Greece for the period 1961-2012 is 0.61 which range between 0.48 and 0.74). The precipitation CI values in Turkey were lower than those shown in other parts of the EM and range between 0.46 and 0.72) with an average of 0.57 during the study period.

Previous studies in other parts of the Mediterranean region like peninsular Spain showed that the concentration index CI of series of precipitation varied between 0.55 and 0.70 for (an average of 0.61 over the period 1951 - 1990) (Martin-Vide, 2004). In Algeria, these values ranged between 0.57 and 0.70 (an average of 0.63 for the period from 1970 to 2008) (Benhamrouch *et al.*, 2015). Coscarelli and Caloiero (2012), for a small part of Italy, showed that a very inhomogeneous daily rainfall temporal distribution characterizes the eastern side of this region with a clear tendency toward a weaker seasonality of the rainfall distribution detected by Mann-Kendall test. Cortesi *et al* (2012) used the CI to investigate the statistical structure of daily precipitation across Europe based on 530 daily rainfall series for the period 1971–2010. The annual CI showed a northwest to southeast increasing gradient (excluding Turkey and Greece). Moreover, high annual and seasonal daily concentrations of rainfall were detected in the western Mediterranean Basin, mainly along the Spanish and French coastlands. The range of CI values in the Mediterranean region is clearly lower than that presented in China (0.74–0.80) by Zhang *et al* (2009). This difference can be explained on the basis of the different climate systems and precipitation mechanisms responsible for rainfall in China (such as a typhoon).

Abrupt changes were detected in precipitation CI in the northwestern parts of the EM. Fig 4.29 illustrates that abrupt changes of CI at most stations occurred in the late 1970s and early 1980s and indicates that interannual precipitation CI was uniformly distributed during those years, whereas the abrupt changes in northern parts of the EM occurred mainly after 2003. It is evident that abrupt changes of the annual CI detected later than in those located in the southern and southeastern parts. The abrupt change in precipitation CI might be occurred due to sudden highly intensive rainfall in these parts and it can be seen from Fig 4.29 that the values of annual CI in most stations that located in northern EM have increased after the change point, whereas stations in the other parts have exhibited an increasing or a decreasing tendency in CI values after the change point. Three representative stations of these two parts (northern and southern EM) were selected to demonstrate the abrupt changes that occurred in annual precipitation CI along different areas (Fig 4.29). For example, for last four stations which are located in Turkey as shown in Fig. 4.29, it can be seen from the time series plots and CUSUM charts of the annual precipitation CI a steady rise in CI values since 2004 which was statistically significant at $\alpha=0.001$. The results obtained for Beer–Sheva in Israel showed also a steady rise in CI values from 1978 till 1992, then detected a decreasing trend till 2005 followed by a further rise till the end of the record in 2012. The analysis in Har kanaan (Israel) detected two changes which occurred in 1963 and 1997 (Fig.4.29).



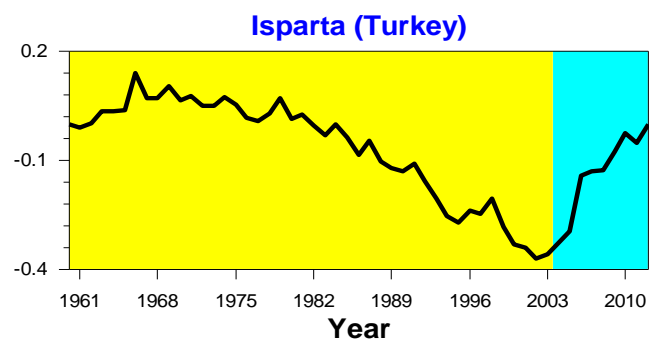
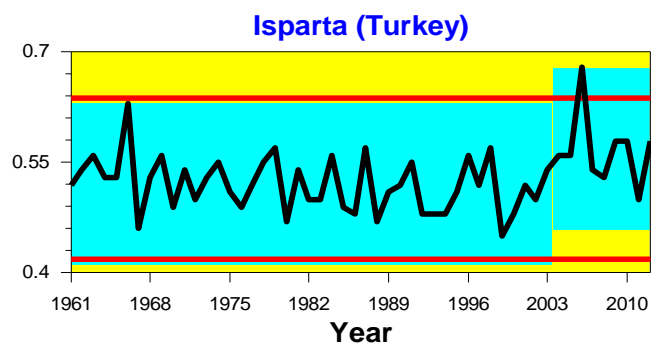
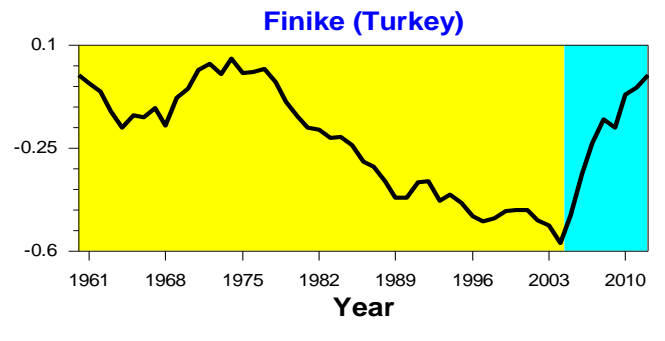
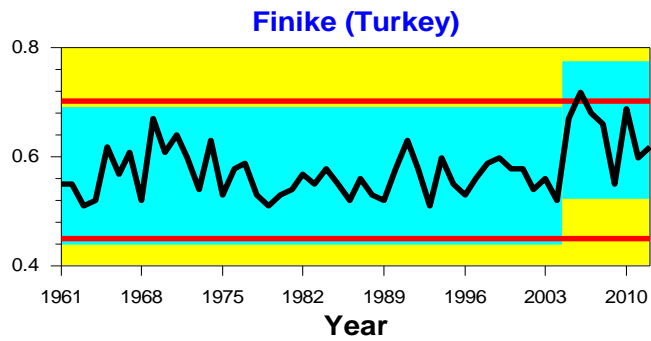
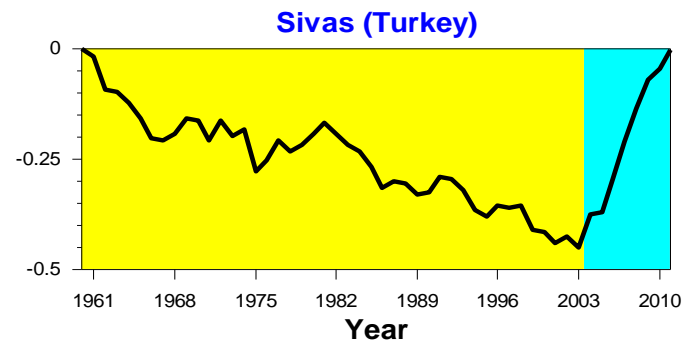
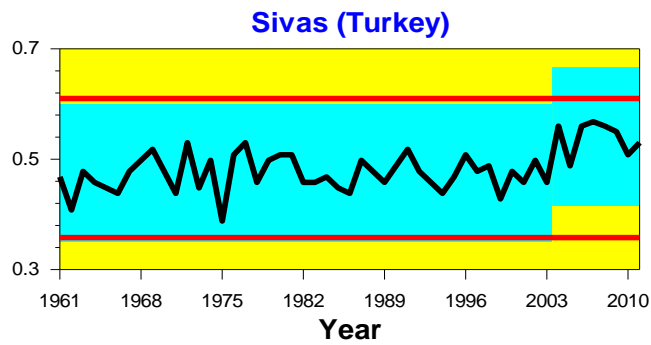
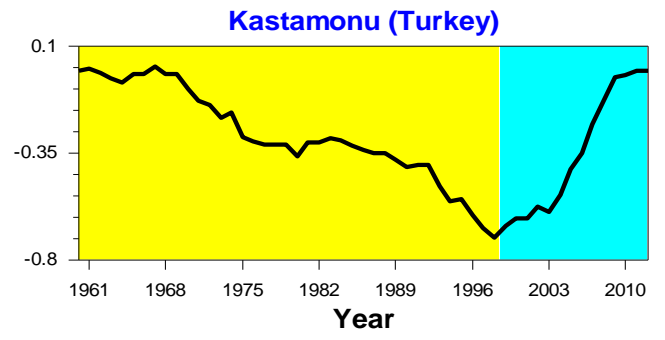
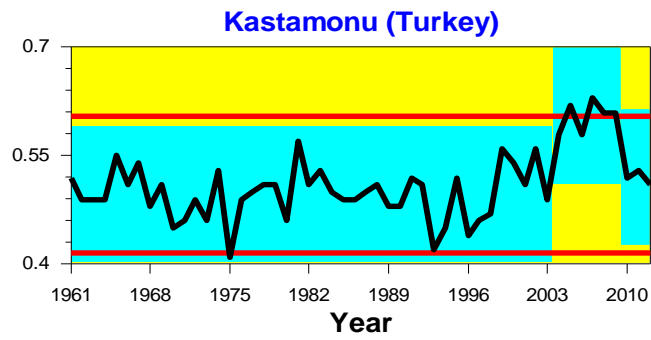
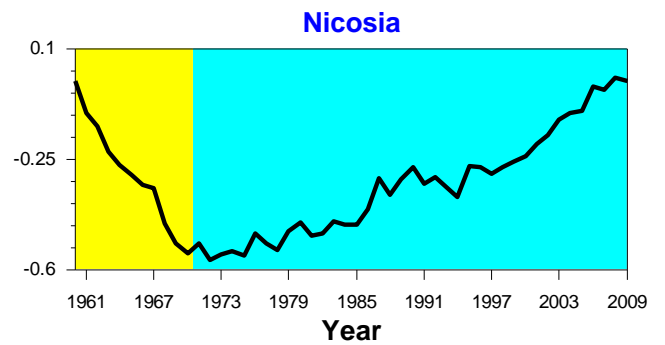
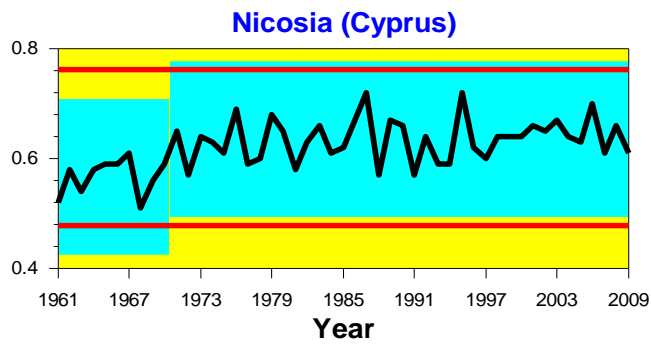


Figure 4.29 CI precipitation time series data (left) and their abrupt changes (right) between 1961 and 2012, as determined by CUSUM charts for some selected stations over the EM.

The first and most important change point is estimated to have occurred between 1963 and 1965 with $\alpha=0.01$ confidence level. Prior to 1997 mean annual CI values were about 0.52 while and after the first change they were 0.6 and, then, 0.63 after the second change. A significant increasing of mean CI values at $\alpha=0.05$ confidence level occurred during one subsequent year in both Nicosia (Cyprus) and Lod Airport (Israel). The mean CI has increased from 0.57 to 0.64 and from 0.57 to 0.62 in Nicosia and Lod Airport respectively. In Limassol (Cyprus), the analysis of abrupt change detected three steps of change which occurred in 1974, 1990 and 1998. The first and most important change point is estimated to have occurred between 1969 and 1979 at $\alpha=0.01$ confidence level. Prior to 1974 the average value of annual CI was found to be 0.63, while after the first change it decreased to 0.56. The change point occurred both in 1990 and 1998 occurred at the same confidence level ($\alpha=0.05$) with an increasing of mean precipitation CI during (1987-1992) from 0.56 to 0.64, while the third change led to another decrease till 0.55.

4.5 Spatial and temporal distribution of the annual Precipitation Concentration Index PCI.

The spatial distribution of an annual PCI across the study area was computed for the 103 monthly stations. The results are mapped in Fig 4.30

In the northern regions of the EM, the PCI values between 11 and 20 denote the seasonality of the rainfall distribution. Differently, the southern and southeastern areas have $PCI > 20$, with a steep increasing gradient from north to south, denoting a high monthly variability in the rainfall amounts. The highest PCI values are observed in the southeastern parts across the Mediterranean Sea (Syria and Israel), with PCI ranging from 22 to 55, indicating that most of the precipitation in this area falls in only a few months. The water stress is very intense in these regions during the hot summer season due to the lack of rainfall.

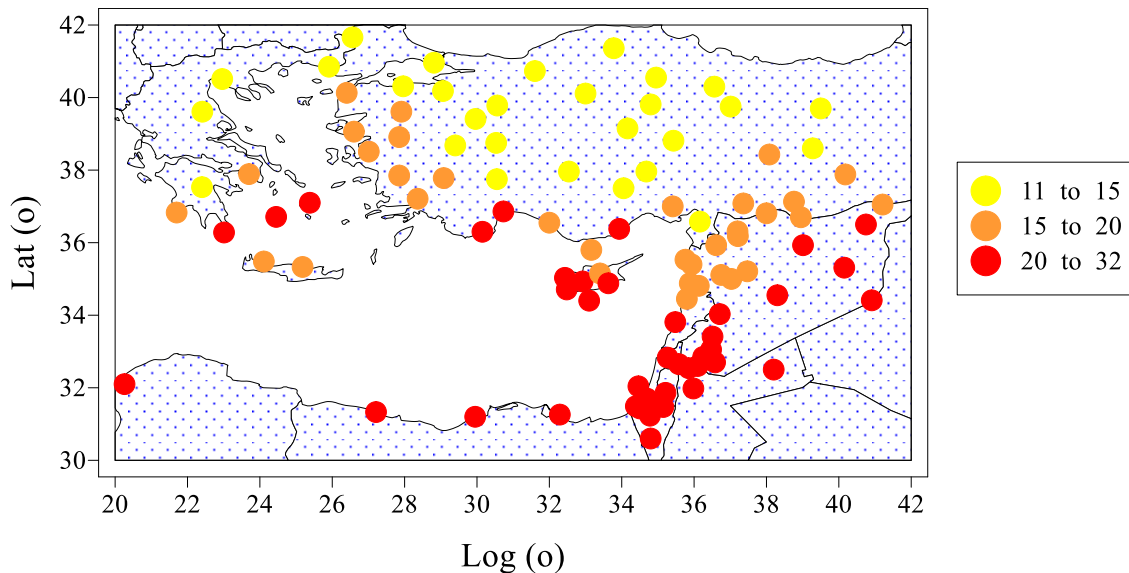


Figure 4.30 Mean value of the Precipitation Concentration Index (annual scale) during the period 1961-2012.

On an annual scale, PCI in the EM can be described as strongly irregular in the south and southeastern parts (more influenced by the Mediterranean). PCI values are distributed from high distribution in south and southeastern parts to moderate and uniform distribution in the northern parts. During the wet season (October to March) PCI is lower and it is distributed according to a clear north to south gradient (from uniform precipitation concentration in the northern and northwestern parts to moderated seasonal distribution in the southern parts across

the Mediterranean coast) (not shown). Therefore, the annual PCI values showed a statistically significant and negative correlation with latitude ($r=-0.91$) (Fig 4.31).

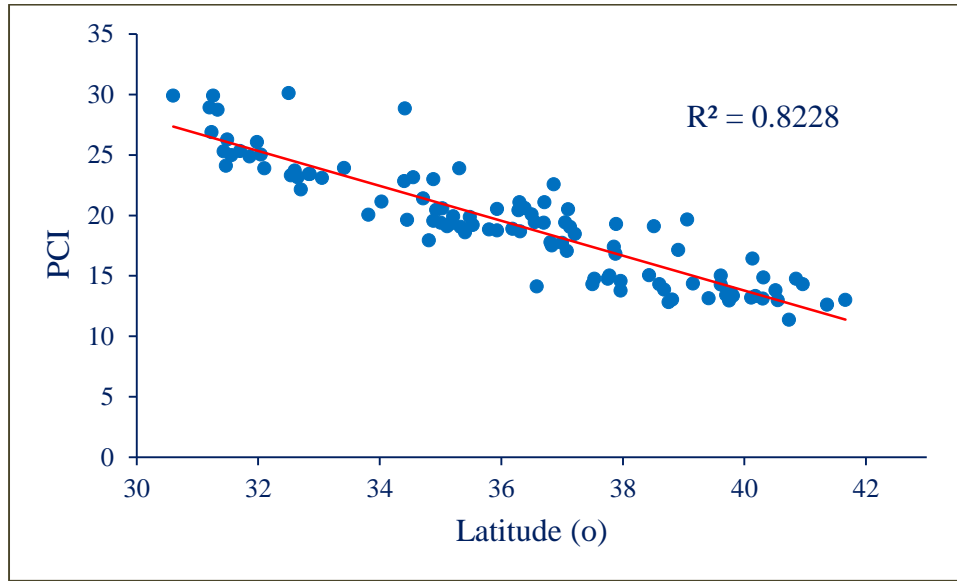


Figure 4.31 Relationship between annual PCI values and latitude.

We applied the PCA to annual PCI values computed for all stations. Based on Scree test (Cattell, 1966) to determine how many components should be retained, we have selected four principal components for Varimax rotation. The idea behind choosing a varimax rotation is to simplify the structure of loadings (Jolliffe *et al.*, 2002) by maximising the variance of the squared correlation coefficients (such as loadings) between each rotated and original component. The four leading PCs explain 63% of the total variance which tallied with Briffa *et al* (1994) recommendation. High loadings indicate good correlations between the PCIs variables and the PCs. The PC1 and PC2 loadings explains about 26% and 20% of the total variance, respectively. They have high positive loadings in the northwestern and southeastern parts of the EM (the inner parts of Syria, Greece and south and west parts of Turkey). For winter precipitation, the PC1, which explains 30% of the total variance, showed positive loadings in Syria, Egypt and Libya (Fig 4.32).; while the PC2 showed a high concentration of winter precipitation in western Turkey and Greece which means that these parts of the EM are characterized by considerable rainfall amount and percentage in winter.

The PC1 and PC2 loadings together cover identical extension areas in both annual and winter analyses.

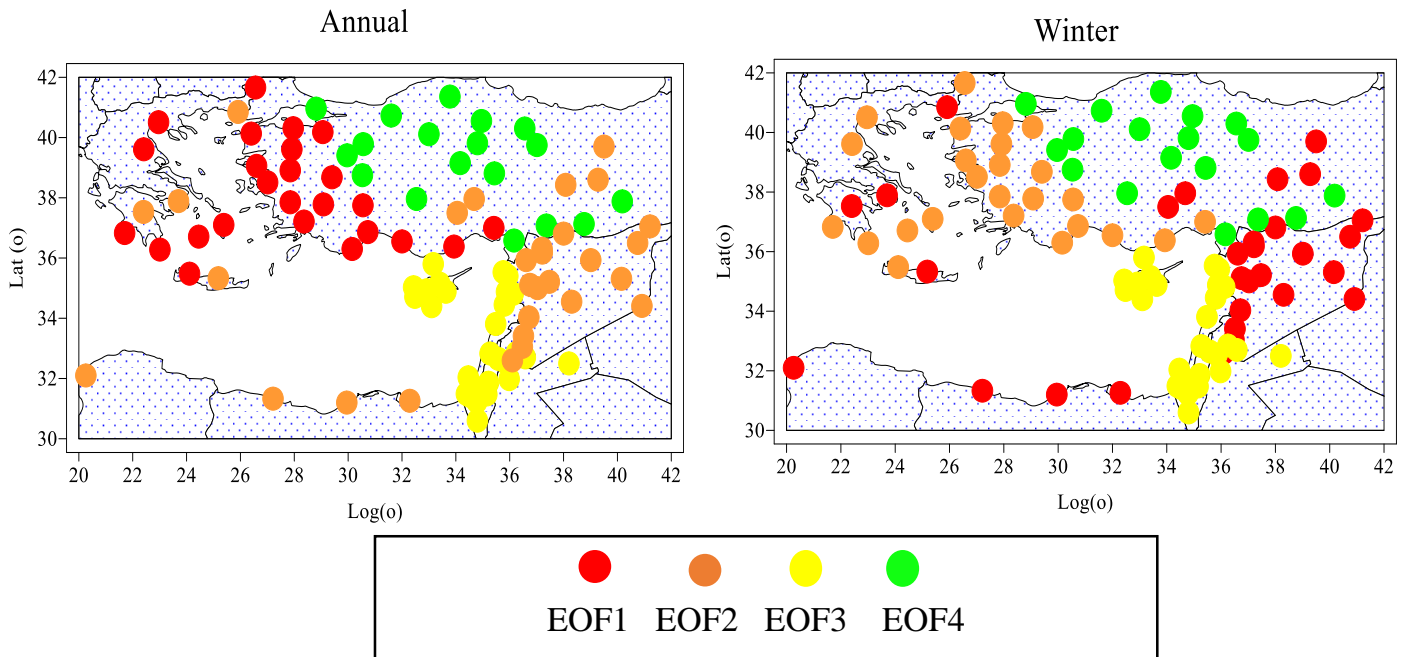


Figure 4.32 Spatial distribution of the rotated PC loadings (EOFs) across the EM applied to annual PCI values

The PC3 loading, with 11% and 16 % of explained variance in annual and winter precipitation, respectively, had high positive values on annual and values in Cyprus the southeast parts of the EM across the coastal region of Syria, Lebanon, Israel, and Jordan. This spatial pattern indicates that these areas are characterized by high amounts in winter and high seasonal rainfall regime and resulted mainly from passages of extratropical cyclones over the EM (Ziv *et al.*, 2006). These authors found a negligible correlation between the winter rainfall in Israel and the sea-level pressure (SLP) over the EM, but significant positive correlations over the other parts of the Mediterranean and over Europe.

Finally, an analysis of the spatial and temporal patterns in the EM has been carried out by means of annual precipitation PC1 and PC2 scores dataset. They show a different behaviour between southern parts, with the most critical rainfall concentration, and north parts where precipitation concentration was lower compared to those of southern parts. The application of the Mann–Kendall test

showed a general non-significant trends in annual and winter PCI over those stations under EOF1 and EOF2 domains. (Fig 4.33).

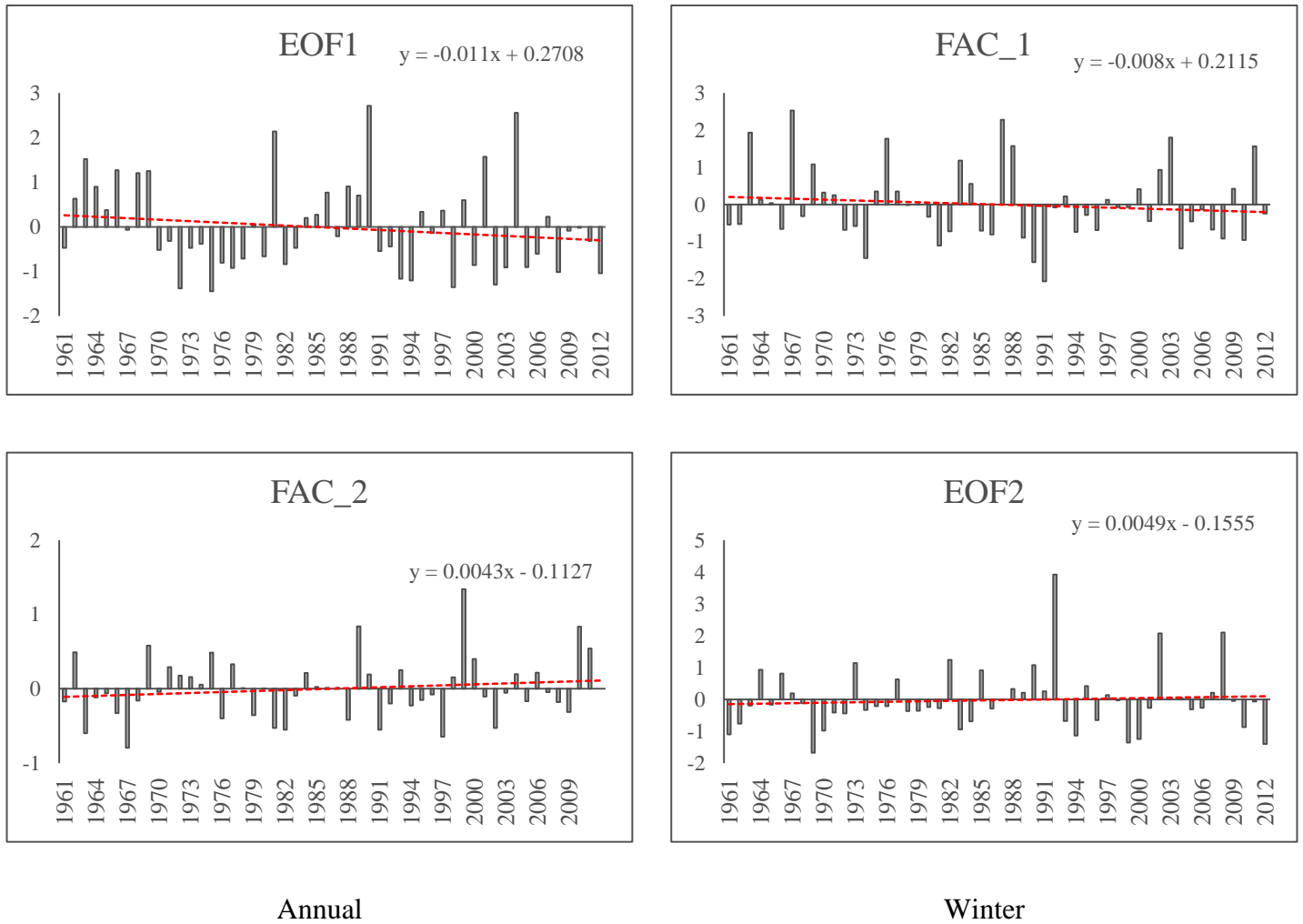


Figure 4.33 Temporal patterns of corresponding EOF1 and EOF2 scores derived from FAC values in winter and annual precipitation

4.6 The spatial distribution features of entropy over the EM.

The value of the entropy of a rainfall series is determined by its probability distribution. For a given rainfall station, the entropy of the rainfall series reaches its maximum when the probability distribution is uniform without any deflection; however, it would reduce to zero if any particular value of the rainfall series occurred with the probability of one (Maruyama *et al.*, 2005). The variability of precipitation is measured using the entropy. In order to investigate the variability of annual, monthly and daily precipitation, the mean entropy is calculated for individual stations respectively for each time series. The spatial distribution of entropy on monthly and daily scales is shown in Fig 4.34. The value of the entropy ranges between 5.33 and 6.18 for monthly precipitation, 5.12 and 8.5 for daily precipitation, whereas all the stations have similar values of annual entropy ranging between 3.8 and 3.9.

It is clear that the distribution of the entropy values for both monthly and daily rainfall series varies between the north and south parts. Overall, the variability is high in southern relative to northern parts of the EM. The low values of entropy are detected in south and southwestern parts where the highest seasonality values represent a big disorder in the rainfall amounts associated with high variability in this area.

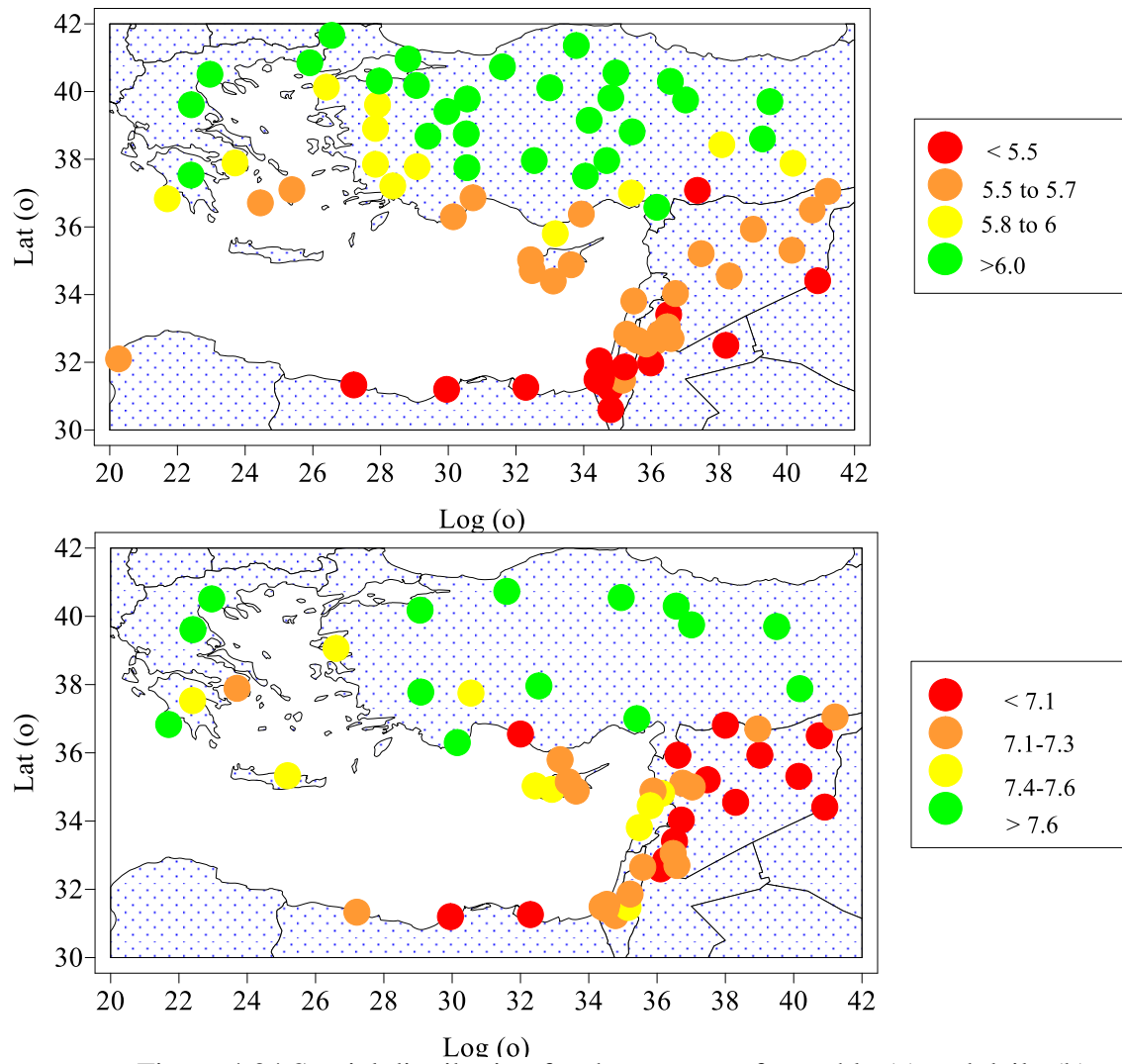


Figure 4.34 Spatial distribution for the entropy of monthly (a) and daily (b) rainfall amounts during 1961-2012 over the EM.

It is observed that the spatial variability of monthly series is less than that of individual time series (These results agree with those obtained in (Mishra *et al.*, 2009). The entropy would reach its maximum only when the monthly rainfalls are equal at a given station. The entropies in the EM are relatively small, mostly, which implies that the distribution of rainfall is discrete in time with interannual variations except in the northern parts which might be due to the climatic conditions and topographies (e.g., closeness to Black Sea and altitude above 1,000 m in the center of Anatolian plateau).

4.6.1 The relationship between entropies, longitude, latitude and CV.

The entropy and the coefficient of variation (CV) for a given station can both indicate the variability of temporal rainfall distribution. The relationship between the entropy and both longitude and latitude is analysed to reveal the spatial structure of the precipitation (Fig 4.35).

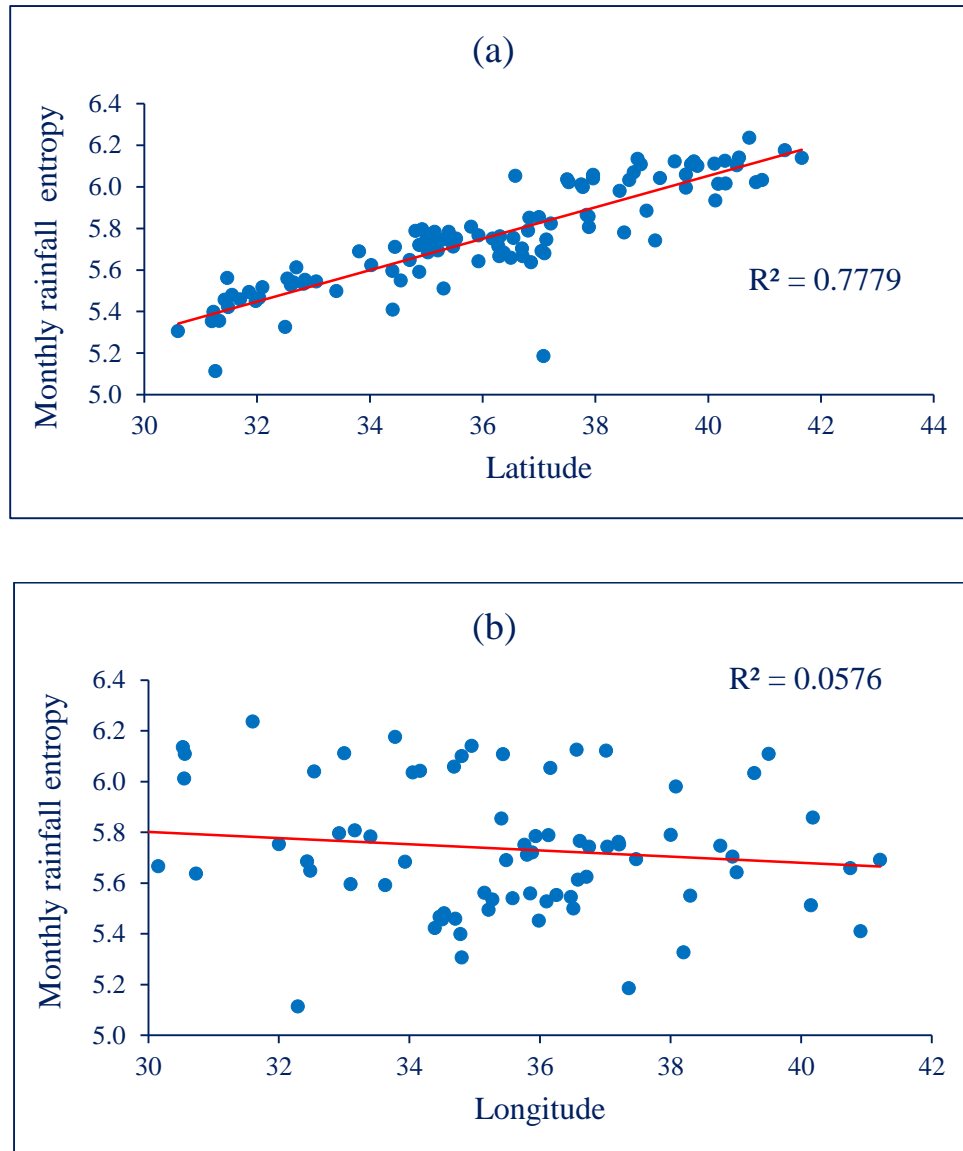


Figure 4.35 Relationship between monthly entropies and both longitude and latitude over 1961-2012.

It can be seen in Fig 4.35a that the monthly rainfall entropies are highly and significantly correlated with the latitude ($r = 0.88$) at ($p = 0.01$), i.e., entropy

increases with latitude (from south to north); whereas the relationship between daily rainfall entropies and latitude was lower ($r=0.63$) at ($p=0.01$) due to high variability in the daily rainfall amounts (Fig 4.36).

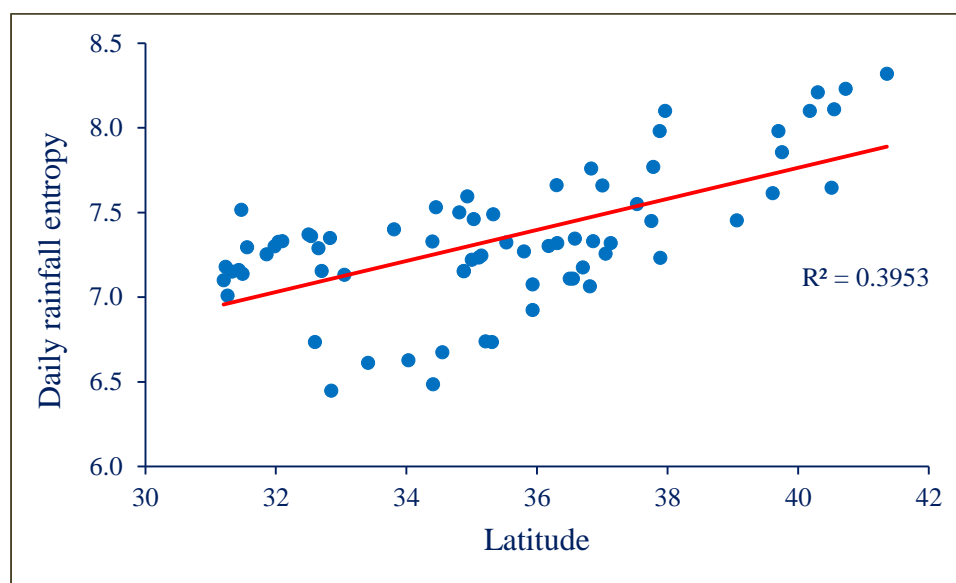


Figure 4.36 Relationship of daily entropies and latitude over 1961-2012

No statistical relationship was observed between any temporal entropy and longitude. Entropies in the longitude direction or from west to east are widely scattered without any correlation ($r= -0.24$) (Fig. 4.35b), showing great differences in rainfall distributions from west to east. The results show that the entropy was linearly and positively related to the latitude, but it was not linearly correlated with the longitude. It was suggested that the precipitation possesses the latitude zonality, which implied that precipitation might increase with the latitude from the south to the north. The same results were obtained by Zhao *et al* (2011), they found a significant correlation between the monthly rainfall entropy and latitude with a correlation coefficient of 0.8 in Xinjiang, located in an arid area in north China.

The results show that the correlations between seasonal CVs and entropy values are significant at ($p=0.01$) and these correlations are negative. The highest correlation is detected in spring ($r=-0.84$) (Fig 4.37a) and autumn ($r=-0.77$) (Fig 4.37b), whereas the entropy values in winter have a moderate negative correlation

with CVs ($r=-0.47$) (Fig 4.37c). Among others, similar results were observed in China (Liu *et al.*, 2013). Sang (2013) has also found that the measures of CV and entropy perform differently in describing the complexity of daily precipitation processes in and so they also have different performances. Ebrahimi *et al* (1999) showed that both the variance and entropy reflect concentration, but their performances are different. The former measures concentration only around the mean, while entropy measures diffuseness of the probability density function (PDF) but does not consider the location of concentration. They also found that entropy may be related to high-order moments of a distribution which could offer a much closer characterization of the PDF because it uses much more information about the probability distribution than the variance does. Koutsoyiannis (2005) has also detected high negative correlation between CV and Entropy values for numerous hydrological data sets on several time scales.

Therefore, the entropy is more effective than CV for quantifying the complexity and variability of the changing climatic systems and it can be an effective alternative measure of dispersion and scattering (Mishra *et al.*, 2009; Sang *et al.*, 2012), because it can show the impact of urbanizations on the variability of both daily precipitation and precipitation extremes.

In recent years, an Entropy Theory approach has been adopted as a good method to evaluate the disorder, which is based on spatial and temporal precipitation variability patterns. It has been used in a wide range of applications, assessing variability in the hydrological variables (Koutsoyiannis, 2005; Delsole and Tippett, 2007; Mishra *et al.*, 2009; Zhao *et al.*, 2011).

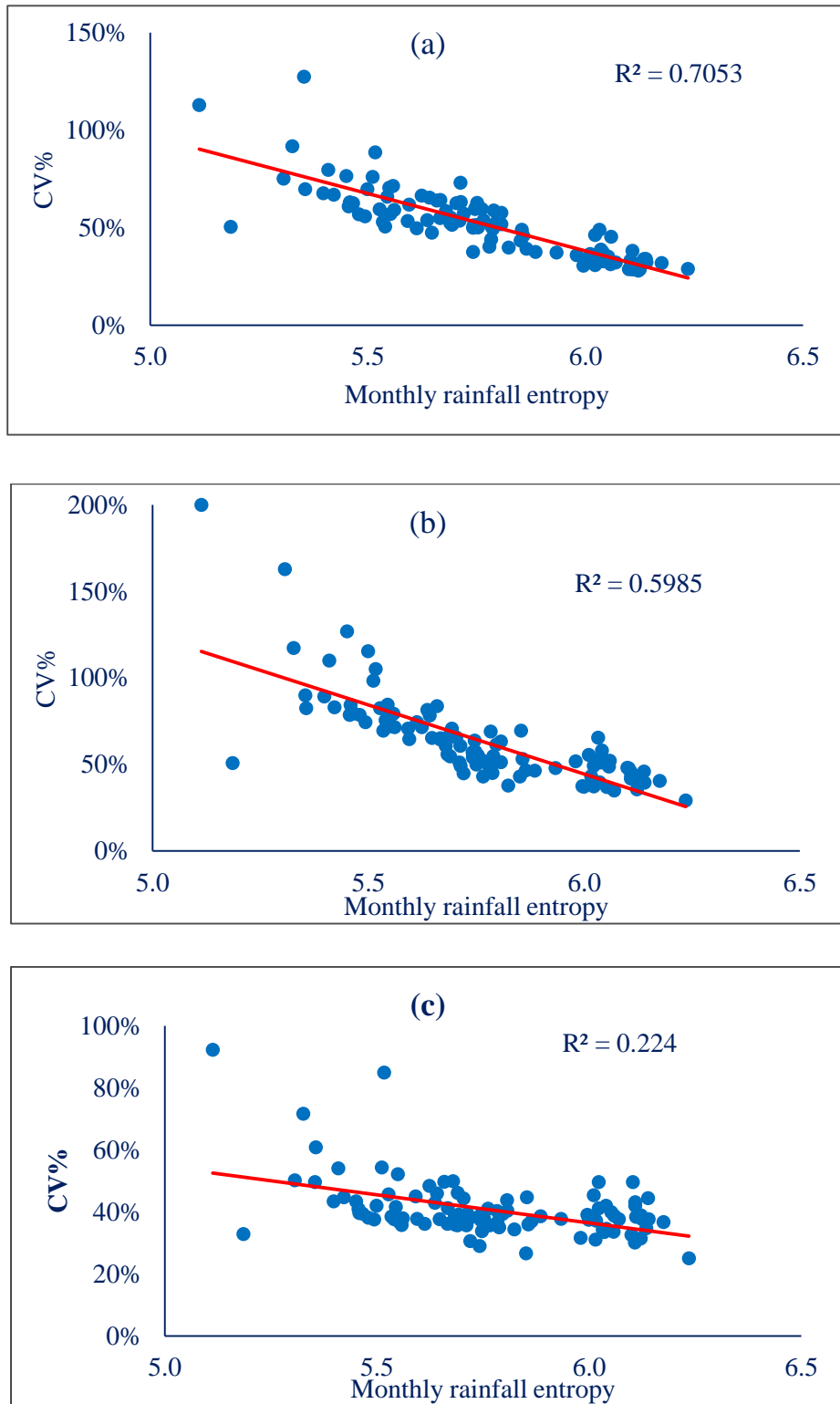


Figure 4.37 Relationship between entropies and CV in autumn “a” , spring ”b” and winter “c” during 1961-2012 over the EM.

4.7 Spatial and temporal changes in rainfall frequency distribution patterns

Annual rainfall totals in the EM were analysed to reveal any long term changes in their temporal and spatial distribution patterns since the 1960s. We investigated the behaviour of the changes in the shape and scale parameters of the fitted gamma distribution to the annual rainfall data between two 26-yr periods (1961-1986 and 1987-2012). The values of the shape α and size parameters $1/\beta$ for each of all 103 meteorological stations, separately, are shown in Table 4.5.

Table 4.5 The values of parameters α and $1/\beta$ for each station during two 26-yr periods (1961-1986 and 1987-2012) and the percent of change over 1961-2012.

Station	Period 1		Period 2		Change%	
	1961-1986		1987-2012			
	α	β	α	β	α	β
Abu Kamal (SYR)	5.22	26.52	3.64	30.16	-30.30	13.71
Adana Incirlik (TUR)	10.10	66.96	10.32	65.95	2.18	-1.52
Afyon (TUR)	20.16	19.69	36.21	11.33	79.62	-42.44
Akhisar (TUR)	18.89	31.72	16.76	31.63	-11.27	-0.29
Alanya (TUR)	16.82	65.60	11.24	96.86	-33.15	47.64
Aleppo (SYR)	22.68	14.72	7.01	43.45	-69.07	195.28
Alexandria (EGY)	9.90	17.65	5.41	36.86	-45.31	108.84
Alexandroupoli Airport (GRC)	18.65	30.22	13.22	37.23	-29.11	23.21
Amiandos (CYP)	15.23	68.36	9.12	93.73	-40.10	37.10
Amman Airport (JOR)	12.61	21.62	3.19	88.96	-74.66	311.58
Ankra Esenboga (TUR)	26.37	15.65	19.25	20.95	-26.99	33.80
Antalya (TUR)	12.92	85.67	8.17	131.85	-36.77	53.91
Ashdod (ISR)	7.05	71.72	5.48	93.47	-22.33	30.33

Ashdot Ya'akov (ISR)	23.14	17.59	8.21	45.71	-64.50	159.86
Athalassa (CYP)	18.88	17.51	8.86	36.13	-53.05	106.40
Athria (SYR)	15.86	12.43	5.57	31.73	-64.86	155.29
Aydin (TUR)	27.57	23.61	13.70	43.93	-50.30	86.09
Balikesir (TUR)	25.20	23.48	18.19	30.48	-27.84	29.84
Bandirma (TUR)	24.73	29.69	21.41	31.98	-13.44	7.72
Beer Sheva (ISR)	7.73	27.00	5.78	31.59	-25.20	17.00
Beer Tuvia (ISR)	8.61	61.78	9.12	58.72	5.90	-4.95
Beirut Airport (LBN)	16.92	48.06	13.11	52.95	-22.54	10.17
Benina (LBY)	9.93	27.42	6.60	35.47	-33.57	29.37
Bolu (TUR)	43.25	12.71	33.59	16.27	-22.35	28.00
Bursa (TUR)	38.02	18.03	21.15	32.01	-44.37	77.59
Canakkale (TUR)	19.65	32.33	18.30	30.61	-6.91	-5.31
Corum (TUR)	30.07	13.18	37.60	11.96	25.03	-9.26
Damascus-Airport (SYR)	10.02	14.62	4.78	24.67	-52.30	68.83
Daraa (SYR)	11.20	24.06	5.67	37.64	-49.41	56.46
Deir Ezzour (SYR)	7.66	20.80	3.30	38.15	-56.95	83.40
Denizil (TUR)	22.33	25.83	19.06	29.49	-14.63	14.20
Diyarbakir (TUR)	14.37	34.71	17.02	27.51	18.43	-20.72
Edleb (SYR)	30.00	16.90	8.90	54.19	-70.34	220.56
Edirne (TUR)	32.52	17.96	22.33	25.58	-31.33	42.42
Elazig (TUR)	16.56	26.81	16.65	23.51	0.60	-12.31
Eregli / Konya (TUR)	19.32	15.85	22.31	12.97	15.48	-18.14
Erzincan (TUR)	25.16	14.90	16.75	22.06	-33.40	48.05
Eskisehir (TUR)	43.94	8.91	29.25	11.59	-33.44	30.10
Finike (TUR)	10.15	95.28	9.32	102.10	-8.25	7.16
Gazianteb (TUR)	23.46	32.43	10.69	51.15	-54.43	57.72

Gazit (ISR)	22.96	21.38	8.18	57.37	-64.38	168.38
H-4 Irwaidhed (JOR)	3.68	2.84	22.94	28.76	-22.73	25.47
Hama (SYR)	23.41	15.28	9.23	33.07	-60.55	116.44
Har Kanaan (ISR)	14.16	47.28	12.14	45.64	-14.26	-3.48
Hasakah (SYR)	8.67	33.20	4.35	52.30	-49.79	57.53
Hellinikon Airport (GRC)	20.77	18.23	11.04	31.63	-46.86	73.51
Herakilon Airport (GRC)	16.89	30.61	15.73	28.98	-6.89	-5.32
Hmemiem Airport (SYR)	29.71	29.35	10.61	71.20	-64.28	142.60
Irbid (JOR)	22.76	21.26	8.93	47.11	-60.76	121.58
Iskenderun (TUR)	15.99	45.56	34.76	21.52	117.35	-52.76
Isparta (TUR)	11.22	49.89	15.69	31.73	39.83	-36.39
Istanbul-Ataturk (TUR)	22.69	30.23	5.60	119.62	-75.33	295.74
Izmir/Cigli (TUR)	16.59	41.60	11.77	58.40	-29.08	40.38
Izraa (SYR)	23.31	13.18	6.69	39.38	-71.31	198.84
Jarablous (SYR)	12.35	26.70	7.85	36.75	-36.41	37.67
Jerusalem (ISR)	18.91	29.56	8.68	60.02	-54.13	103.09
Kamishli (SYR)	10.79	40.96	4.86	71.41	-54.91	74.34
Kastamonu (TUR)	35.38	13.37	22.17	21.08	-37.35	57.71
Kayseri / Erkilet (TUR)	34.04	10.84	18.66	20.69	-45.17	90.82
Kfar Menachem (ISR)	9.29	51.24	8.94	56.24	-3.80	9.76
Kharabo (SYR)	15.58	10.72	5.25	26.04	-66.31	142.91
Kirsehir (TUR)	25.08	14.73	31.71	11.59	26.43	-21.35
Kithira Airport (GRC)	22.70	24.07	9.33	49.59	-58.92	106.04
Konya (TUR)	19.74	17.20	18.55	16.21	-6.03	-5.73
Kutahya (TUR)	34.50	17.31	34.14	15.16	-1.05	-12.41
Larissa Airport (CYP)	13.99	29.73	24.52	17.05	75.21	-42.64
Larnaca Airport (CYP)	12.73	26.67	8.46	41.22	-33.54	54.58

Lattakia (SYR)	19.59	40.25	9.08	74.14	-53.67	84.21
Limassol (CYP)	16.62	25.55	9.99	42.04	-39.92	64.53
Lod Airport (ISR)	15.58	36.36	6.13	87.58	-60.63	140.87
Malatya/ Erhac (TUR)	16.49	24.90	26.11	13.85	58.35	-44.38
Mersa – Matruh (EGY)	8.72	14.73	7.00	21.90	-19.77	48.63
Meslmia (SYR)	18.53	18.83	9.35	33.88	-49.53	79.89
Methoni (GRC)	19.02	36.87	19.06	35.65	0.22	-3.30
Milos (GRC)	22.20	18.61	6.99	57.07	-68.52	206.57
Mitzpe Roman (ISR)	5.04	15.50	4.41	15.35	-12.49	-0.97
Mugla (TUR)	18.04	68.77	17.79	60.90	-1.40	-11.44
Mytilene Airport (GRC)	30.03	23.13	11.36	51.27	-62.17	121.60
Nabek (SYR)	12.67	9.68	5.01	22.28	-60.50	130.07
Naxos (GRC)	12.49	30.94	8.42	42.69	-32.61	37.96
Nicosia (CYP)	19.85	16.70	9.90	31.96	-50.10	91.45
Nigde (TUR)	20.19	15.72	20.38	16.70	0.90	6.21
Palmyra (SYR)	6.99	19.27	4.39	26.16	-37.17	35.71
Paphos Airort	16.49	24.59	7.86	50.41	-52.33	105.04
Polis (CYP)	15.26	31.90	9.45	44.03	-38.08	38.03
Port Saied (EGY)	3.90	19.59	0.97	102.60	-75.23	423.63
Raqa (SYR)	9.18	23.43	3.99	38.03	-56.52	62.29
Safita (SYR)	20.13	57.48	9.54	102.78	-52.60	78.83
Salamia (SYR)	17.02	18.17	8.80	31.79	-48.27	74.96
Silifke (TUR)	16.35	36.81	9.53	56.87	-41.70	54.51
Sivas (TUR)	29.42	14.16	35.63	13.16	21.11	-7.10
Souda Airport (GRC)	17.53	38.55	9.40	64.98	-46.40	68.55
Swedaa (SYR)	19.32	18.86	9.96	29.85	-48.44	58.29
Tartous (SYR)	18.47	49.04	10.67	77.55	-42.21	58.13

Tel Aviv (ISR)	12.54	43.78	6.02	84.23	-52.03	92.36
Thessaloniki Airport (GRC)	25.67	17.66	19.51	30.97	-24.01	75.34
Tl-Abiad (SYR)	11.60	24.99	5.89	40.06	-49.23	60.30
Tokat (TUR)	44.06	9.31	62.39	7.38	41.60	-20.68
Trepoli (LBN)	18.45	44.18	9.71	77.26	-47.35	74.85
Tripolis Airport (GRC)	26.07	31.68	14.16	45.45	-45.68	43.50
Urfa (TUR)	11.58	41.45	8.47	50.77	-26.84	22.49
Usak (TUR)	28.61	19.21	27.11	19.66	-5.24	2.35
Yozgat (TUR)	27.59	21.00	34.79	17.13	26.09	-18.42

These values from Table 4.5 have been used to draw the scatter plot diagrams in Fig 4.38, which displays distinctively for each of the two periods (1961-1986 and 1987-2012), the values of parameters α and $1/\beta$ and the percent of change. It is apparent that there is a tendency for the points representing α versus $1/\beta$ for two periods to concentrate in distinctively different areas of the scatter plot diagram and becomes more concentrated in the second period.

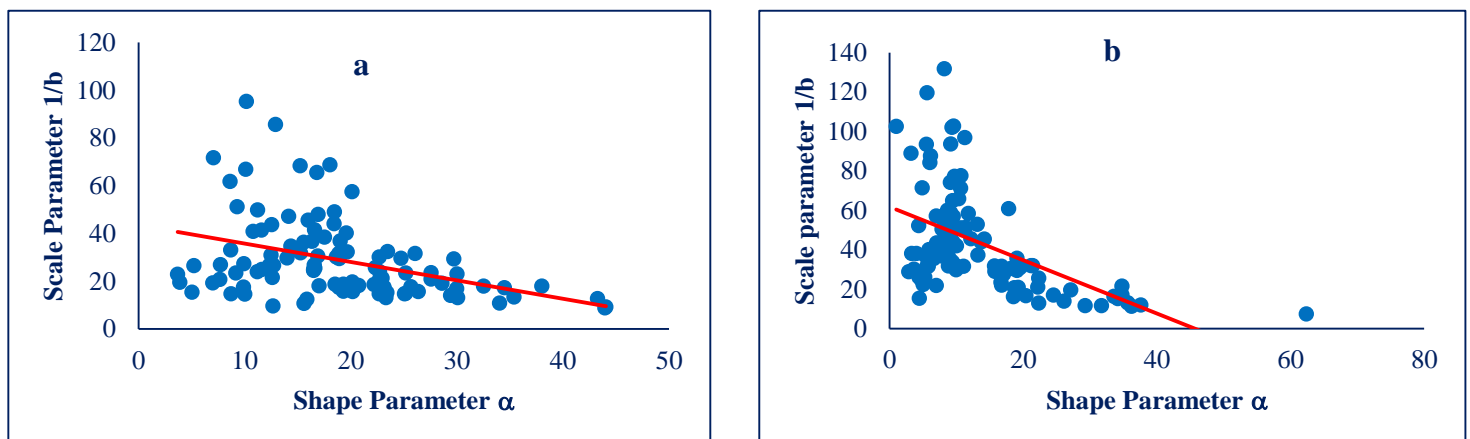


Figure 4.38. Scatter plot diagram of pairs of shape (α) and size parameters ($1/\beta$) for all the rainfall measuring stations, for each of the two 26-yr periods, separately.
a) Period 1 (1961–1986), b) Period 2 (1987–2012).

The results show a statistically significant correlation at ($p=0.01$) between shape parameter α and latitude in both subperiods, $r=0.68$ and $r=0.64$ for the first and second period, respectively (Fig 4.39).

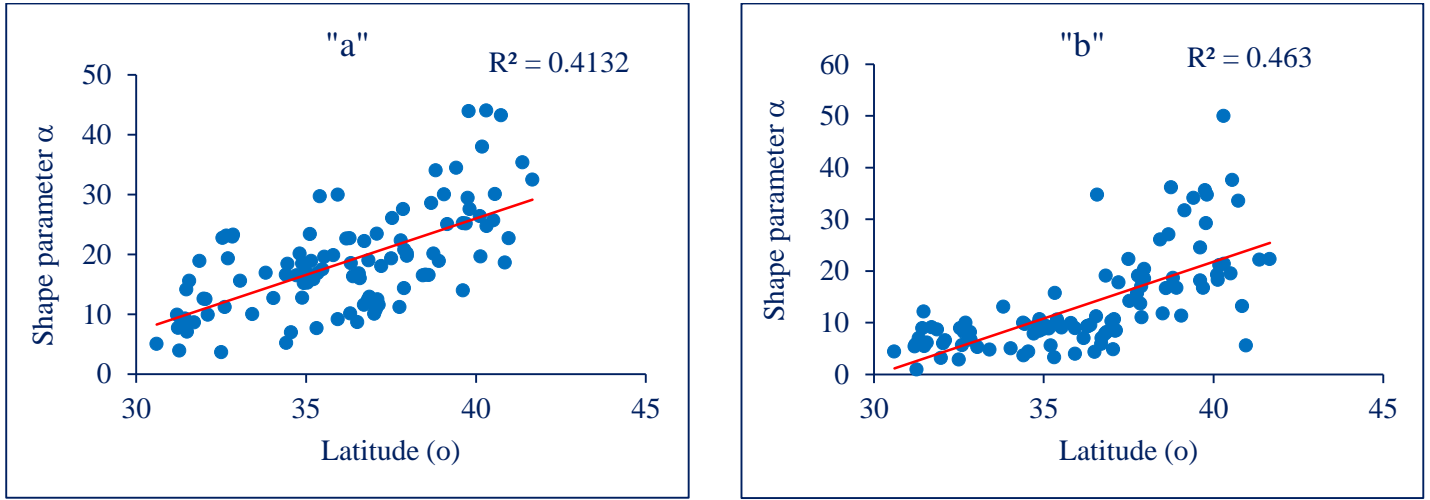


Figure 4.39 Scatter plot diagram of pairs of latitude and shape parameters for all the rainfall measuring stations, for each of the two periods, separately.
a) Period 1 (1961–1986), b) Period 2 (1987–2012).

The shape parameter α ranges between 3.7 and 44.1 in the first period (1961–1986) (Fig 4.40a) and from 0.9 to 62.4 in the second one (1987–2012) (Fig 4.40b). It was seen that the values α in 80% of stations range from 20 to 30 in the first period and these values decrease to be between 10 and 20 in more than 85% of total stations.

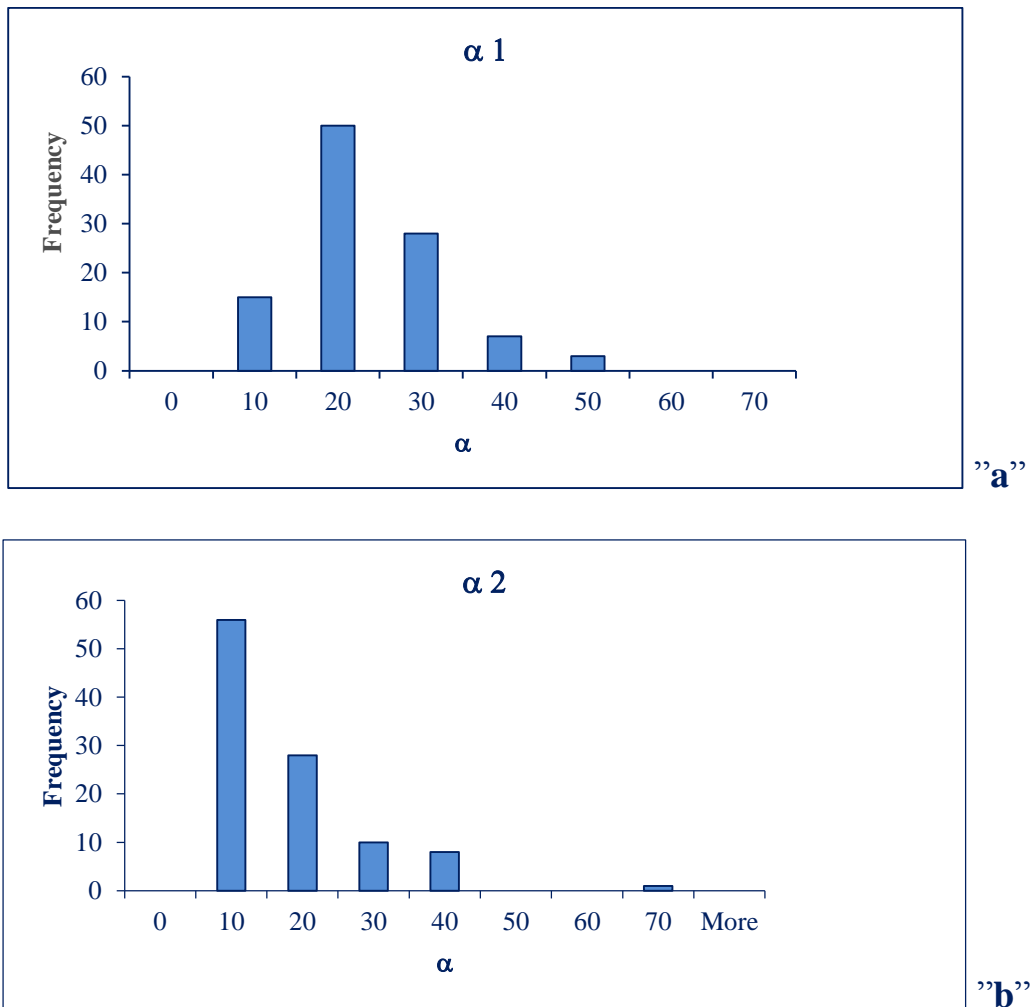


Figure 4.40 Shape parameter distribution for rainfall stations during the two 26-yr periods (a) (1961-1986) and (b) (1987-2012)

There are stations with large α values, whereby the distribution approaches the normal and at the same time for these stations the most likely value of annual rainfall is larger. In the cases where α is small, due to the asymmetry of gamma distribution, smaller annual rainfalls are more likely to happen. The scale parameter $1/\beta$ ranges from 8.91 to 95.28 in the first period and 7.38 to 131.85 in the second period with most stations belonging to the extreme higher tail (e.g. more than 70 percentile).

The fact that most stations are characterized by large values of $1/\beta$ can be interpreted as a characterization of increased occurrence of extreme annual rainfall, at both tails of the distribution, in this period. It was observed that in the second period, both ranges of α and $1/\beta$ values are increased considerably. The increasing in the scale parameter means that the distribution function covers events with extreme rainfall amounts. The clear tendency of the size parameter $1/\beta$ to decrease in the northern parts (Turkey) by the end of the period under study can be interpreted as a tendency for reduced probability of large annual rainfall amounts in the most recent years. This is reflected in a severe water shortage in this area over the last two decades, which in conjunction with the increasing water supply demands.

The results show a north-to-south decreasing trend of the shape parameter which reflects the steep climatic gradients from humid in northern parts, to the semi-arid and arid zones in southern ones. During the first period, the scale parameter increased steadily from the north to the south, reflecting the increasing aridity towards the southern part of the EM. The above drastic changes in the north-south tendencies of the shape and scale parameters are expressed by the percent changes of both distribution parameters during the second period with respect to the first one.

The spatial distribution of the shape parameter of the fitted gamma distribution for the two consecutive periods, as well as the percentage change during the second period, with respect to the first one, are mapped in (Fig 4.41a) and their values were presented in the table above (Table 4.5). As it can be seen, the shape parameters show negative trends in most areas, especially in the southern and

southeastern parts in which the shape parameters have such severe significant decrease. A similar pattern, though opposite in nature-positive is exhibited by the change of the percentage of the scale parameter. The changes in the spatial patterns of the shape and the scale parameters during the two consecutive periods may be indicative of a variety of factors which led to these patterns of change. We can see

an appreciable decrease occurs in the shape parameter, with a concurrent increase in the scale parameter in the second period, compared to the first (Fig 4.41b).

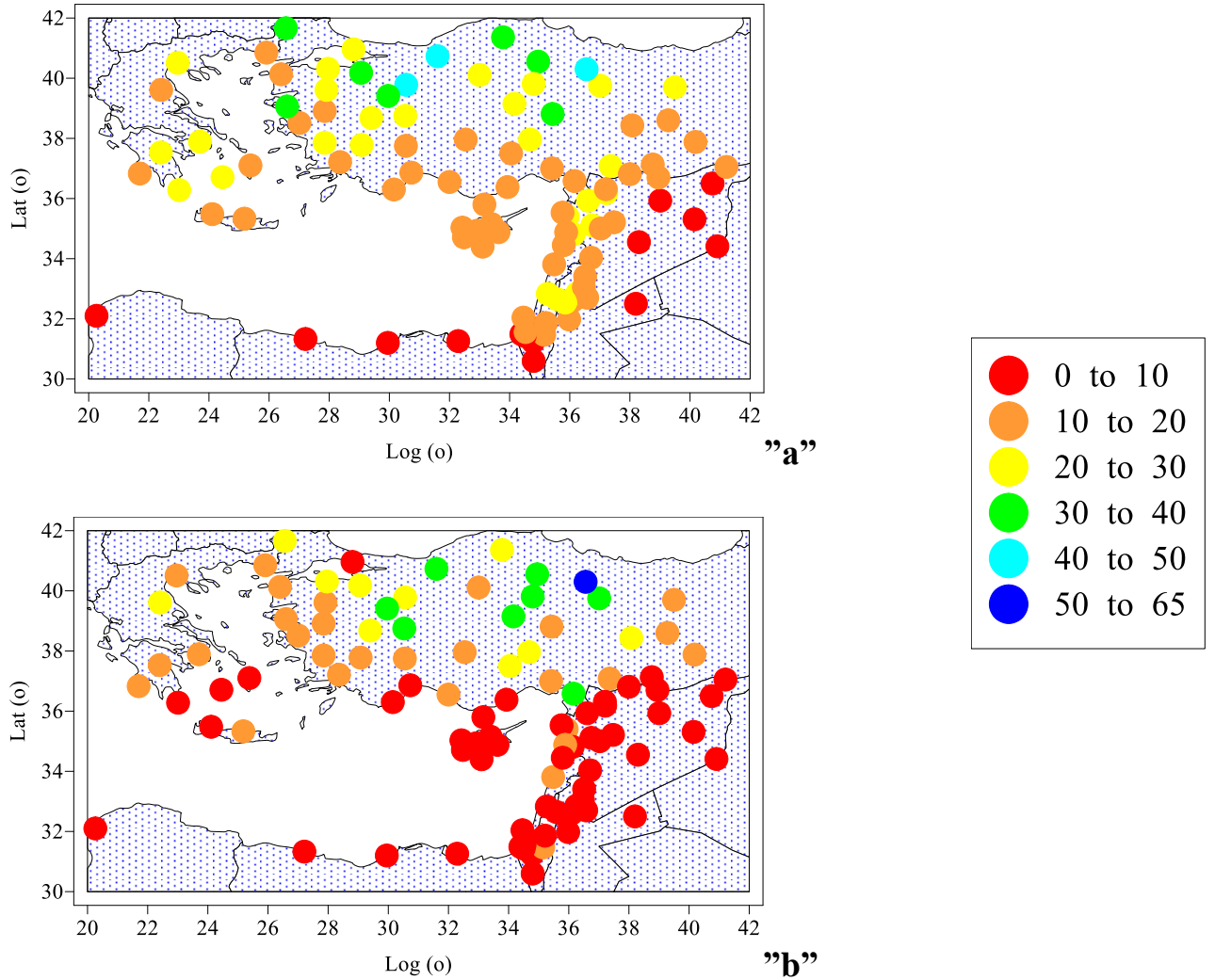


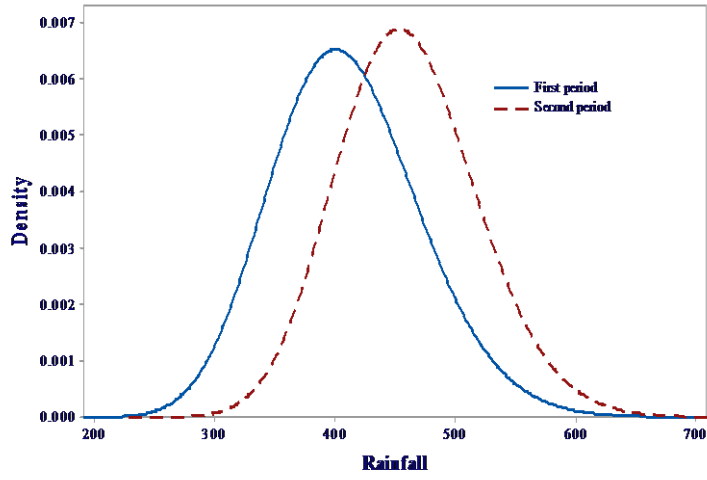
Figure 4.41 Spatial distribution of the shape parameter for (a) the first period (1961-1986) and (b) the second period (1987-2012)

The changes of the distribution parameters were statistically tested at the two levels, 0.01 and 0.05, of significance. These changes are illustrated by the shifting patterns of the PDF curves of the gamma distribution fitted to the annual rainfall amounts of some stations for the two periods. The PDF fitted to the annual rainfall at some selected stations are plotted in Fig 4.42. In general, the percentile changes for this area show an increase in the lower tail and a considerable decrease in the upper tail, which was more detected in the southern and southeastern parts, also showing a trend towards a normal distribution shape. Fig 4.42 shows more

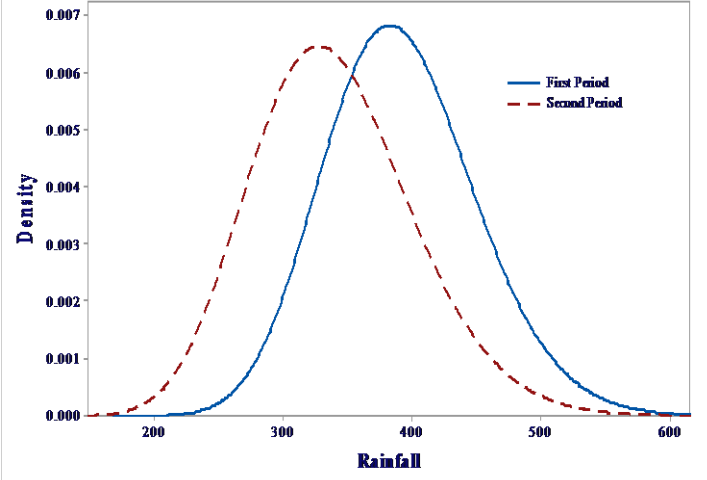
skewed-to-the-left graph in the last period, which reveals significant decreasing in the mean annual rainfall and total annual amounts between two periods.

A parametric statistical analysis of annual rainfall distribution in the southern parts of the EM over the 52-year study period, covering the two 26-yr subperiods, reveals some significant spatial and temporal changes in the shape and scale parameter patterns of the fitted gamma distribution. These changes have some important implications regarding the critical values at the upper tails of the distributions and consequently, the frequency of extreme rainfall events. A similar studies based on temporal changes of parameters α and $1/\beta$ was applied in some Mediterranean areas such as Nastos and Zerefos (2010) in Greece who indicated an increasing tendency in the scale parameter in the western and southern-eastern parts of Greece, especially during the last decade 1991-2000, which in turn revealed the incidence of extreme daily precipitation values since 1980s. Ben-Gai *et al* (1993, 1998) in Israel have also analysed the annual distribution function parameters and found some significant changes in the spatial rainfall distribution patterns in the southern, northern and central parts of Israel. The results from Michaelides *et al.*, (2009) in Cyprus have also shown that there are significant temporal and spatial changes of the annual rainfall amounts, as they can be determined by the characteristics of the gamma distribution.

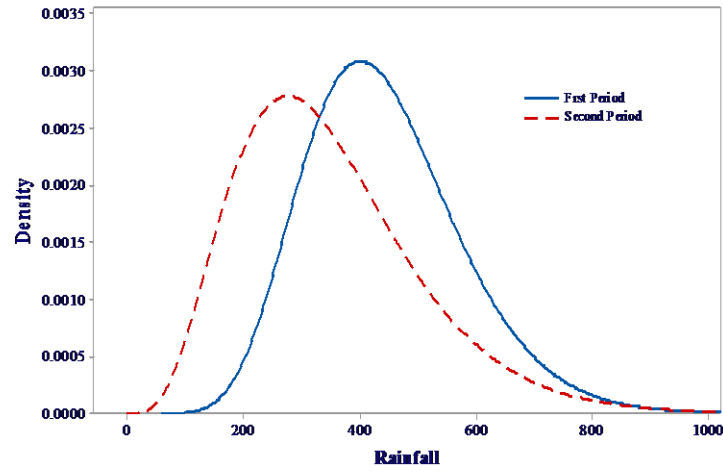
Tokat (Turkey)



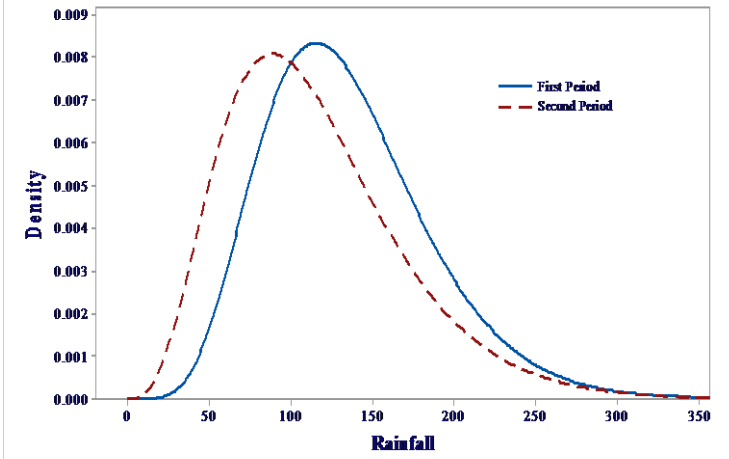
Eskisehir (Turkey)



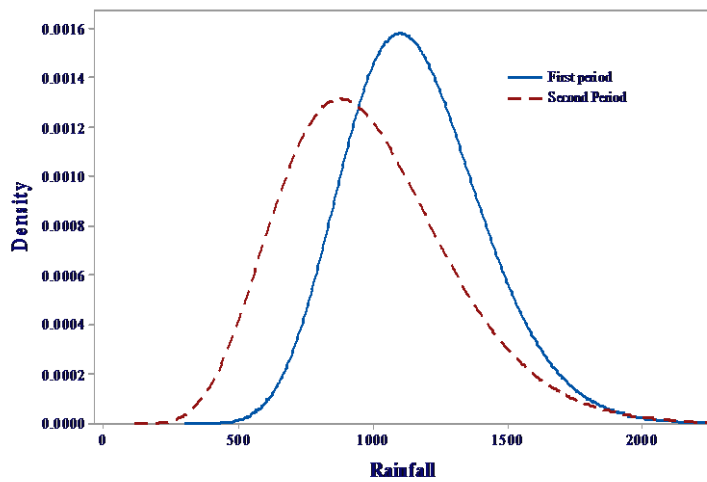
Kamishli (Syria)



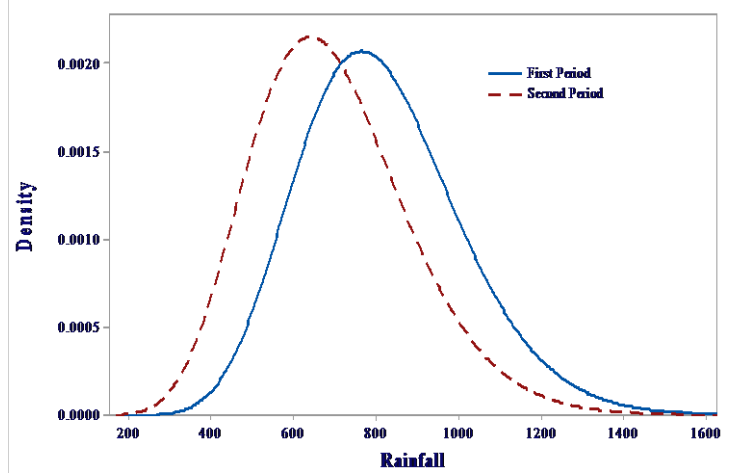
Palmyra (Syria)



Safita (Syria)



Beyrouth Aeroport (Lebanon)



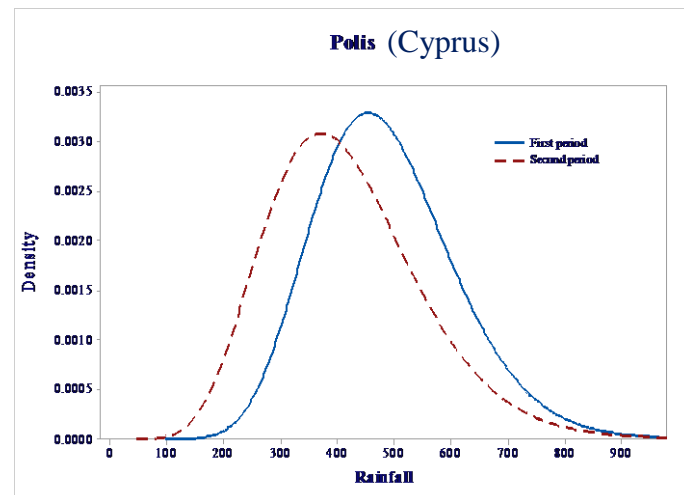
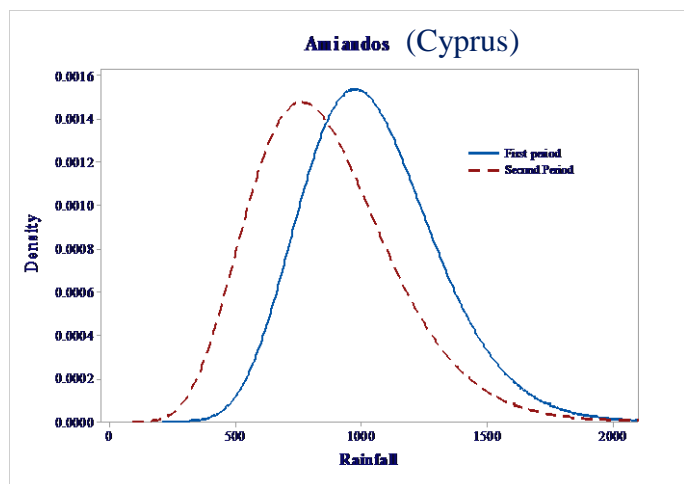
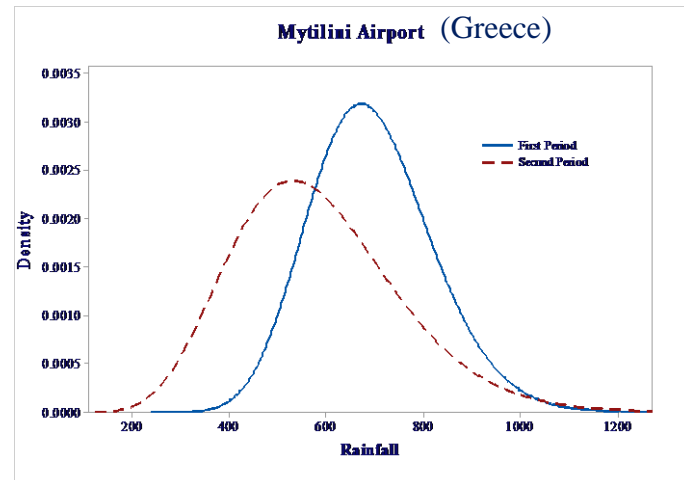
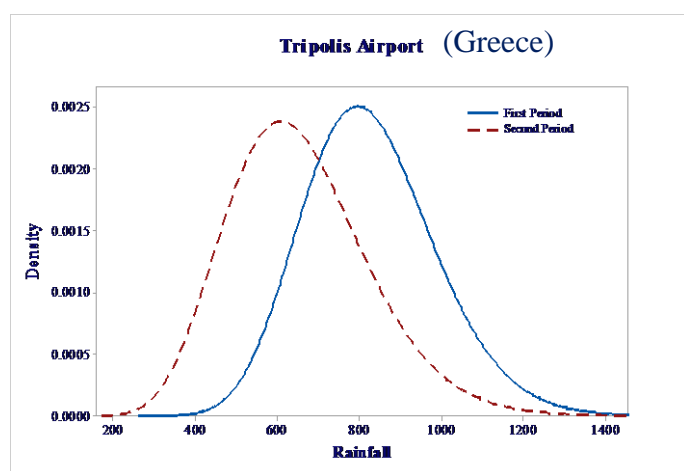
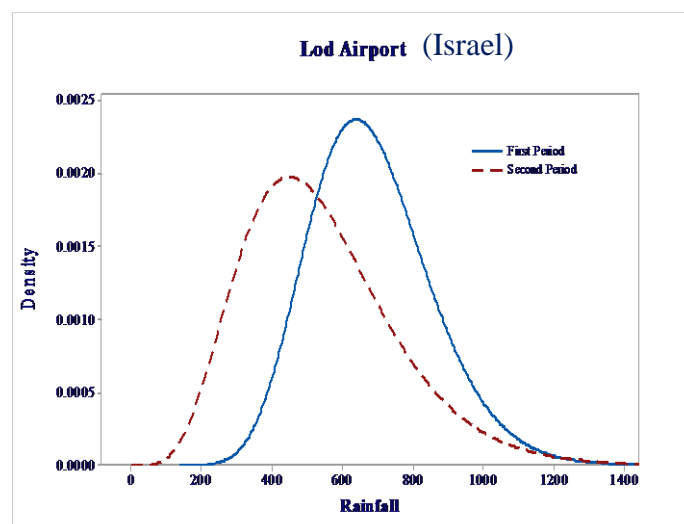
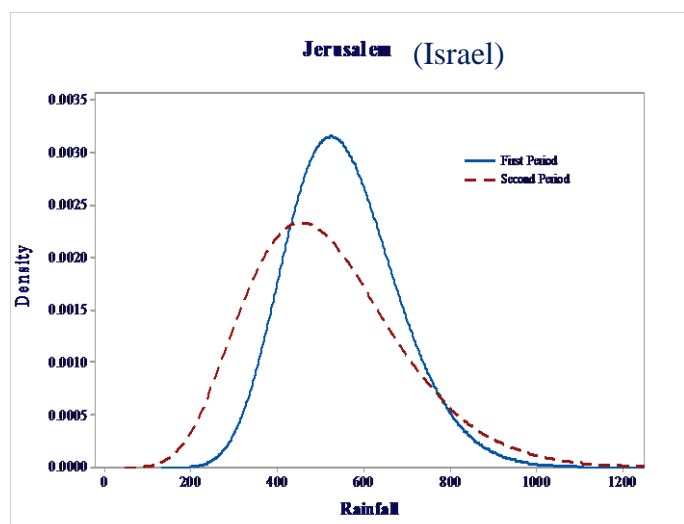


Figure 4.42 Probability density function (PDF) fitted to the annual rainfall in some selected stations during 1961-2012.

Finally, the rainfall distribution in the Mediterranean is very important because this region is at risk of water shortage (Hulme *et al.*, 1999). The accumulated rainfall in the period between September and May accounts for more than the 80 % of the total annual precipitation (Hurrell, 1995). Spatial and seasonal distributions of modern rainfall in the southern parts (Syria, Lebanon, West Jordan and Israel) are controlled by the Mediterranean Sea due to its zonal orientation between three continents and other water basins of the area. It is considered as an important source of heat, water vapour and latent heat for synoptic processes (Trigo *et al.*, 1999; Lionello *et al.*, 2006).

Without the influence of moderating climatic of this sea, this area would be part of the larger northern low middle-latitude warm dry desert extending from North Africa into western Asia.

The possible changes in spatial and temporal distribution patterns and temperature regimes may be of crucial importance to the availability of surface water resources and thus millions of people who are living in this area and may influence governments' policies too (De Luis *et al.*, 2000; Chenoweth *et al.*, 2011). This problem may be enhanced in the Mediterranean because of the constant population increase accompanied by increasing demands for freshwater supply.

4.8 Long term precipitation trends and variability.

The results of statistical analysis at $\alpha = 0.01$ and 0.05 confidence level for annual and seasonal precipitation data using different techniques were approximately similar. Both positive and negative trends were identified by all the tests. All negative trends were significant, and only some positive trends were significant. The annual precipitation is overall decreasing in the EM, except for some stations located in central Turkey, south Israel and Egypt. The most outstanding rainfall decreases are concentrated in the west and south Turkey, and north Syria. On a seasonal time-scale, Mann –Kendall test showed a general trend towards decreasing precipitation in winter and spring which was significant in most areas. On the other hand, autumn precipitation is overall increasing, above

all, in Turkey. Summer season was not considered in these trend analysis because it is almost dry with mean precipitation near 0.0 mm in most of the EM (Fig 4.43).

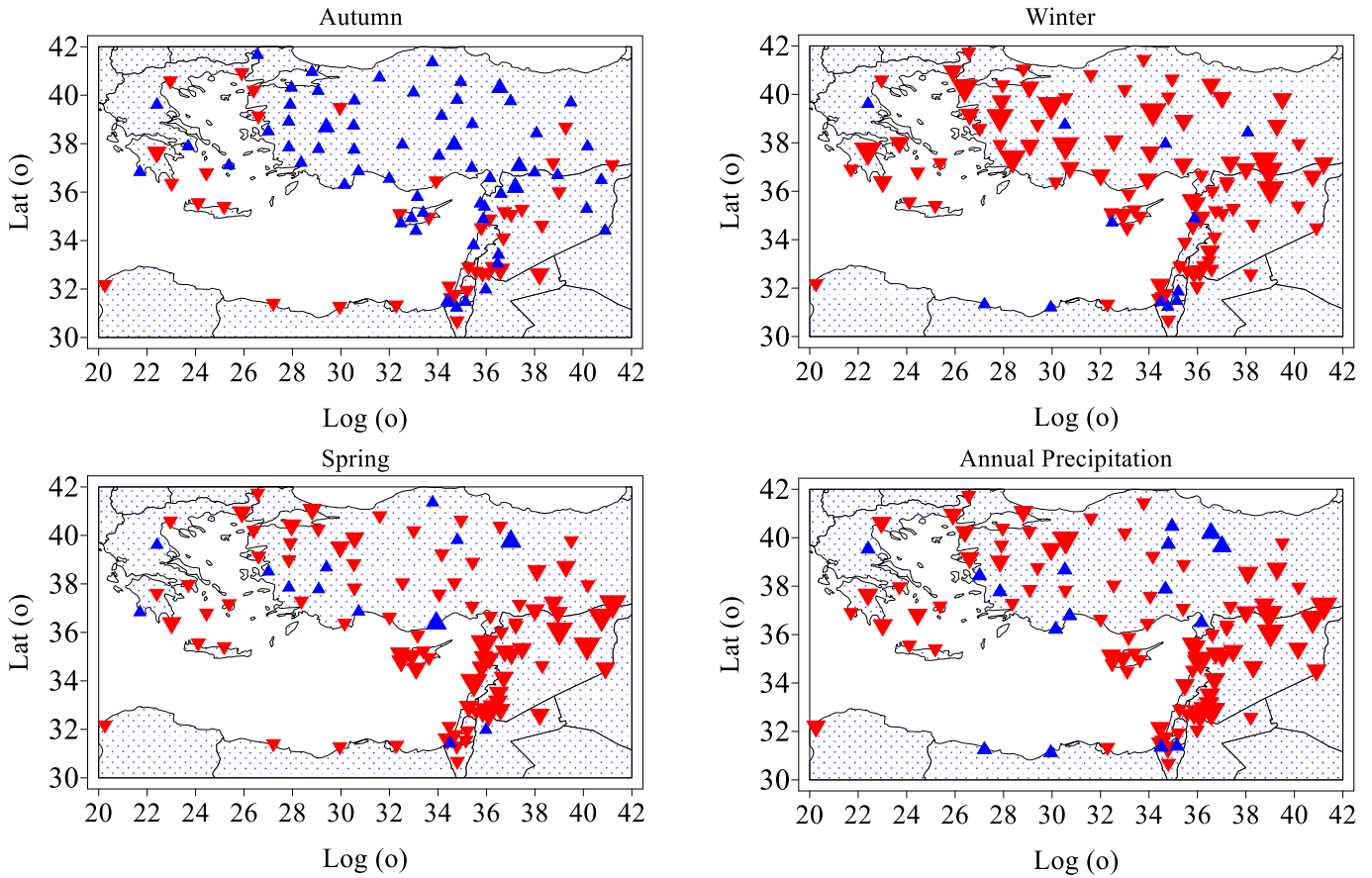


Figure 4.43 Trends in seasonal and annual rainfall over the EM in during 1961–2012. An increase is shown by a blue triangle, a decrease by a red one; big and moderate triangles indicate significance at $\alpha=0.01$ and 0.05, respectively, otherwise small ones are shown.

Fig 4.43 proved that detected trends appeared extremely severe during the last 50 years, when they are significant for almost 95% of the meteorological stations. Evaluation of long term rainfall series on various time scales (annual, seasonal and monthly rainfalls) in some stations showed higher negative trends comparing with short ones. The annual precipitation totals appear to be statistically and significantly (95% confidence level) decreasing in most of the EM during the study period 1961–2012; being much more pronounced during longer periods (1887–2012) in Limassol and Nicosia (Cyprus), (1877–2012) in Beirut Airport (Lebanon) and (1861–2012) in Jerusalem (Israel) (Fig 4.44). The mean annual precipitation for both examined periods exhibits similar patterns with more evident

and significant decrease for the long period. Fig 4.44 depicts the trends of total annual precipitation for the period 1961–2012 and other long periods. During the long period for each station, it is remarkable that the stations from different regions show a statistically significant ($\alpha=0.05$) decrease in the total annual precipitation (-0.61, -0.52 and -1.13 mm/year) in Limassol, Nicosia and Jerusalem, respectively, which was much more pronounced and significant than within the period 1961–2012. For example, an evident decrease of annual precipitation in Limassol was detected in both periods and was statistically significant only during 1887-2012. Decreasing of 15.8% occurred during 1887- 2012, whereas non-less than 10.8% of total annual precipitation was reported over 1961-2012. Fig 4.44 also showed that the values of annual precipitation obtained by the linear regression equations have also decreased in those three stations. For example, in Limassol, a decreasing from 484.1 mm in the long term records (1887-2012) to 446.9 mm in the short one (1961-2012) was shown.

In Nicosia (Cyprus) the mean annual precipitation shows non-significant positive precipitation trend (0.045 mm per year) in the shorter period (1961-2012), where negative trend (-0.52 mm per year) was observed during the longer one (1887-2012). The annual trends of the two different time intervals in Jerusalem (Israel) are quite similar. The annual precipitation trends in this area of the shorter period 1961-2012 is generally higher than those of the longer interval 1861-2012. The 1940s were quite wet period and thus suppressed the positive precipitation trend.

The current studies assess that the future climate change is likely lead to a continuing reduction of moisture availability throughout the whole region (Palutikof *et al.*, 1994). Trigo and Davies (2000) suggested that the decadal-scale changes which are recently observed in the coupled ocean-atmospheric circulation in the northern Atlantic have induced a decline in the intensity of Mediterranean cyclones, which represents the local direct forcing of the decline in Mediterranean precipitation.

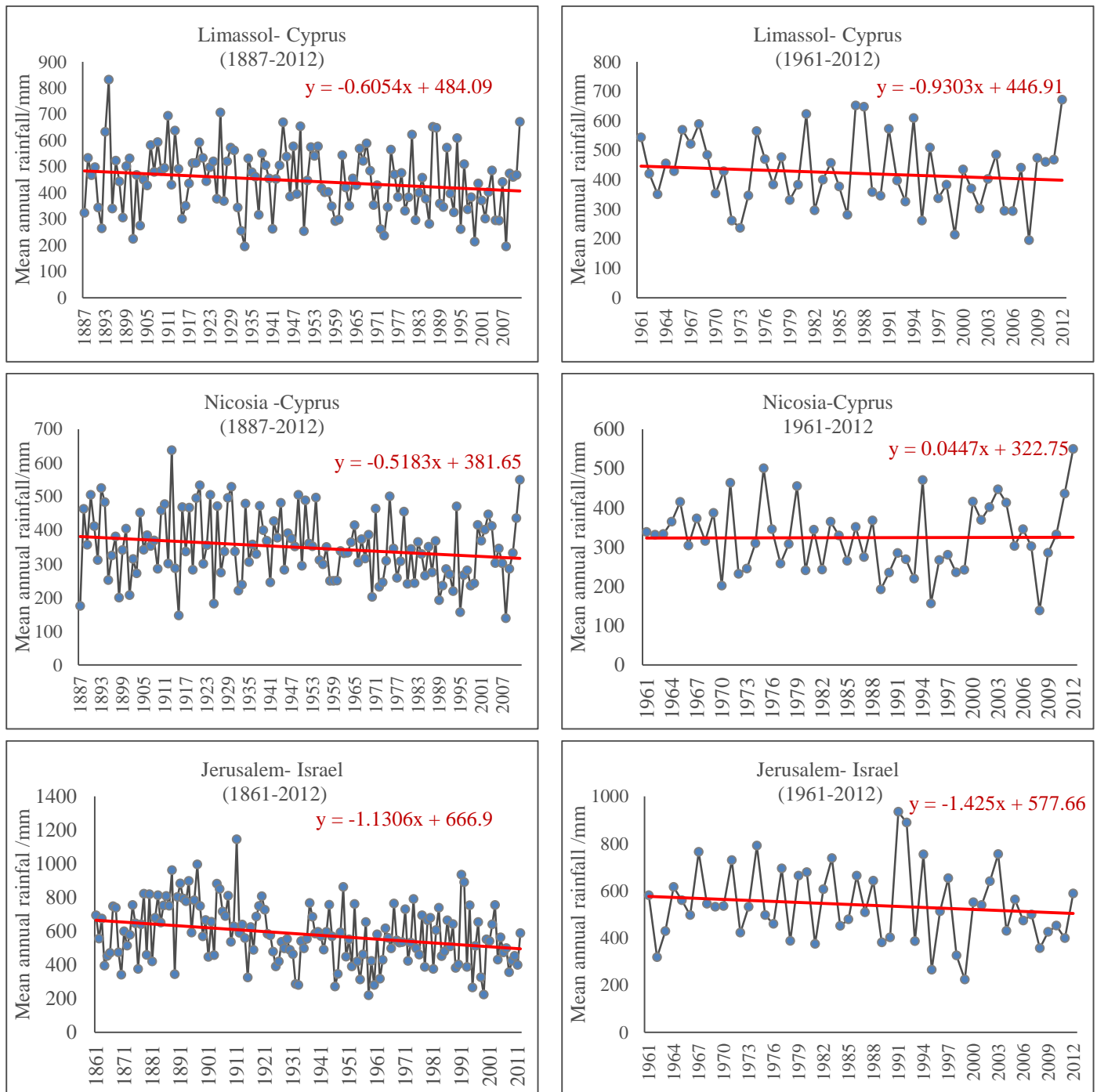


Figure 4.44 Annual rainfall linear trends for different periods in some selected stations from the EM with long period data.

The same results have been proved by Hoerlin *et al* (2012) who have found a change in wintertime Mediterranean precipitation toward drier conditions for the period 1902–2010 and ECSN (1995) demonstrated high regional differences in annual precipitation trends in the 20th century detecting a clear general increase

for northern Europe, with the exception of Finland, and a decrease for southern Europe and the EM. Analysis by Philandras *et al* (2011) showed that statistically significant negative trends of the annual precipitation totals exist in the majority of Mediterranean regions during the period 1901–2009, with an exception of northern Africa (in Fig 4.43 some positive annual trends are seen in Egypt and southern Israel), southern Italy and western Iberian Peninsula, where slight non-significant positive trends appear. The annual number of rain days significantly decreased by 20% in the EM, while the trends are insignificant for west and central Mediterranean (Philandras *et al.*, 2011).

Precipitation patterns for seasons represent significant positive or negative at both 0.01 and 0.05 confidence levels over the EM. However, there is a considerable amount of precipitation decrease for winter and spring, which is statistically significant at $\alpha = 0.01$ and 0.05 confidence during the period of 1961–2012. On the other hand, autumn showed an overall increasing tendency, above all, in Turkey and northern Syria; however, most of these positive trends are not statistically significant.

The annual decreasing trend of precipitation in the EM was also found in EOF1 (Egypt, Israel and Jordan), EOF3 (northeast Syria and southern Turkey) and EOF4 (west Turkey and Greece) regions (Figs 4.2 and 4.45), especially in recent years, whereas the EOF2 (Cyprus, littoral Syria and southwest Turkey) and EOF5 (mid and east Turkey) regions have detected a weak insignificant increase.

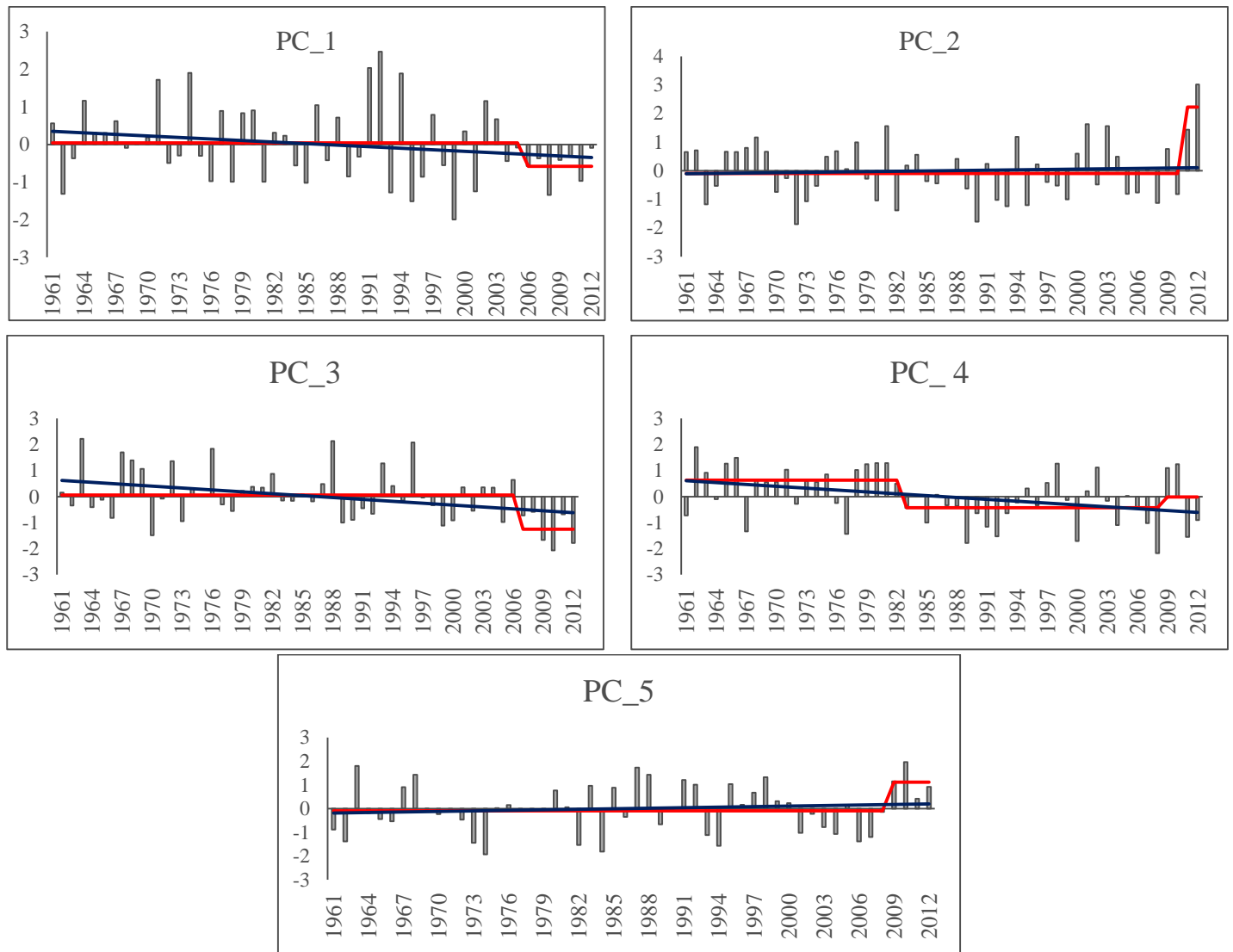


Figure 4.45 Scores time series of the PCs of annual precipitation. Blue lines denote the fitting linear trend, the red ones represent the annual precipitation before and after the regime shift found by the STARS algorithm.

The time scores associated with the EOFs patterns, presented in Fig 4.45, showed a non-significant downward trends in EOF1, EOF3 and EOF4, while both of EOF2 and EOF3 detected weak upward trends. The STARS algorithm test (RSI) reveals the same shift after 2005 ($\alpha= 0.05$) as found for the individual stations. This result leads to the conclusion that the analysis of the PC scores is a powerful tool for detecting a climate signal in the data set.

Results for winter and spring precipitation have revealed an overall decreasing tendency in all regions which was statistically significant at $\alpha= 0.05$ in both EOF1 (Turkey and North Syria) and EOF3 (western parts of

Turkey and Greece) and at $\alpha=0.01$ in EOF4 (eastern and mid parts of Syria) for winter and EOF1 (Syria and southeastern parts of Turkey) for spring precipitation (Fig 4.2). These changes have been detected by a STARS test during the last ten years which reflect the big variability in seasonal precipitation in these regions (Fig.4.46). Non-significant increasing in autumn rainfall reported in all regions except of EOF3 (east and northeast Turkey) which was significant at $\alpha=0.05$.

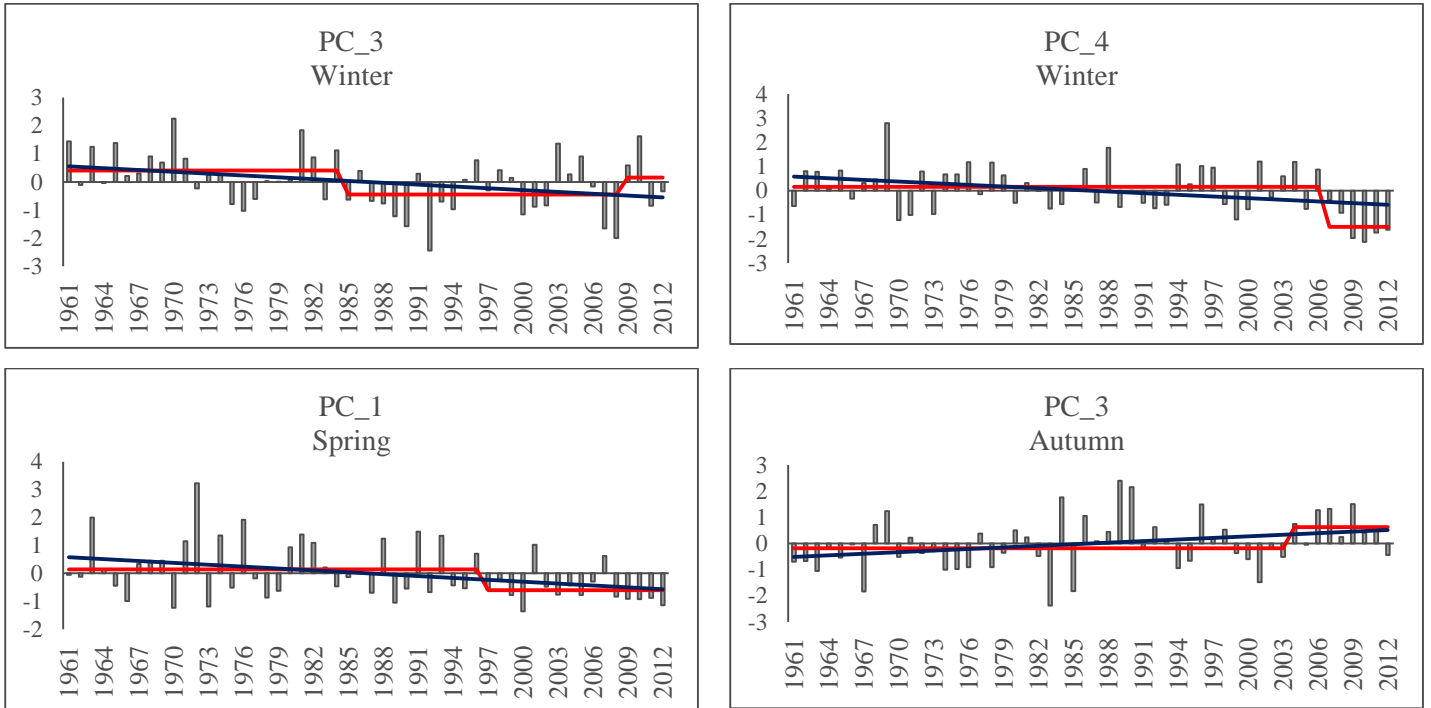


Figure 4.46 Time scores series of the significant PCs of seasonal precipitation. Blue lines denote the fitting linear trend, the red ones represent the annual precipitation before and after the regime shift found by the STARS algorithm.

In all sub-regions, the decreased tendency in total annual rainfall is because of the decreasing rainfall amounts in winter and spring. These reductions are considered as the main factors of the recent droughts, and water supplies and river discharge shortage. The results of change point detection indicated that most of the negative significant mutation points in annual and seasonal precipitation started from 1990s (Fig 4.47). This agrees with the results obtained by (Amanatidis *et al.*, 1993; Türkeş, 1996; Zangvil *et al.*, 2003; Giannakopoulos, 2010) who found a general downward trend over most of Greece, Cyprus, Israel and Turkey with abrupt decreases during the last 20 years.

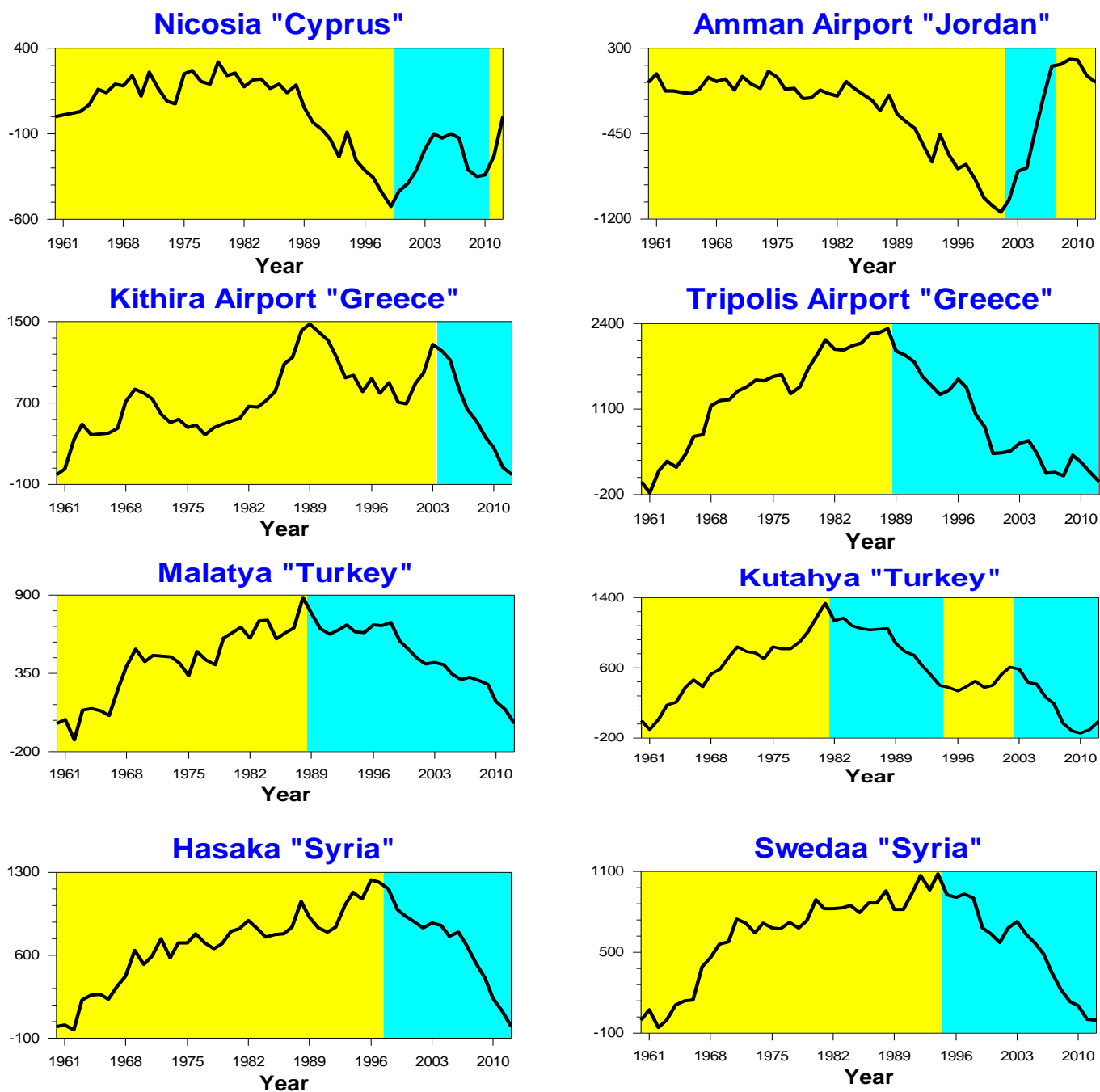


Figure 4.47 Abrupt changes in annual precipitation between 1961 and 2012, as determined by CUSUM charts for some selected stations over the EM.

The most important reasons for mutation point in precipitation and series include station relocation, change in instruments, changes in observation time and methods for calculation of mean and climate changes and changes in atmospheric circulation (Smadi, 2006). For example, abrupt changes in the surface circulation and water masses have been recognized at decadal time scales in the EM

(Malanotte-Rizzoli *et al.*, 1999) as well as Roether *et al.* (1996) and Klein *et al.* (1999) demonstrated an abrupt and major change occurred in the oceanography of the EM during the late eighties of the last century which affected the climatic conditions. A global analysis has shown that abrupt changes of rainfall are more likely to occur in arid and semi-arid regions due to the strong positive feedbacks between vegetation and climate interactions (Narisma *et al.*, 2007). Recent studies have also pointed to the role of rainfall seasonality in abrupt climate change in the Mediterranean region (Denton *et al.*, 2005; Dormoy *et al.*, 2009; Pross *et al.*, 2009). These abrupt changes may be indicative of a transition into another climatic/rainfall regime for the sudden and persistent nature of recent drought events (Scheffer *et al.*, 2001; Alley *et al.*, 2003). This means that the eastern Mediterranean faces a severe water crisis and water supply decreases due to rapid and abrupt climate change, while demand increases due to rapid population growth (Tielborger *et al.*, 2010).

In each subregion included in the annual EOFs, long-term changes and trends in their monthly precipitation time series data were calculated to evaluate long term temporal variability of monthly precipitation in each area. Precipitation series for total seasonal time scale in each subregion obtained by seasonal EOFs were also analysed to determine the slope of the liner trend in each one. The significance of trend for the precipitation amounts was identified by the Mann–Kendall test for the general period 1961–2012, then the direction and magnitude of significant trends were then calculated using the Sen’s slope estimator (Sen, 1968).

Table 4.6 shows the results of applying the Mann–Kendall and Sen’s slope test values, for all five subregions during 1961–2012. This study showed that there is a great similarity between the statistical results from the Mann–Kendall and Sen’s statistical methods at $\alpha = 0.05$ significant level. A similar conclusion has been confirmed by Partal and Kahya (2006), Tabari and Hosseinzadeh Talaei (2011) and Gocic and Trajkovic (2013).

Table 4.6 Monthly, seasonal and annual results of Mann–Kendall and Sen’s slope tests of least square linear fitting for all subregions over the period 1961-2012.

	EOF1		EOF2		EOF3		EOF4		EOF5	
Month	M K Z value	Sen’s slope	M K Z value	Sen’s slope	M K Z value	Sen’s slope	M K Z value	Sen’s slope	M K Z value	Sen’s slope
January	-0.53	-0.12	-0.80	-0.46	-1.46*	-0.32*	-0.96	-0.28	-0.96	-0.28
February	0.81	0.22	-1.32*	-0.54*	-1.10	-0.22	-0.50	-0.14	-0.50	-0.14
March	-1.03	-0.16	-1.65 *	-0.44*	-2.12 *	-0.40*	-1.29	-0.27	-1.29	-0.27
April	-1.99 *	-0.17*	-0.61	-0.13	-1.42*	-0.24*	-0.04	-0.01	-0.04	-0.01
May	0.61	0.01	-0.34	-0.03	-0.56	-0.05	-0.31	-0.05	-0.31	-0.05
September	1.16	0.00	0.12	0.01	1.17	0.02	0.50	0.08	0.50	0.08
October	-0.85	-0.08	-0.58	-0.17	0.04	0.00	1.13	0.28	1.11	0.28
November	-0.09	-0.02	0.89	0.34	0.43	0.06	-0.53	-0.17	-0.53	-0.17
December	-1.14	-0.39	-0.99	-0.58	-2.36 *	-0.55*	-1.63	-0.56	-1.63	-0.56
Autumn	0.13	0.01	-0.97	-0.01	2.53 *	-0.42*	0.23	0.02	-0.45	-0.01
Winter	-0.50	-0.01	-0.92	-0.01	-2.38 **	0.41**	-2.15 *	-0.41*	0.54	0.01
Spring	-2.77 **	-0.42**	-0.99	-0.01	-0.34	-0.01	-0.72	-0.01	0.81	0.01
Annual	-0.62	-0.01	-0.89	-0.01	-0.73	-0.01	0.29	0.01	-0.07	-0.01

** Significant trends at a $\alpha=0.01$ significance level

* Significant trends at a $\alpha=0.05$ significance level

The analysis, including all months from January to December (except June, July and August) (JJA) were applied to evaluate the long-term variations and trends in monthly precipitation over all subregions (Table 4.6).

During winter (December, January and February) and spring (March, April and May) seasons, almost all results pointed out to a reduction in monthly

precipitation during over all sub regions, which occurred most strongly in the months of December, March, April and January. In EOF3 (southeast Turkey and northeast Syria), the results are statistically significant at $\alpha=0.05$ in January, March, April and December are ranging between 5.5 mm per decade in December and 2.4 mm per decade in April. Other trends in monthly precipitation in EOF3 precipitation series in these two seasons were not significant. The EOF2 (west and south Turkey, Cyprus, Greece, Lebanon and west Syria) has also showed this decreasing tendency in all monthly precipitation which was statistically significant at $\alpha=0.05$ in both February and March. Reduction in monthly precipitation (1.7 mm per decade) in April was also detected in EOF1 (Libya, Egypt, Israel, Jordan and south and mid Syria). As shown, the majority of the trends in the monthly precipitation series in autumn (September, October and November) were positive especially in September and all of them were not statistically significant.

On the seasonal time scale, the significant decreasing trend at $\alpha=0.01$ was detected at EOF1 (Syria and southeast Turkey) in spring (4.2 mm per decade) due to the high negative tendency of rainfall amount in April, while both EOF3 (Greece, east and southeast turkey) and EOF4 (Cyprus) were detected significant decreasing trends in winter (4.1 mm per decade for both of them) at $\alpha=0.01$ and $\alpha=0.05$, respectively. This decreasing tendency in winter precipitation has basically resulted from the strongest downward trends in December in these two regions. In autumn, the significant increasing trend was found only at the EOF1 (Syria, Lebanon, Jordan, Israel, Cyprus and south Turkey). The annual trends are not statistically significant. This appears to be resulted from the high inter-annual variability and differing trends in individual months that make up the various seasons. This increase in dry spring seasons, and wet autumn seasons which, were observed even in wet years will affect the timing when crops receive water and their yields (Ramos, 2001).

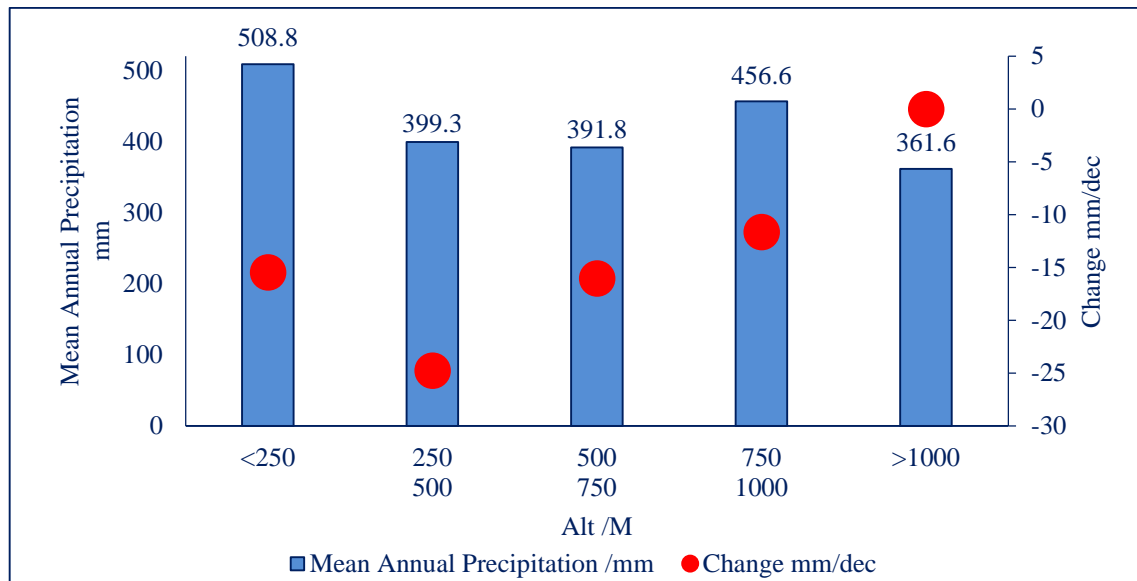
These results agree with previous studies which demonstrated a decreasing trend in winter rainfall in the Mediterranean region in the recent decades marked by widespread decreases in the Mediterranean area linked to particular changes over time in several of the associated circulation patterns. Thus, different regional

rainfall changes are integrated into an overall interrelation between Mediterranean rainfall patterns and large-scale atmospheric circulation (Jacobeit, 2000; Dunkeloh and Jacobeit, 2003). As well as, Kitoh *et al* (2008) and IPCC (2013) mentioned to the projected decrease in precipitation is concentrated in the Mediterranean Sea and coastal areas of Southern Turkey, Syria, Lebanon and Israel mainly projected in the winter and spring.

The concomitant changes in the atmospheric circulation, a recent trend towards rising pressure, especially since the 1970s, is well documented for most of the Mediterranean area (Schonwiese *et al.*, 1994; Brunetti *et al.*, 2002). In particular, the strengthening of sea level pressure during the winter months, both at the surface and at upper tropospheric levels, is highly significant (Schonwiese *et al.*, 1994 Brunetti *et al.*, 2002). This is related to the accumulation of positive modes of the NAO in winter during the last few decades (Hurrell and van Loon, 1997; Jacobeit *et al.*, 2001; Philandras *et al.*, 2011). For instance, Türkeş and Erlat (2006) have pointed out that annual and, in particular, long winter precipitation amounts in Turkey tended to decrease during the positive NAO phase and to increase during the negative one.

Additionally, in spring, mostly insignificant pressure increases are identified in the Mediterranean area, with the greatest enhancement in the southwestern and southeastern sector (Schonwiese *et al.*, 1994; Schonwiese and Rapp, 1997; Brunetti *et al.*, 2002). Lionello and Giorgi (2007) suggested in their study that the reduction in the number of Mediterranean cyclones is a main contributor to the projected decline in precipitation in the South and East Mediterranean regions in winter.

The highest decrease of annual mean precipitation occurred in the stations up to 250-500 m (-25mm /decade), whereas the stations with high altitude (>1000m) detected non-significant trends near zero, (0.002 mm per decade) (Fig 4.48.).



Number of
Stations

Figure 4.48 Trend in precipitation over the EM with altitude over the EM

Despite the large spatio-temporal variability of precipitation, the large-scale circulation changes at different heights can explain a significant part of this variability. The advective processes can be considered as an important factor which controls the regional change of precipitation especially in winter. Furthermore, many shifts in general atmospheric circulation can associate the precipitation changes such as jet streams, storms, monsoon circulations, or can be accompanied by changes in the thermodynamic structure of the atmosphere (Jacobeit 2000; Giorgi, 2002).

These changes in rainfall direction and rainfall distribution may add to existing problems of desertification, water scarcity, crop production and food production, while also introducing new threats to human health, ecosystems and national economies of countries.

4.9 Meteorological drought analysis using several drought indices

In this study the overall meteorological drought vulnerability in the EM was assessed by reconstructing historical occurrences of droughts at varying time steps and drought categories by employing several meteorological drought indices.

4.9.1 Study of observed spatial characteristics of meteorological drought using the Standardized Precipitation Index (SPI)

SPI is a drought monitoring index developed by McKee *et al.* (1993) to quantify the rainfall deficit for multiple timescales. This index uses long term rainfall data for a specific period, which will be fitted to a probability distribution. The PCA is employed to analyze the spatial variation of drought severity in the region. It is an important technique to identify spatially homogenous drought regions (Karl and Koscielny, 1982; Bonaccorso *et al.*, 2003; Vicente-Serrano *et al.*, 2004)). The loading generated by the PCA can be mapped to show the spatial patterns of drought characteristics and the temporal patterns of drought can differ due to the temporal succession of SPI values.

In this study, the SPI used to explore the spatial and temporal features of meteorological droughts in the EM by the identification and probabilistic characterization of historic drought events on precipitation data during the period 1961-2012. From the SPI series of EM, we applied fifth PCAs, one for each time scale, to examine if there is any change in drought spatial patterns of drought in relation to time scales of drought event or they are stable by the changing of the time period. Regarding the PCA, the number of components that explain a significant portion of the total variance was determined by means of the Scree test (Cattel, 1966), then the retained components were rotated using a Varimax procedure (White *et al.*, 1991; Serrano *et al.*, 1999). The number of PCA components extracted using the SPI series increased as the time scale increased (Table 4.7). It can be seen that explained variance was more distributed among the components for the longer time scales, than for the shorter ones and the total explained variance was greater too. Vicente-Serrano (2006) has also found that the number of components increased as the time scale did, which means great spatial

complexity in drought analysis and uncertainty in drought classification, especially at the 24 month time scale and above. Table (4.7). Results obtained from PCA analyses for SPI at different time scales over the EM during 1961-2012.

Total	% of variance	Cumulative %	Total	% of variance	Cumulative %
3month			6 months		
13.84	13.43	13.43	13.34	12.95	12.95
11.16	10.83	24.27	12.47	12.11	25.06
9.99	9.70	33.96	10.12	9.83	34.89
8.88	8.62	42.58	8.93	8.67	43.55
7.35	7.13	49.72	8.13	7.89	51.44
3.99	3.87	53.59	4.91	4.76	56.21
3.98	3.86	57.45	2.85	2.77	58.98
3.83	3.72	61.17	2.42	2.35	61.32
			2.16	2.10	63.42
9 months			12 months		
13.76	13.23	13.23	14.40	13.85	13.85
13.70	13.17	26.40	13.80	13.27	27.12
11.32	10.88	37.28	11.42	10.98	38.10
8.91	8.57	45.85	9.16	8.81	46.91
8.33	8.01	53.86	8.09	7.78	54.69
4.64	4.46	58.32	5.13	4.94	59.62
3.00	2.88	61.20	3.37	3.24	62.86
2.62	2.52	63.72	2.61	2.51	65.36
2.35	2.26	65.97	2.50	2.40	67.76
2.26	2.18	68.15	2.22	2.14	69.90
2.10	2.02	70.17	2.18	2.09	71.99
			2.16	2.08	74.07
24 months					
26.45	25.93	25.93			
15.90	15.59	41.52			
7.40	7.26	48.78			
7.40	7.25	56.03			
4.40	4.31	60.34			
4.11	4.03	64.37			
3.19	3.13	67.50			
3.08	3.02	70.51			
2.98	2.92	73.43			
2.76	2.70	76.14			
2.72	2.67	78.80			
2.30	2.25	81.06			
2.18	2.14	83.19			

At 3- months scale, 8 components were extracted which explained 61% total variance of the SPI series. Using series for 6 month time scale, 9 components were extracted which explained 65% of total variance. For 9, 12, 24 months, the number of components obtained increased to 10, 12 13, respectively. The percentage of total variance explained by these components was 70%, 74 and 83%, respectively. This observation can reflect a higher distribution of total variance among the components selected. At 12 and 24 months, it is clear that the number of components was significantly greater than in the shorter scales (3 and 6 months).

The first six patterns which explained about 54 %, 56%, 58%, 60% and 64% of the total variance in the original SPI series at 3-, 6-, 9-, 12- and 24 month time scales, respectively were mapped (Fig 4.49).

The spatial extent of the first six component series was characterized by mapping the values of the factorial matrix (loadings). For a given time scale this matrix contains the correlations between each component and the SPI series loadings at the 103 rainfall stations. We considered the representative region based on loadings larger than 0.5 (White *et al.*, 1991; Lopez-Bustins *et al.*, 2015).

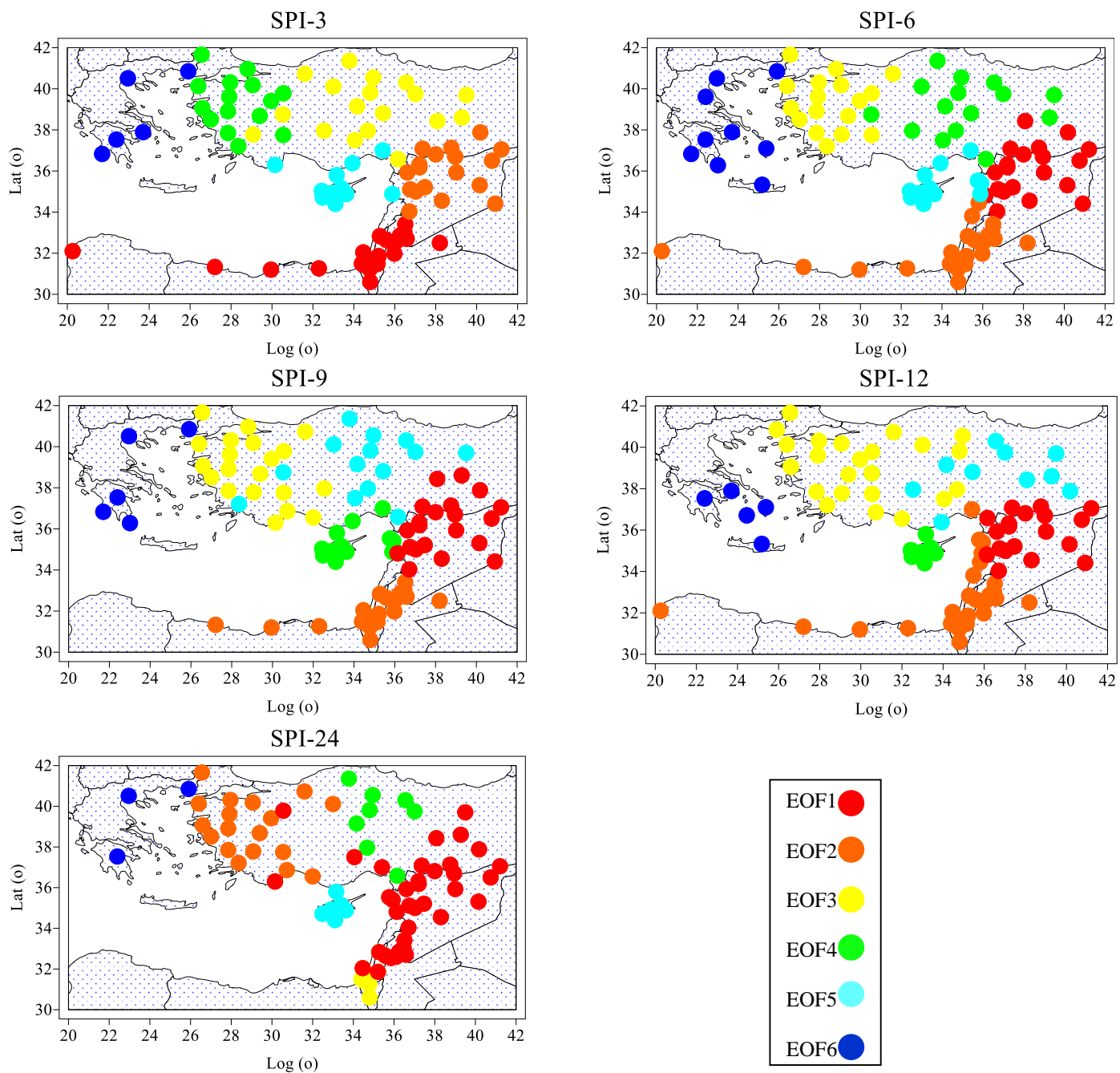


Figure 4.49 Spatial distribution of the first sixth PCs loadings (EOFs) for SPI series at different time scales.

For a 6-months' time scale, spatial drought patterns were similar to the shorter ones (3 months'), although the spatial pattern of first component was replaced by the second and the third by the fourth. In spite of these small differences, the patterns were consistent with those obtained for shorter time scales, and their spatial order was also similar.

At 24 months' time scale, we can see that the spatial distribution of drought caused by higher number of components extracted was greater comparing with those in shorter time scales (1, 3, 6 or 9 months'). On this time scale, the area represented by each component was smaller and it can be found that some areas represented by a single component at 1, 3, 6 or 9 months' time scale were divided. For example, Turkey was represented by only two components (3 - 4 for SPI-3) and (3-5 for SPI-9 and SPI -12) at all short time scales, whereas at 24 months, it was represented by three components (1 and 2 and 4) (Fig.4.49). The southern and southeastern parts of the EM were also represented by two components (1-2) at shorter time scales, where at 24 months, this area was represented by three components (1-2 and 3). It can be seen that at 24-month time scale the areas represented by each component had small surfaces comparing with those obtained in shorter periods, and new components for smaller areas were also presented and identified, which indicated more complexity in the spatial distribution patterns of drought over the EM.

Fig 4.49 shows that between the first three components PC1, PC2 and PC3, the regions with significant correlation (higher than 0.6) do not overlap, being clearly spatially disjunctive. They explain between 10% and 25% of total variance. For all SPI time scales, except for 24 months SPI, both first and second components highlight areas located in the south and southeastern parts of the EM across Syria, Lebanon, Jordan, Israel, southeast Turkey and northern parts of Egypt and Libya. For the SPI at the 24 month time scale, it can be seen that the first component highlights the eastern parts of the EM (Syria, Lebanon and east Turkey) and the second one covers the western parts of Turkey. They explain 26% and 17% of total variance respectively. The third component covers whole Israel. In all time scales, the sixth component covers Greece and explains about 4% of total variance.

In these classifications, the first component, which explained the highest percentage of variance (about 13% for 3, 6, 9 and 12 months' time scale) and (25% for 24 time scale) represented a drought evolution in a big area in the southern parts of the EM (Syria, Lebanon, Jordan, Israel and south Turkey), north Egypt and north Libya. These results detected that the shortest time scales produce clear

spatial patterns of drought evolution and the spatial distribution in these regions showed an evident coherence due to the big homogeneity in this area. These results agree with those obtained by Vicente-Serrano (2006) in Iberian Peninsula using different time scales for SPI. The spatial loadings are almost positive having higher values in these two areas, and the correlations among the values of this component and of the SPI series are higher than 0.80 which means a clear individualized pattern. Thus, the fluctuating time series scores of these particular regions give a clear idea about the dry and wet conditions. The PC3 explains between 10 and 11 % of the total variance for 3, 6, 9 and 12 months' SPI and only 7% of the total variance is explained for SPI-24. The EOF4 explained between 4-9% of the total variance with higher values of loadings in the northern parts in mid and north east Turkey for SPI-6, Cyprus for SPI 9 and 12 which have the highest rainfall rates compare with other parts of the EM. The spatial difference between the first four EOFs may be caused by a difference in seasonal precipitation regime. The south and southwestern parts of the EM do not receive precipitation in summer and almost has a long dry season (as mentioned before) and more rain falls over this region in winter. On the other hand, Cyprus receives between 2% and 4% of their rainfall in summer, while the north and northwestern parts (Turkey) can receive between 5-16% of their annual rainfall in summer.

The previous results indicated that with these main components a spatial classification is achieved, with many well-defined regions (EOFs) which differed depending on the time scale. They are located in the south, south east, northwest, northeast and the intermediate region (Cyprus) which promotes the transition from the wet north to the arid and semiarid south. The spatial classification was similar for all the time scales used.

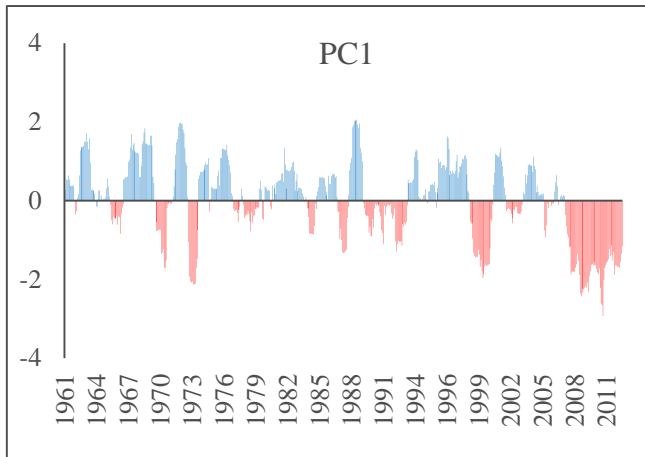
4.9.1.1 Temporal variability of meteorological drought using the Standardized Precipitation Index (SPI)

The temporal evolution of the main PCs using their score values is shown in Fig 4.50. This figure shows that most areas of the EM suffered several extreme droughts, starting at the beginning of the 1970s, mid 1980s, 1990s, and end 2000s

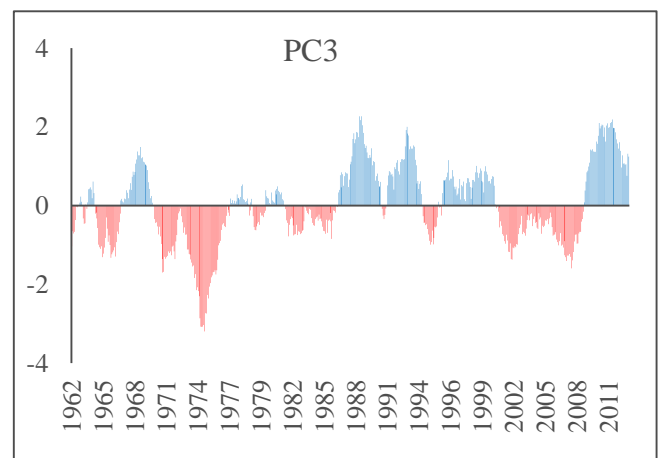
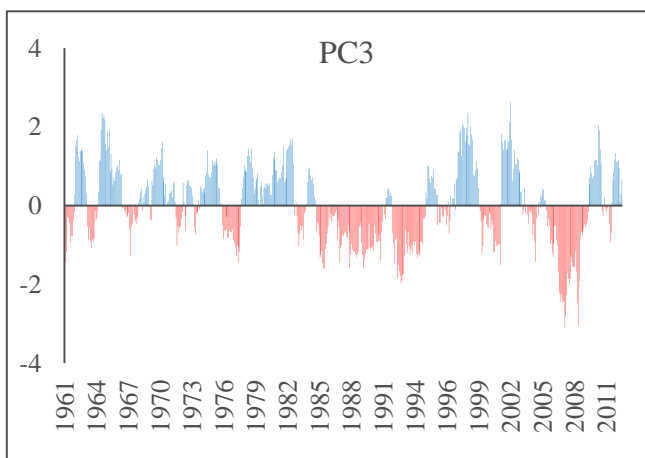
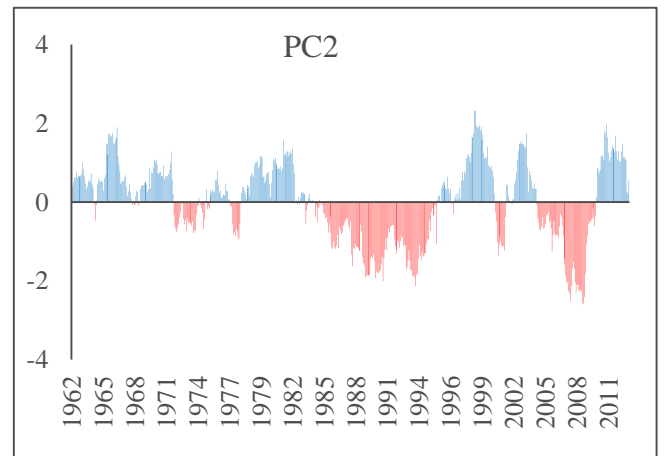
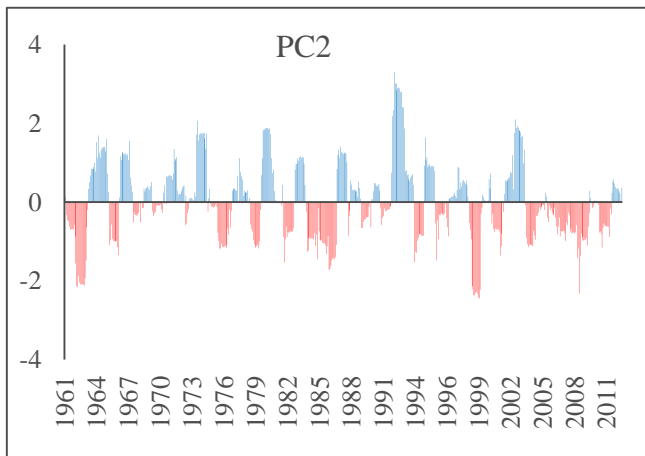
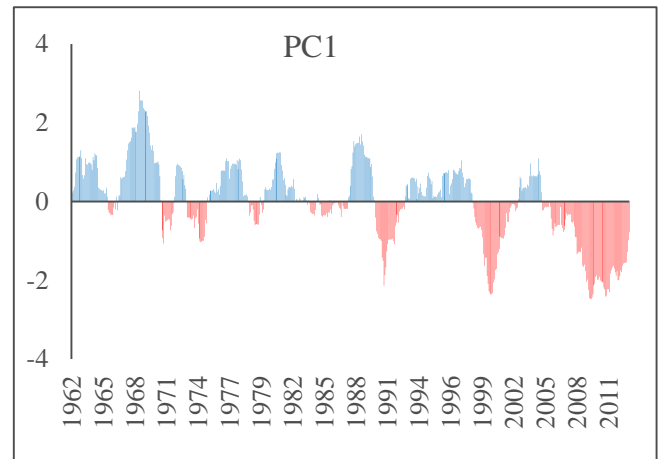
which enhance with an increasing of the time scale. Some of those droughts were particularly severe as they were prolonged in time such as the one in the end 2000s. In general, the north and northwestern parts of the EM have fewer drought events compared with other parts of the EM. Two extreme droughts are quite clear: one in the mid-1970s and the other in the beginning of the 1990s. The first episode was short and the second one more prolonged in time, which were closely linked to the positive anomaly phase conditions of the NAO dominating in those years (Türkeş and Erlat, 2003).

It can be seen that several dry episodes were detected having larger negative values, yielding critical situations for several years. Consecutive severe and extreme dry periods were detected, especially by 12 and 24 months. For example, for a 12- month time scale, the longest and most extreme drought periods were detected in (1989-1993), (1999-2001) and (2007-2012) for EOF1, (1991-1994), (1999-2001) and (1985-1991) for EOF2, (1986-1991), (1999-2011) and (2006-2009) for EOF3, (1995-1999), and (2005-2007) for EOF4, (1972-1975) and (2002-2008) for EOF5, and (1989-1991), (1991-1996) and (2004-2007) for EOF6.

SPI 12



SPI 24



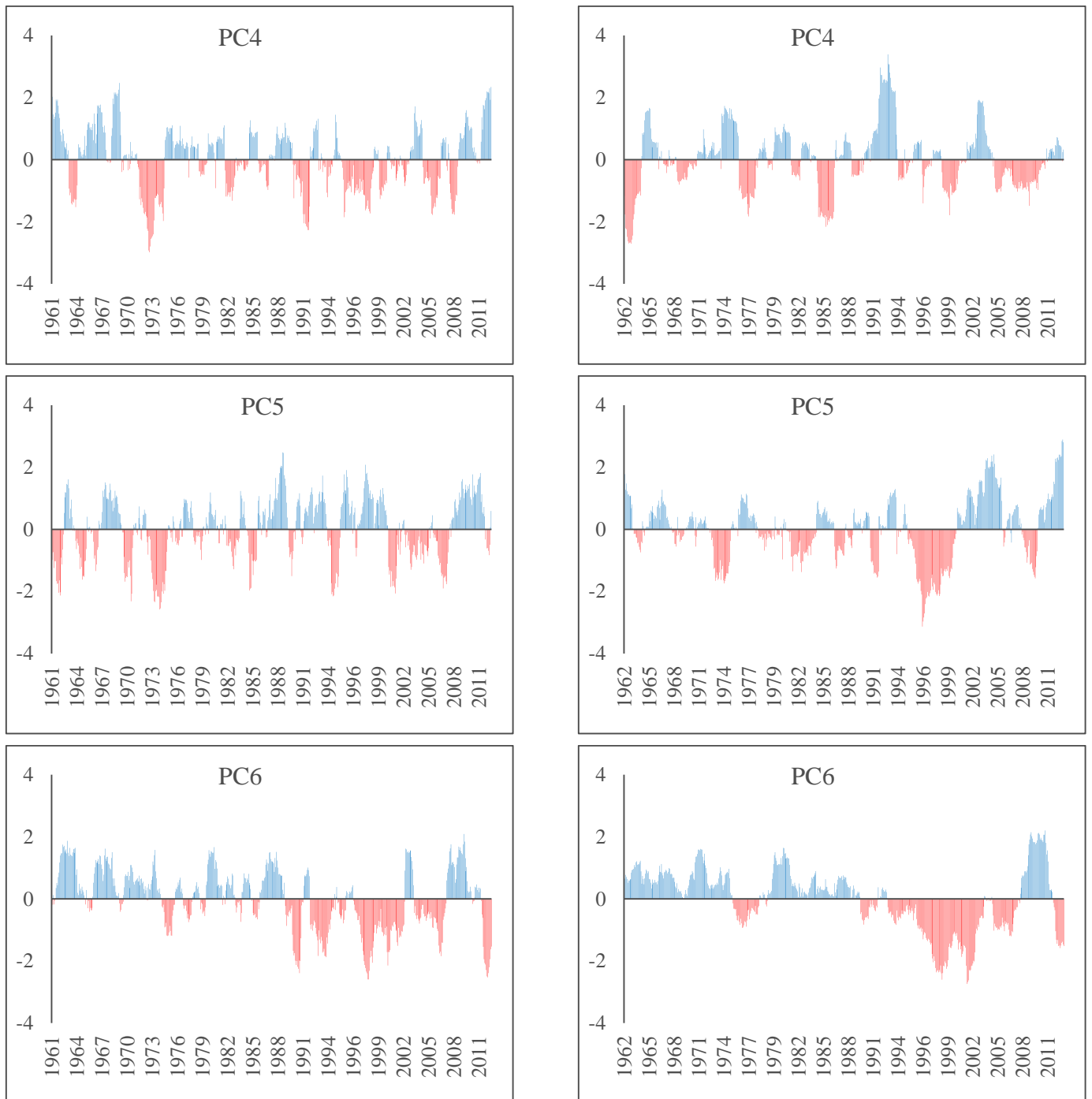


Figure 4.50 Evolution of the 12- and 24-month SPI from the scores series representing for the first six components PC1, PC2, PC3, PC4, PC5, PC6

Very extreme and long drought periods were detected at time scale for 24 months. For EOF1, the most extreme drought period was recorded in (2005-2012) with SPI average -1.4 in 94 consecutive months. Two long extreme periods were shown in EOF2, (1984-1995) and (2004-2010) with values of SPI -1.1 and -1.5, respectively. Very long and extreme drought period was also detected in EOF3 (1970-1977) with a severity of -1.29 for 84 consecutive months. The most severe drought periods for EOF4, EOF5 and EOF6 were detected in (2005-2010), (1995-2000) and (1992-2007), respectively.

Depending on the MK test, decreasing trends of SPI values at different time scales were detected at both 95 % and 99% confidence levels (Fig 4.51). In this respect, according to the SPI values at the regional level, during the second half of the twentieth century and the first decade of the twenty-first century, the driest years (from most dry to least dry) were 2008, 2007, 1999, 2000, 1989, 1997, 2001 and 2012. By contrast, the wettest years were 1980, 2003, 1967, 1963, 1968, 2002, 1978, 1996 and 1971. These results also emphasize that the persistence of lower-than normal precipitation is the primary cause of drought in the EM, whereas other meteorological factors, such as temperature, wind, and humidity usually contribute to the intensification of the impact of drought.

According to the SPI values characterising the categories of dry and wet conditions, the temporal evolution of the monthly SPI during the wet season (September to May) showed the periods of drought (from most dryer to least dry): 1999–2001, 1972-1973, 1989-1991, 2005-2012, 1983-1986 with an average ranges between -0.21 and -0.61 during these periods (Fig 4.52 a and b).

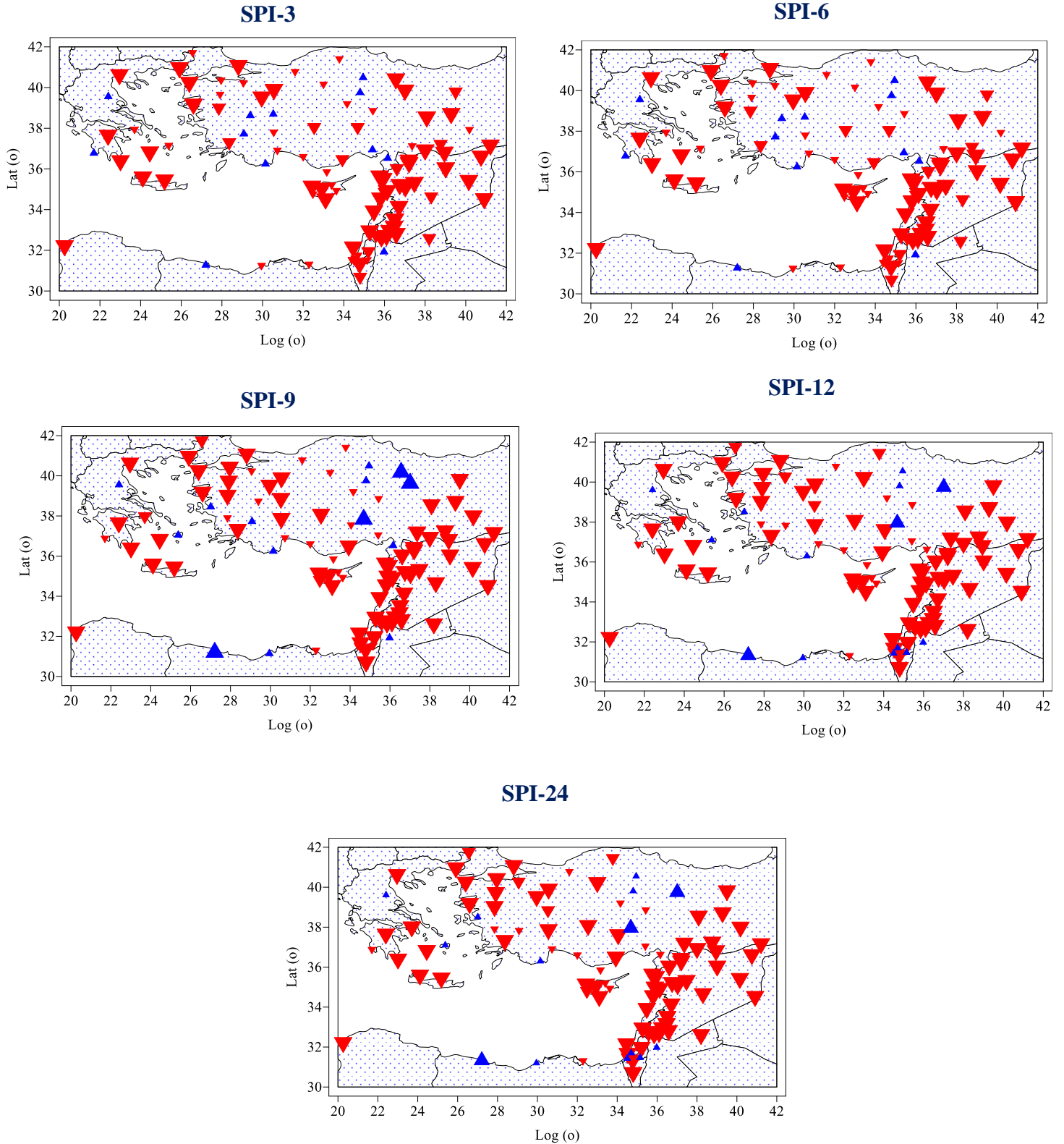


Figure 4.51 Observed trend of SPI at different time scales. Positive trends are in blue and negative ones in red. Large and medium-sized triangles represent significant trends at $\alpha=0.01$ and 0.05 . Otherwise small triangles are shown.

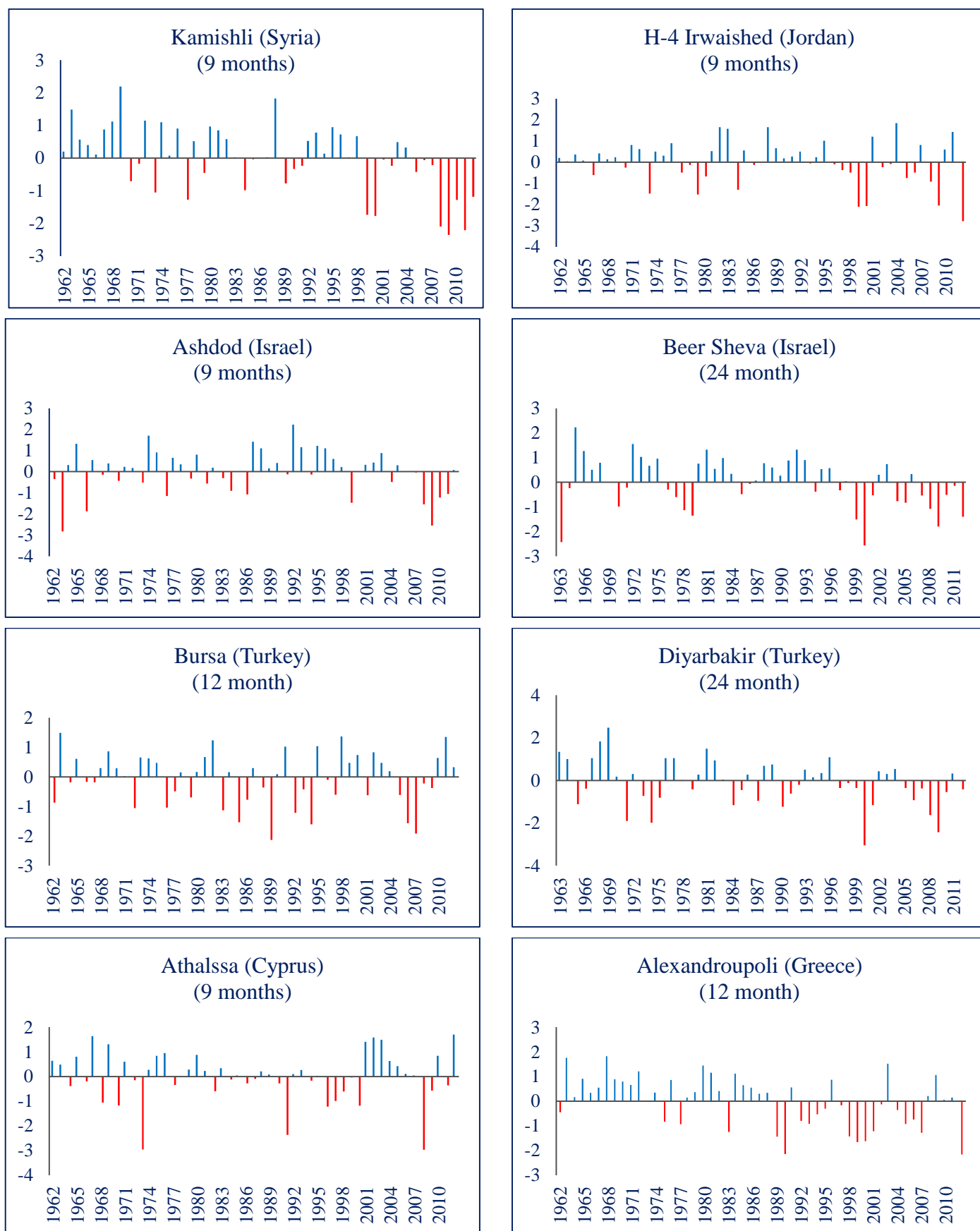
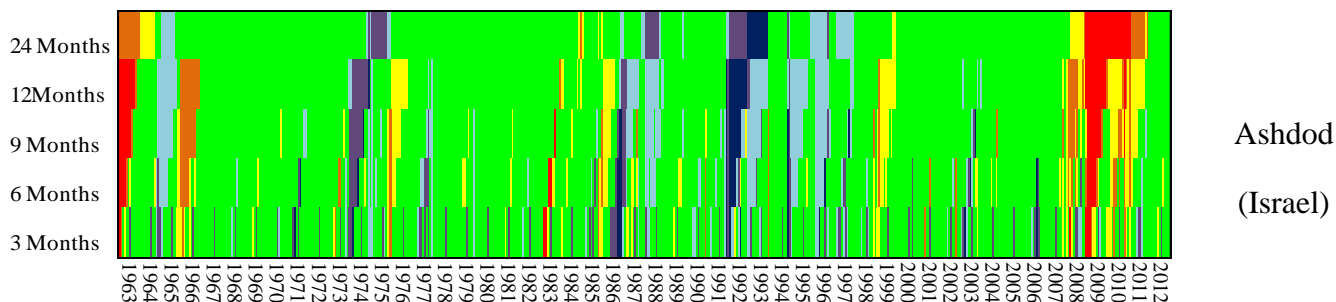
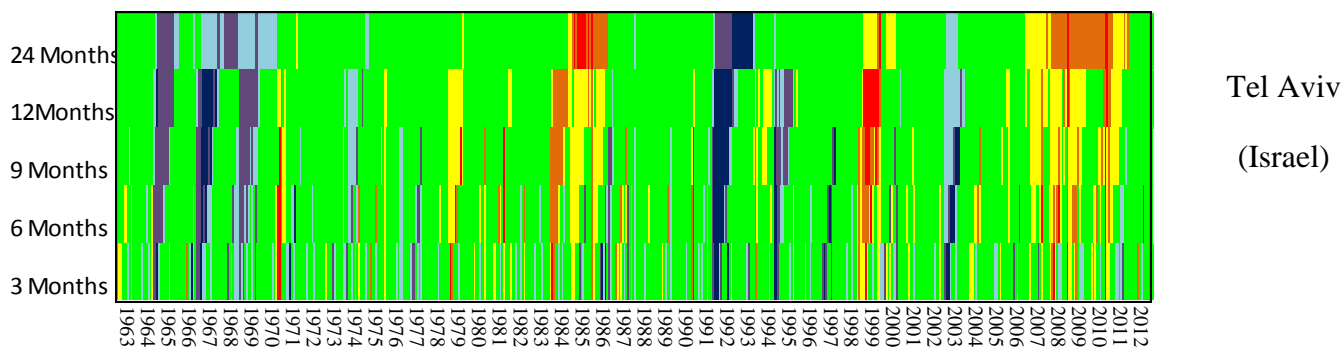
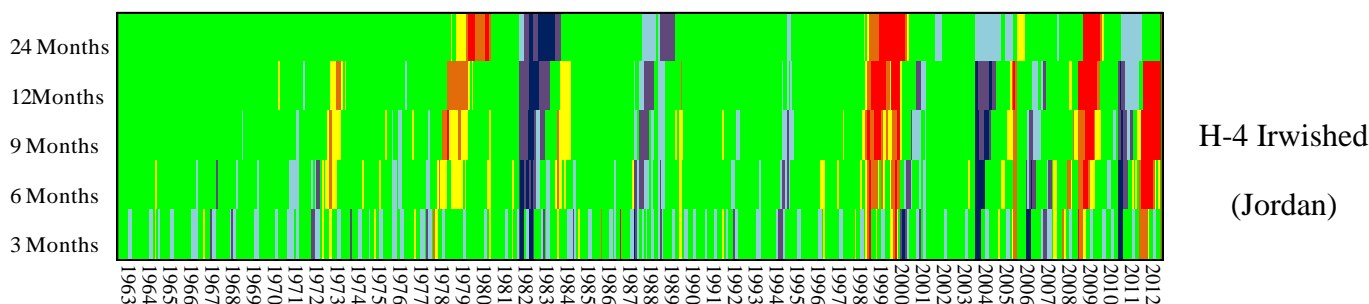
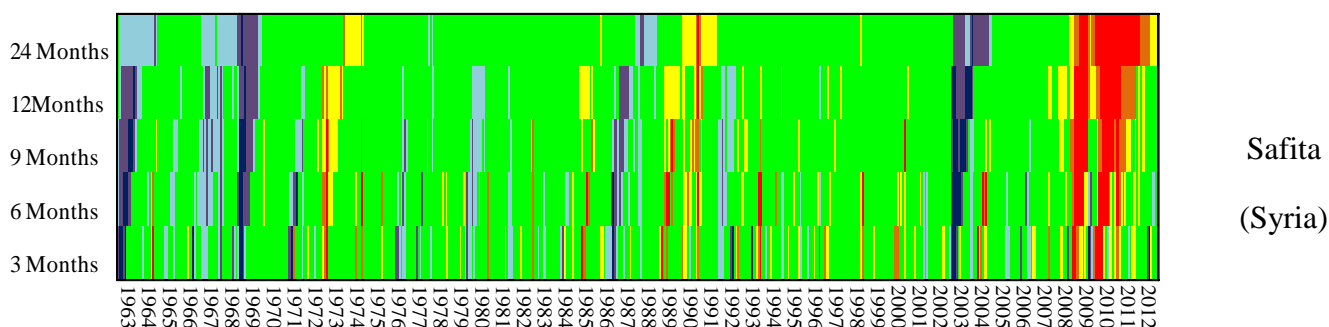
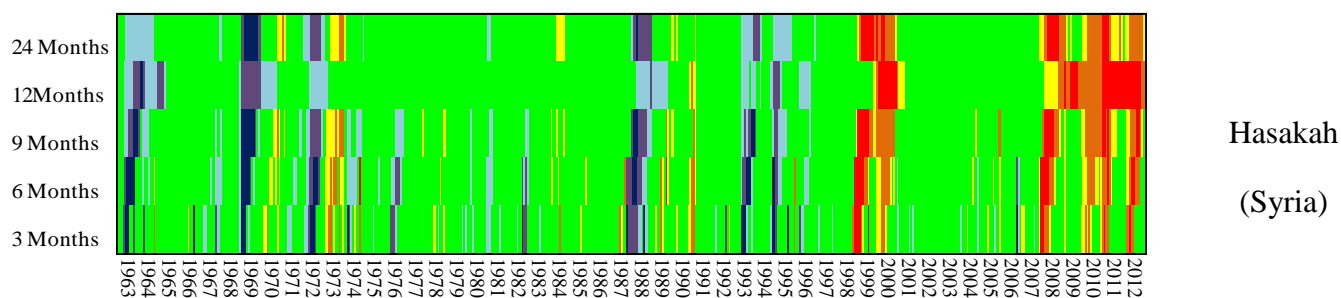


Figure 4.52 Temporal evolution of the averaged SPI over the wet period (September–May) at various time scales (9, 12, and 24 months) for some selected stations.



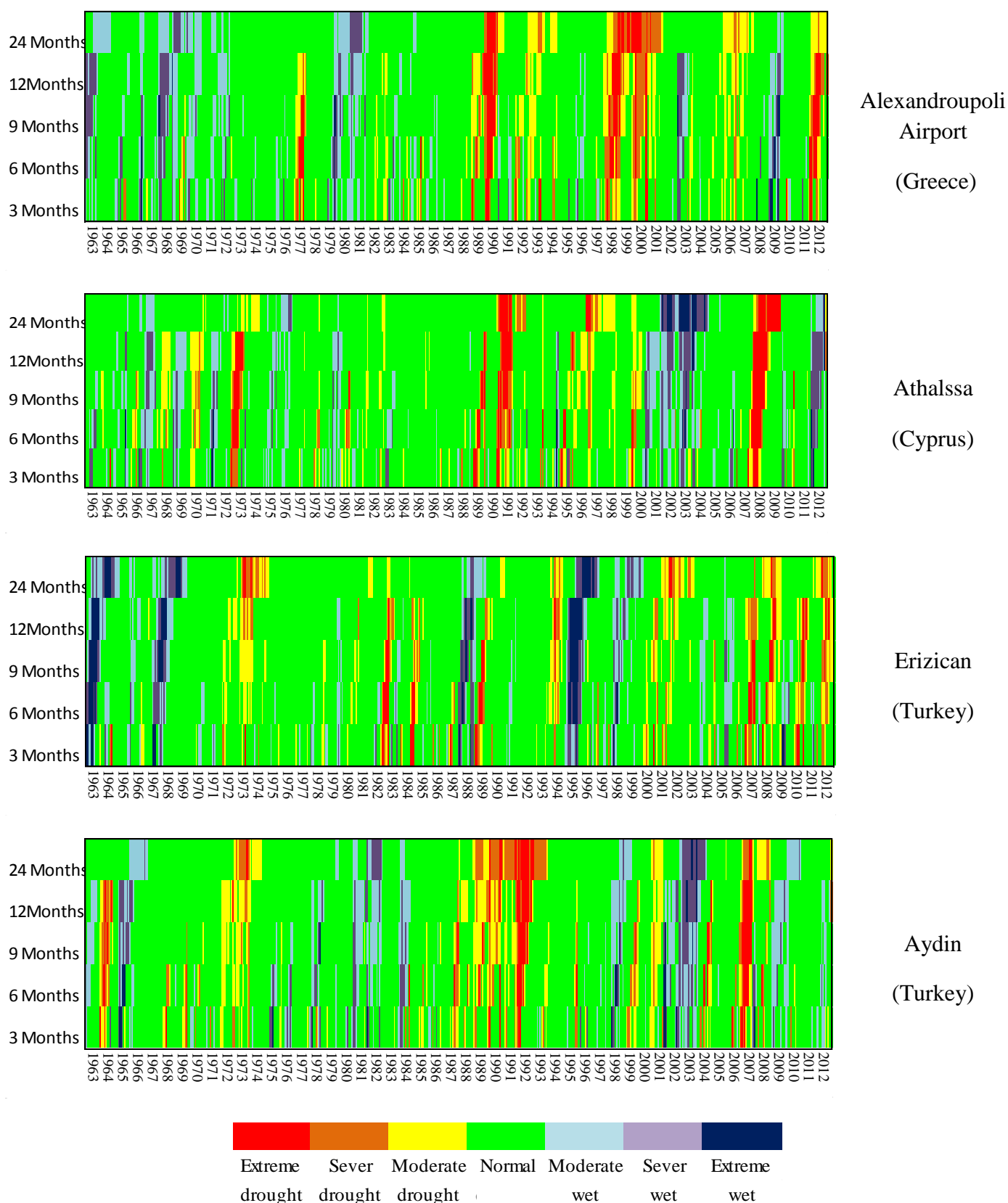





















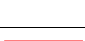


Figure 4.53 Evolution of the SPI index of observed rainfall records in some stations at different time scales over 1961-2012

Fig 4.53 shows an aggregated picture of monthly SPI at five time scales during the period 1961–2012 in several stations located in different regions. The figure emphasises the evolution of moisture characteristics as quantified by the SPI at 3- to 24-month time scales. It can be seen that the severe and extreme drought events were more frequent after 1990 and the drought severity has increased by time scale increasing. At longer time scales (e.g., 12 and 24 months) the dry ($SPI < 0$) periods show a high temporal frequency, whereas when the time scale decrease the frequency of dry periods decreases. This result was very clear in all some stations such as Hasakah and Safita (Syria), H-4 Irwished (Jordan), Tel Aviv and Ashdod (Israel), Athalssa (Cyprus) and Alexandria Airport (Egypt). At the time scale of 12 and 24 months the most important and severe dry periods (as mentioned above) were recognised in 1972-1976, 1989-2000 and 2005-2012, and the average duration of the dry periods ($SPI < 0$) has evidently changed as by changing of time scale. At the time scale of 3 months, the average duration is 4.3 months, at the time scale of 12 months is 10.4 months and the longest mean duration is recorded at the time scale of 24 months with an average duration of 16.5 months.

Abrupt changes in annual SPI values have occurred in the last twenty years between the late of the 1980s and 1990s in the southern and southwestern parts of the EM, which reflect the most extreme drought episodes in this period. This might be a result of the rapid decrease and the abrupt change in the annual precipitation detected around the same period. The northern parts of the EM had several changes during 1961-2012 starting in 1970s at confidence levels range between 90 and 99.9%. Table 4.8 shows the results of a change-point analysis of the annual SPI values (12 month) in the EM and gives a level associated with each change; the level is an indication of the importance of the change.

Table 4.8 Significant abrupt changes in the annual SPI values during 1961-2012.

Station	Country	Point of change	Confidence level	From	To	Level	
Abu kamal	Syria	2009	92%	0.173	-0.201		1
Alexandroupoli	Greece	1989	99.9%	0.450	-0.524		1
Amiandos	Cyprus	1989	98%	0.354	-0.373		3
Amman Airport	Jordan	2002	97%	-0.210	1.558		1
		2008	92%	1.558	-0.17		2
Balikesir	Turkey	1982	97%	0.371	-0.252		1
Bandirma	Turkey	1982	99.9%	0.358	-0.317		3
Beirut Airport	Lebanon	1963	94%	-0.635	1.007		3
		1972	92%	1.007	0.098		3
		1989	98%	0.098	-1.005		1
		2000	92%	-1.005	0.125		1
Damascus Airoprt	Syria	1995	98%	0.335	-0.629		1
Daraa	Syria	1993	98%	0.372	-0.592		1
Deir Ezzour	Syria	2007	92%	0.223	-1.682		1
Eskisehir	Turkey	1982	99.9%	0.533	-0.415		1
Hama	Syria	1989	96%	0.394	-0.458		1
Hasakah	Syria	2007	97%	0.185	-1.410		1
Kamishli	Syria	2007	99%	0.202	-1.535		1
Kharabo	Syria	1995	90%	-0.128	-0.666		2
Lattakia	Syria	1989	95%	0.351	-0.409		1

Hmemim Airport	Syria	1980	92%	0.351	-0.409		4
		2004	98%	0.481	-0.128		2
Istanbul -Atatork	Turkey	1979	99%	-0.006	1.340		4
		1983	96%	1.340	-0.521		3
		1991	90%	-0.521	2.563		2
		1994	93%	2.563	-0.405		5
Kithira Airport	Greece	2005	97%	0.226	-1.234		5
Kutahya	Turkey	1982	99.9%	0.614	-0.698		5
		1995	97%	-0.698	0.241		5
		2004	98%	0.241	-0.663		4
Malatya	Turkey	1989	94%	0.378	-0.387		5
Mytilene Airport	Greece	1985	94%	0.445	-0.378		3
Polis	Cyprus	1989	99.9%	0.363	-0.422		1
Raqa	Syria	2005	99%	0.223	-1.210		1
Tartous	Syria	1989	91%	0.635	-0.170		1
Thessaloniki Airport	Greece	1988	91%	0.333	-0.358		1
TL Abiad	Syria	2008	94%	0.174	-1.580		1
Tokat	Turkey	1985	94%	-0.467	0.401		1
Tripolis Airport	Greece	1989	99.9%	0.450	-0.524		1
Usak	Turkey	1982	95%	0.220	-0.547		4
		1997	98%	-0.547	0.005		6
		2012	96%	0.005	2.930		6

This analysis detects one change in several regions and more than two changes in others, such as Istanbul Ataturk in Turkey (1979, 1983, 1991 and 1994), Usak (Turkey) in three years (1982, 1997, and 2012), Beirut Airport in Lebanon (1963, 1972, 1989 and 2000), Hmemim Airport in Syria (1980 and 2004) and Amman Airport in Jordan (2002 and 2008).

Associated with each change is a confidence level indicating how confident the analysis is that the change actually occurred. For example, the first change in Amman Airport (Jordan) occurred with 97% confidence, whereas the second change occurred with 92% confidence. We are much more confident about the first change than others. Table 4.8 also gives a level associated with each change. The level is an indication of the importance of the change. The level (1) is the first change detected and that is most visibly apparent in the plot. Level (2) is detected on a second pass through the data. Any number of levels can exist depending on the number of changes. Change-point analysis is more powerful at detecting smaller sustained changes and it better characterizes such changes (Taylor, 2000 a, and b).

As it can be seen, the most important change is estimated to have occurred during 1989-2000 with 95-99.9% confidence level and high change levels in the southern and southwestern parts of the EM, whereas the change was detected earlier in the northern parts (Table 4.8 and Fig 4.54).

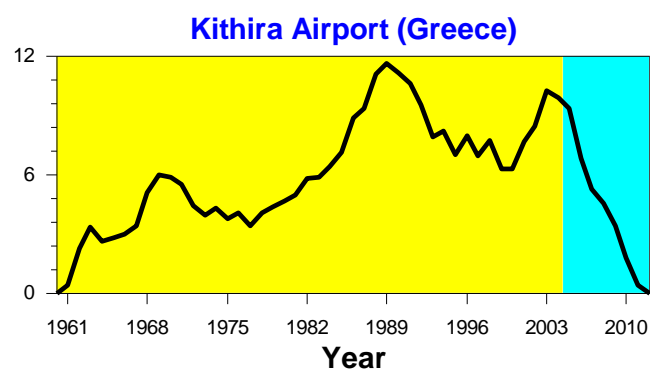
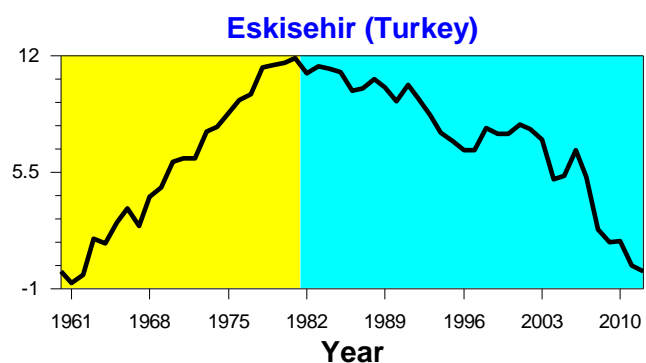
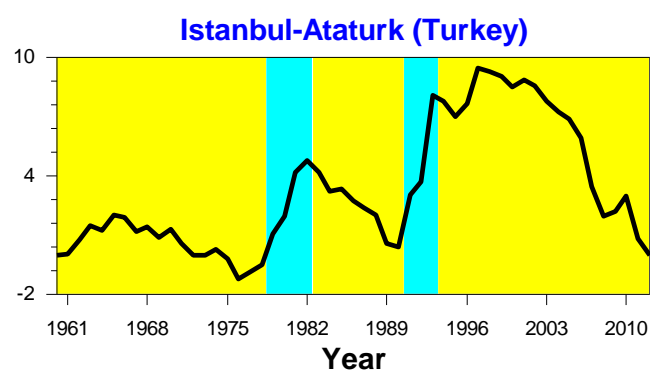
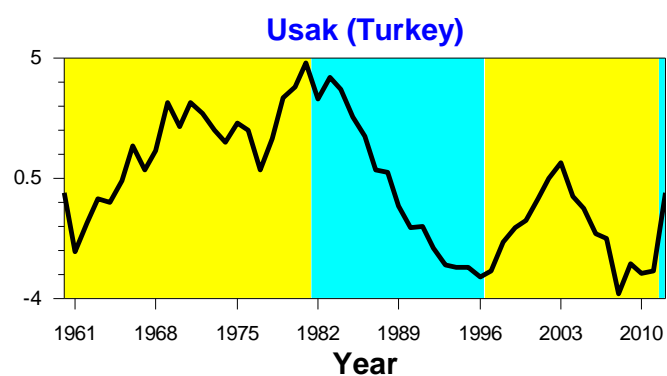
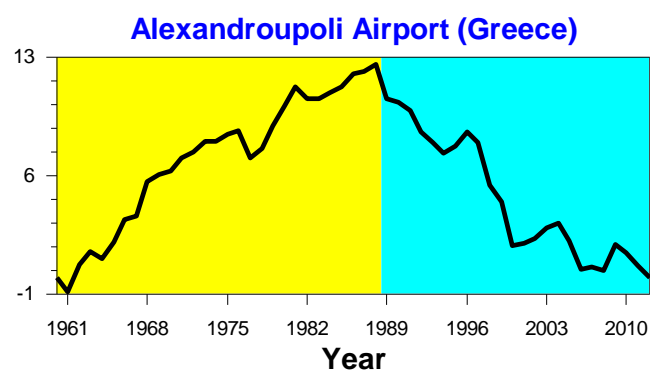
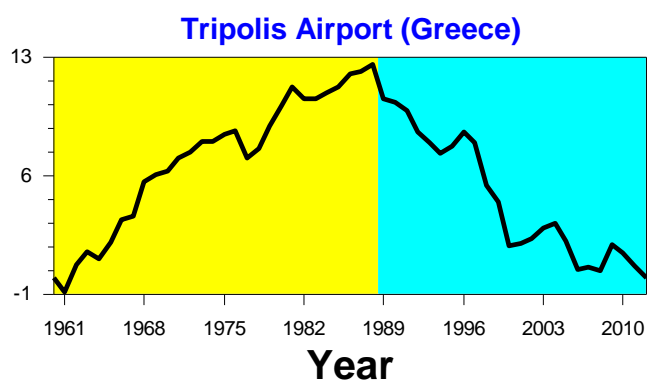
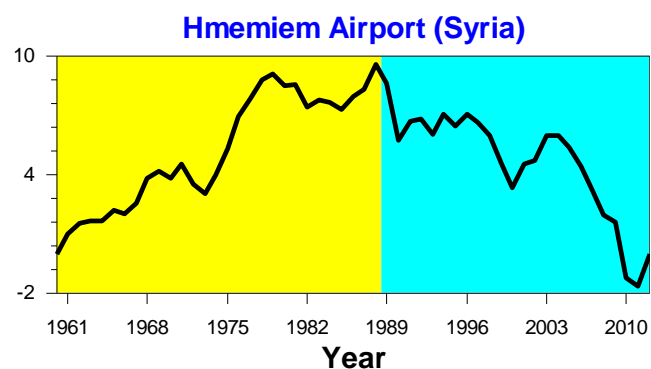
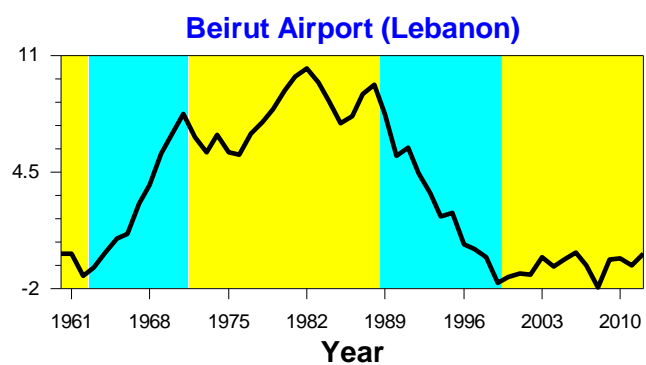


Figure 4.54 Abrupt changes in annual SPI values between 1961 and 2012, as determined by CUSUM charts for some selected stations over the EM.

The SPI is comparable in both time and space, but it is not affected by geographical and topographical differences (Lana *et al.*, 2001).

This versatility makes SPI as one of major drought indices and allows it to monitor short term water supplies, such as soil moisture, important for crop production and long term water resources such as low flows, ground water supplies and Lake Reservoir levels (Hayes *et al.*, 1999). Kito *et al* (2008) concluded a decreasing tendency in most of rivers in the East Mediterranean region, For example, the annual discharge of the Euphrates River will significantly decrease by 40% (Nohara *et al.*, 2006) as well, the stream flow in the Jordan River (82-98%) (Kito *et al.*, 2008). The percentage decrease in river discharge is larger at the Ceyhan River region in Turkey (39-88%).

The combination between the decreased precipitation and increased temperature in the EM may lead to extended periods and frequencies of drought (IPCC, 2013) which would result in a prolonged reduction in agricultural output. This could possibly lead to economic, environmental and social impacts. Additionally, the weakening of winds that bring moisture-laden air from the Mediterranean and hotter temperatures that cause more evaporation can together put this area under a great response to the recent increased of greenhouse gases emissions.

4.9.1.2 Drought frequency distribution using SPI

Drought occurrence is investigated on the basis of the frequency distribution of the SPI values in their seven classes (Table 3.2). The frequency was calculated as the ratio between the number of occurrences in each SPI category and the total number of events counted for all stations in a given region and for a given SPI calculated for various time scales (3, 6, 9, 12 and 24 months). The aim was to identify the spatial patterns of frequency distribution of moderate, severe and extreme droughts (Table 4.9) over the EM for various SPI time scales based on individual station frequency distribution. The frequency distribution of the SPI values was calculated at each station, and the frequency distribution of the three drought categories (moderate, severe and extreme) was then plotted at the regional level (Fig 4.54). The occurrence of these drought categories according to SPI classes at various lags was also analysed on a regional basis to highlight the drought characteristics of the five climatic regions (Table 4.9).

In Table 4.9, the percentage of drought and wet occurrence is expressed in seven classes of moisture and dryness categories (in percent) (Table 3.2) based on the SPI series calculated at 3, 6, 9, 12 and 24 months for each individual region for the period 1961–2012. The normal conditions represent between 64.1 and 85.8 % of the total values of the SPI for all timescales in all five regions. Moderate drought conditions are distributed approximately between 4.5% and 9.2%, whereas the moderate wet conditions are highly occurred (7.9 to 15.3%). The differences in extremely dry conditions compared with extremely wet conditions increased with increasing SPI time scales; for example, the percentage of extreme drought for the SPI at 3 and 24-month lag in the first region was 2.1% and 6.2%, whereas the percentage of extreme wetness was 0.6 % and 1%, respectively.

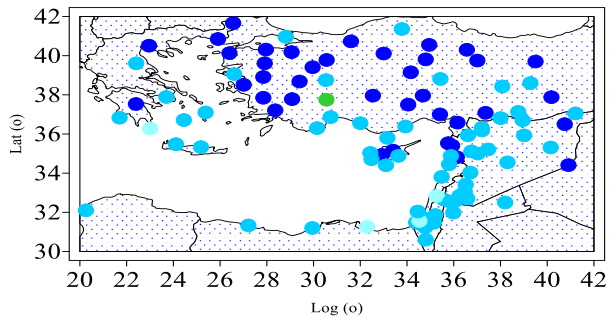
Table 4.9 Frequency distribution (in percent) of the annual SPI values in seven classes of moisture /dryness categories for the SPEI at 3-, 6-, 9-, 12-, and 24-month time scales in first six EOF regions.

	EOF region	Extreme drought	Severe drought	Moderate drought	Normal	Moderate Wet	Severe wet	Extreme wet
SPI-3	1	2.0	2.7	9.0	63.7	15.3	4.9	2.4
	2	1.9	3.8	7.5	66.4	13.5	4.6	2.3
	3	2.8	4.5	8.6	68.0	10.0	4.4	1.7
	4	2.3	4.4	8.6	69.9	8.5	4.3	2.0
	5	2.0	4.4	7.9	69.6	10.1	4.2	2.0
	6	2.7	4.4	7.5	68.9	9.9	4.5	2.1
SPI-6	1	3.4	4.4	8.0	68.3	9.0	4.5	2.4
	2	3.0	3.9	8.7	69.4	7.9	4.5	2.6
	3	2.9	4.2	7.6	68.6	10.1	4.1	2.6
	4	3.2	4.3	6.1	68.7	10.2	4.1	3.5
	5	3.0	4.4	7.9	68.4	10.3	3.8	2.3
	6	3.4	3.6	8.0	68.9	9.8	4.5	1.9
SPI-9	1	3.8	4.7	7.6	68.1	9.1	4.3	2.4
	2	3.9	3.9	8.6	68.5	8.3	4.5	2.3
	3	3.9	4.6	8.0	68.1	9.8	3.8	1.8
	4	3.0	4.0	8.0	67.9	9.6	4.2	3.3
	5	2.9	4.6	5.8	68.8	10.3	4.2	3.5
	6	3.5	3.8	8.8	68.7	9.0	4.5	1.8
SPI-12	1	3.5	4.6	7.4	68.6	8.9	5.2	2.0
	2	3.5	3.9	8.9	69.0	8.6	3.8	2.4
	3	2.8	4.7	7.7	69.0	10.2	3.9	1.7
	4	3.2	4.2	8.2	69.1	9.5	4.1	1.7
	5	2.6	5.2	9.0	67.6	8.3	4.5	2.7
	6	2.9	4.1	8.6	69.3	9.1	4.1	2.0
SPI-24	1	4.0	4.2	7.0	68.6	9.0	5.1	2.1
	2	1.5	5.5	9.5	67.3	9.2	5.3	1.7
	3	2.7	4.4	7.6	70.4	8.3	4.1	2.5
	4	2.8	3.5	8.2	69.4	10.1	4.0	2.0
	5	3.8	3.8	8.8	68.8	8.5	4.1	2.2
	6	3.3	4.6	4.5	68.5	12.3	4.2	2.7

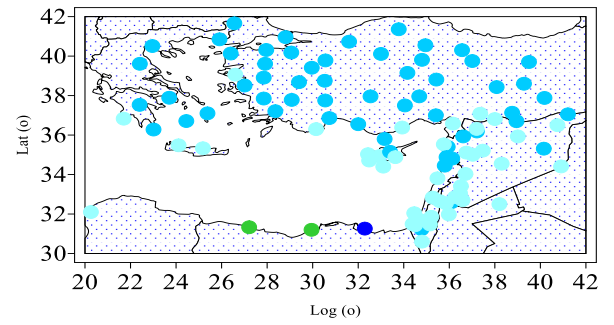
The results presented in Table 4.9 indicate that the occurrence of extremely dry conditions (SPI value lower than -2) tended to prevail over the occurrence of extremely wet conditions (SPI value higher than $+2$), mostly for all time scales and more evident in the SPI calculated for longer accumulation periods (12 and 24 months). The occurrence of extreme drought has the lowest values for 3 months timescale ranging between 1.9% in EOF2 and 2.8% in EOF3, whereas the EOF1 region has the highest percentage for SPI (4.0%) at the 24 month time scales.

As it can be seen in Fig 4.55., the highest percentage of the SPI values falling into the moderate drought category tended to occur in regions with relatively low precipitation in southern parts of the EM. The moderate drought frequency ranges between 1.6% and 10.6% for short-term drought. As the lag increases from 6 to 12 months, no major changes are observed in the distribution of maximum frequency (16.6 % for SPI-12). At a 24- month time scales, moderate drought tends to occur more frequently. The frequency of drought occurrence ranges between 0.5% and 13.6%, and the maximum frequency lies southwestern parts of the EM (Israel, Syria and Lebanon) and western parts of Turkey (Fig 4.55.).

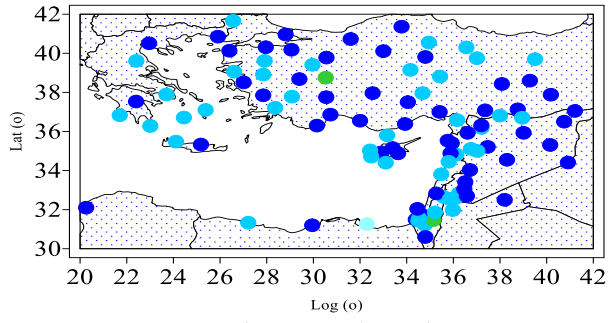
The occurrence of severe drought at short time scales (3 months) and for 6 and 9 months was detected in the regions in southwestern parts of Turkey and northern parts of Syria (6-8%). According to the spatial distribution of the frequencies of the SPI values, the highest occurrence of severe drought (9–10%) was detected for the long term (12 and 24 months, hydrological drought) in the western and southeastern parts of the EM (Israel and Jordan). The highest frequency of severe drought occurrence ranges between 6.3% and 9.8%, whereas on average, at the regional level, it was 4.2% for all SPI lags.



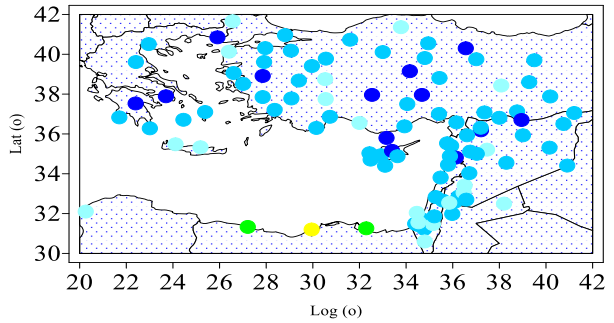
3 months sever drought %



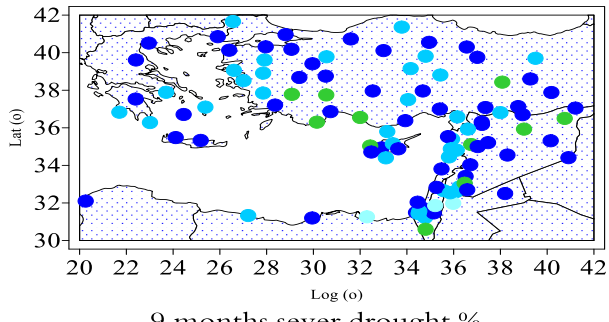
3 months extreme drought %



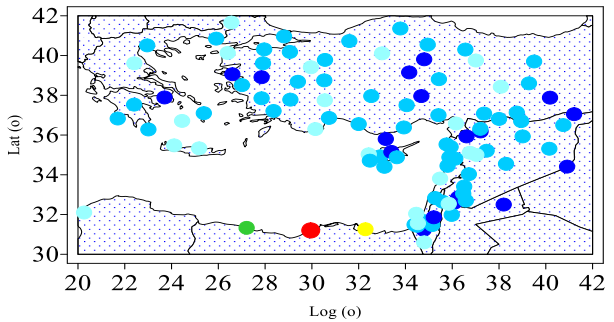
6 months sever drought %



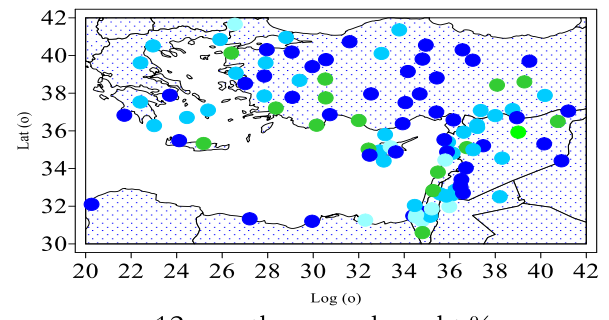
6 months extreme drought %



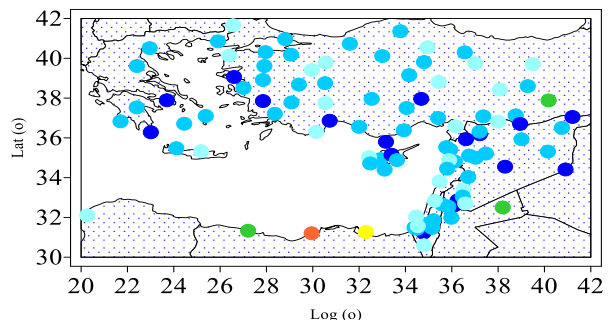
9 months sever drought %



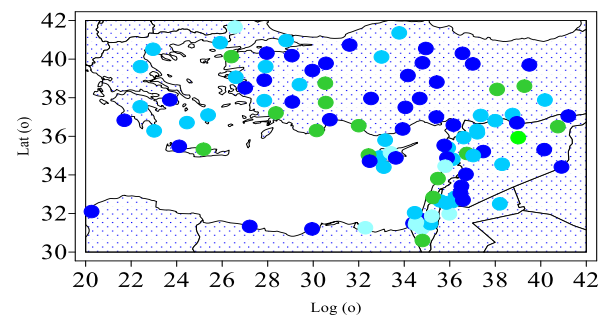
9 months extreme drought %



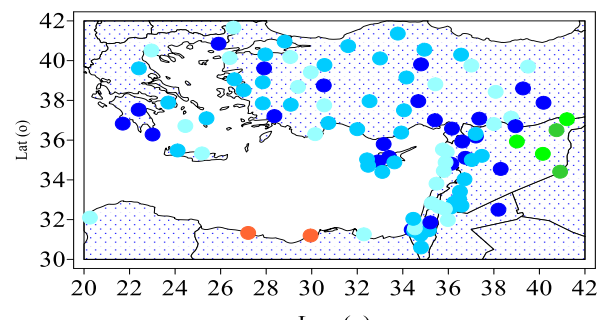
12 months sever drought %



12 months extreme drought %



24 months sever drought %



24 months extreme drought %

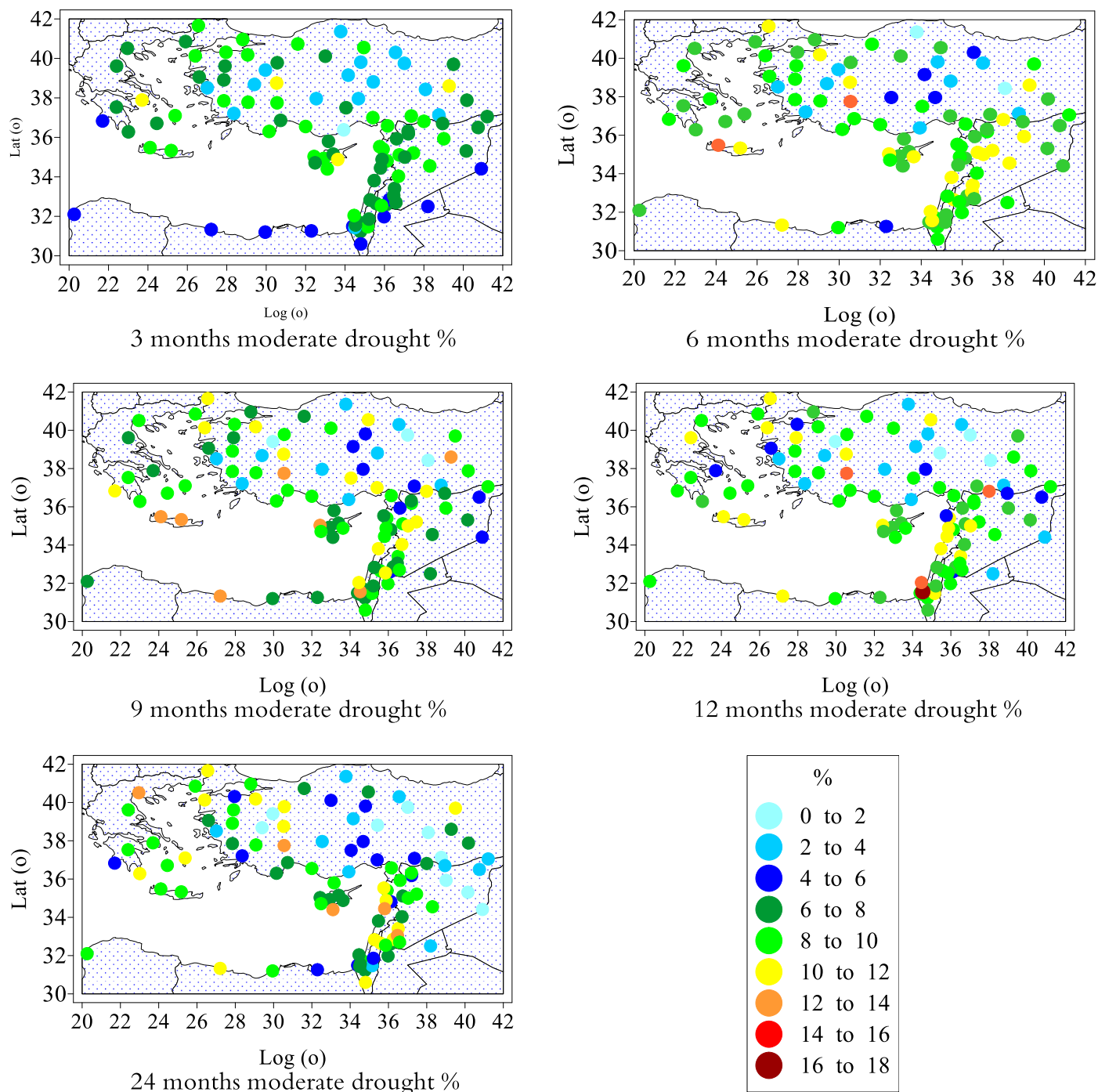


Figure 4.55 Spatial distribution of the frequency (in per cent) of the SPI values falling into the category of moderate, severe and extreme drought based on the station values of the SPI at various lags (3, 6, 9, 12 and 24 months).

The areas affected by extreme drought expand gradually as the time scale of the SPI increases from 3 months (meteorological drought) to 12 and 24 months (hydrological drought). The highest percentage of extreme drought occurrence is 7 % at the short time scale (SPI-3), whereas at longer time scales (SPI-12, SPI-24), the highest percentage of extreme drought increases and ranges between 12 and 13 % and it was recorded in northern Egypt. It can be seen that as the time scale increases, drought occurs at higher frequencies at the coastal stations while the inner stations experience longer-duration droughts at lower frequencies, indicating that seasonal droughts are more common in the coastal areas while the interior parts suffer from prolonged droughts. These results agree with the results of Komuscu (1999) in Turkey who found that for the 3- and 6-month time scale coastal stations suffered more often from moderate droughts than the inland stations, but the differences between these frequencies were, probably, not statistically estimated. However, on 3- and 6-monthly time scales, the Greek, Syrian and Lebanese coastal stations experience more severe drought events than inland ones, while on a 12-month time scale severe droughts have almost the same frequency at all stations. In all cases these, events were related to cases of high persistence of drought conditions. Drought frequency at 12 and 24 time scales detected high values in some agricultural regions (especially in Turkey and Syria). This region has massive projects for developing agricultural sectors and water resources on the Turkish side of the Euphrates and Tigris river basins. This region receives very little rainfall in the summer, creating very dry conditions coupled with high temperatures, which make the goals of the project are the irrigation of large areas to reduce the impact of severe droughts.

4.9.2 Drought analysis using the Modified China Z Index (MCZI) and Statistical Z –scores and Deciles.

The median precipitation was used in place of the mean precipitation in the calculation of the CZI, which is now called the Modified CZI (MCZI), attempting to reduce the differences between the SPI and MCZI. MCZI values have detected several dry periods during 1961-2012. On the other hand, there are four extremely dry peak points (2008-1999-1973-1991) with MCZI values lower MCZI < -2 in most regions.

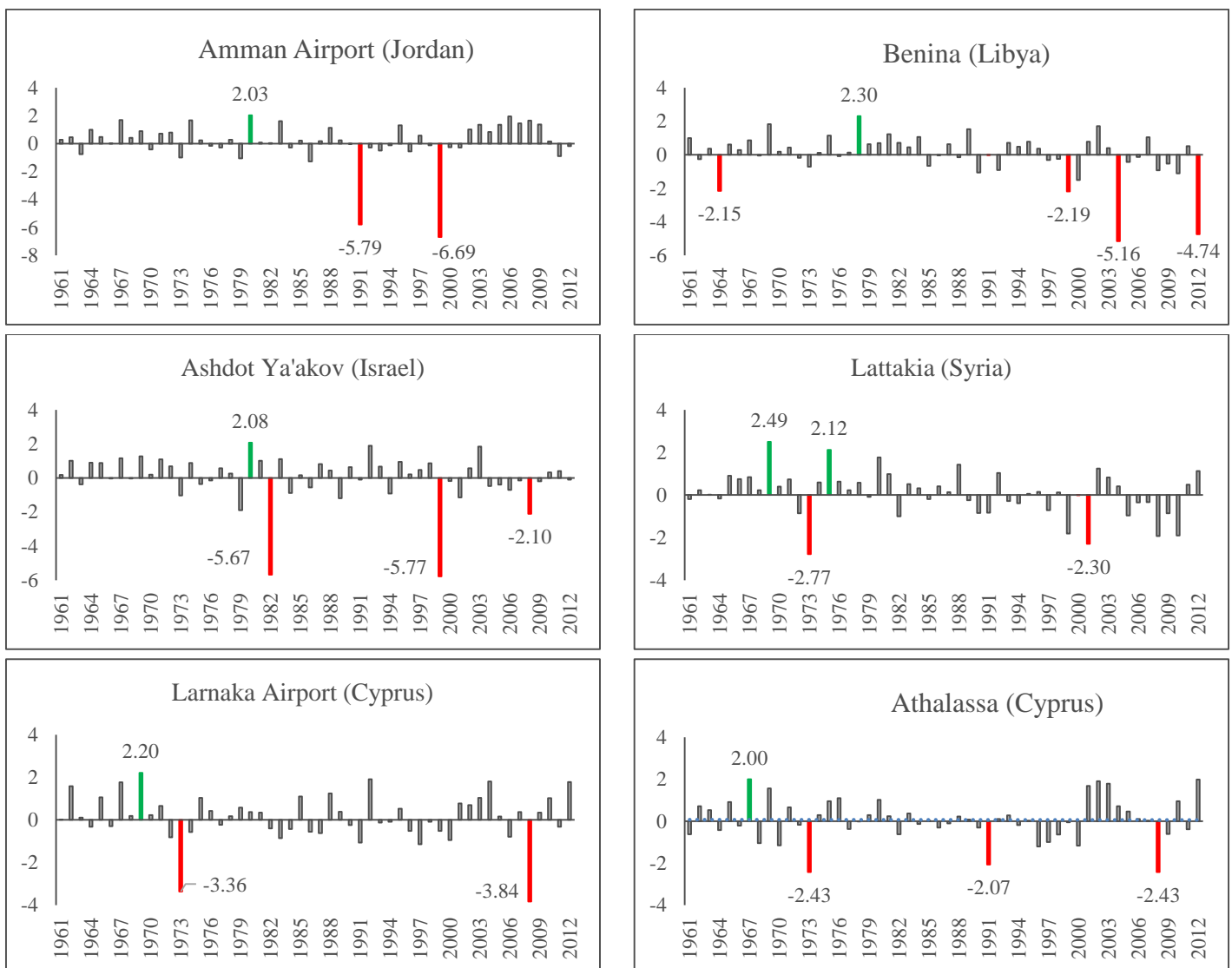


Figure 4.56 Temporal evolution of the averaged MCZI over the wet period (September–May) for some selected stations during 1961-2012. Red columns indicate extreme drought (MCZI ≤ -2), and green columns indicate extreme wet conditions (MCZI ≥ 2)

We can see only one or two peak points with MCZI >2 in the whole period before 1990s (between 1967 and 1980) in the southern and southwestern parts of the EM, whereas some other years have recorded extreme MCZI values between 1990 and 2000 (Fig 4.56). For example, in Lattakia (Syria), there are two points peak of extremely wet (1969, 1975) with MCZI values 2.49 and 2.12, respectively, but we can see one peak point in Athalassa and Laranaka Airport in Cyprus (1969). Both of Amman Airport (Jordan) and Ashdot Ya'akov (Israel) have the same peak year (1980) with MCZI values of 2.03 and 2.08, respectively, whereas Benina in Libya detected the peaked value 1978 with a 2.03 MCZI value. It can be concluded that the driest years are 2007, 1989, 2001 and 2012 in most stations over the EM. Percentage of years affected by various drought severity levels in the EM during the period 1961–2012 is illustrated in Fig 4.57a. Approximately 70%, or precisely 67.4%, of the frequency of drought belongs to the near normal drought category. The frequency of drought was 14.4%, while the frequency of wet periods was 18.2%. The percentage of the EM affected by drought during the period 1961–2012 is presented in Fig 4.57b. The results reveal a deterioration of drought conditions after 1990, especially, in 1999 and 2008.

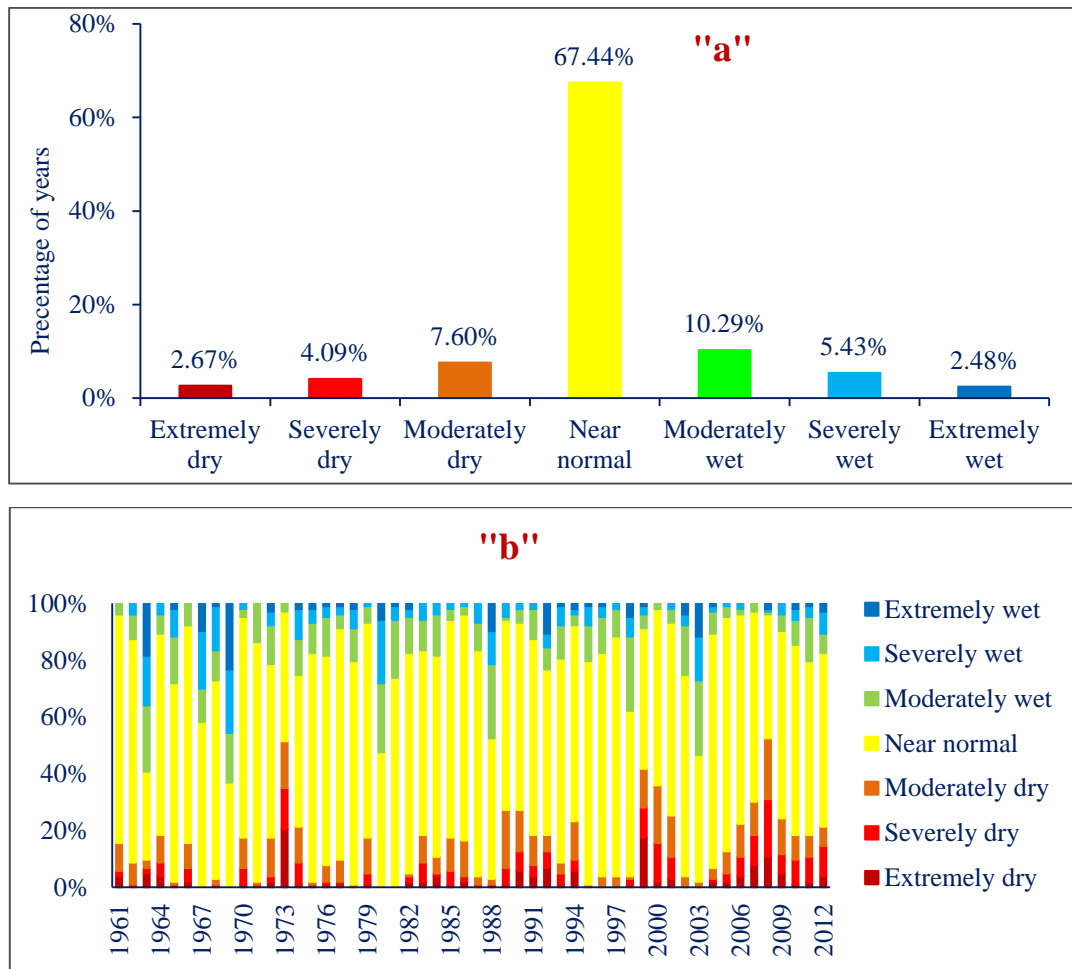


Figure 4.57 Percentage of years affected by various drought severity levels according to MCZI index (a) and percentage of the EM area affected by drought categories (b).

It can be seen that 20 % of the EM had extreme droughts during the 1973, 17 % in 1999, 11% in 2008 and 8% in 2007. Furthermore, the majority of the EM had severe and extreme droughts during the years 1973, 1999, 2008 and 2012.

By applying the PCA for the MCZI index during the wet period (September to May), five distinct sub-regions were identified, representing high coherence with SPI spatial distribution (Fig 4.58).

The cumulative total explained variances of the five retained PCs are 62%. The first component explains the highest percentage of variance around 15% of the total variance, and has the highest positive loading over the eastern part of the EM (Syria and east Turkey).

The second component, PC2, highlights an area located in the southern parts of the EM (Egypt, Libya, Israel, Jordan, Lebanon and the coastal region of Syria) and it explains about 14% of the total variance. The first and second components coincide with the dry sub-humid and semi-arid areas in the EM. The PC3 is mainly representative of the western parts of the EM (west Turkey and Greece) and explains 13% of the total variance. 11% of the total variance was explained by PC4 and its loadings which are found over Cyprus.

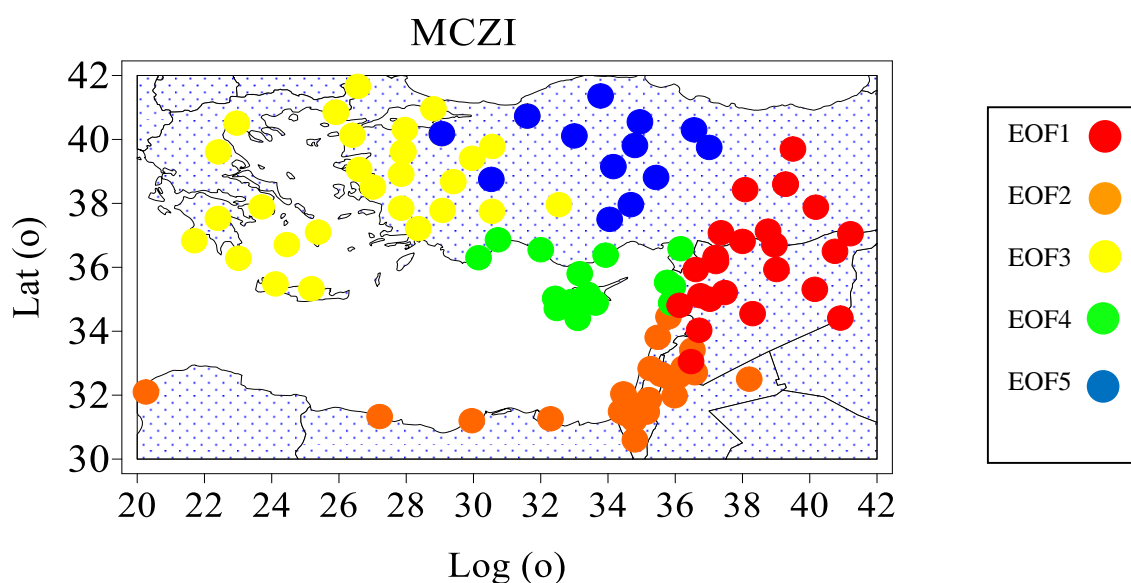


Figure 4.58 Spatial distribution of the PCs loadings for MCZI series in wet period over 1961-2012.

Apparently, PC5 coincides relatively well with the humid areas in the north EM (northern Turkey). Figure 4.58 shows that between all components, the regions with significant correlation (higher than 0.5) do not overlap, being clearly spatially disjunctive. These results indicate that with the five main components a spatial classification is achieved, with five well-defined regions.

The percentage of drought and wet occurrence expressed in seven classes of MCZI in the wet period for each individual region for the period 1961–2012 is illustrated in Fig 4.59

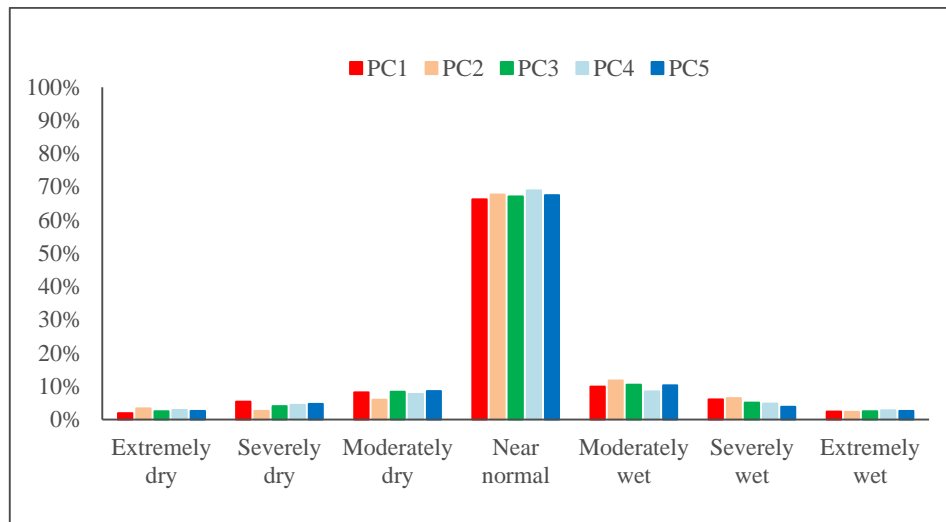


Figure 4.59 Frequency distribution of the MCZI values in the wet period for each individual region during the period 1961–2012.

The frequency of moderate drought ranged between 5.93% in EOF2 and 8.55% in EOF5 and the near normal situations were recorded in the same rates in all regions and ranged between 66.22 and 68.99%. The highest frequency of severe drought occurrence was 5.35%, which was located in the region EOF1 region. The average of severe drought occurrence at the regional level was 4.2%. According to the spatial distribution of the frequencies of the MCZI values, the highest frequency of extreme drought (3.37%) was detected in the south and southwestern parts of the EM (EOF2 region) ranging between 1.92 and 2.88% in other regions (Fig 4.58). It is found that the seasonal MCZI observational time series of area under drought shows a significant negative trend in both winter and spring and was more evident in winter at a significance level of 0.05 due to the significant decrease in seasonal rainfall amounts in these areas.

Mann–Kendall statistical test was also employed to analyse the trends for MCZI of each season. 84% stations were characterized by decreasing MCZI trends in spring, which were statistically significant at 33% of these stations at $\alpha=0.05$ (Fig 4.60). These trends can also be identified in winter. Figure 4.60 shows that the major parts of the EM were characterized by decreasing MCZI trends in the winter (85% of stations). Most stations located in south and southeastern parts of

the EM show a significant drying tendency at $\alpha=0.05$ (35% of total stations). These decreasing trends in winter and spring indicate that a drying tendency dominates in the large majority of the EM areas. The results also indicate that a large majority of the EM had a positive trend of MCZI in autumn which was significant in several areas in the northern parts (Fig 4.60) Showing the same behaviour of SPI index (shown in Fig 4.51). Very high pair-wise correlation (>0.90) was obtained between MCZI and SPI for the same time steps. Linear regressions between the monthly values of the SPI and Z-Score, and MCZI 1961 to 2012 indicate a high relationship between the SPI and MCZI. This is resulted from using the median precipitation instead of the mean precipitation in calculation MCZI which makes SPI and MCZI values are closer and the difference between the values of these two indices is small.

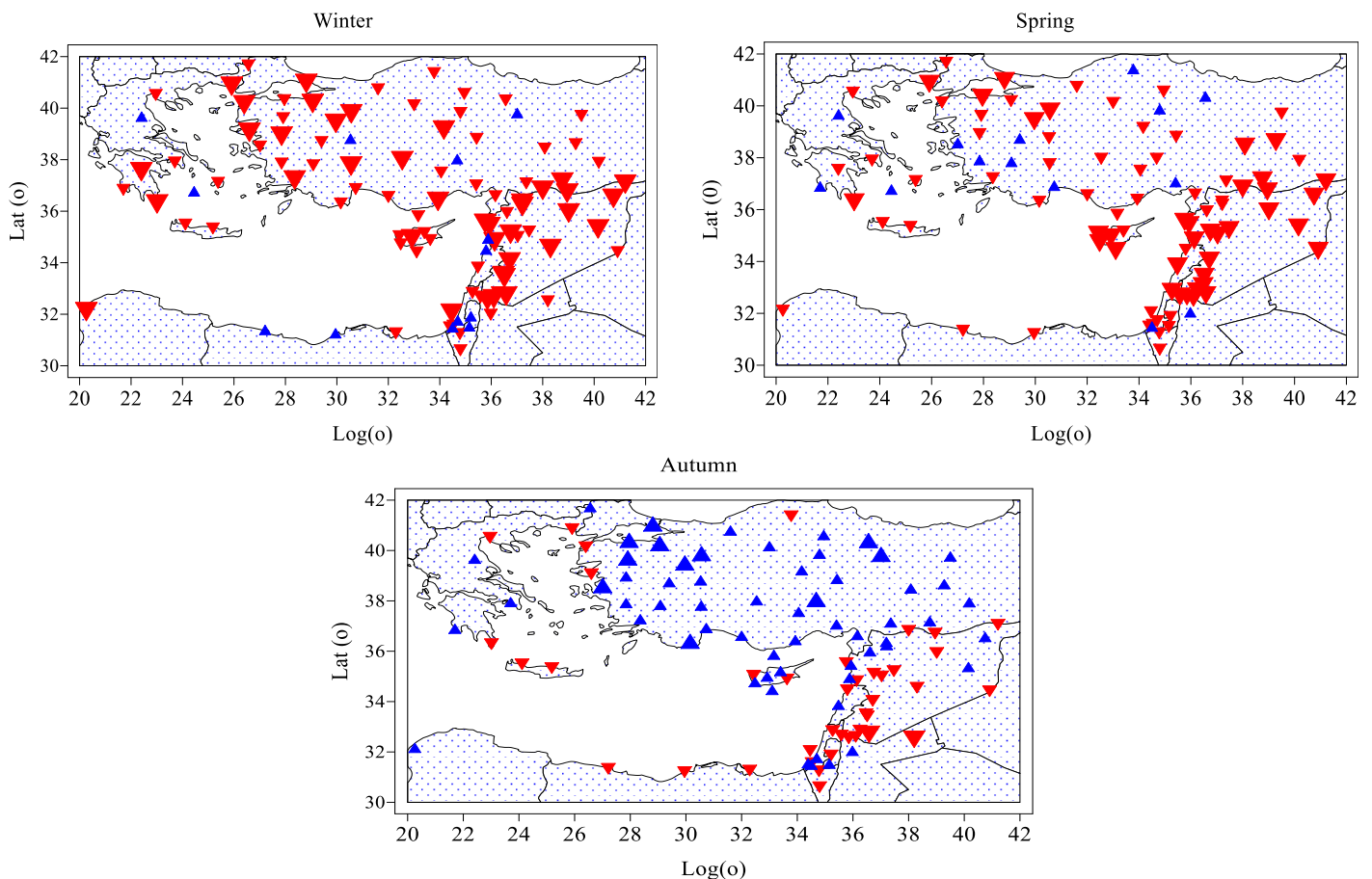
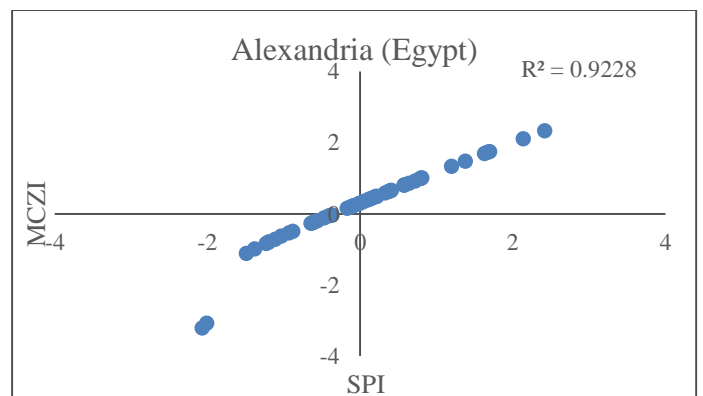
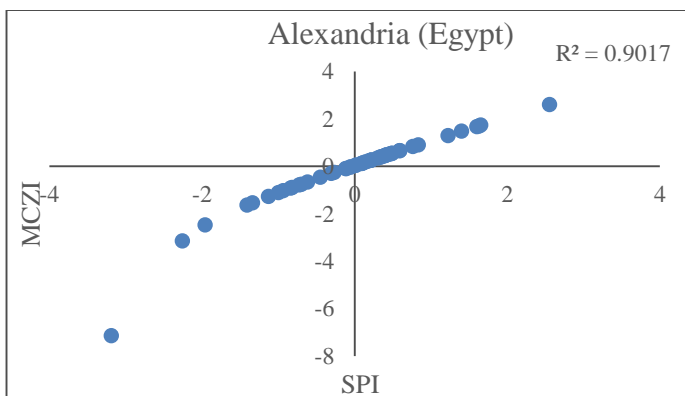
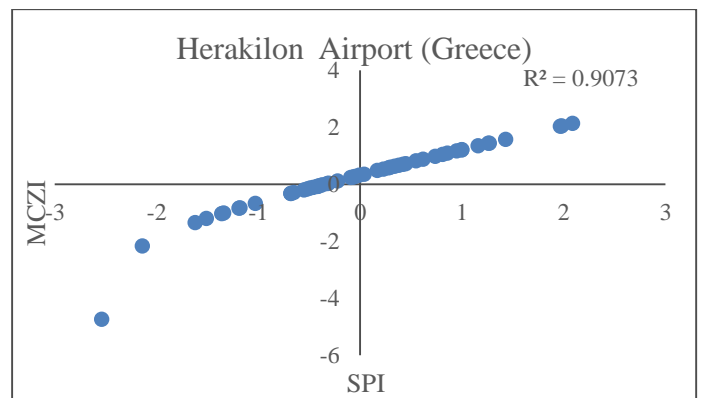
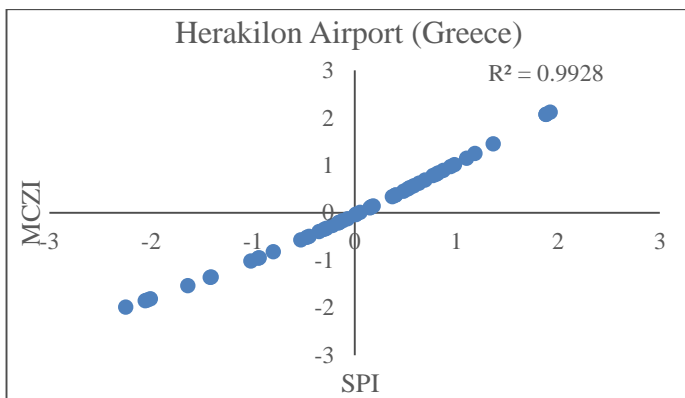
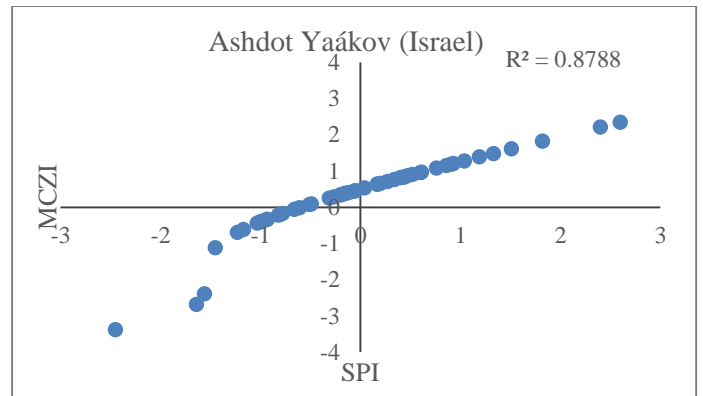
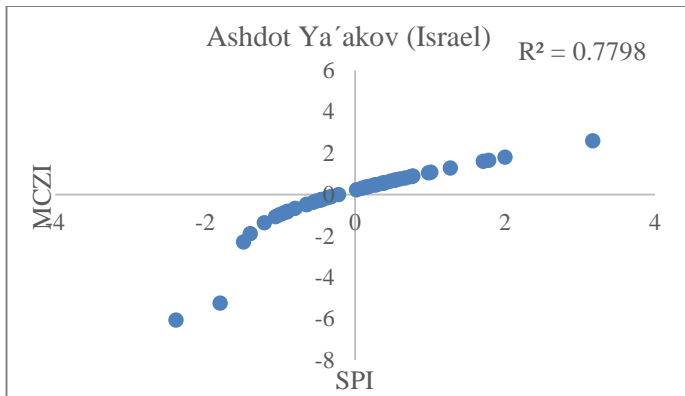
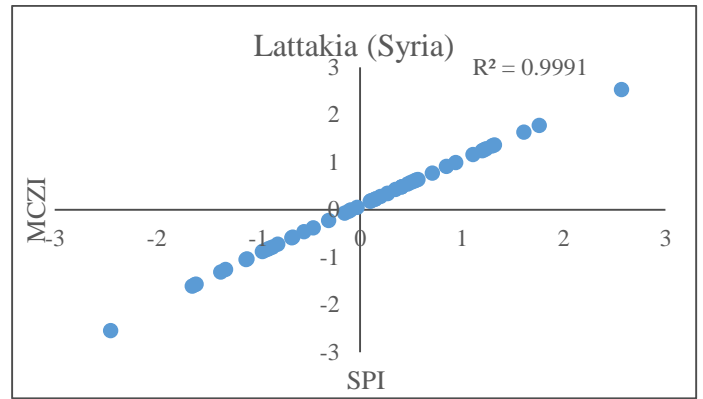
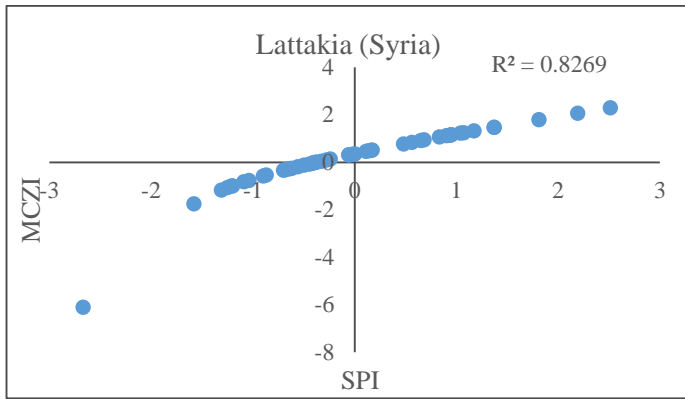
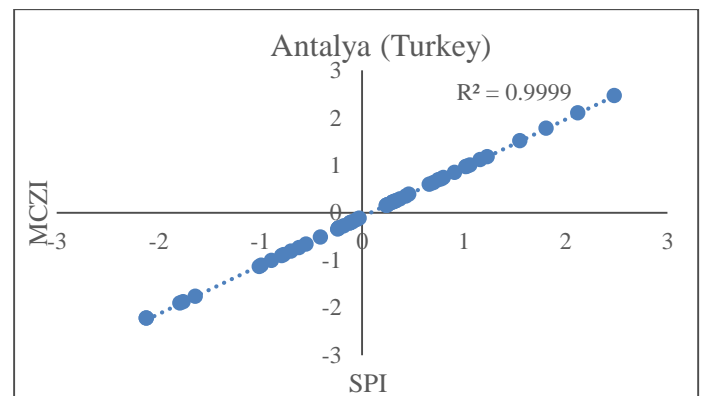
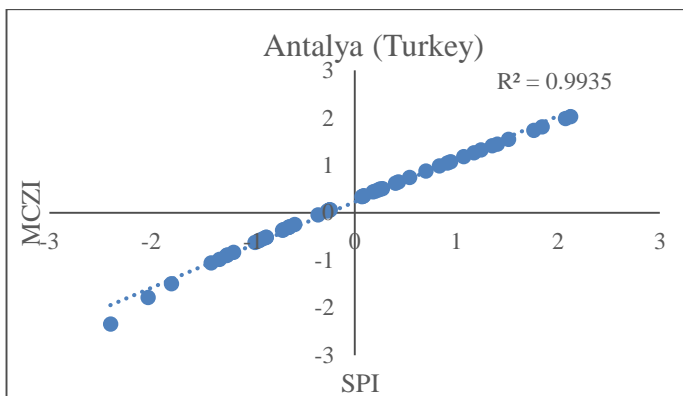
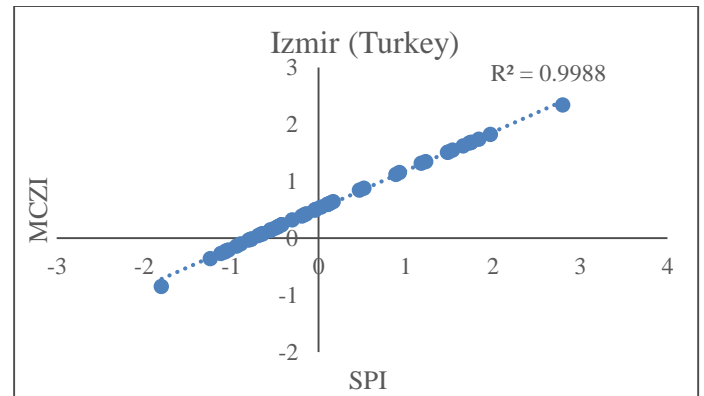
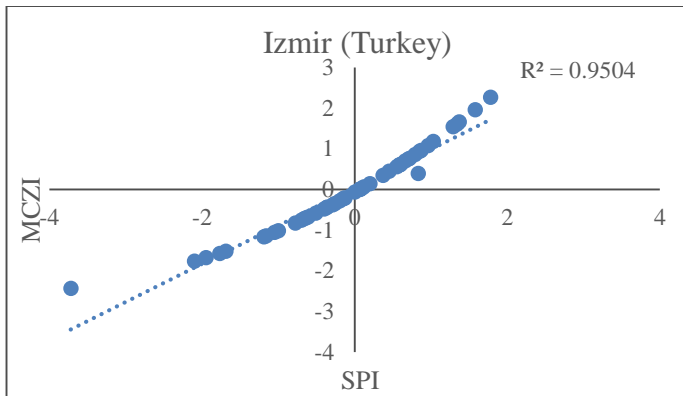
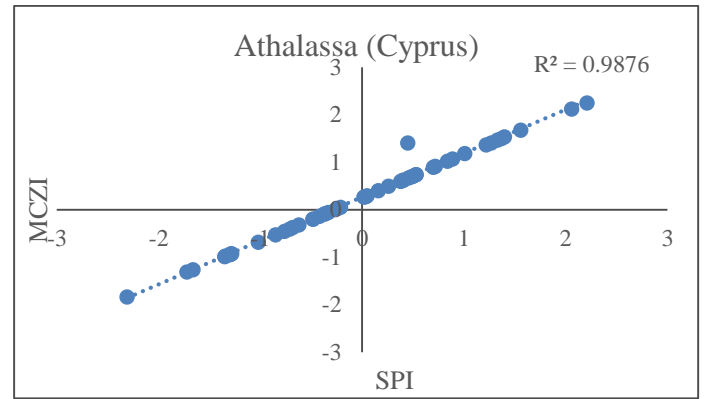
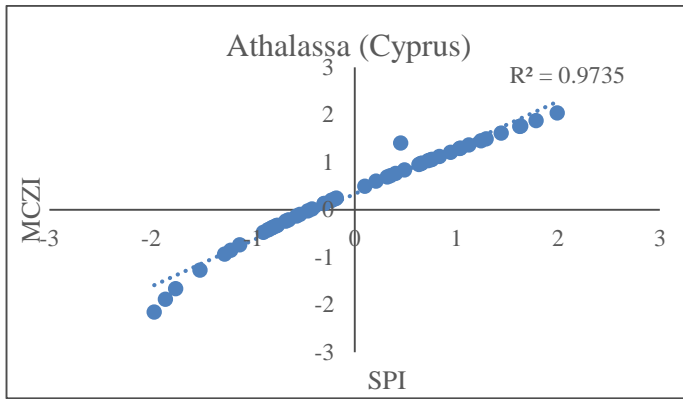


Figure 4.60 Observed trend of seasonal MCZI. Positive trends are in blue and negative ones in red. Large triangles represent significant trends at $\alpha=0.05$ otherwise small triangles are shown.

(No significant trends at $\alpha=0.01$ were obtained).

Nevertheless, these relationships depend on the period, timescale and climatic region. The strongest relationship was found between SPI and MCZI especially in rainy months in the coastal areas (Fig 4.60). This figure shows the linear regression between the values of the SPI and MCZI from 1961 to 2012. It indicates that the two indices generally have a strong relationship, particularly during the rainy season (Fig 4.61), and the coefficient of correlation ranges between 0.85 and 0.99). Using MCZI instead of CZI reduces all the discrepancies which can be found during drier months, as the SPI tends to have larger negative values than the CZI, which in turn is considered as a strong point of MCZI index. For example, high correlation coefficient between SPI and MCZI values in autumn was detected over the EM which ranges between 0.80 and 0.98).





“a”

“b”

Figure 4.61 Scatter diagram for the SPI-3 and MCZI for the selected stations for winter (a) and autumn (b) from 1961 to 2012

The results indicated that the MCZI tended to have lower negative values than the SPI especially in the southern parts of the EM which are drier comparing with the northern ones, which means that MCZI can express very dry conditions that do not show in the SPI. For example, MCZI values in Ashdod (Israel) fall between -3.1 and -1.1 when corresponding SPI (Fig 4.62).

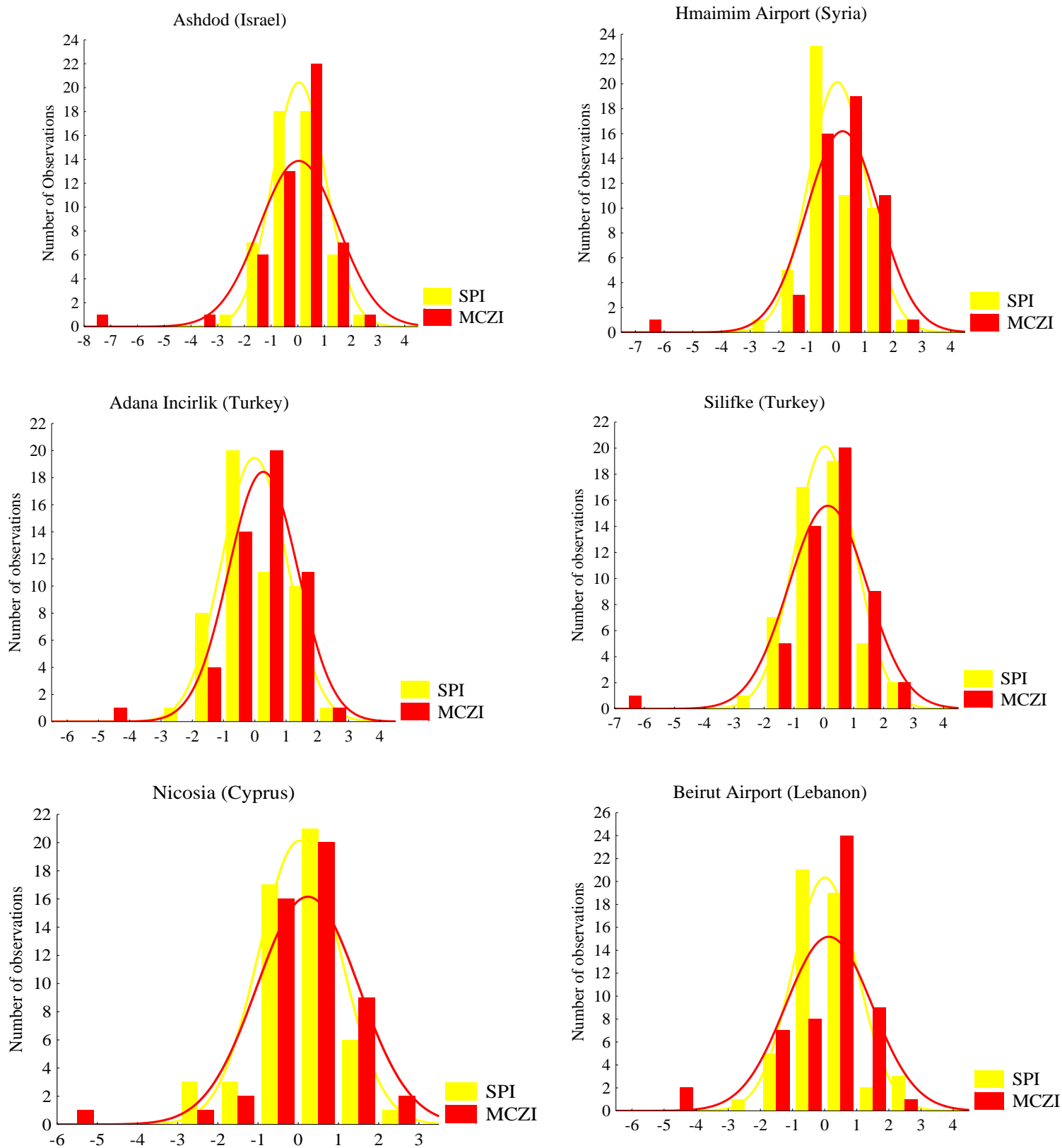
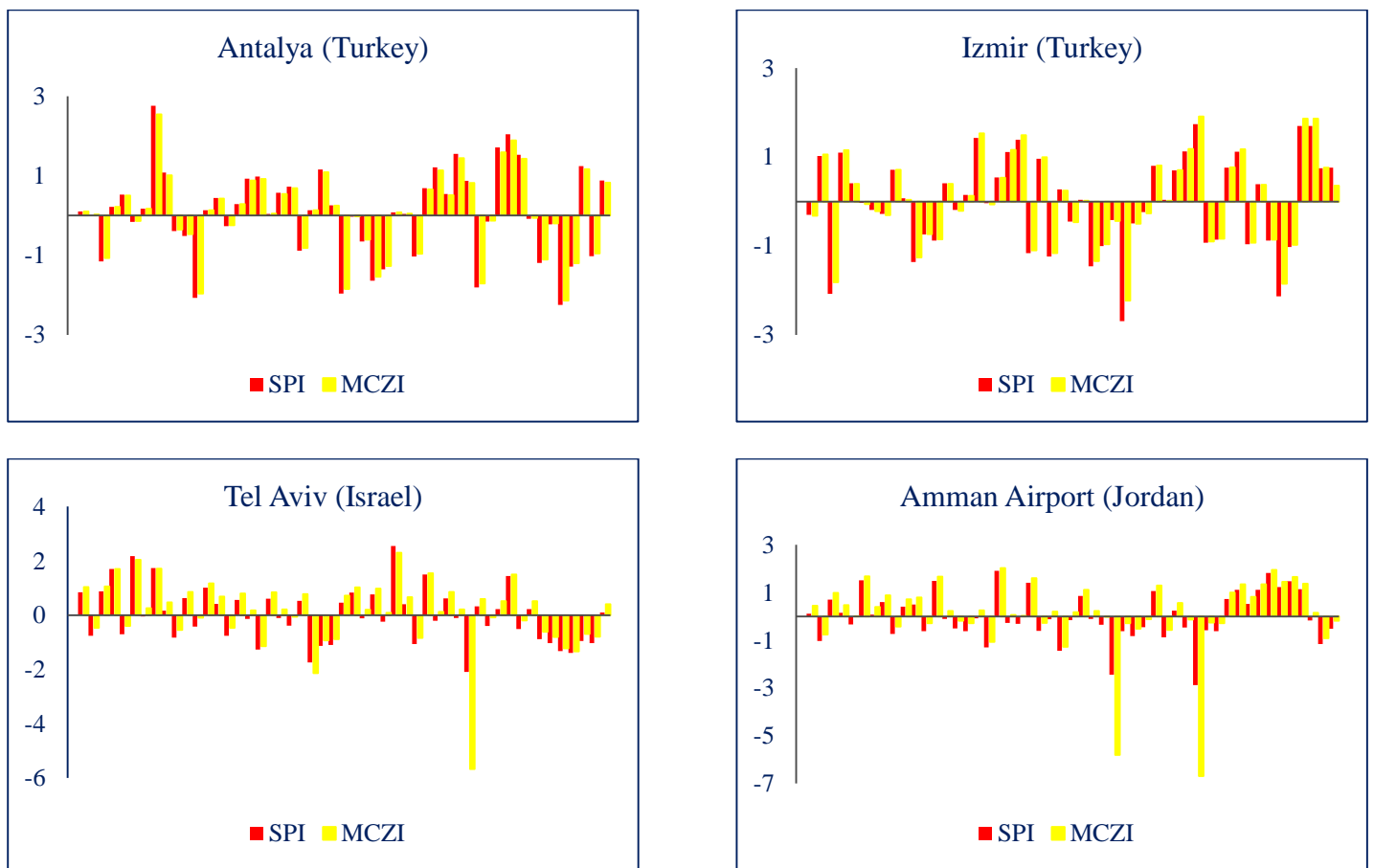


Figure 4.62 Histogram plot of the SPI and MCZI distribution in winter for some selected stations over 1961-2012.

In other words, since SPI and MCZI are distributed normally as stated in the assumptions associated with these relationships, the left tail of the MCZI distribution curve shifted away from the normal curve (Fig 4.61), creating the observed increasing differences between the SPI and MCZI in extremely dry conditions. Also, in wet periods (winter and spring), MCZI detected higher values than SPI in all the EM. Wu *et al* (2001) and Morid *et al* (2006) reported that MCZI showed larger negative values compared to SPI, which totally agree with our results in whole regions over the EM (Fig 4.63).



Figur 4.63 Comparisons of the SPI-9 and MCZI-9 in the wet period for 1961–2012 for some selected stations in several areas in the EM

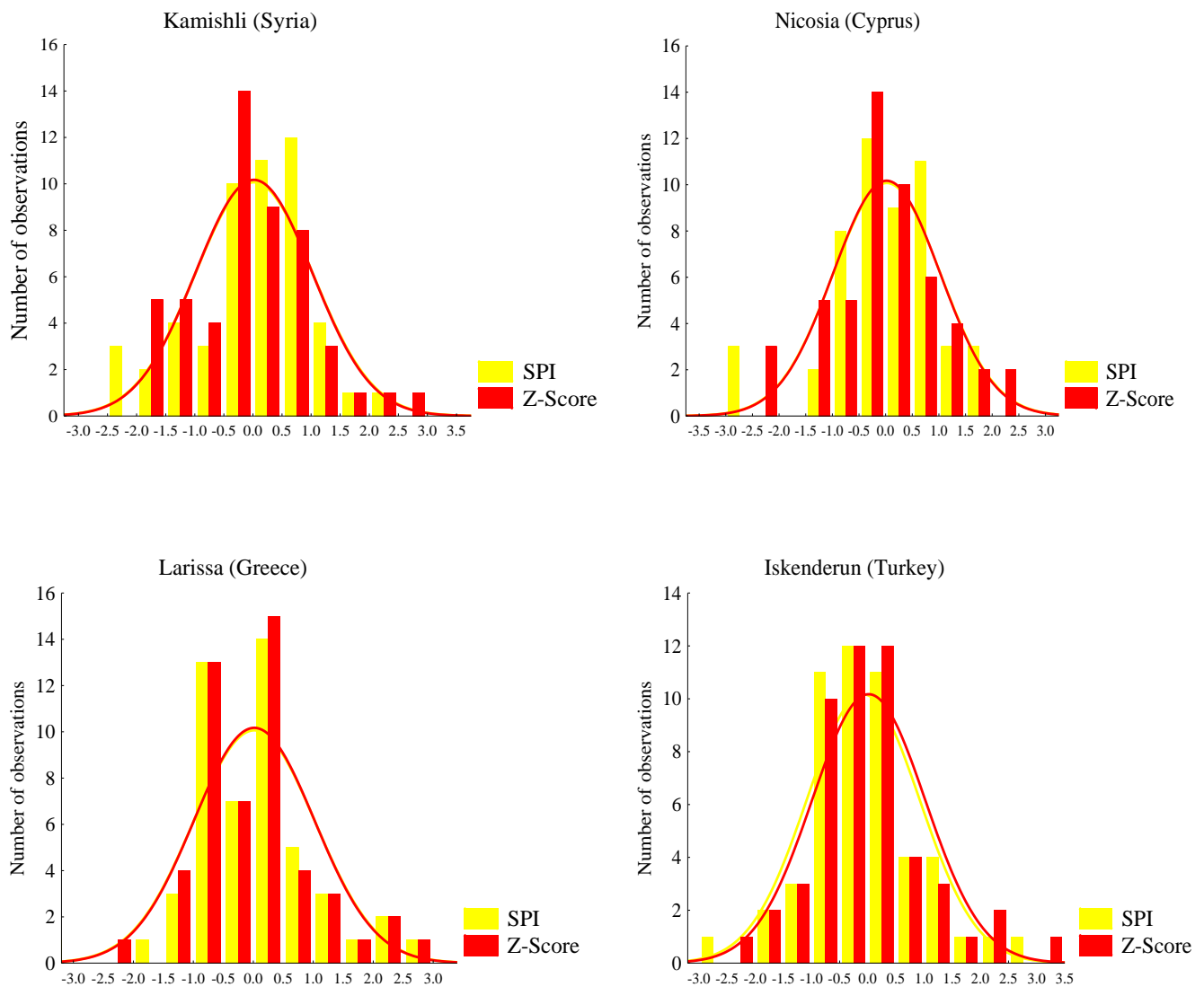


Figure 4.64 Histogram plot of the SPI-9 and Z-Score-9 (wet period) distribution for some selected stations over 1961-2012

Very Similar results were found in an intercomparison of SPI and Z-score. It can be seen that the Z-Score tends to have lower values than the SPI during drier periods (Fig 4.64). This Fig 4.63 illustrated that both of SPI and Z-Score matched the same distribution and the Z-Score generally appears more positive (or wetter) than the SPI in both extremely wet and dry conditions. For example, when the SPI is +2.18 in Larissia (Greece) the corresponding Z-Score is

+3.21, and when SPI is +2.7 in Iskenderun (Turkey) the corresponding Z-Score +3.5 (Fig 4.65). The Z-Score, on the other hand, has a wet bias compared to the other two indices in extreme wet and dry conditions, and may not detect serious drought conditions as shown in previous charts.

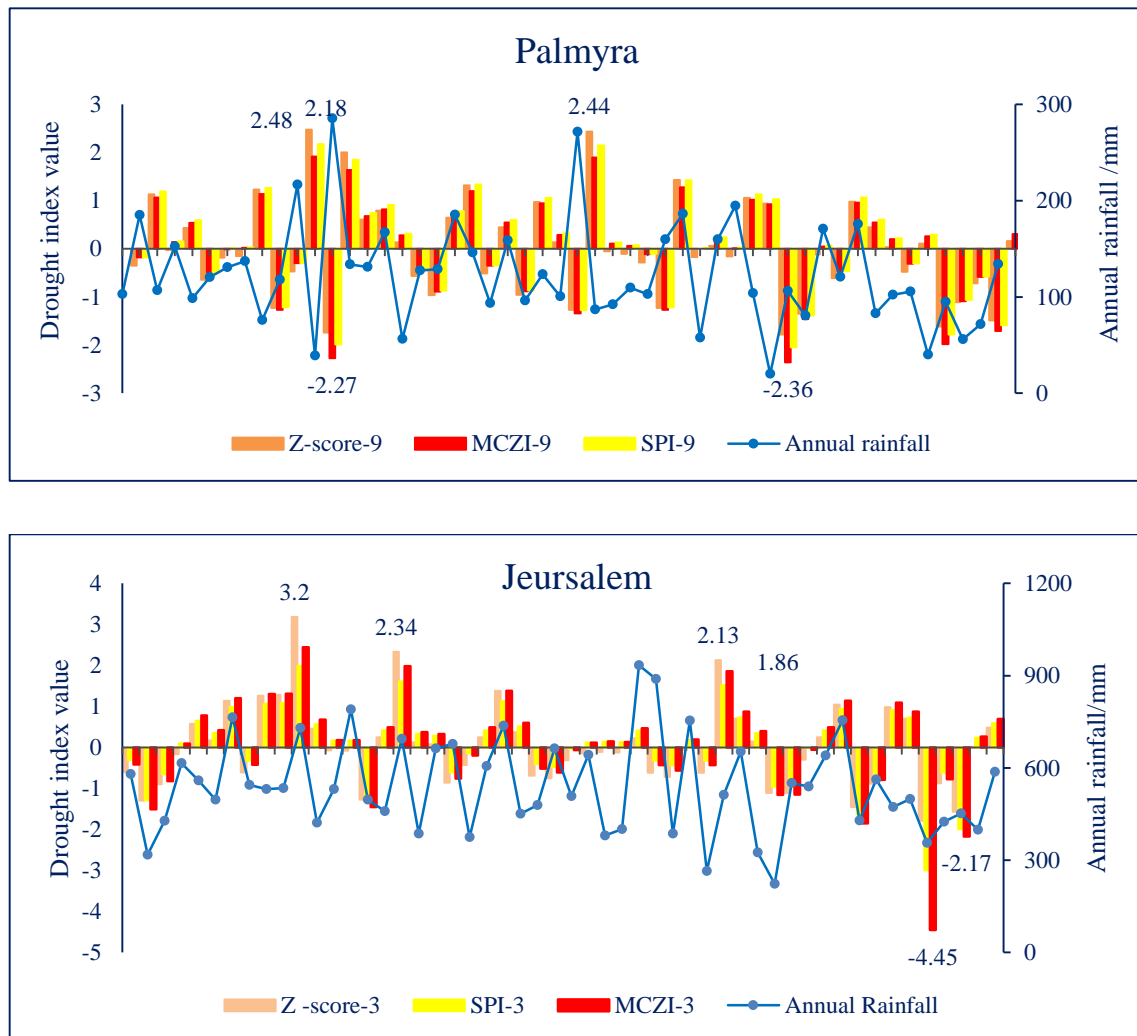


Figure 4.65 Time series of drought indices and rainfall at two Stations (Palmyra), time steps 9 months, and Jerusalem (Israel) 3 months.

This figure showed how MCZI has the most negative values comparing with both SPI and Z-Score, whereas the Z- score has the most positive values comparing with others. For example, in Jerusalem (Israel), the 3-month MCZI for May 2008 was -4.45 when the annual precipitation was 58% of the mean (355.9 mm), while the corresponding SPI and Z-Score values were -3.0 and -1.79, respectively. Contrary, Z-score detected the highest positive value in 1971 (+3.18), whereas MCZI and SPI values were less (+2.44 and +1.99), respectively. Except in

extremely dry or wet conditions, the MCZI and Z-Score provide the same measure of conditions as the SPI. In certain situations, the MCZI and Z-Score can be considered more appropriate tools for monitoring droughts and floods than the SPI because they are easier to calculate (Wu *et al.*, 2001).

Compared with the relationship between the SPI and MCZI, the SPI has a closer correlation with the Z-Score. The results show that the SPI is highly correlated with both the MCZI and Z-Score at all-time scales. In addition, in wet events these indices have a higher correlation than in dry events due to the high variability of precipitation amounts in the EM in dry periods. This evaluation showed similar behaviour of the MCZI and Z-Score with the SPI. For the Z-score, the frequency of dry periods differs from that of the SPI and MCZI, especially in the humid areas. The magnitude of this class in the Z-Score is higher than in the MCZI between 1.25 times (arid areas) to 2.6 times (humid areas) (Fig 4.66).

This study shows that the SPI, MCZI and Z-Score are good tools to define, detect, and monitor droughts and floods and manage of water resources or precipitation anomalies at different time scales. The MCZI and Z-Score are very similar to the SPI for 3-, 6-, 9-, 12- and 24 -month time scales. The major advantages of the MCZI and Z-Score against the SPI are that the calculations of these two indices are simpler than the SPI. The MCZI is more responsive to precipitation deficits than the other two indices in extremely dry conditions. When the actual precipitation is much lower than the mean precipitation for a period, the MCZI could reach large negative values compared to the other two indices. The same results were obtained by Wu *et al* (2001) and Shahabfar and Eitzinger (2013).

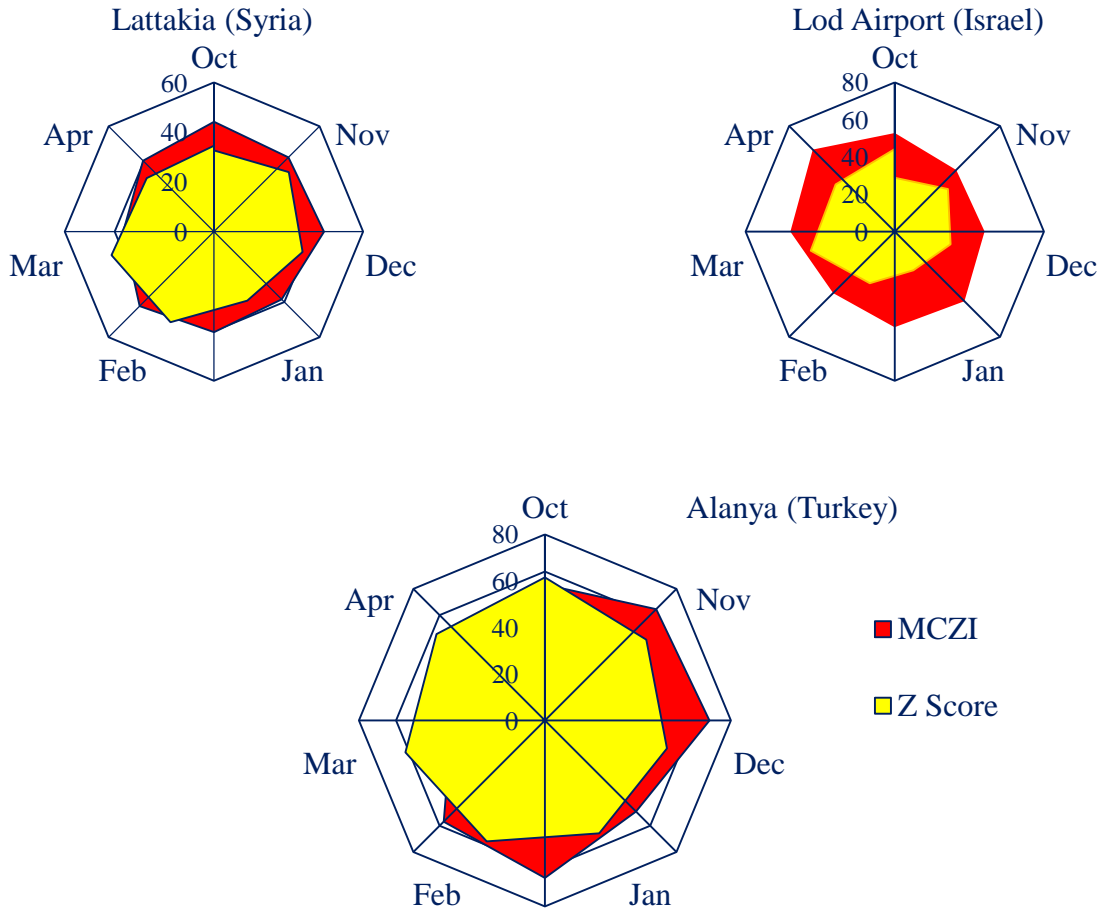


Figure 4.66 Monthly drought risk occurrences (%) according to Z-score and MCZI for the humid period in some selected stations over 1961-2012

Results from Decile Index (DI) showed that it can capture some of the drought events of 1970, 1989, 1990, 1999, 2007, 2008 and 2010 especially in the southern parts of the EM. The figure shows that the Rainfall DI, at regional scale, also captured some of the drought events. Those years whose precipitations are below the D line are the years with “much below normal”, which significantly increased after 1990. The results demonstrated the period 1989–2008 as the most extreme and long-lasting drought event, especially in whole regions over the EM (Fig 4.67).

These environmental stresses such as the prolonged severe drought periods, worsened by a warming climate, were an overlooked factor in creating the recent

crisis in Syria. These situations lead to increase poverty and relocation to urban areas and helped spark a bloody civil war in Syria. All these factors, combined with high unemployment and bad government, helped tip Syria into violence. This civil war and other environmental problems contributed to the displacement of 1.5 million Syrian farmers with subsequent impact on political stability (Gleick, 2014). FAO and World Food Program (WFP) reported that up to 60 % of lands in Syria experienced one of the worst long-term droughts in modern history during 2008-2012 and the recent conflict will exacerbate the dangerous throughout whole ecologic and socioeconomic systems in the absence of drought risk management investments and programs. The United Nations estimates that half of the country 22 million people have been affected, with more than six million have been internally displaced. The recent precipitation variability and decrease and subsequent environmental stresses in the EM and Middle East might play a big role in the new Middle East situations such as the Syria revolution. The second look at Egypt and Libya addresses the role that climate change in North Africa, as well as related stress like droughts, which likely contributed in re-establish a new Libya, highlighting the possibility of action on climate change and water security as a tool for conflict resolution and peace building.

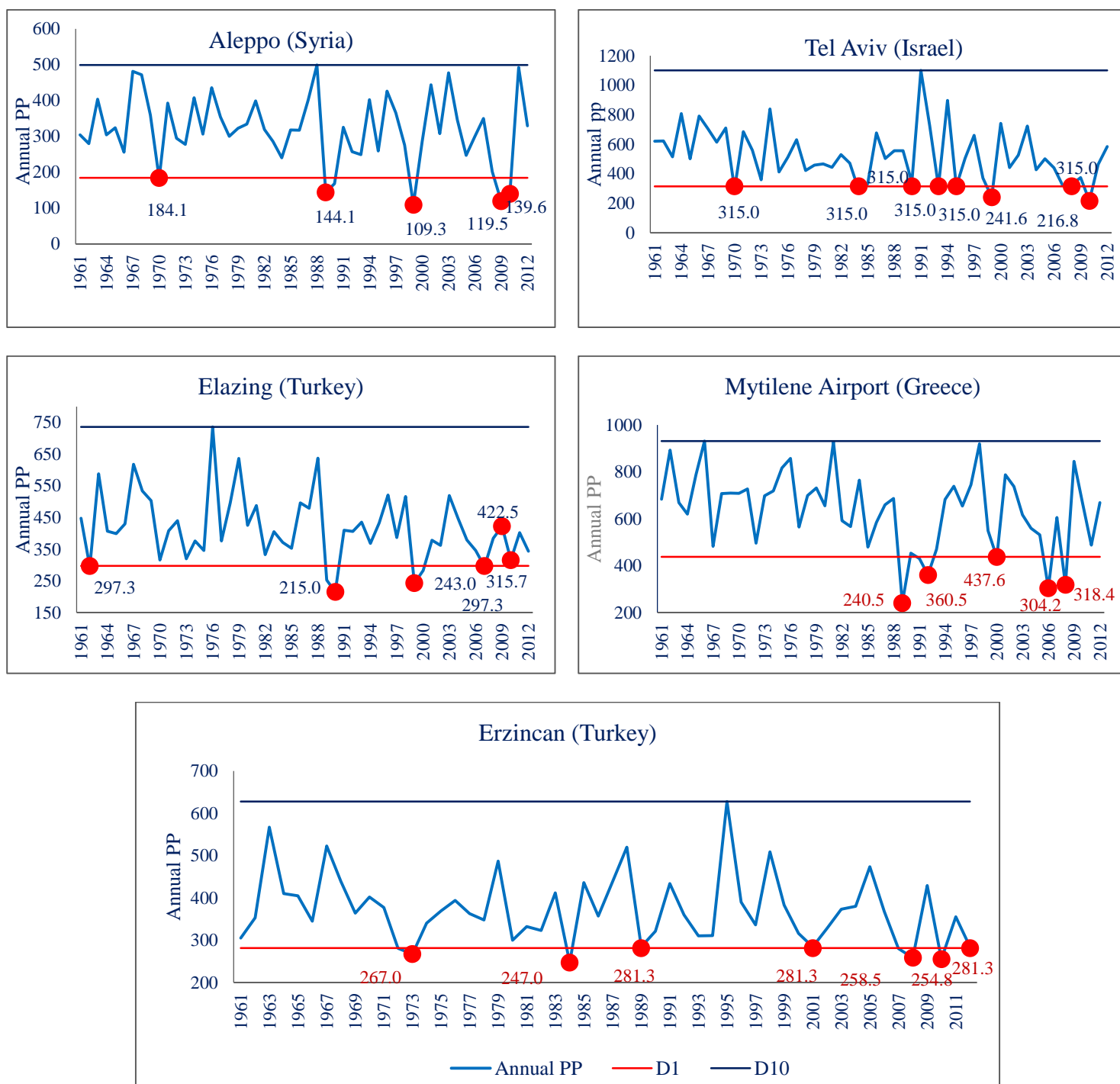


Figure 4.67 Annual rainfall variability in five stations representing five regions in the EM over 1961-2012. Red circles are the precipitation amount below the D line “much below normal”.

These results showed that the lowest DI values were detected in EOF1 (Libya, Egypt, Israel, Jordan and south and mid Syria) with high variability in the

same region too (CV=36.7%) then in EOF3 (Libya, Egypt, Israel, Jordan and south and mid Syria) (Fig 4.2), whereas CV values in the EOF5 was the lowest one (CV= 30.5%) (Fig 4.68).

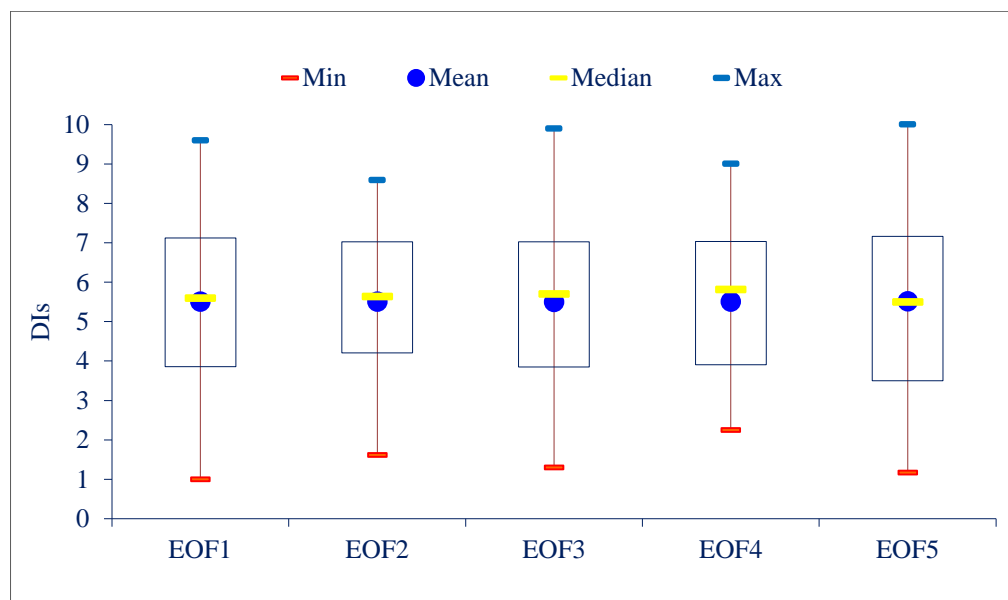


Figure 4.68 Box-Whisker diagram of DI values in five regions over 1961-2012 in the EM.

In other hand, the minimum values of DI ranged between 1.0 in EOF1 and 2.3 in EOF4, whereas the highest value ranged between 10 in EOF5 and 8.6 in both EOF3 and EOF5.

The same evaluation has been used for the DI (Fig 4.69). The frequency of dry and wet cases differs from that of the SPI, especially in the “normal and near normal classes” which is from 3 (in the northern parts) to 3.5 (in the southern parts) times higher than in the DI (Fig 4.69).

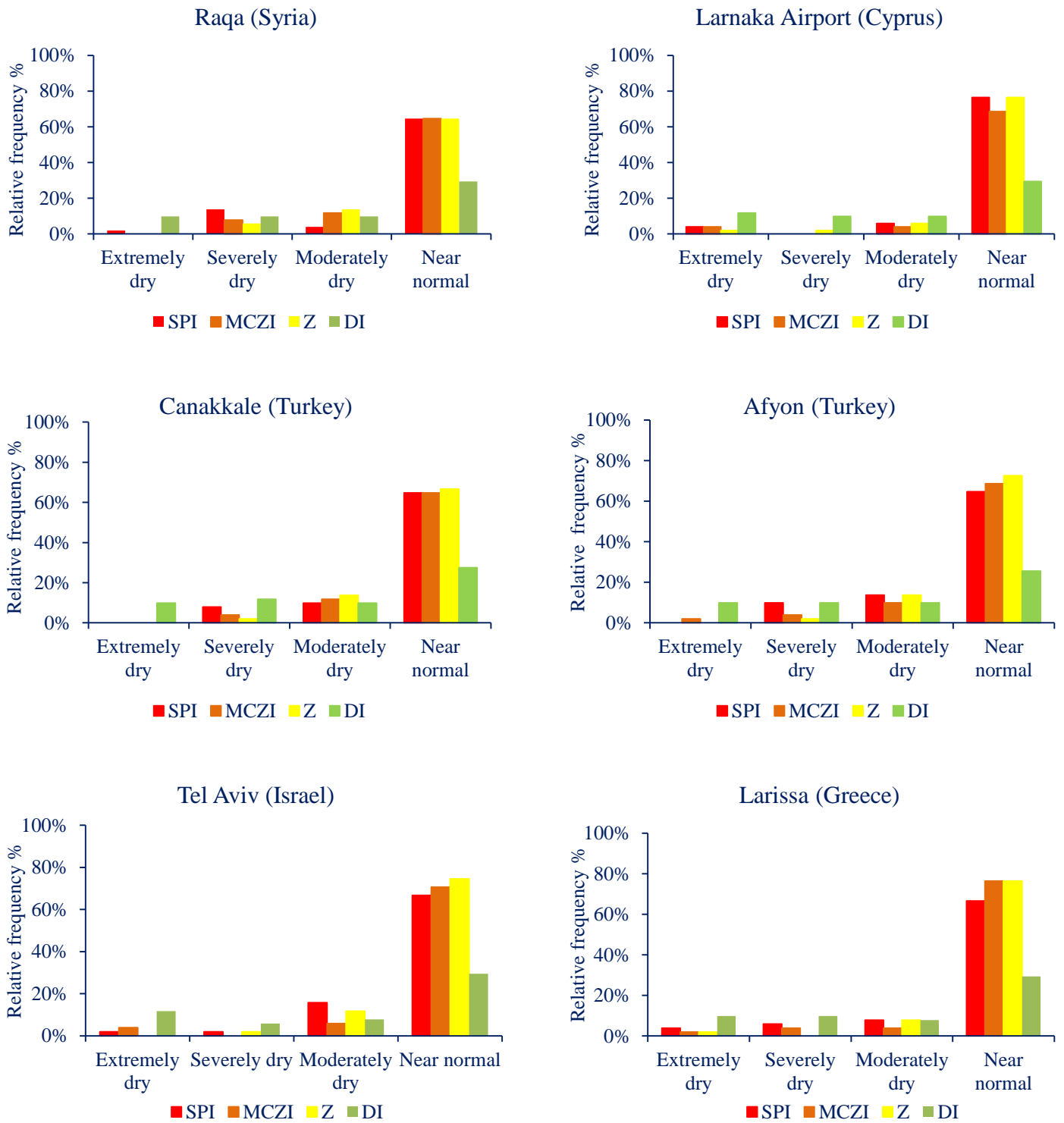


Figure 4.69 Histograms of the drought frequency classes of the SPI, MCZI, Z score and DIs for the some selected stations over 1961–2012.

Fig 4.69 shows the histogram of the relative frequency of the dry classes according to the SPI, MCZI, Z-score and DI. This evaluation showed similar behaviour of the MCZI and Z-Score with the SPI in all classes and different behaviour for DI in the “near normal” period. These indices have detected between 65-77% of the months in the ‘near normal’ situation, but the DI have been more responsive to the dry situation. The DI detected only 25-29% of the period in the ‘near normal’ class. These results agree with Dogan *et al* (2012) in Turkey and Morid *et al* (2006) in Iran who found that the SPI detects between 63.8-77.7% of the months in the near normal situation whereas the DI detects only 13.8-38.8% for the same class.

4.9.3 Assessment drought severity using daily Effective Drought Index (EDI).

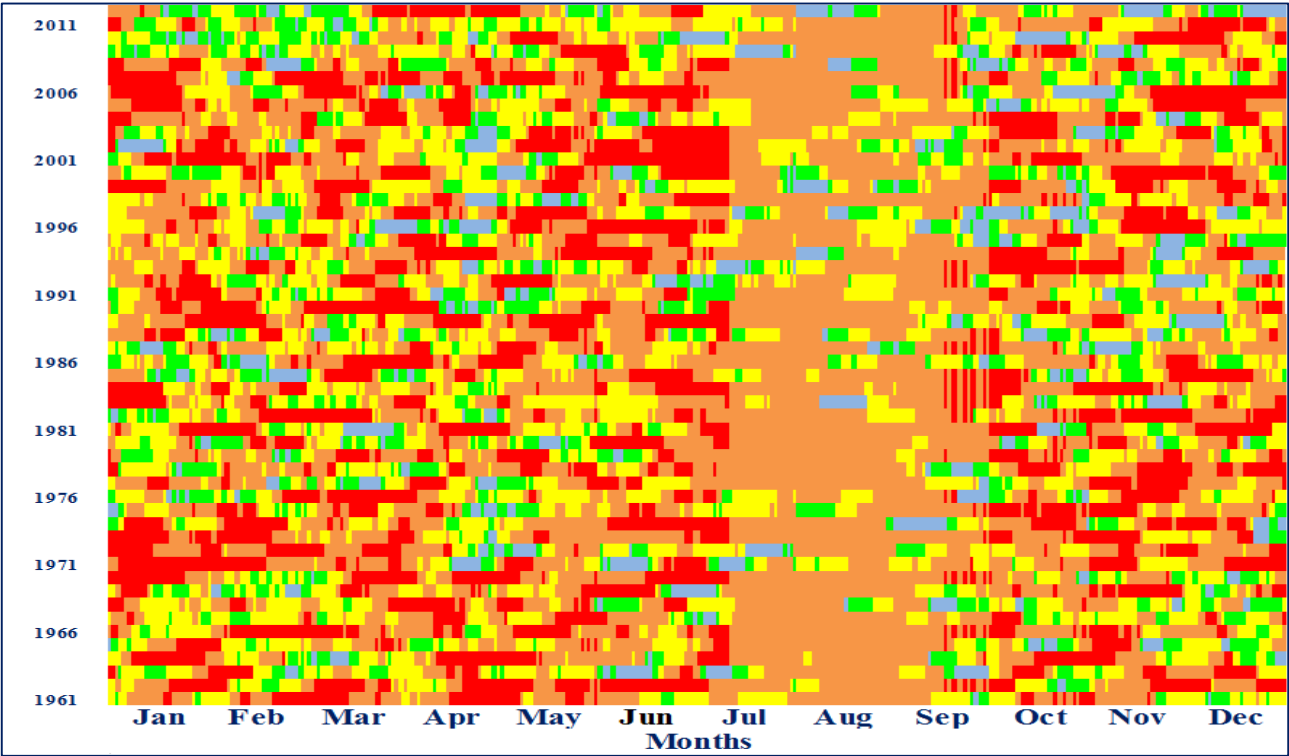
4.9.3.1 Analysis of EDI values.

In order to unveil any patterns in drought occurrence behaviour in the observed data, EDI values are plotted in function of the year (y axis) and the day of the year (x axis) for some selected stations representing all previous sub regions (Fig 4.70). Thus, a qualitative assessment of any seasonal patterns as well as the inter-annual variability can be made. From the plots, it can be seen that droughts seem to occur more often in Sivas and Kastamonu (Turkey) than in Thessaloniki Airport (Greece) and Lattakia (Syria). This figure reveals that drier (low EDI) and wetter (high EDI) periods seem to span over multiple years in whole regions represented by these four stations.

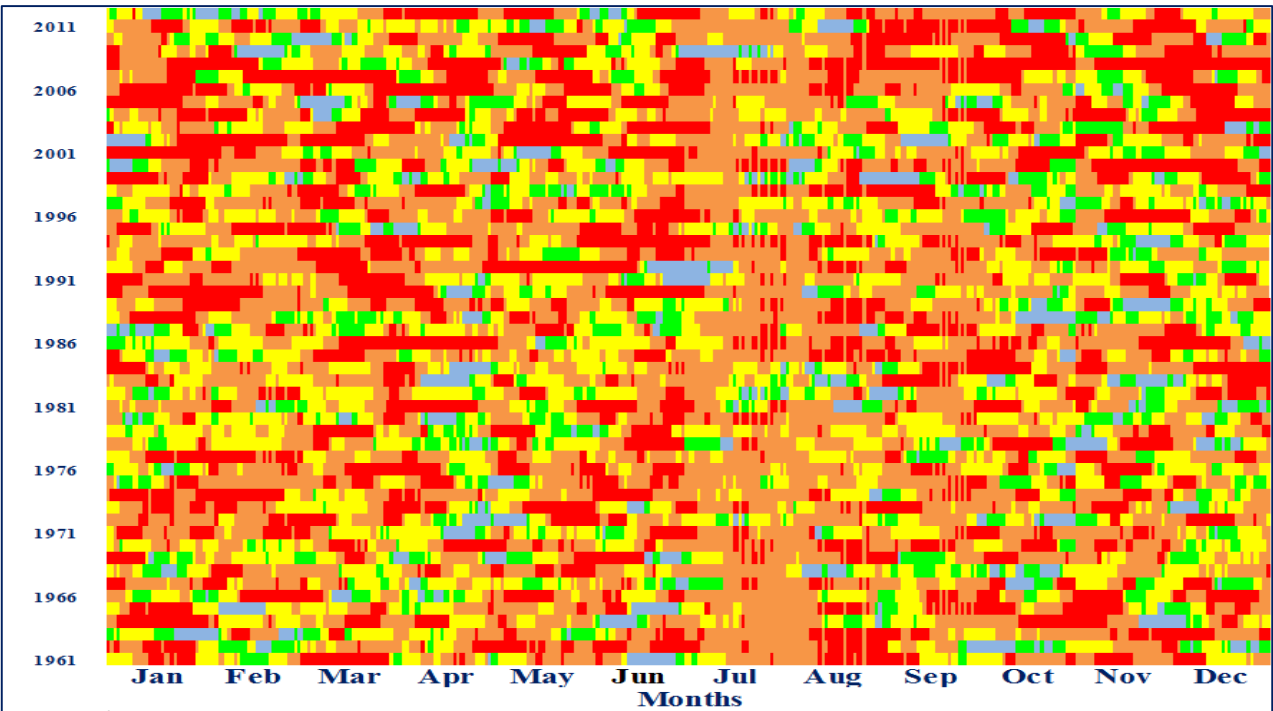
It is obviously seen that the severe and extreme droughts in the period from (June to October) have a lower frequency of occurrence than this during the period from November to May, that includes both wet seasons (winter and spring) especially in Jerusalem (Israel) and Ammandus (Cyprus). These areas have low precipitation amounts in summer and autumn which explains the absence of extreme drought events (red colour) during these two periods. In figure 4.70, we can also see the interannual variance of the EDI for all data sets. The intra-annual variances for the Sivas, Kastamonu and Thessaloniki Airport are higher than those

for Lattakia and which means that, on average, the EDI values obtained from the first three stations time series fluctuate more throughout the year than those derived from observed rainfall series.

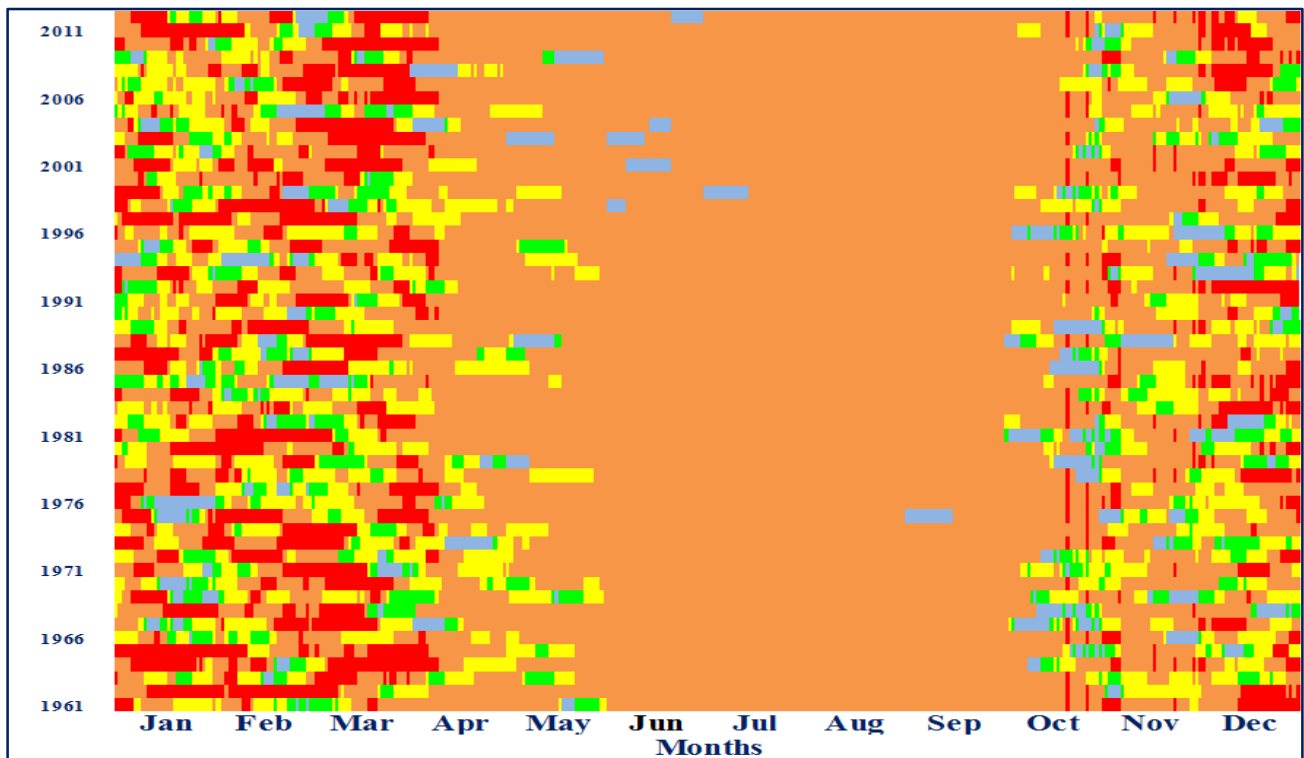
Sivas (Turkey)



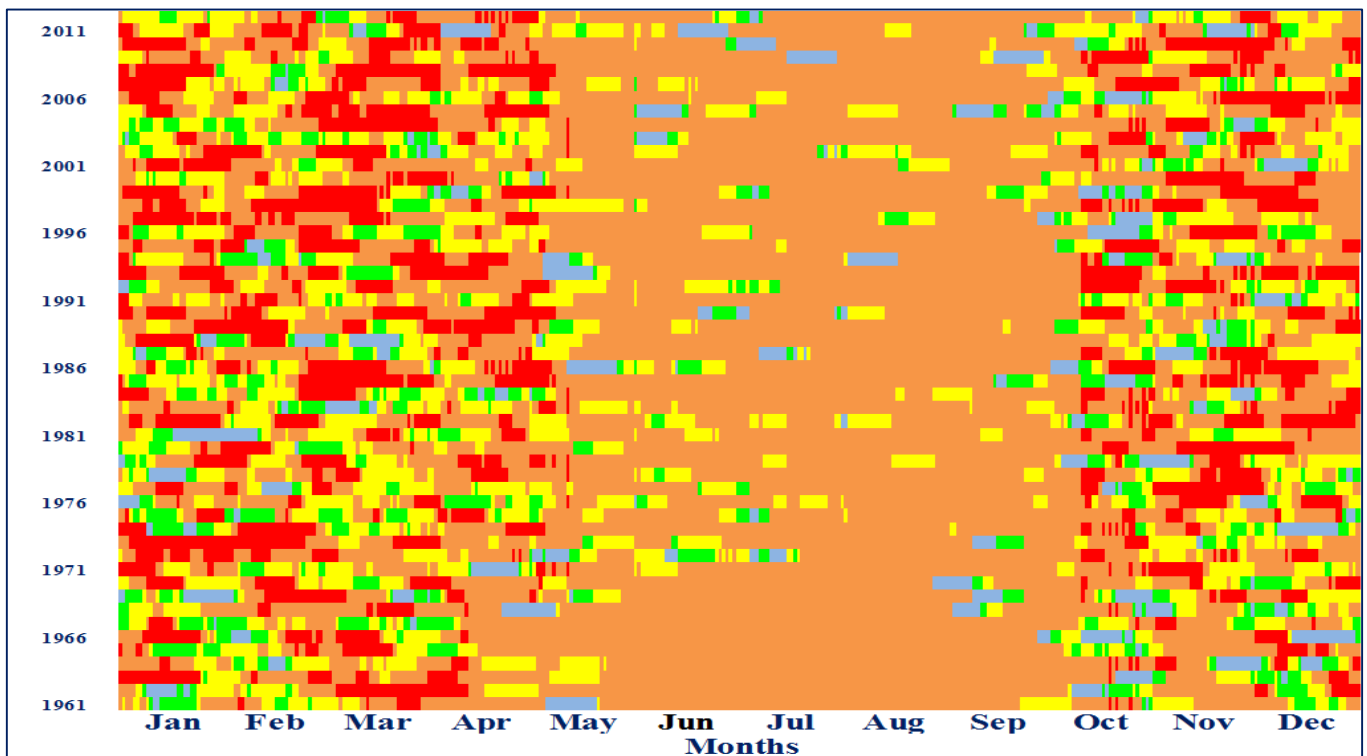
Kastamonu (Turkey)



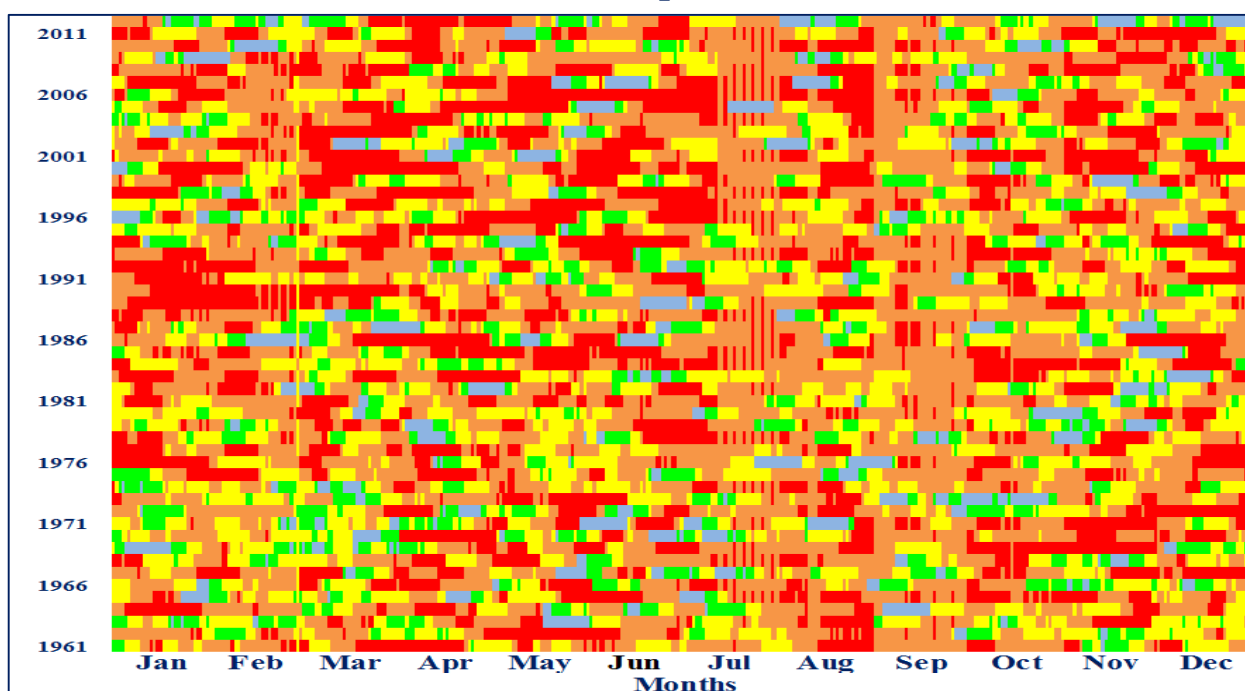
Jerusalem (Israel)



Lattakia (Syria)



Thessaloniki Airport (Greece)



Amiandos (Cyprus)

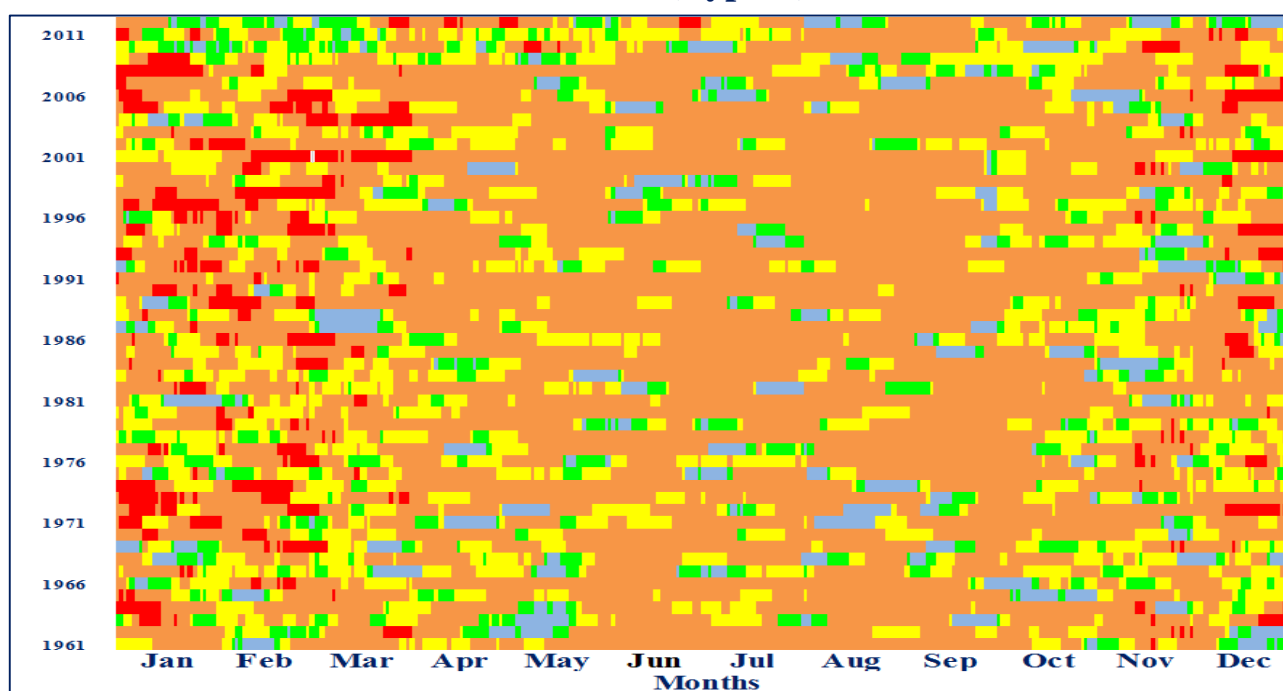


Figure 4.70 Evolution of the EDI index of observed rainfall records in some stations over 1961-2012

It can be seen that the extreme dry events stop in May in Amiandos, Lattakia and Jerusalem, which have different mean annual precipitations (948.1mm, 730.8 mm and 539.9 mm, respectively). Nevertheless, all of them have originally long dry periods with very low precipitation amounts (between 0.0 mm and 25 mm) covering 5 months (from the first June till the end of October) with some variability between each other. Other stations like Thessaloniki Airport (Greece), Sivas and Kastamonu (Turkey) showed a continuous moderate and severe periods without interrupt in summer, which relatively has high precipitation amounts comparing with those in the southern parts of the EM; the mean summer precipitation in Kastamonu, Savis and Thessaloniki airport is 129.8 mm, 55mm and 70mm, respectively.

The run-sum method (Yevjevich, 1967) was utilized to calculate the sum of the drought severity over the period in which the EDI values fall below the standard ones. In this research, we considered the classification proposed by Morid *et al* (2006) who defined an extremely dry to moderately event as the dry period in which the EDI index is continuously less than -0.7 . When this method is applied to the EDI, the sum total of continuous negative EDI values is called the Accumulated EDI (AEDI). By applying the AEDI and calculating the sum of all the negative EDI values using an annual unit, we can express drought severity on an annual basis. This method is used for a comparative analysis of severity between drought events and for the estimation of the accumulated damage by representing the accumulated negative values of EDI which in turn can characterize an accumulated rainfall and real water shortage because droughts depend not only on the absolute quantity of the precipitation shortage, but also on the temporal distribution of precipitation. For instance, annual precipitation for the year 1974 in Lattakia (Syria) was recorded as 1096.8 mm, 150% of the average annual precipitation over 1962-2012 period (730.77mm). 1974 had the third highest precipitation during 1961-2012; however, the year was determined to be very severe drought with prolonged drought 6 months. This means that there was an extremely poorly-balanced distribution of precipitation in 1974. Therefore, when we viewed this from a simple annual precipitation perspective, this year could be

classified as a “flood” period. However, when you use the YAEDI, it is categorized as a severe drought year, thus showing the practicability of the YAEDI. Depending on AEDI and from the previous figure we can define the droughts that had occurred in several regions and the most severe droughts were selected (Table 4.10). Within the 52-year period, droughts were more severe from 1990 to 2010.

Table 4.10 Top 10 drought cases based on the AEDI values for 52 years in three stations represented to four different regions over the EM

Station	Rank	Onset date	AEDI	Dry duration (Day)	Severe drought (%)
Savis (Turkey)	1	11/06/1984	-107.6	173	23.1
	2	02/04/1989	-103.3	159	38.4
	3	11/03/1994	-100.5	143	40.6
	4	05/11/2000	-84.6	48	80.0
	5	21/02/2007	-83.3	106	69.8
	6	11/10/1982	-76.9	109	63.3
	7	14/06/1998	-75.9	137	13.9
	8	22/02/1986	-70.0	81	51.8
	9	11/08/1993	-63.5	100	44.1
	10	22/06/2007	-61.2	117	9.4
Thessaloniki Airport (Greece)	1	05/04/1985	-139.4	232	46.2
	2	27/04/2006	-127.7	164	9.1
	3	15/11/1991	-104.6	147	83.0
	4	16/07/1965	-96.2	135	44.4
	5	20/12/1989	-91.4	111	67.6
	6	01/07/1993	-81.5	138	34.1

	7	26/12/1988	-71.6	88	78.5
	8	09/05/1984	-67.7	98	48.1
	9	15/04/1981	-60.9	103	32.1
	10	04/07/2010	-60.8	94	42.6
	1	29/02/2008	-111.7	209	100.0
	2	25/05/1993	-105.8	226	100.0
	3	19/02/1985	-102.7	208	100.0
	4	29/05/1980	-102.6	222	100.0
Lattakia	5	06/02/2004	-93.2	199	100.0
(Syria)	6	30/03/1974	-91.7	235	100.0
	7	14/10/2000	-81.2	130	98.5
	8	29/11/1972	-78.0	97	100.0
	9	17/02/2005	-72.0	124	100.0
	10	17/11/2009	-62.8	104	100.0
	1	01/07/1998	-79.4	201	16.1
	2	01/07/2010	-76.3	214	12.2
	3	19/03/2012	-69.1	195	7.73
	4	10/11/2008	-65.5	103	48.5
Jerusalem	5	29/02/2008	-62.7	113	32.1
(Israel)	6	01/07/1999	-61.4	188	7.0
	7	26/02/2004	-58.6	116	33.1
	8	20/02/2005	-54.4	120	20.0
	9	07/02/2002	-52.1	134	10.5
	10	23/01/2006	-46.1	67	61.2

In particular, the drought that began after 1998 (shown in Table 4.10) was the most severe drought within the 52-year period in Syria (represented by Lattakia) and Israel (represented by Jerusalem). This drought was distinguished from the other droughts by its AEDI of -111.7 in Lattakia and -79.4 in Jerusalem, rather than by the minimum EDI of -2.47 in Lattakia and -3.1 in Jerusalem. Severe and moderate drought percentages were more consistent and high in all top ten drought events in Lattakia (98-100%) and occurred in the wet periods which in turn would affect water availability in reservoirs substantially and the recurrent extreme drought events could lead to potentially dramatic emergencies in terms of water quality and availability in the next decades. As it is shown from the table, 7 out of 10 most severe droughts occurred after 1989 in Sivas (Turkey) with the highest frequency 80% for the fourth rank which started in the 5th of November and lasted only for 48 days, but with very low EDI values during this period which proved that the severity of droughts did not solely depend on the values of drought indices. That is, some droughts have low intensity, but are maintained for a long period of time. Some droughts have high intensity, but are of short duration.

The same case was shown in Jerusalem (Israel) which detected the highest extreme drought frequency (61.2%) during 67 days for AEDI (-46.1) in winter. It can be seen that the highest frequencies of extreme drought occurred during the winter in all previous stations or started in autumn and extended till winter or spring.

For more explanation, a comparison between frequency distributions of EDI values of the wet period (September to May) and the dry one (June to August) in Lattakia (Syria) and Sivas (Turkey) is shown in Fig 4.71. Fig 4.71 showed that Lattakia has detected lower EDI values in the first period (January to May) than Sivas with higher frequency for the values less than -1 in Sivas, (7.1% in Lattakia -13.8% in Sivas). In the second period (June to October), lower values of EDI were shown in Sivas comparing with Lattakia and the ratio of drought - wetness showed that the probability of severe and extreme drought/wetness ($-1.0 > \text{EDI} > 1.0$) was higher in Sivas (2.9% vs 0% in Lattakia)

and the frequencies of severe and extreme drought decreased from the first period to the second one.

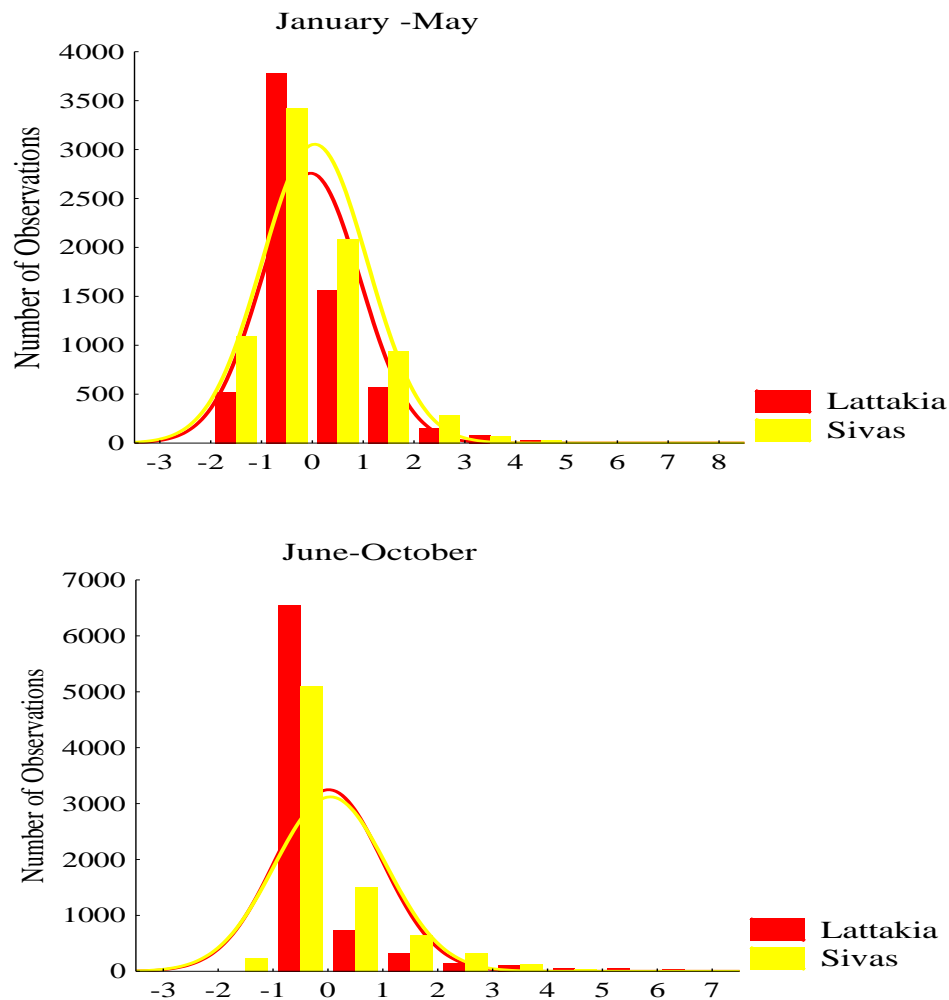


Figure 4.71 Comparison between frequency distributions of EDI values in two periods in Lattakia (Syria) and Sivas (Turkey) over 1961-2012.

These results are coherent with those proved by Oikonomou *et al* (2008) who expected a long dry spells over whole regions of the EM and will be longer in its southern parts in winter and spring. Extreme wet spells are getting shorter everywhere during all seasons, except autumn, due to the high reduction in seasonal precipitation amounts in winter and spring. The greatest reduction (1.3 days) was noticed in Turkish coast and southern continental Greece (Holt and Palutikof, 2004). The maximum increase of dry spell length is expected in winter

in the southern part of the EM basin, as well as in spring, reaching up to about 7 days (Oikonomou *et al.*, 2008). Thus, the frequencies of dry spells ($EDI < 0$) in the dry areas of the EM are larger than those detected in the northern parts, but the frequencies of severe and extreme ones are less.

Fig 4.72 demonstrates these results in 16 stations representing most regions over the EM for $EDI < -1$ and $EDI < 0$.

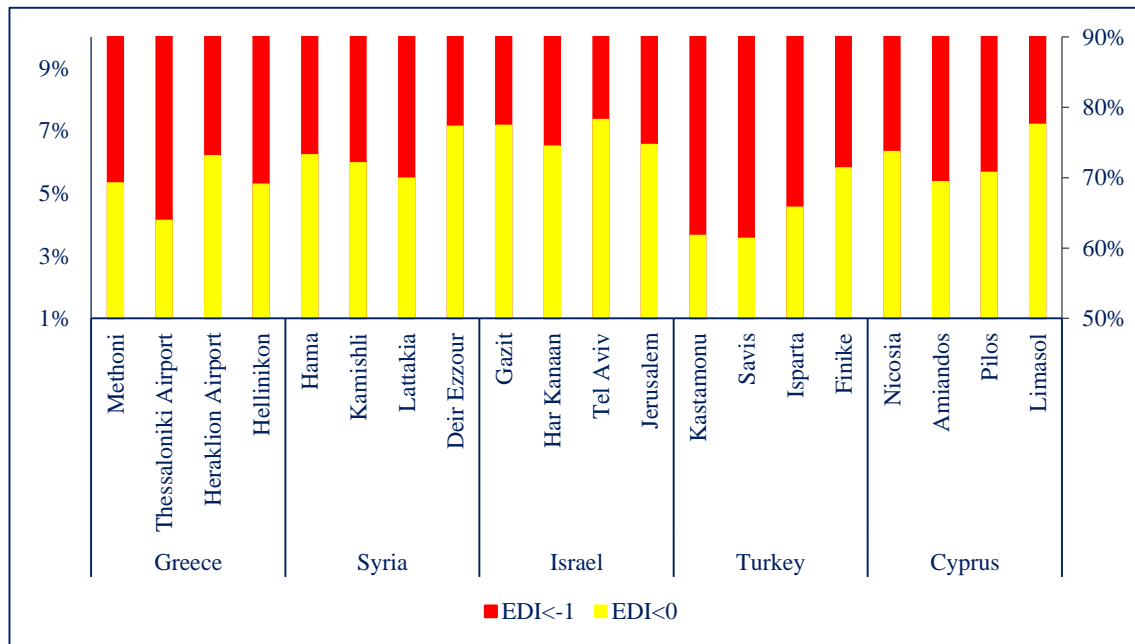


Figure 4.72 Frequency distribution of the daily EDI values in some selected stations during the period 1961–2012.

For example, the frequency of negative EDI values (dry spells) in Tel Aviv (Israel) is 78.3% of total days, but 3.7% of them is extreme. The same case of Deir Ezzour (Syria) in which the EDI has the lowest rate of extreme (1.9%) but a high rate of dry days (77.3%). On the other hand, both Savia and Kastamonu (Turkey) showed moderate rates of dry days (61.5%) accompanied by high rates of extreme drought frequency (8.6% and 9.3%, respectively). The correlation between $EDI < 0$ and $EDI < -1$ values showed a strong negative relationship with a correlation coefficient ($R = -0.75$).

It can be seen that several droughts were concentrated between the 1961 and 2012. In particular, the 2008, 1973 and both 1999 and 2012 droughts were the severest ones. Fig 4.73 shows the histograms of the frequency of drought durations whose EDI is less than -1.0 (drought duration) and less than 0 (dry duration) for the month of the year and for whole year indicated for some stations over the EM.



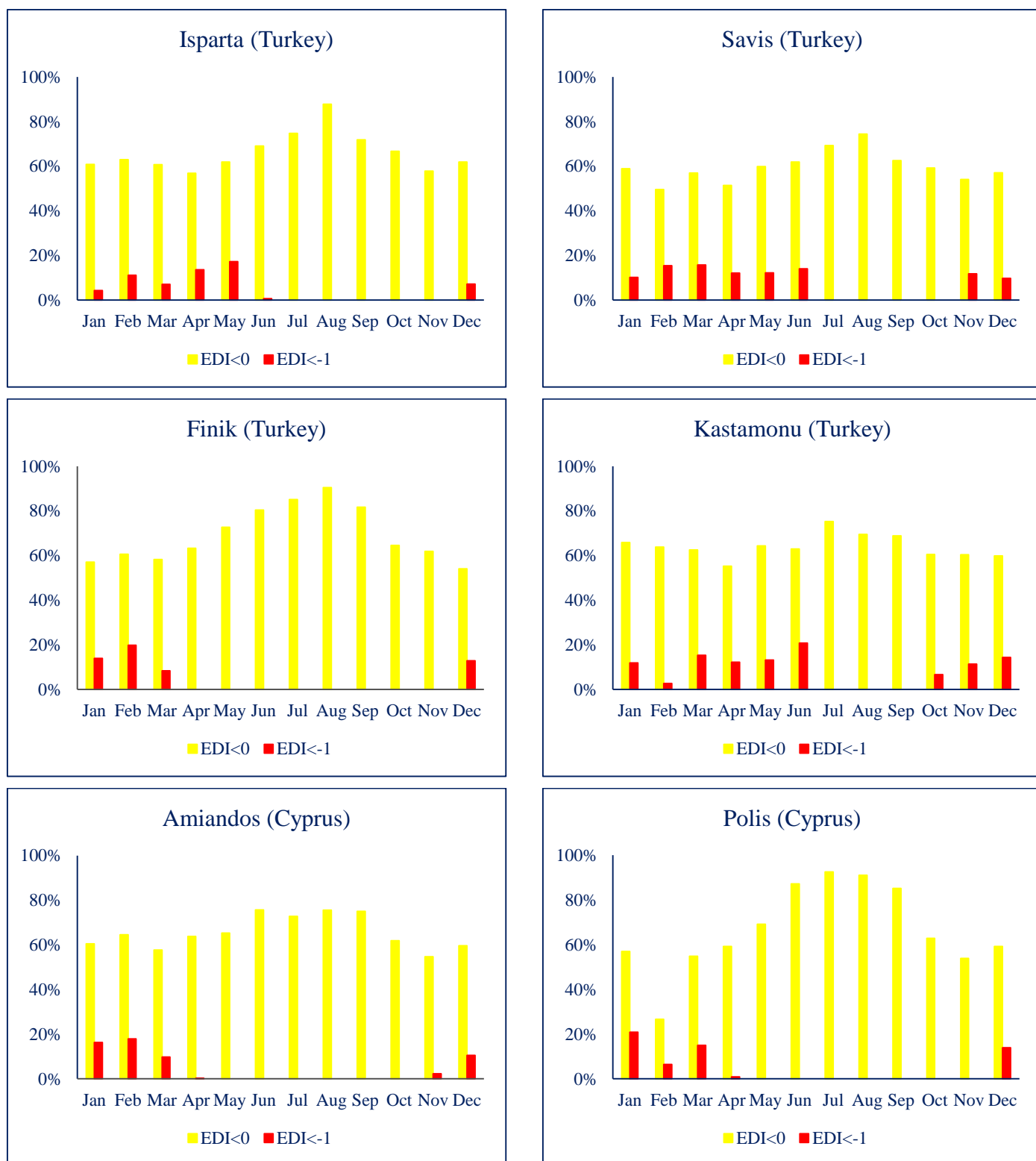


Figure 4.73 Histograms of the frequency of drought duration corresponding to $EDI < 0$ and $EDI < -1$ in some selected stations over the 1961–2012 period.

The results showed a general increase in severe drought frequency in the wet period (December, January, February and March) in most areas which extended to May and June in the northern parts of EM as shown in Fig 4.73. The frequency of extreme drought ($EDI < -1$) ranges between 0% in summer and (10-25%) in the rainy season for all representative stations which means that 60% of severe drought occurred in the wet period.

For drought characteristics at annual scale, the frequency of long term-drought with durations of about 270 days was the highest one. The second frequency peak occurs in the drought of about 280–290 days (Fig 4.74).

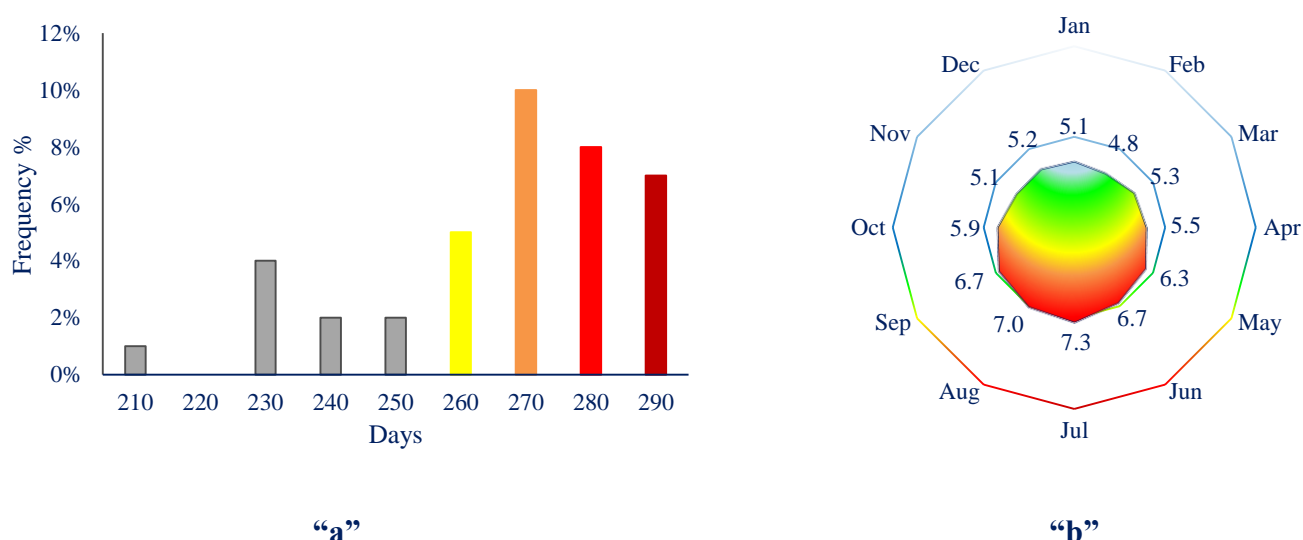
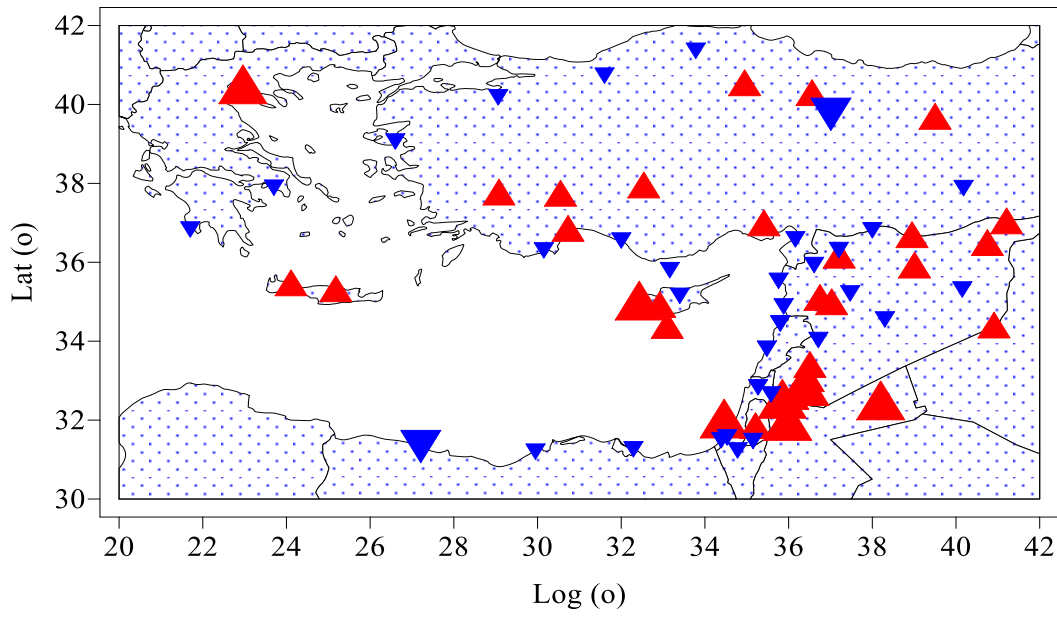


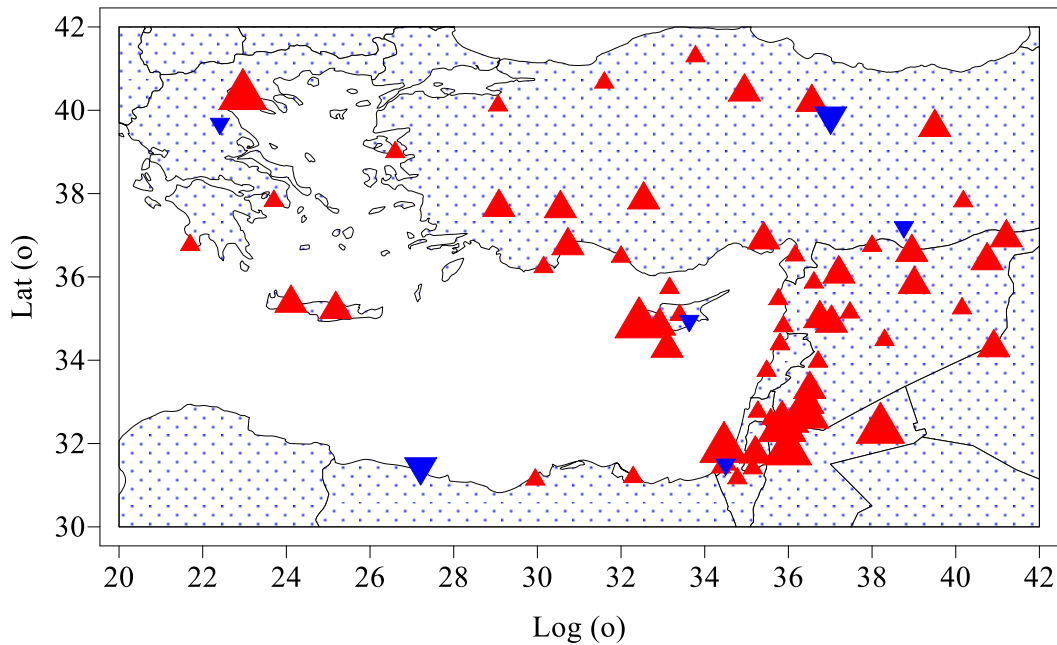
Figure 4.74 Observed frequency of long term drought durations (a) and monthly frequency of dry periods (b).
Droughts are defined by EDI from 70 daily stations during 1961 -2012.

Fig 4.74 showed that 21% of all droughts occurred during the summer (June –July- August). Droughts also occurred in autumn (17.8%) and 15 % of droughts occurred in winter and spring. The average number of dry days in summer is 77 days, whereas this number decreases to 63 days in autumn. The drought duration in spring and winter is 65 and 55 days, respectively.

Maps of the spatial distribution of total dry days ($EDI < 0$) and severe dry days ($EDI < -1$) trends for 70 weather stations across the EM can be seen in Fig 4.75 a, b, respectively.



“a”



“b”

Figure 4.75 Observed trend of total dry days $EDI < 0$ “a” and severe dry days $EDI < -1$ “b”. Positive trends are in red and negative ones in blue. Large and medium triangles represent significant trends at $\alpha=0.01$ and 0.05 , respectively; otherwise small triangles are shown

This figure indicates that major parts of the EM are characterized by positive significant trends of severe drought periods at the 0.05 significance level with a few exceptions which detect a significant trend at 0.01. Severe drought periods

showed an evident increasing trend comparing with total dry periods which no significant decrease in several stations over the EM. As a result, the number of drought periods and drought duration were increased over the last decade of the 20th century.

4.4.3.2 Drought event and its return period

A drought event was defined as the period in which the minimum EDI value is less than -1.0 (Kim *et al.*, 2011). The onset of drought was defined as the date on which the EDI first drops below 0, and the secession of drought was defined as the date on which the EDI last has exceeds this value while maintaining a negative value after the onset. The duration of drought was defined as the period between the onset and secession date. The frequency analysis of the drought events based on the EDI, calculated using daily precipitation data over 70 stations from 1961 to 2012, indicated that about 20% of the droughts were temporarily relieved within a week and redeveloped thereafter. An example of temporary relief from drought is presented in Fig 4.76.

In 2008, Mytilene Airport (Greece) experienced a long drought period because the precipitation during the latter part of January 2008, February 2008 and March 2008 due to less precipitation during this period which was 35% less than an average year. This drought continued for a long time (till April 2008) because the precipitation during March 2008 was not enough to end the drought. On 15th January 2008, an exceptional precipitation of 40.4 mm occurred and the EDI rose rapidly to a positive value. The precipitation shortage continued again, however, and eventually the precipitation during the January in 2008 was 67.7% less than the mean annual precipitation for that year.

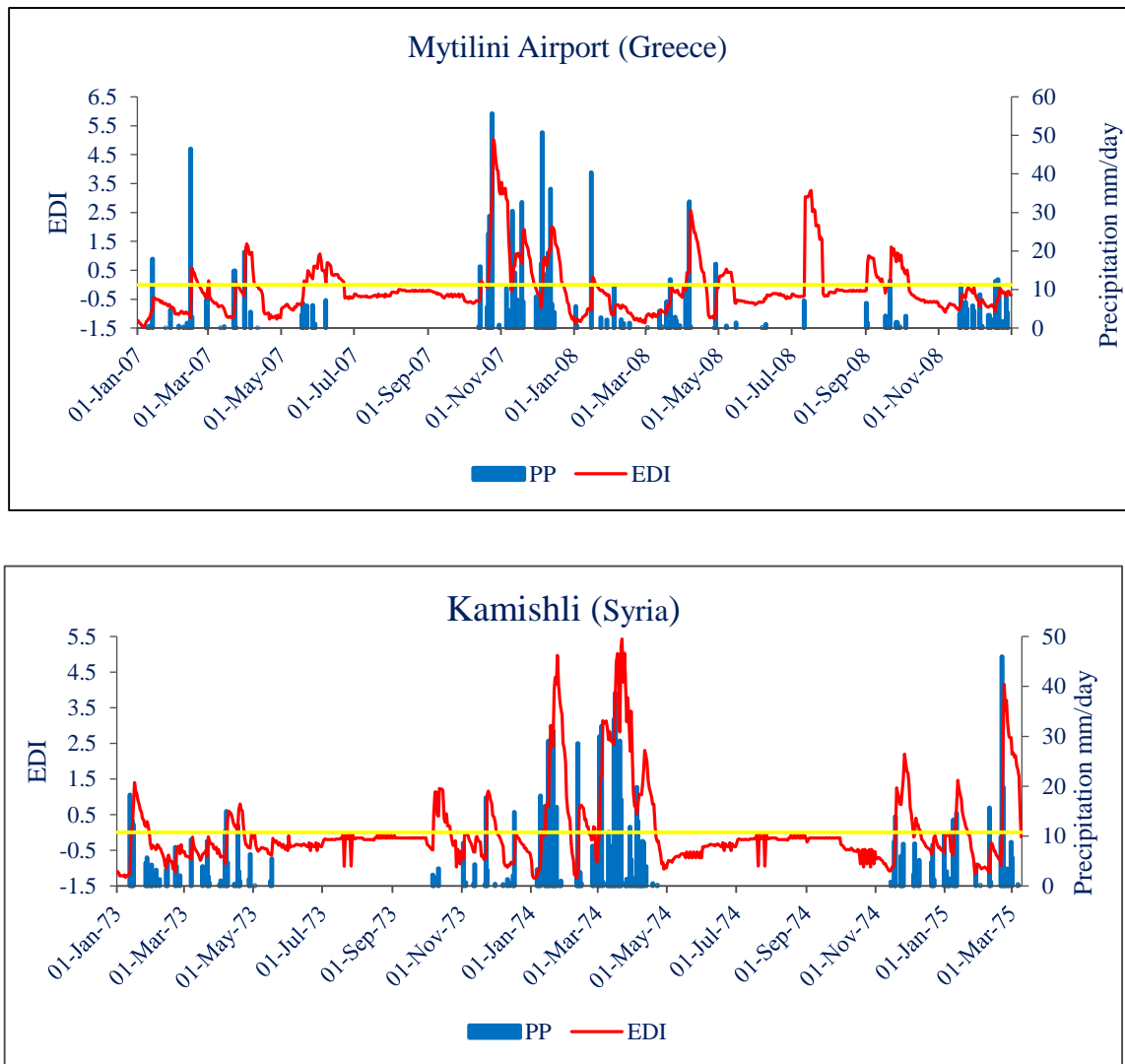


Figure 4.76 Time series of daily precipitation and EDIs calculated for the same period from two selected stations: Mytilene Airport (Greece) (2007-2008) and Kamishli (Syria) (1973-1975).

In Kamishli (another example) on 18th November 1974, a precipitation of 13.4 mm could change the long period of severe drought, which lasted from 21st April 1974 into a wet period rapidly and the EDI values became positive. Since the Period of Return to Normal conditions (PRN) is defined as one day's precipitation needed for a return to normal conditions, the statistical return period in this case, for example, shows that only 7.2 mm is enough to return to the normal conditions. As a consequence, the drought began on 21st April 1974 and it was temporarily relieved for a few days on 18th November 1974, and continued until 20th February 1975. This example illustrates well that even though an exceptional

one-day precipitation could bring temporary relief, if no or low precipitation days continue after that, the water resource generated by the precipitation is lost over time because of outflow and evaporation and drought aggravates rapidly again.

Use of the Available Water Resources Index (AWRI), which represents the total amount of currently available water resources, as supplementary information for determining the drought status can overcome these limitations to a certain extent. The AWRI is an alteration of the Effective Precipitation (EP) and represents currently available water resources based on total precipitation over the previous 365 or 15 days (here we applied it for previous 15 days for several stations). For example, the AWRI was applied to 2006 in Thessaloniki Airport (Greece), when the most severe droughts out of the most recent 10 years occurred (Fig 4.77). When the EDI was used, the period from April to early May was deemed to be a moderate drought, the months of January and early March to the end of May, September and early October to the end of December were deemed to be a severe drought. SPI12 detected severe droughts that occurred from June to December with a mean value of -1.44. The AWRI value is much lower in spring and summer than in autumn. For example, the value of 160.3 mm, corresponding to a severe water shortage, was recorded on spring due to the severe water deficit in May. On the other hand, depending on EDI values in this same year, the meteorological drought was more severe in autumn than in spring (EDI were -0.32 and 0.43, respectively).

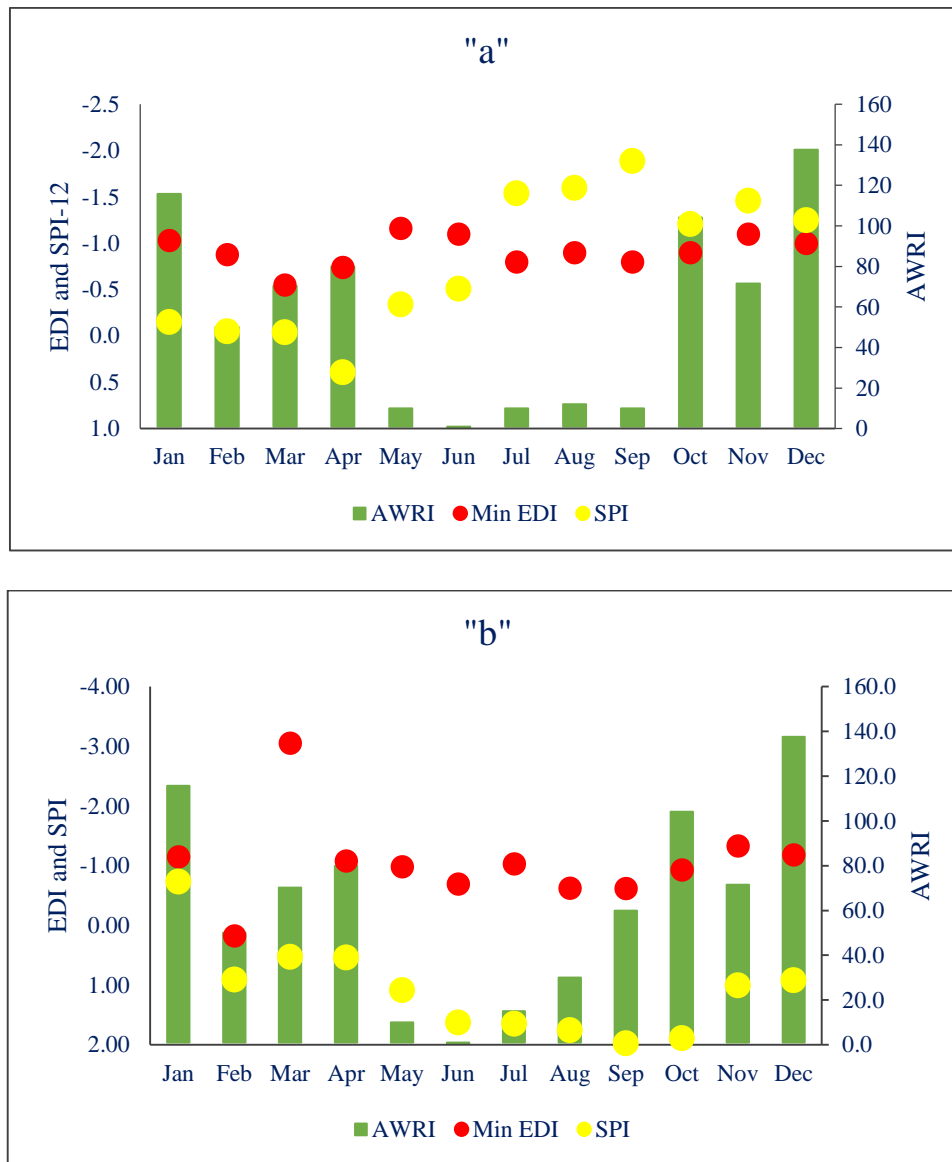


Figure 4.77 Scatter plot EDI, 12-month SPI and AWRI for the years 2006 (a) and 1986 (b) in Thessaloniki Airport (Greece).

However, the AWRI confirms that the shortage of available water was more severe in the spring. In a normal year, such as 1986, we can see that the AWRI value is lower in summer and autumn than in winter (272.6, 283.9 and 344.4 mm, respectively) related to low effective precipitation amounts in April and March, but the lowest EDI values were recorded in winter (-0.22 vs 1.07 and 0.33 in summer and autumn) (Fig 4.77).

4.9.3.3 Comparison between the SPI and EDI.

EDI had greater total drought percentages (22-27%) than for any timescale of SPI. Therefore, it means that EDI resulted in more values indicating any drought classes than did SPI (Fig 4.78).

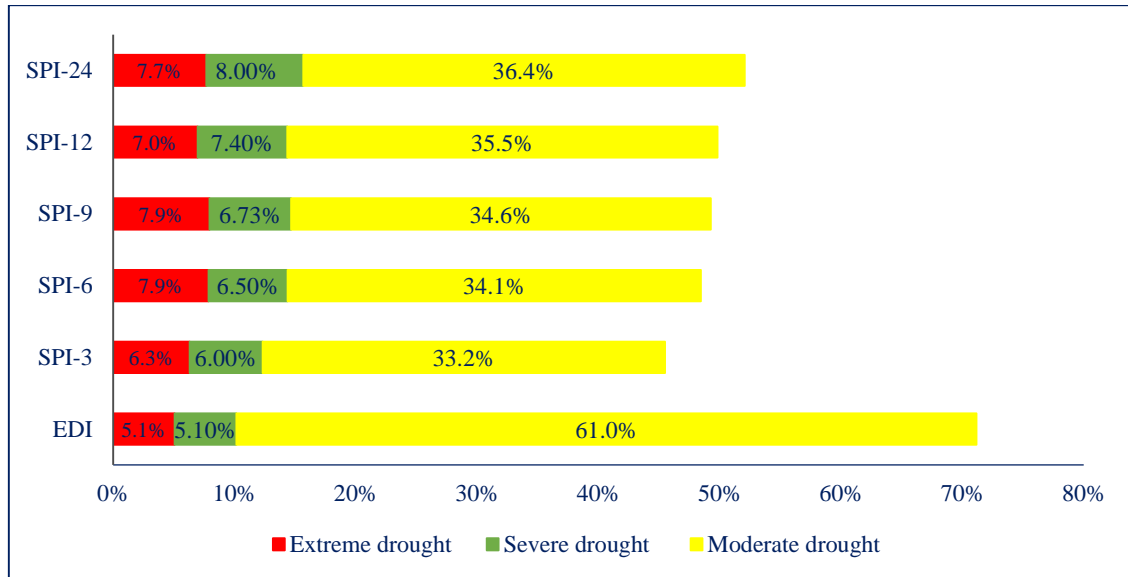
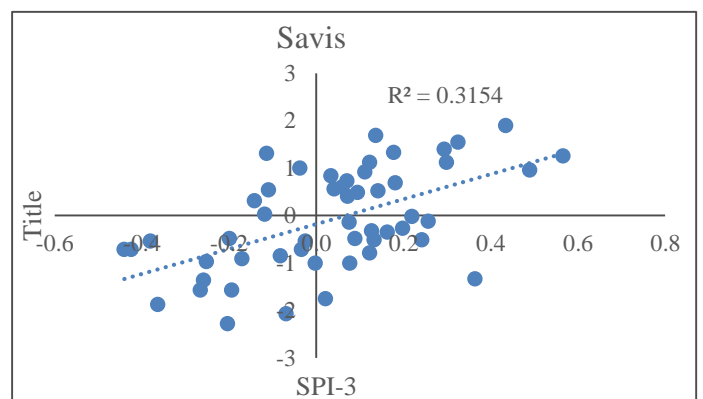
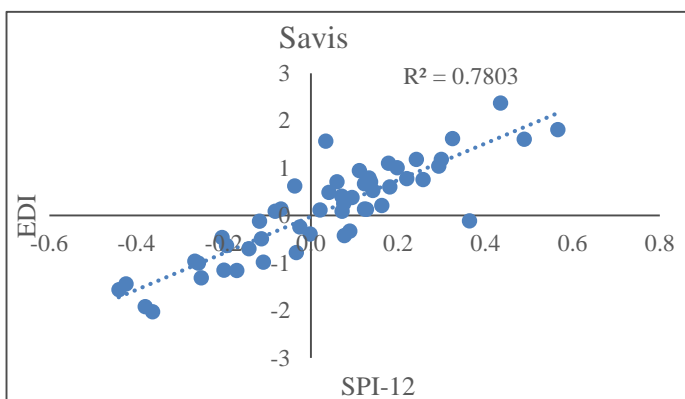
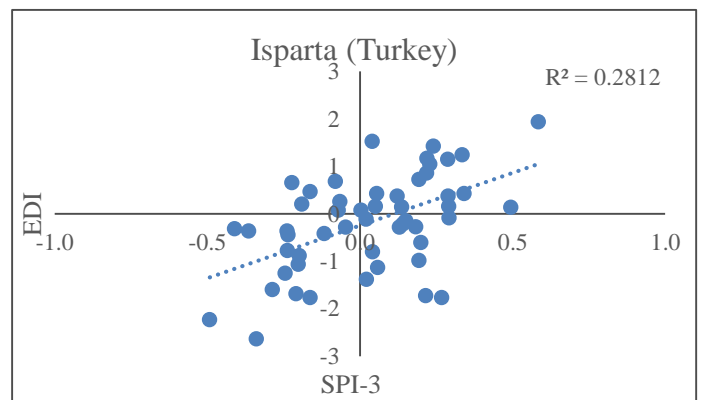
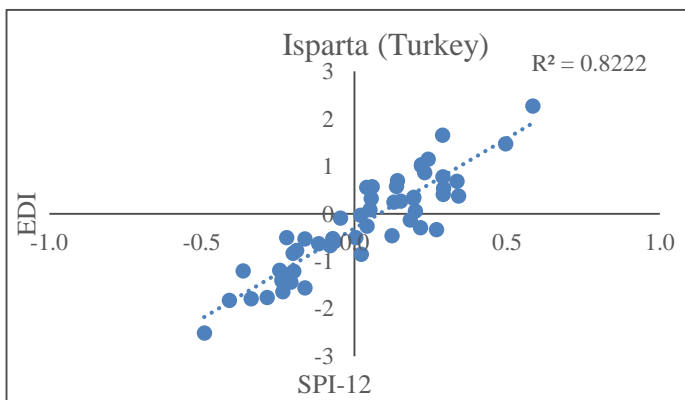
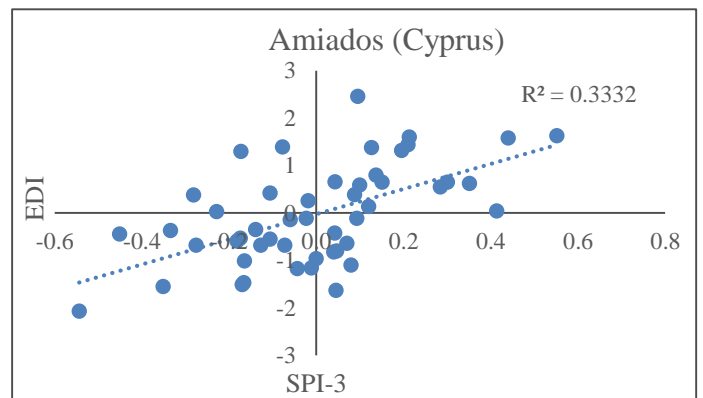
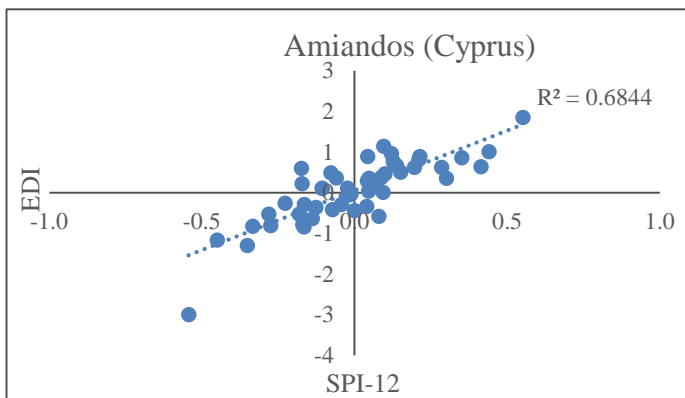
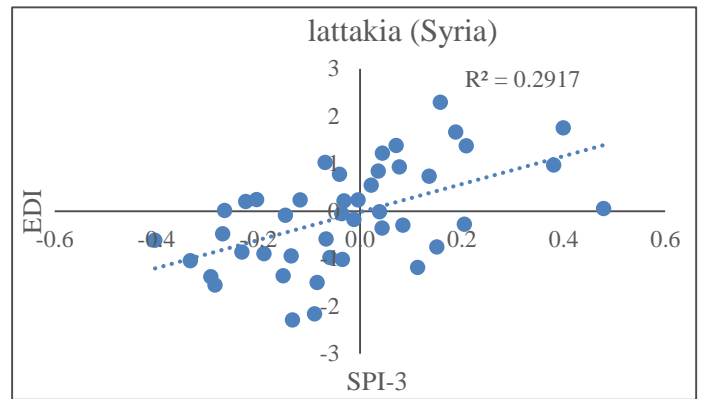
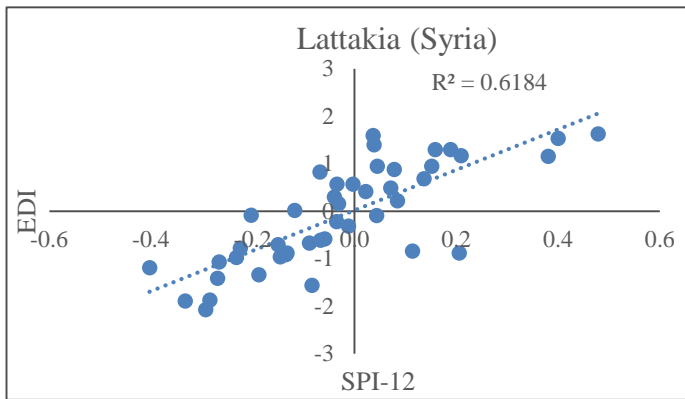


Figure 4.78 Drought class percentages by EDI and SPI time scales as an average of daily 70 stations in the EM for the 1961–2012.

On the other hand, severe droughts were underestimated by EDI (5.1%) and ranged between 6 and 8% for SPI at different timescales. The highest rate of extreme drought was detected by both SPI-6 and SPI-9. EDI detected 5.1% extreme drought, while SPI-3, SPI-6, SPI-12 and SPI-24 detected 6.3%, 7.9%, 7.9%, 7.0% and 7.7%, respectively. SPI-3 was less consistent on detecting extreme drought, and it obtained a 39.2% as severe and moderate drought. Both extreme and severe drought percentages increased from SPI-3 to SPI-24.

As the EDI is effectively a non-parametric index, with a daily timescale, it was necessary to average daily values for computing the monthly EDIs. Fig 4.79 shows the scatter plot of the index versus the SPI in some selected stations.



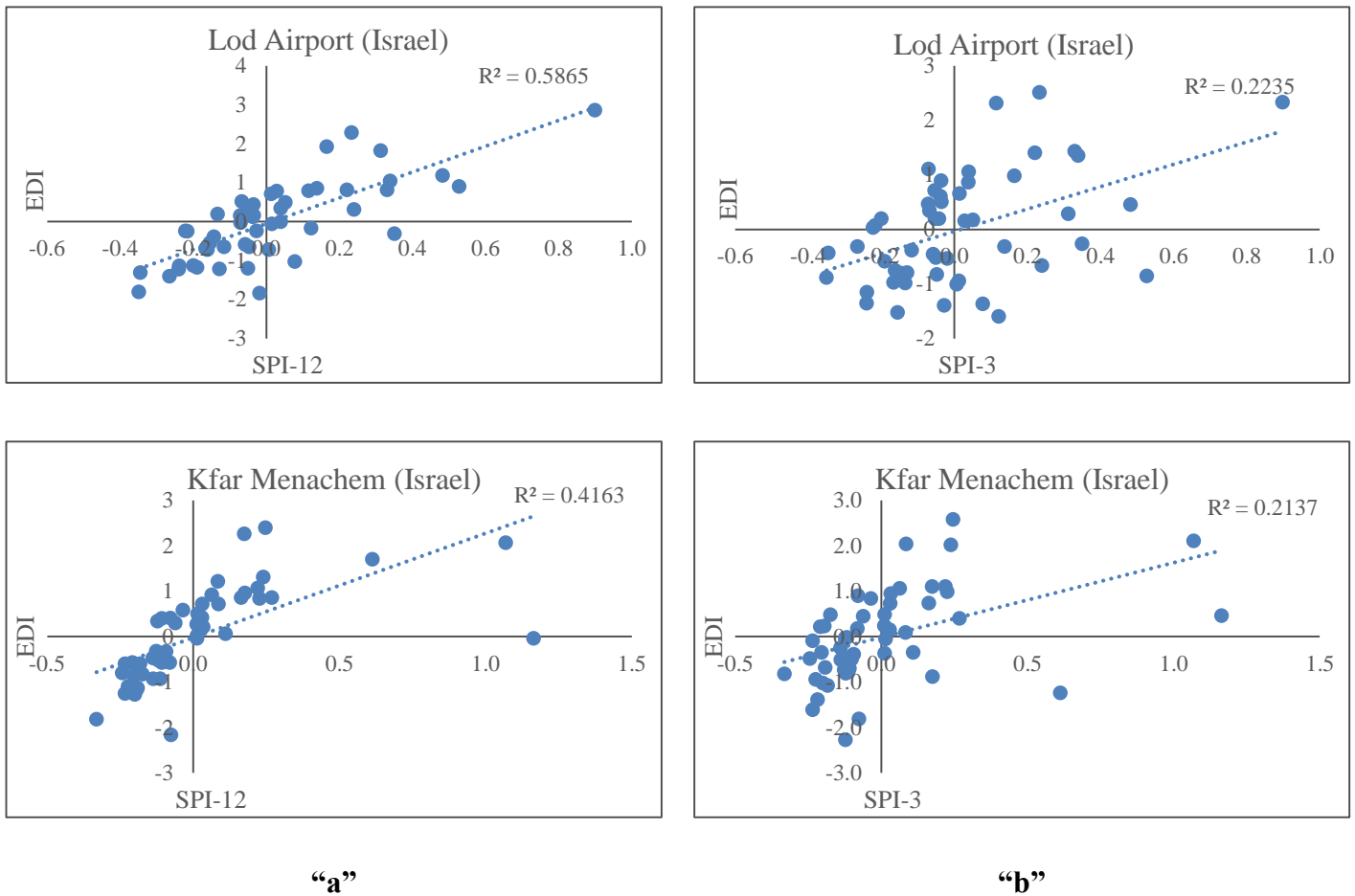


Figure 4.79 Scatter diagram for the SPI and EDI for some selected stations for 12 months (a) and 3 months (b) from 1961 to 2012

It is evident that the correlation is stronger for SPI-12 than SPI-3 at ($p=0.01$) in all stations. For more accurate relative frequencies of the dry classes identified by the two indices were compared for the 52 year-long period. The histogram of the dry and wet classes is shown in Fig 4.80.

The figure indicates that the two indices generally have a good relationship, particularly at 12 month timescale. This means that SPI-12 responded very similarly to EDI within drought period evolution and also responded with high sensitivity to monthly rainfall deficiency.

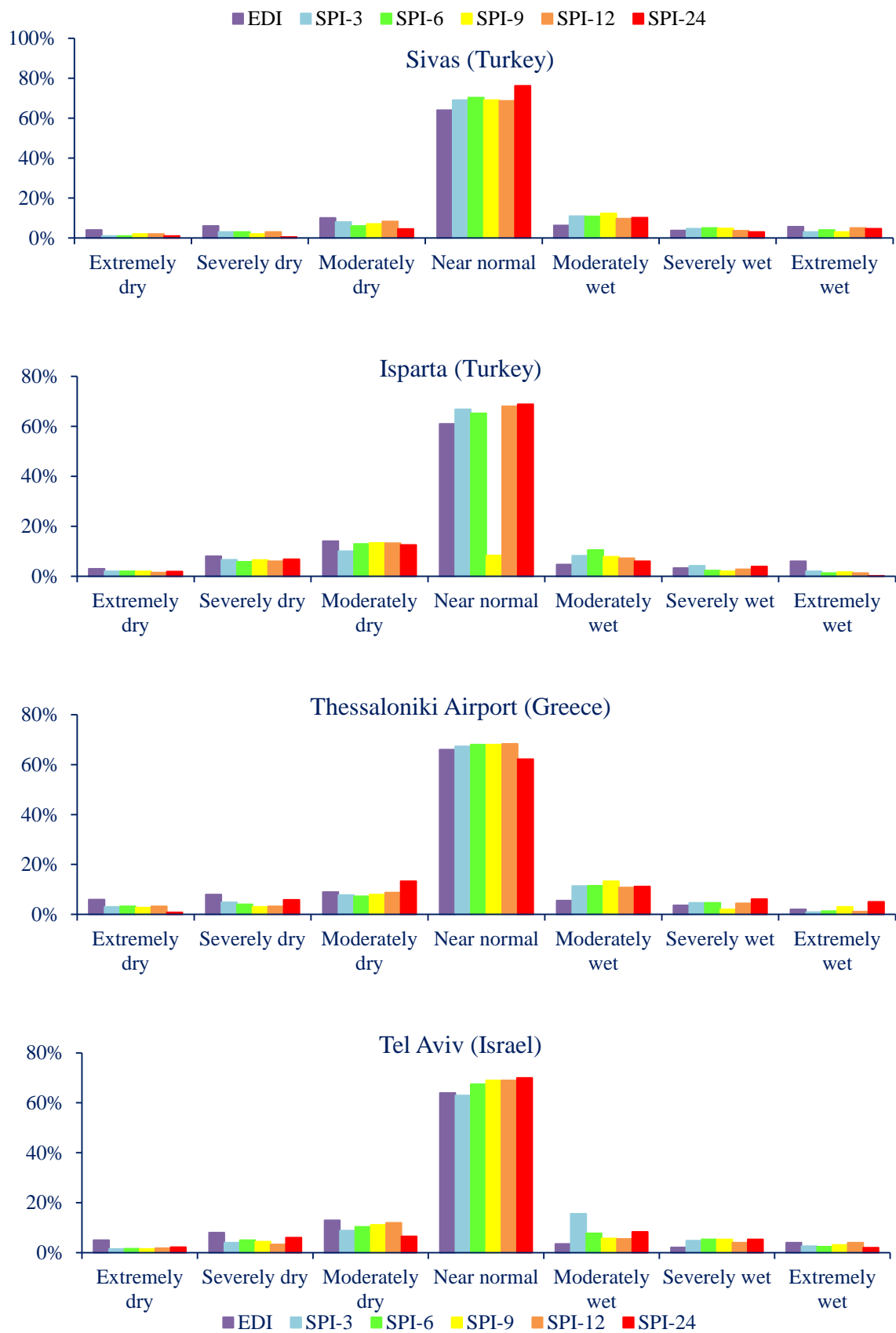


Figure 4.80 Histograms of the drought frequency classes of the SPI and EDI for some selected stations in 1961–2012.

Both indices in Fig 4.79 have a bell-shaped histogram, but the ‘normal class’ of the SPI is much larger than that of the EDI. Conversely, other classes in the EDI are higher than those in the SPI. This fact points to a larger sensitivity of the EDI to changes in precipitation, compared to the SPI.

Analysis of monthly EDI values show that EDI is more sensitive to monthly rainfall changes with respect to multi-monthly cumulative rainfall changes. Resemblance between the sensitivity of EDI and that of others increases from 3-month to 12-month timescales, that was proved before by Morgan *et al* (2012).

DIs were evaluated to see how they responded as time series to monthly rainfall data to better distinguish their responses by the change of rainfall. (Fig 4.81) shows a dry spell of the year 2010 in Raqa (Syria) by using index values of SPI, MCZI, Z-Score and rainfall variables at 3, 6 and 12 month timescales for the first three indices and the average monthly values of EDI for this year. Multi-monthly cumulative rainfall data was also involved to understand the response of these DIs. There were four rainfall variables involved: monthly rainfall (the rainfall received in that month), monthly rainfall average, moving cumulative rainfall representing the sliding sum of rainfall of preceding months relevant to timescales, and multi-monthly rainfall average (the average of the sum of particular months).

As it can be seen, DIs values, in this year, went below -1 on January 2010 and the negative values continued for 12 months till December 2010. This year was one of the longest and most severe dry periods that affected this station and most of other stations that are located in the southern parts of the EM.

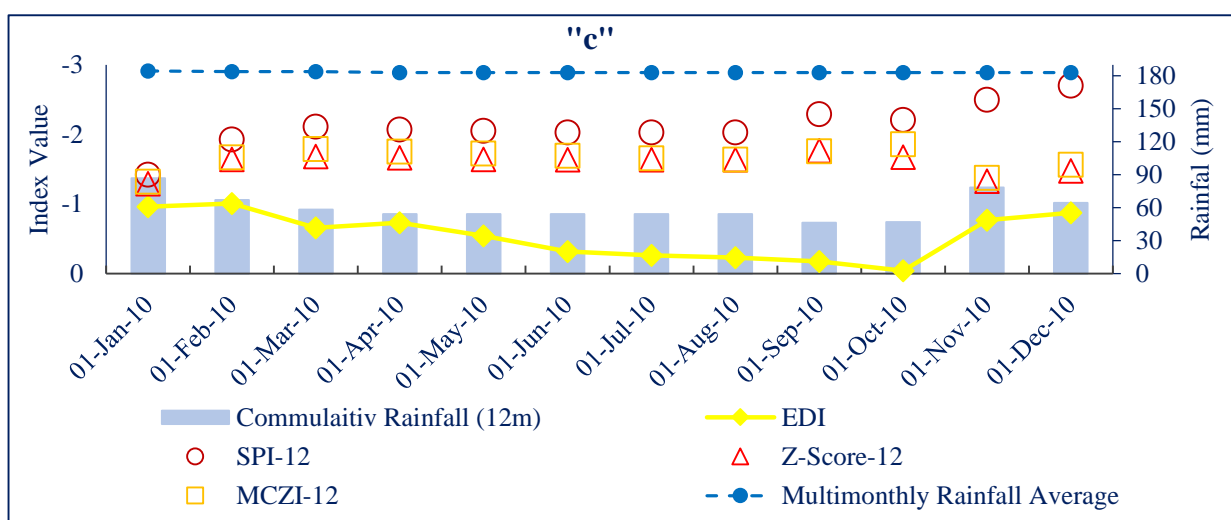
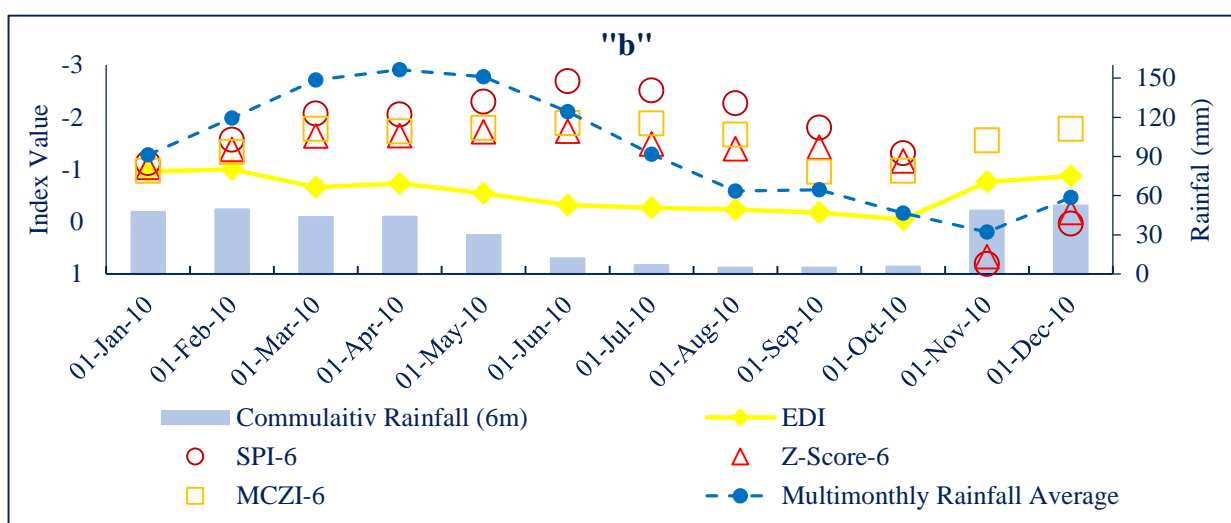
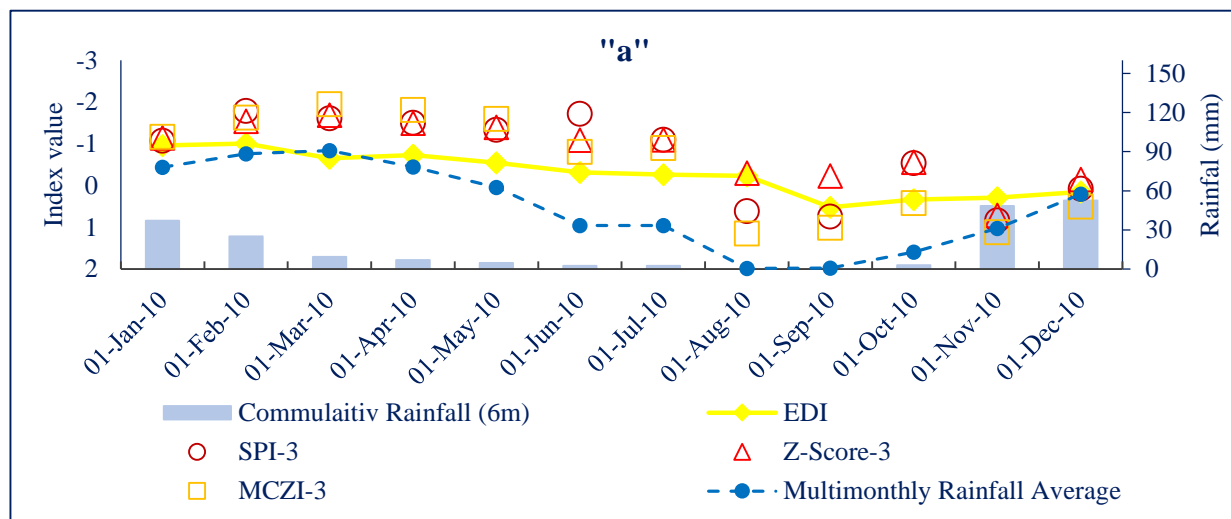


Figure 4.81 Time series of drought indices (DIs) and rainfall in Raqa (Syria).
for 3 months (a), 6 months (b), and 12 months (c)

Fig 4.81 shows an important and essential difference between EDI and SPI-3, MCZI-3, ZScore-3 series. The monthly rainfalls received in January 2010 were less than the monthly averages (85% below the average of this month), but 3-month cumulative rainfalls were well below the 3-months rainfall averages (9.4 mm of rainfall, 89.6% of the average, received in 3 months while the 3-month average was 90.9 mm for March), so EDI was not able to detect 3-month rainfall deficiency very well for this month. Monthly rainfall (45.4 mm) was again above its average value (18.3 mm) in November 2010; this led 6-month cumulative rainfall (48.5 mm) to its 6-month average (32.1 mm). SPI-6, MCZI-6 and Z-Score-6 responded as initiation of recovery from the deficiency, but EDI could not reach it. The same case was detected for the 12-month timescale in November 2010, which means that EDI was not able to detect 6 and 12-month rainfall increasing very well in this month. For 6 and 12-month timescales, all DIs have detected very low values in September 2010 and responded in the same way to the high rates of water deficiency. Only 4.8 and 46.2 mm were received in 6 and 12 months, respectively; whereas the rainfall cumulative averages were 64.3 and 182.9 mm for the same period which, in turn, affected all DIs values in this month, except for EDI value. EDI almost recovered its average value and recorded a positive value (0.52). In June 2010, all DIs responded decreasingly to the high decreasing of the 6-month cumulative rainfall comparing with the average (6.9 mm to its average 90.5 mm). EDI showed less responding to this decrease in this month because of the monthly rainfall which just had met its average (0.1 mm to its average 0.7 mm). The cumulative average for the 12-month timescale for all months was the same and ranged between 182 mm and 184 mm, whereas all the monthly cumulative amounts were less by 52-74% leading to very low values for all DIs ranged between -1.70 and -2.29. It can also be seen that EDI and all DIs had the highest negative correlation with cumulative rainfall amounts at 3-month timescales. SPI-6 and SPI-12 detected this dry spell as an extreme drought by the excess of threshold level within this year, in March (-2.2,-2.1), April (-2.1,-2.2), May (-2.3,-2.1), June (-2.7, -2.2), July (-2.5,-2.3), August (-2.4, -2.1) and both September and October had also detected an extreme drought period for 12-month timescales with

SPI values -2.4 and -2.2, respectively. SPI-6 had also recorded high negative values (-1.8 and -1.3), in September and October, respectively detecting a severe drought period. MCZI-6 and Z-score-6 had also showed the same results in this dry spell (Table 4.11).

Table 4.11 Pearson correlation coefficients of indices with same time scales for 2010 dry spell in Raqa (Syria).

	Time Scale (Month)		
	3	6	12
EDI-SPI	0.78	0.54	0.40
EDI-MCZI	0.85	0.51	0.40
EDI-Z-Score	0.81	0.50	0.40
SPI-MCZI	0.94	0.85	0.98
SPI-Z-Score	0.92	0.96	0.98
MCZI-Z-Score	0.94	0.82	0.97

From the Table 4.11, EDI was highly correlated with lower time steps than other DIs, except Z-Score-3 which had much higher correlations than EDI for 3 and 6-month time steps. The same results were detected previously by Dogan *et al* (2012) who found that median time steps (5-month to 18-month) had better correlations (>0.5) with other time steps

To compare between several DIs, a correlation matrix was created for all timescales and for all considered DIs. All calculations were made for each station and then relevant results were averaged to obtain the final result to represent the whole EM. Fig 4.82 shows the distribution of correlations by timescales. Four different indices (EDI, SPI, MCZI and Z-Score) were combined for each timescale. The median timescales (6 and 9 months) showed better correlation (>0.6), while lower and higher timescales showed less correlation. This can be explained by the fact that the median timescales obtained better correlation with both lower and higher ones (longer range was correlated), while lower/higher timescales were

only correlated with nearby ones and the strength of the relationship between median timescales with closer ones was stronger (shorter range was highly correlated). However, EDI showed higher correlations with most of the timescales, and this made EDI the best correlated DI overall.

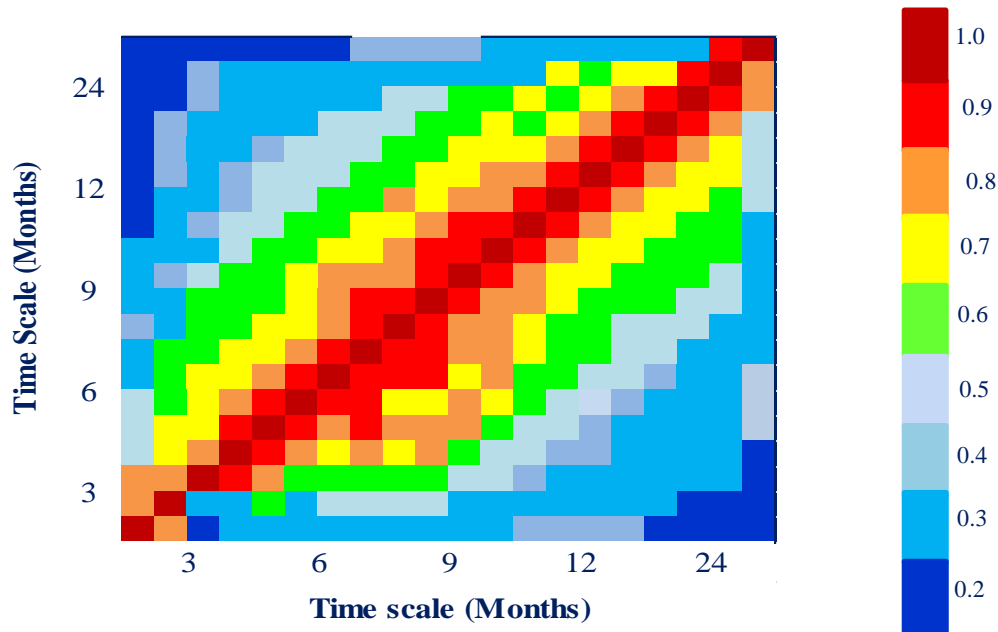


Figure 4.82 Correlation of drought indices for five time scales. Each time scale consists of four different indices (EDI, SPI, MCZI and Z-Score) during 1961-2012 over the EM.

As it can be seen from Fig 4.82 there is not much difference between DIs correlations at the same time scale. This means that the average correlation of a DI with particular timescale against all DIs time steps has similar average correlation with the other DIs of the same timescale (EDI, SPI, MCZI and Z-Score1. They were all similar). Timescale is also very important when comparing the robustness of DIs. It is clear that the least correlation is for short and long timescales. It would be beneficial to not only use lower timescales, but to involve at least 6-month and 9-month time scales of any DI when studying short or long term drought in arid and semi-arid areas.

On the other hand, a drought is an accumulation of water deficiencies by time, so the analysis of drought at different timescales would be a better indicator, especially for semi-arid and arid regions because short-term water deficiencies are

common in these areas. A 1-month timescale was used by some researchers in their DIs comparative studies (Keyantash and Dracup, 2002; Morid *et al*, 2006).

Finally, our results demonstrated two long dry periods (1998-2001) and (2007-2012) over the EM with a significant increase detected in dry period length especially in the southern parts of the EM. This result expands on previous drought studies (Kutiel *et al*, 1996; Tolika *et al*, 2004) that also found a general future tendency towards drier EM with reduced rainfall intensity. Longer dry spells are expected in all seasons, except autumn, with the largest increase in the southern part of the study area. Recent studies have shown an increasing tendency of dry spell length during the last two decades in the EM (Oikonomou *et al*, 2008; Hatazaki *et al*, 2008; López-Franca *et al*, 2013). On other hand, concerning dry periods, a long-term trend of drying was already evident over the Mediterranean area from 1900 to 2008 (Dai, 2011), and the risk of these events is likely to increase in the future. Furthermore, Weiß *et al* (2007) assess that 100-year droughts will occur more frequently in the future over large parts of the Mediterranean area. Table 4.12 summarizes the relative strengths and weaknesses of drought indices.

Table 4.12 Summary of the commonly used DIs and their strong and weak points.

Index	Description and use	Strengths	Weaknesses
Standardized Precipitation Index (SPI) McKee <i>et al.</i> (1993). (Monthly)	Calculated depending on the probability of precipitation for any time scale basing on the concept that precipitation deficits over varying periods or time scales influence ground water, reservoir storage, soil moisture and streamflow.	<ul style="list-style-type: none"> -Computed for different time scales. -Provides early warning of drought and help assessing drought severity. -Used as an approximation of streamflow and groundwater droughts. -Its values are well comparable in quite different climate locations (Guttman, 1999) 	<ul style="list-style-type: none"> -Precipitation is the only input data and it requires a long time series of observed data. The minimum precipitation record for calculating the SPI is 30 years, but it is recommended to use ≥ 50 years of data (Wu <i>et al.</i>, 2005). -The SPI is strongly influenced by record length (Wu <i>et al.</i>, 2005). -The SPI is strongly influenced by the presence of missing data and the replacement of these missing data (Guttman, 1999).
Modified China Z Index (MCZI) Wu <i>et al.</i> (2001). (Monthly)	Calculated based on the Wilson–Hilferty cube-root transformation assuming that precipitation data follow the Pearson Type III distribution to monitor drought conditions.	<ul style="list-style-type: none"> - Computed in a simple way at different time scales for detecting drought severity at monthly time step. It can be preferred over SPI when some rainfall series have gaps. - Highly correlated with SPI. -More efficient and has a better performance than SPI in the arid and semi-arid areas in detecting and measuring drought conditions. 	Precipitation is the only input and needs long series data.
Z- Score Palmer (1965). (Monthly)	Calculated to indicate how many standard deviations a rainfall value is above or below the mean.	<ul style="list-style-type: none"> -It is a good indicator for meteorological and agricultural drought. -Provides spatial and temporal representations of historical droughts. 	Drought is declared more often with shorter duration of the drought spells.

Deciles (DI) Gibbs and Maher (1967). (Monthly)	A simple calculation by grouping precipitation into deciles distributed from 1 to 10. The lowest value indicates conditions drier than normal and the higher value indicates conditions wetter than normal.	<ul style="list-style-type: none"> -Accurate statistical measurement of drought. -Simple calculation -Provides uniformity in drought classifications. 	Accurate calculations require a long climatic record of precipitation data.
Effective drought Index (EDI) Byun and Wilhite (1999). (Daily)	Calculated using daily precipitation data and it was designed for detecting the onset and termination of drought events and monitor the duration and severity of drought on daily time steps.	<ul style="list-style-type: none"> - EDI is more sensitive to monthly rainfall changes with respect to multi-monthly cumulative rainfall changes. - EDI is found to be a good choice for the assessment of drought characteristics and monitoring of drought conditions, because of its ability in detection the drought onset and quantification of severity of drought events especially in arid and semi-arid regions (Jain <i>et al.</i>, 2015; Dogan <i>et al.</i>, 2012). -EDI was found to be able to describe spatial and temporal developing of drought conditions and more responsive to the emerging drought conditions compared with other drought indices (Morid <i>et al.</i>, 2006). 	<ul style="list-style-type: none"> - It is relatively unknown so its ability to accurately monitor drought conditions remains largely untested (Morid <i>et al.</i>, 2006). It needs a long continuous daily precipitation record. - Using only precipitation data and the methodology for calculating the EDI is not straightforward. - It lacks the nice statistical properties of some of the other precipitation-based indices (SPI, deciles, etc.). For example, Morid <i>et al</i> (2006) demonstrated that the EDI is not normally distributed.

-
- EDI can thus measure both long-term and short term droughts, and it is superior to SPI in determining the accumulated water resources which are important for drought monitoring (Byun, 2009).
 - The EDI was the best index in assessing drought severity worldwide and the PRN was the best suited for limited areas in a timely manner (Byun and Wilhite, 1999).
 - EDI is found to be well correlated with other DIs for all time steps and coherent with many time steps of other DIs (Jian *et al.*, 2015; Dogan *et al.*, 2012).
-

In such arid and semi-arid environments, changes in precipitation have one of the greatest impacts on ecosystem dynamics more than the singular effects of the rising CO₂ concentration or temperature (Weltzin *et al.*, 2003), because the spatio-temporal availability of water will directly affect plant recruitment, growth and reproduction, nutrient cycling and net ecosystem productivity (Knapp *et al.*, 2002). Therefore, alterations in precipitation regimes could significantly affect the functions of desert plant, soil communities and ground water through their effects on overall ecosystem carbon and water balance (Huxman *et al.*, 2004). For example, in a period of 33 years, a decrease of 14.3 meters in the groundwater level in Konya Basin (Turkey) has taken place, with 80% of this fall during the last 10 years and after 1980's almost all groundwater levels in Central Anatolia have begun to decrease year to year (Dogdo and Sagnak, 2008). They have also announced that the big cities in Turkey that are most vulnerable to droughts are Ankara, Istanbul and Izmir. These cities depend on fresh water storage in reservoirs. This is because of the NAO has detectible influences on the hydrology of the EM area with different magnitudes. Kahya (2011) illustrated the NAO

influence on the formation of streamflow homogenous region and on the probability distribution functions of critical droughts. The results have also showed that NAO during winter was found to influence both precipitation and streamflow patterns in Turkey. Positive significant correlation values was also found between the NAO index and total precipitation in central and south Israel and with some of the rainfall categories due to the role of NAO in controlling the Atlantic heat and moisture fluxes into the Mediterranean region (Turkes, 1996) which in turn can explain the relationship between the EM and Atlantic sector.

Sirdas and Sahen (2008) demonstrated that high level sunshine duration and solar irradiation ratios correspond to moderate, severe and extreme drought levels in Turkey. They concluded that the the variation of precipitation can also be depicted according to solar irradiation and sunshine duration. Cullen and de Menocal (2000) found that the decreasing trend in rainfall associated with long dry periods and long term trend in the NAO index have strongly affected crop yields and have contributed to high level political disputes on water withdrawals from the rivers between Turkey, where most of the rain falls, and Syria, a downstream riparian neighbour. The balance between precipitation and evaporation influences the circulation and the quality of the waters in the Mediterranean Sea (Mariotti and Struglia, 2002). The variability of precipitation during the wet period affects the hydrological budget in this region and considered as an important factor in managing the regional agriculture, water resources, ecosystems, environment, economics and social development and behaviour.

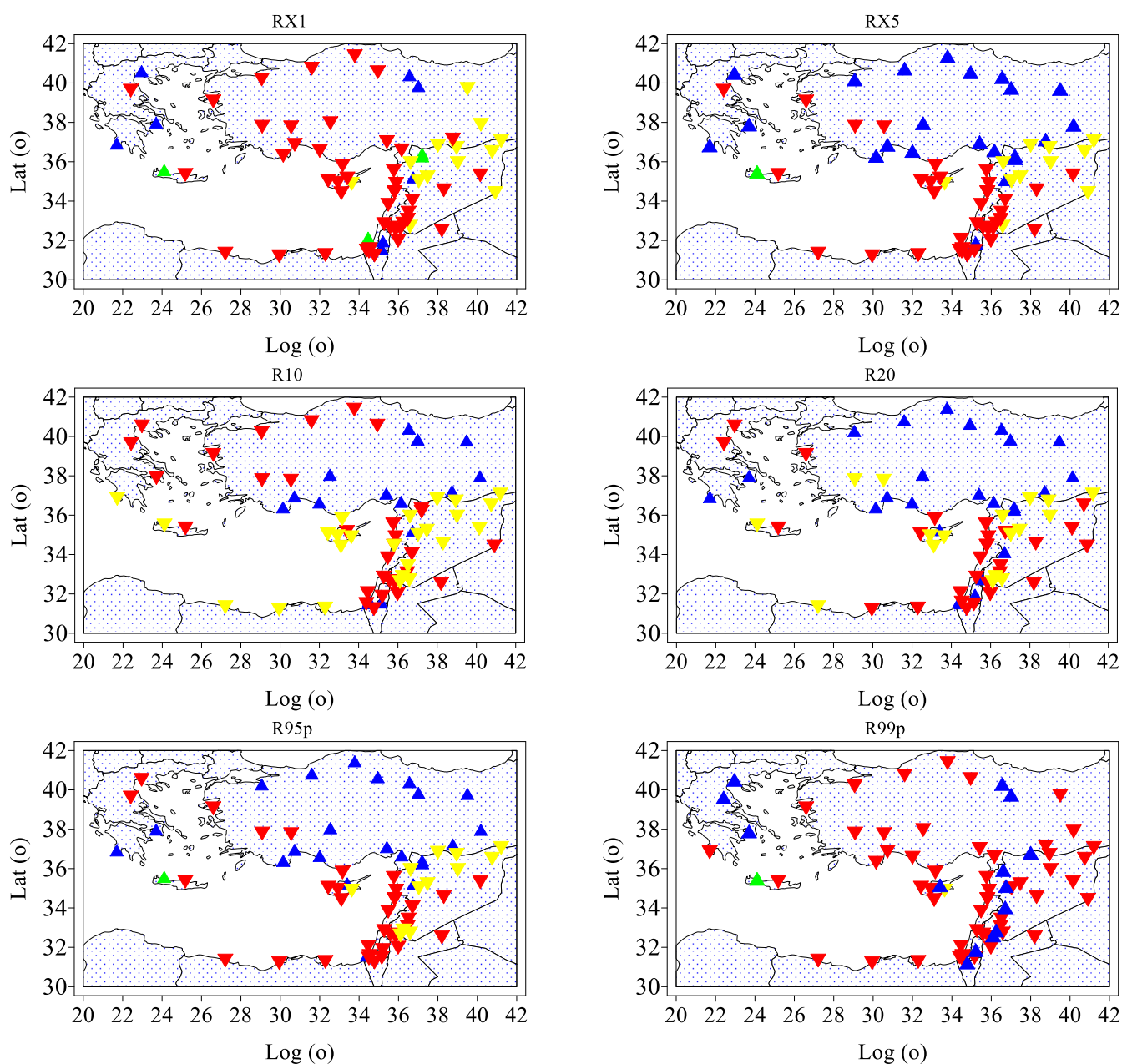
Finally, many states in the EMME will see growing competition and conflict between urban and rural water needs and these conflicts may lead to social and political unrest. Moreover, there is the possibility that growing water scarcity, severe and frequent drought events and other effects of climate change could exacerbate existing political tensions and conflicts in this region.

New analysis by NOAA scientists and colleagues at the Cooperative Institute for Research in Environmental Sciences (CIRES) found that the climate change from greenhouse gases explained roughly half the increased dryness of 1902-2010 which contributed to increasing drought frequency in the

Mediterranean region. They assessed that winter drought has emerged as a new normal that could threaten food security. All of these factors have demonstrated that drought was one of reasons of recent conflict in some sensitive areas such as Syria that has experienced the worst drying in the region (Mohtadi, 2012). Femia, and Werrell (2012) have assessed that severe drought from 2006 to 2010, coupled with the Syrian government's failure to mitigate its negative impacts on farmers, water and agricultural sectors, were possible drivers of the civil unrest and big crisis that happened in Syria in 2011.

4.10 Observed changes in daily precipitation extremes.

The results of trend analyses of 10 daily precipitation indices' time series (presented in Table 3.8) for the period 1961–2012 are summarized in Table 4.12 and Fig 4.83. Table 4.13 gives the percentage of precipitation stations that had positive/negative trends in annual precipitation indices calculated individually for the 70 stations with daily data and the corresponding percentage of statistically significant results at 0.05 level. Fig 4.83 shows the trends in annual regional precipitation indices and the corresponding 95% confidence intervals.



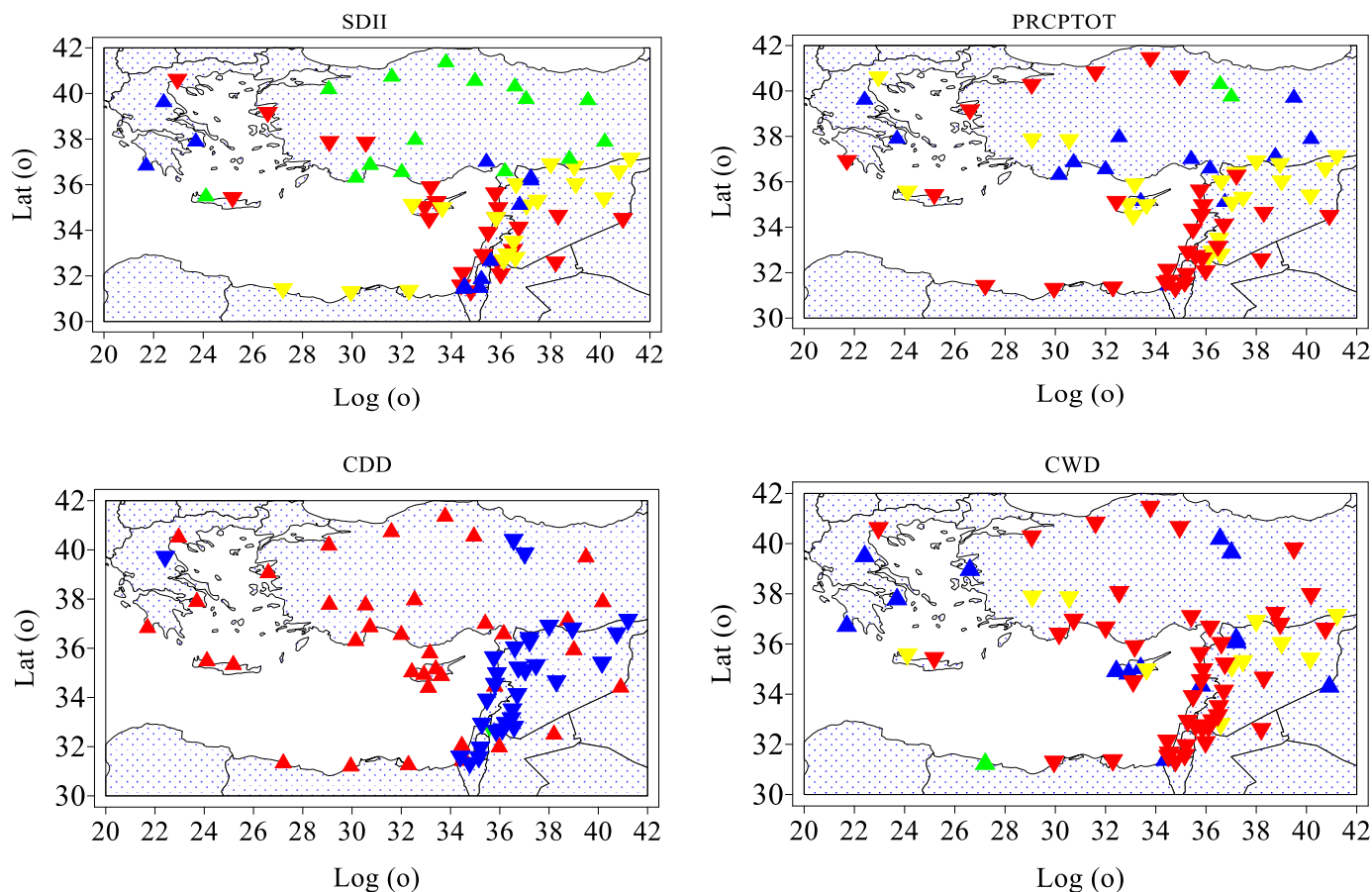


Figure 4.83 Spatial patterns trend in the annual indices of precipitation (RX1day, RX5days, R10, R20, R95p, R99p, SDII, PRCPTOT, CDD and CWD) for the 1961-2012 in 70 stations with daily data over the EM. Statistically significant ($\alpha=0.05$) positive trends are in blue and negative ones in red. The green and yellow triangles present non-significant positive and negative trend, respectively. Positive indicates wet trends and negative indicates dry trends (it is the opposite for the CDD).

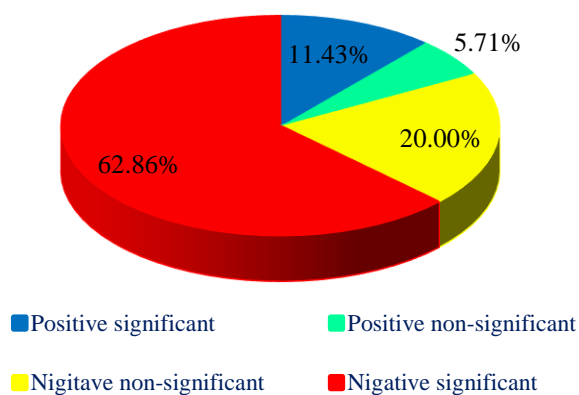


Figure 4.84 Frequency of the 10 extreme precipitation indices trends shown in Fig 4.83 over the EM during 1961-2012.

Table 4.13 Percentages (%) of the daily 70 precipitation stations with linear positive (+) and negative (-) trends in annual precipitation indices (RX1day, RX5days, R10, R20, R95p, R99p, SDII, PRCPTOT, CDD and CWD). (Positive indicates significant wet trends and negative indicates significant dry trends; this is the opposite for the CDD index).

		Sig (-)	Non-sig (-)	Sig (+)	Non-sig (+)
Non-thresholds indices	RX1day	62.9	20.0	11.4	5.7
	RX5days	50.0	17.1	31.5	1.4
	SDII	32.9	28.6	17.1	21.4
	PRCPTOT	45.7	30.0	20.0	4.3
Fixed-thresholds indices	R10	41.4	37.2	21.4	0.0
	R20	38.6	25.7	35.7	0.0
	CDD	44.3	1.4	52.9	1.4
	CWD	62.9	15.7	20.0	1.4
Station-related thresholds indices	R95p	48.6	18.6	31.4	1.4
	R99p	74.3	1.4	20.0	4.3

Table 4.13 gives the percentage of precipitation stations that had positive/negative trends in annual precipitation indices calculated individually for the 70 stations' data and the corresponding percentage of statistically significant results at the 0.05 level.

The overall analysis of extreme precipitation indices reveals that decreasing trends are more frequent than the positive ones (except CDD index). The results show statistically significant decreasing trends in extreme precipitation indices ranging between 32.9% and 74.3% of total stations, indicating significant dry trends.

Negative trends in very heavy or intense rainfall which measured by the RX1day (Max 1-day precipitation amount) and RX5day indices (Max 5-day precipitation amount) were found in 83% and 67% of the stations, respectively. 63% and 50% of total stations exhibited a statistically significant decrease, respectively.

The SDII monitors precipitation intensity on wet days and presents decreasing trends in 61.5% of total stations, about 40% of these stations were statistically significant. SDII takes into account not only the total amount of precipitation throughout the year but also reflects changes in daily rainfall.

Frich *et al* (2002) stated that SDII has showed significant positive trends over Italy but negative ones over the EM.

The annual total wet-day precipitation (PRCPTOT) is probably the most important index reflecting rainfall variations over the entire year. The regional average series indicate a significant decrease in this index (PRCPTOT) of 3.1% per decade over 1961-2012. Most stations (about 50%) show significant decreasing trends ranging from -6 to -18% per decade. Significant increase in total precipitation was detected in 20% of stations (1-3.4% per decade) (Table 4.13 and Fig 4.84).

The persistence of intense precipitation which was measured by the number of cases of daily rainfall exceeding the 10mm, 20mm and 25mm limits have been defined by means of R10mm and R20mm indices. Both of them showed negative trends in 78.6% and 64.3%, respectively. This decreasing was significant in 37.2% and 25.7 at $\alpha=0.05$ significant level, respectively. These results are compatible with those obtained by Frith *et al* (2003) who indicated a negative trend in the number of days with precipitation greater than 10mm over the EM. Kostopoulou and Jones (2005) and Kioutsioukis *et al* (2010) have also assessed a significant decreasing trend affects the annual number of events with daily precipitation greater than 10 mm over the EM. In winter the amount of precipitation due to these events has also exhibited a negative trend in Greece by 74.2 mm/50 year over 1950-2000 (Narrant and Douguédroti, 2006).

The trend for consecutive dry days (CDD) showed a positive tendency in 54.3% of total stations. The trend is significant in 53% of the stations at $\alpha=0.05$ significant level. The CWD (Consecutive wet days) showed a decreasing tendency for the majority of stations, 78.6% of total stations, significant decreasing trends were detected in 62.9% of these stations at $\alpha=0.05$.

The stations' percentile-based R90p and R95p indices showed consistent trends. High percentage of total stations reported a significant decreasing in very wet days (R95P) and in the extreme wet days (R99p) by 48.6 % and 74.3%, respectively. Precipitation variation is characterized by strong interannual variability without any significant trend in any of the precipitation indices analysed.

4.10.1 Trends in seasonal precipitation indices

Trends observed for seasonal precipitation are, in general, statistically significant. Only two out of all precipitation indices, RX1day and RX5day, have data available for sub-annual timescales. On a seasonal basis, extreme precipitation amount and its relation to total precipitation were expressed by the indices RX1day (monthly maximum 1-day precipitation) and RX5days (monthly maximum consecutive 5-day precipitation). The statistical downscaling results for both R1Xday and R5Xdays yielded widespread increase in extreme precipitation over the northern parts of the EM (especially in Northern and Western costs of Turkey) (Fig 4.85). In these areas, the increase in extreme precipitation is visible across all seasons but tends to be more statistically significant during autumn (Fig 4.85).

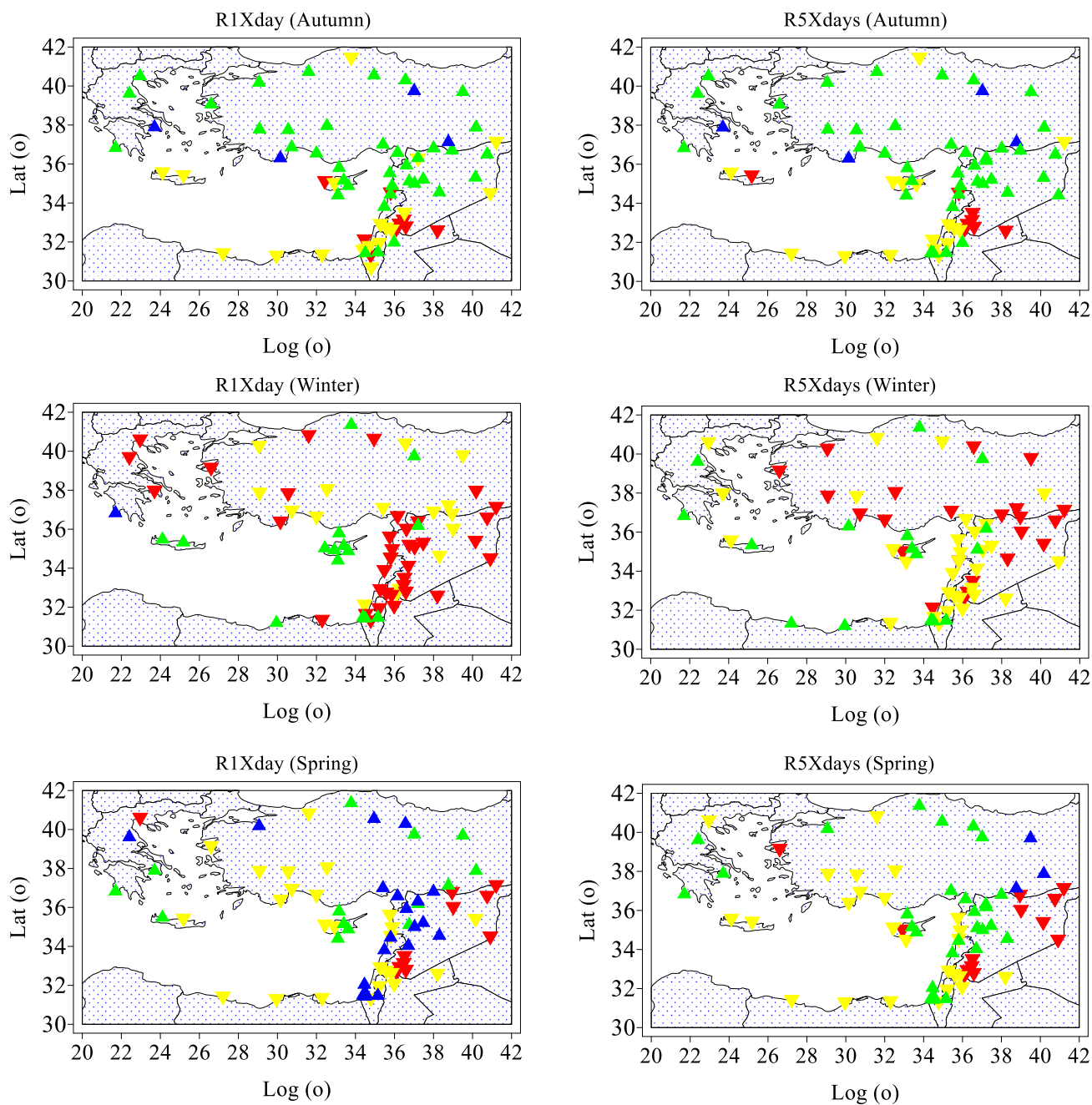


Figure 4.85 Spatial patterns trend in the seasonal R1Xday and R5Xday indices for the 1961-2012 in 70 stations with daily data over the EM.

Statistically significant ($\alpha=0.05$) positive trends are in blue and negative ones in red. The green and yellow triangles present non-significant positive and negative trend, respectively. Positive indicates wet trends and negative indicates dry trends.

Other areas of the EM displayed significant decreasing trends in extreme precipitation across the seasons, particularly in winter (DJF) (Fig 4.85). These results are in line with previous ones which concluded that extreme wet spells in the EM will become shorter in all seasons, except in autumn (Oikonomou *et al*, 2008). In summer, reductions of RX5 days were assessed over the southern parts of the EM and increased in the northern parts.

In autumn, between 5.2% and 11.4% of the stations reveal statistically significant increasing and decreasing trends of RX5days respectively; in winter, 32.9% of the stations have statistically significant decreasing trends whereas 22.9% of the total stations showed statistically non-significant increasing trends. In spring, statistically significant increasing trends of very wet days were detected in 41.4% of stations and only some stations (18.6%) reveal significant decreasing trends (Fig 4.86)

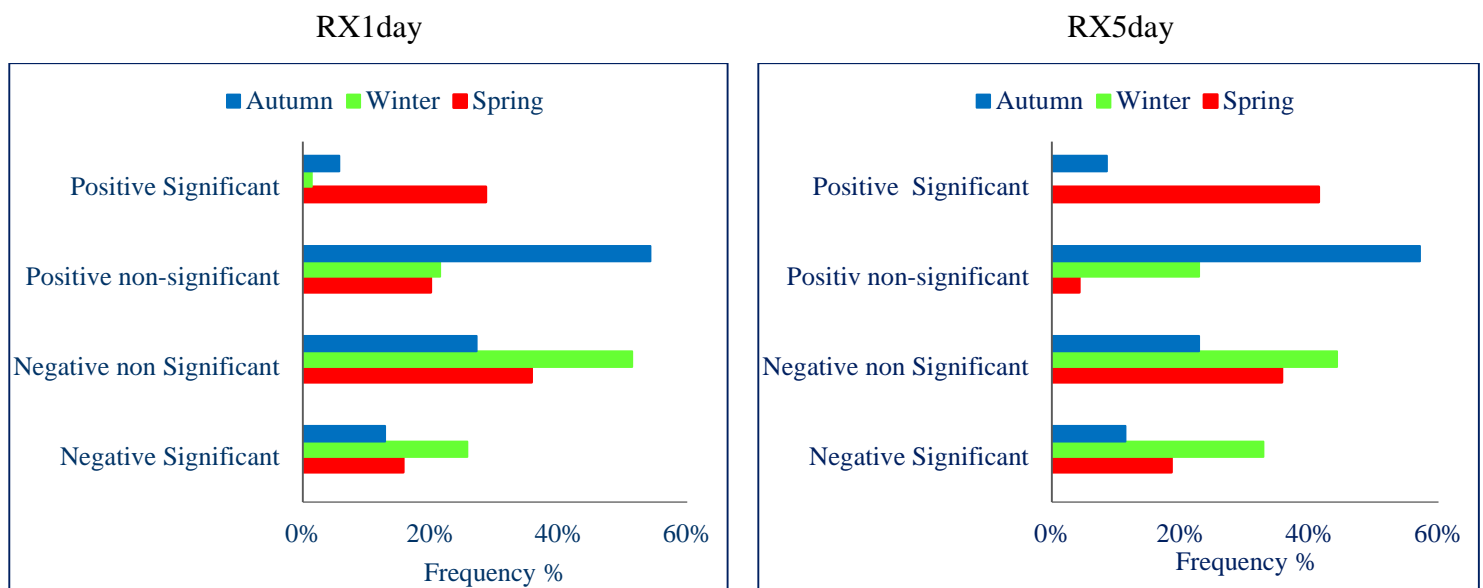


Figure 4.86 Frequency of seasonalRX1 day and RX5 day trends type in the EM over 1961-2012

The spatial pattern of RX5days and total seasonal precipitation changes show large similarities in the whole regions in autumn and winter and high correlation coefficients were also detected. The highest values were found in autumn (0.75-0.93). In spring, non-significant increases of RX5days can mainly be found over Greece, the north eastern parts of Turkey and many parts of Syria and Israel. Regarding changes in RX1day, an increasing tendency in autumn has been detected, the issue that has been proved by several RCMs which also displayed a strong increase of RX1day values in autumn and a small change in winter with a general tendency towards decreases over the Mediterranean region (Frei *et al*, 2006). RX1day decreasing also dominated in almost all regions of the EM in winter and spring but in a lower correlation with the total precipitation in these seasons comparing with RX5days (Fig 4.87) which illustrates the average correlations for all the stations between the RX1day and RX5day indices and total precipitation.

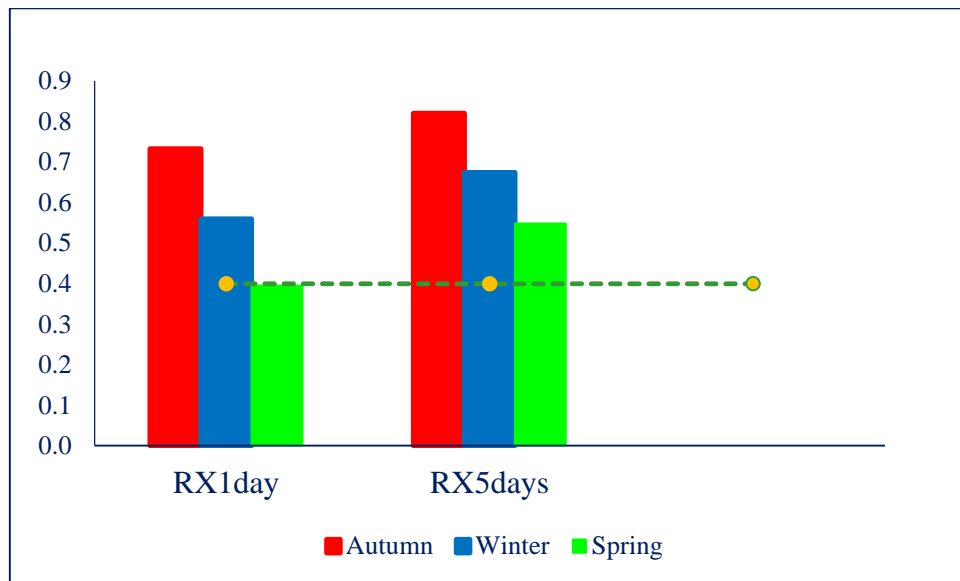


Figure 4.87 Mean correlations between the RX1day and RX5day indices and total precipitation for three rainy seasons (autumn, winter and spring) over the EM during 1961-2012 (green dashed horizontal line indicates where the 95% level starts)

It can be seen in Fig 4.87 that there is a significantly high correlation in autumn and winter between both precipitation indices and total seasonal precipitation with coefficient correlations varying between 0.72 and 0.91 in

autumn, 0.60-0.74 in winter and 0.30 and 0.67 in spring for RX5days. In spring, the correlations are lower than in winter and autumn, but they are still statistically significant. For spring, the highest correlation values can be found in the northern parts of the EM (in Turkey) in which small values of precipitation variability can be detected in this season comparing to whom found in the other parts of the EM (not shown). Correlations between RX1day and total seasonal amounts of precipitation were coherent with the results obtained from RX5days, but they were weaker and not statistically significant in spring.

4.10.2 Indices of maximum length of dry and wet periods

As it can be seen from Table 4.12, the consecutive dry days (CDD) showed a significant positive dry trend in 52.9% of all stations, 1.4% of them exhibited a statistically non-significant increase, whereas 44.3% of stations reported a significant decrease wet trends.

The positive slopes of CDD are concentrated especially in the northern parts of the EM as well as in North Africa (coastal regions of Egypt and Libya) and Cyprus (Fig 4.88). The annual CDD index presents the maximum increase in the northern parts of the EM and the maximum values being found mainly in west Greece (17-31 days per year) in Thessaloniki Airport and Souda Airport, respectively, and southwest Turkey (13 days per year) in Finike. In Cyprus the highest increasing was detected in Limassol Airport (26 days per year), whereas the maximum increasing of CDD values was small in the southern parts of the EM and did not exceed 5 days per year in Tel Aviv (Israel) and in some other stations in Syria.

The positive trend of CDD is in accordance with the projections for the increase in dryness for the Mediterranean area and central Europe (IPCC, 2012). Additionally, these results support the previous ones which were reached by Oikonomou *et al*, 2008 who reported the same increasing of CDD values in the same regions. Hertig *et al* (2013) proved that the overall change pattern of CDD is characterized by shortening of the period of consecutive dry days over the southern parts of the EM, particularly over Israel with values up to 11 days. Brandt and

Thornes (1996) have also pronounced positive trends for the islands of Cyprus highlighting the fact that southern Mediterranean areas and especially the islands are threatened by future drought and desertification. The results from Kostopoulou and Jones (2005) demonstrated significant positive trends of CDD in many southern stations in the EM during the period 1958-2000.

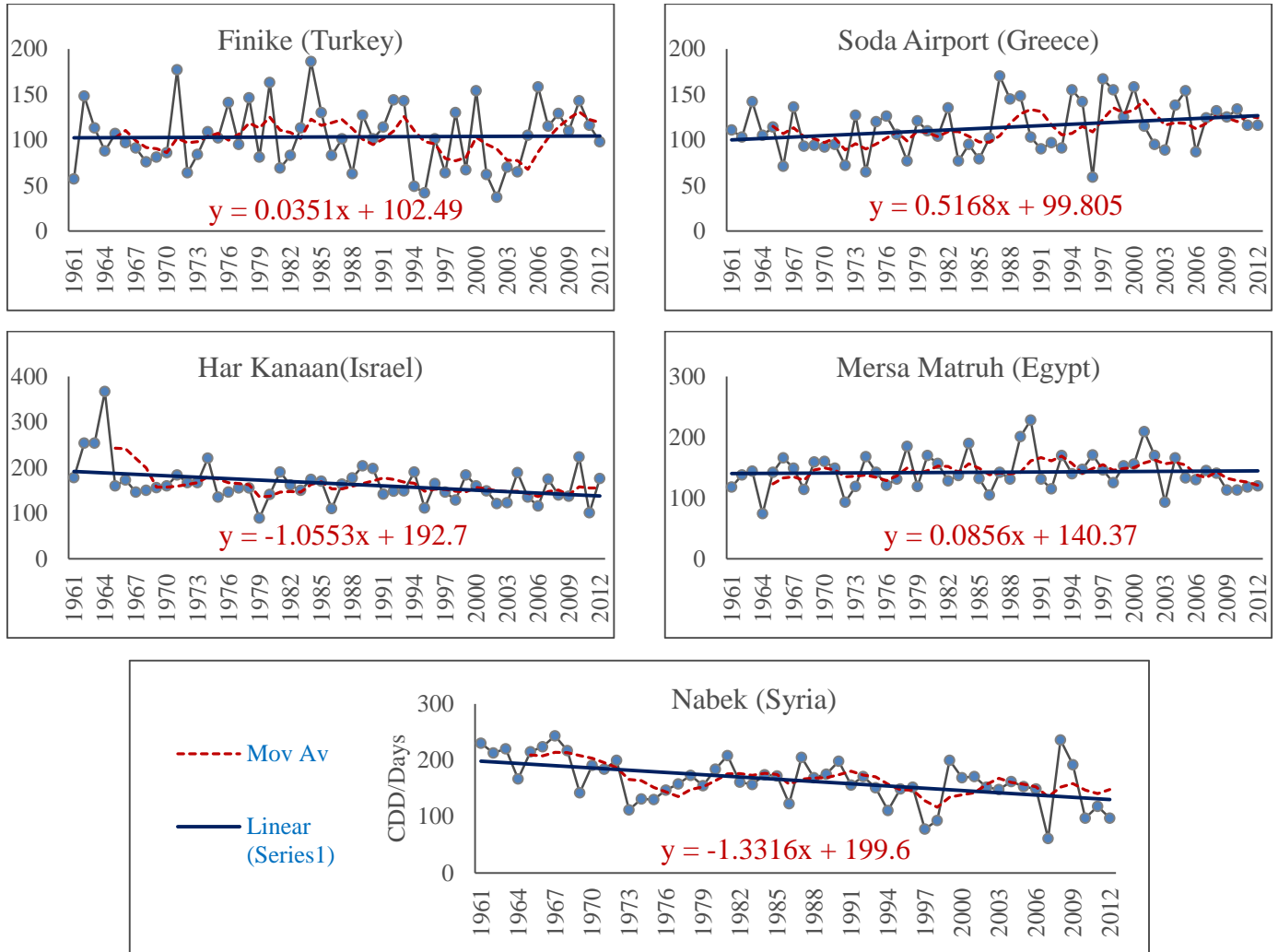


Figure 4.88 Interannual variability of CDD in some selected stations over 1961-2012.

These results agree with Sillmann and Roeckner (2008) who assessed significant increases of the CDD index in regions around the Mediterranean Sea, especially along the African coast. This finding is in accordance with a study of Oikonomou *et al* (2008). Tebaldi *et al* (2006) and Gibelin and Deque (2003) have also found a statistically significant increase in dry days (defined as the annual maximum number of consecutive dry days) in this region. Consecutive wet days (CWD) index showed a decreasing tendency for the majority of stations (78.6%)

which was statistically significant in 15.7% of the total stations. A very small percentage of stations have statistically positive significant trends (only 1.4%). The highest increasing was detected in the last ten years especially in 2008 and also in 1999. The CWD annual indices take the lowest values (<6 days) between 2004 and 2010, that also correspond to the largest absolute values of the negative anomalies (Fig 4.89).

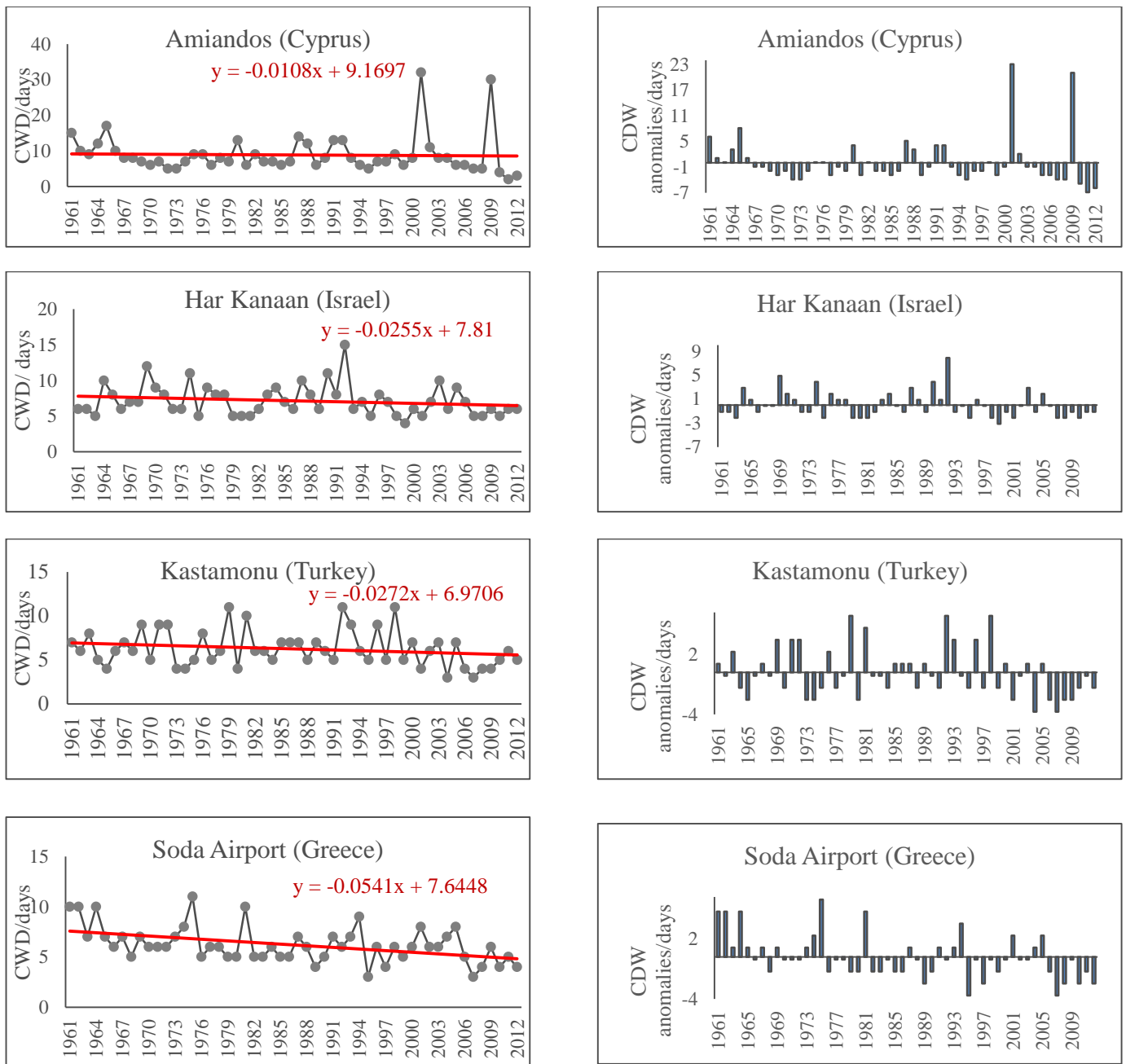


Figure 4.89 Annual anomalies for CWD index (right) and trend lines (left) calculated for the period 1961-2012 for some selected stations in different regions.

For example, CWD decreases by 0.11 day per decade in Amiandos (Cyprus), and 0.54 day per decade in Soda Airport (Greece). A decreasing with 0.03 day per decade was detected in both Har kanaan (Israel) and Kastamonu (Turkey) (Fig 4.89).

4.10.3 Daily precipitation absolute threshold indices

Regional indices' time series indicate fewer days with precipitation above 10, 20 and 25 mm (R10, R20, respectively, heavy, very heavy daily events) in 2008 and 2010 than in 1974 and 1988. Values of R10 distressed to less than 4 days in more than 57% of the total stations in 2008 and 34% in 2010. Regionally, the results showed that the highest values of R10 were observed in 1974 and 1988 (Fig 4.90).

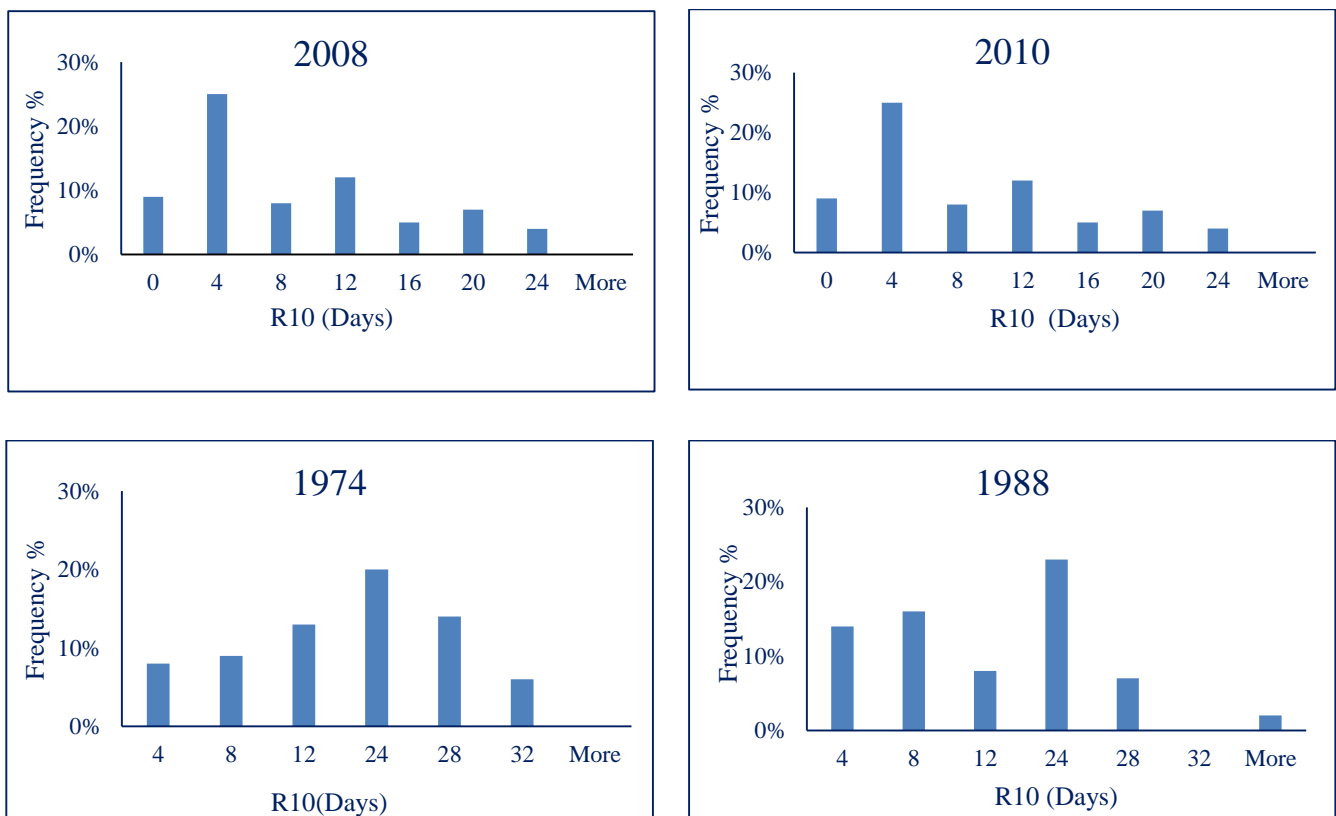


Figure 4.90 Histograms of the R10 frequency values in different periods for the 70 daily meteorological stations throughout the EM during 1961-2012.

The frequency of heavy and very heavy precipitation daily events in the data of the station generally followed the tendency of their respective regional average. Decreasing trend excited at 78.5 % of the meteorological stations for R10 and at 64.3% for R20. The statistically significant trends are found in more than 37.1% and 25.7% of these stations, respectively during the 52-yr study period. In some stations, the percentages of change in the precipitation amount and number of wet days have opposite signs (i.e. negative/positive; when one decreases the other increases).

4.10.4 Indices of extreme precipitation events of 1- and 5-day durations

RX1day index displayed decreasing trends in 80% of the total stations, which were statistically significant in 62.9% of them and the highest decreasing was reported in Raqa (Syria) with 4.7 mm per decade. RX5days values have a decreasing trend in 67.1% of the total stations, 50% of the stations showed a statistically significant trend. The highest decreasing was also detected in Raqa (Syria) with 7.5 mm per decade. The most statistically significant negative trends were observed in spring and winter in all regions, the matter which was reported by Hertig *et al* (2012). They concluded that total and extreme precipitation decreases prevail over the whole Mediterranean area in spring. Total and extreme precipitation decreases mostly come along with increases of the maximum dry period length. The northern parts of the EM have evident statistically significant positive trends in RX5days with 31.4% frequency. This conclusion is consistent with others which were reached in the Western Mediterranean regions by Ramos and Martínez-Casasnovas, 2006 who found that many stations in Catalonia (northeast Iberia) have statistical significant increasing trends in RX5days. Both RX1day and RX5days showed the highest increasing in Greece with 4.1 mm/decade and 6.6 mm/ decade, respectively.

4.10.5 Daily precipitation percentile threshold indices and simple daily precipitation intensity (SDII)

Percentile-based R95p (very wet days) of the stations and R99p (extreme wet days) indices showed consistent trends except in the regions located in the northern parts of the EM. For R95p, 48.6% of the daily stations showed statistical decreasing trend, whereas 31.4% of total stations detected statistical increasing trends. 27.1% of the stations which showed this significant increased tendency to be located in the northern parts (Turkey). This result confirms the concentration of precipitation in single events or a higher concentration in shorter time periods.

This percentage was relatively higher for R99P since 74.5% of the total stations displayed a statistical decreasing trend showing a predominance of negative trends in the majority of the stations, and only 20% of stations detected an increasing statistical trend.

The results showed a statistically significant decrease in the amount of extreme precipitation (R99P) in whole parts of the EM and in heavy events (R95P) in the southern parts. These decreasing trends in both R99P and R95P are accompanied with a decrease in total precipitation amount (PRECPT), and a significant increase in daily intense precipitation events (SDII) in the northern parts of the EM.

In general, the regional average series of these indices show negative trends that accompany the PRCPTOT (Annual total wet-day precipitation) trend. Nevertheless, the statistically significant negative trends of frequency in the R99p and PRCPTOT have different values (45.7% for PRCPTOT vs 74.3% for R99p), whereas both of them have the same frequency rate (20.0%) for statistically significant increasing trends (Table 4.13). The highest decreasing for R95p and R99p was detected in Kamishli (Syria) with 18.7 mm per decade and Lattakia (Syria) with 6.9 mm per decade.

The contribution of very wet precipitation (R95p) to total precipitation (R95p/ PRCPTOT) represents the percentage of the annual total wet-day precipitation due to events with precipitation above the 95th percentile; it can be used to analyze the possibility of having a relatively larger variation in extreme

precipitation events than in the total amount (Groisman *et al*, 1999; Albert *et al*, 2002; Kioutsioukis *et al*, 2010; Brugnara *et al*, 2012).

The (R95p / PRCPTOT) has significantly increased in the northern parts of the EM, this increasing was more evident in Turkey. Many stations (in the northern parts of the EM) detected a statistically significant increasing trend in the contribution of very wet days (R95p) to the total precipitation amount averaged with 25% (ranged from 20% and 30%). Similarly, the average contribution of extreme precipitation wet days (R99p) was 7.5% (ranged between 5.0 % and 10%) (Fig 4.91), which had a non-significant decreasing trend in more than 80% of the total stations. The spatial pattern for R95 values demonstrated that increasing trend occurred mainly in the northern parts of the EM, especially in Turkey. In contrast, these northern parts had a decreasing trend for R99p values.

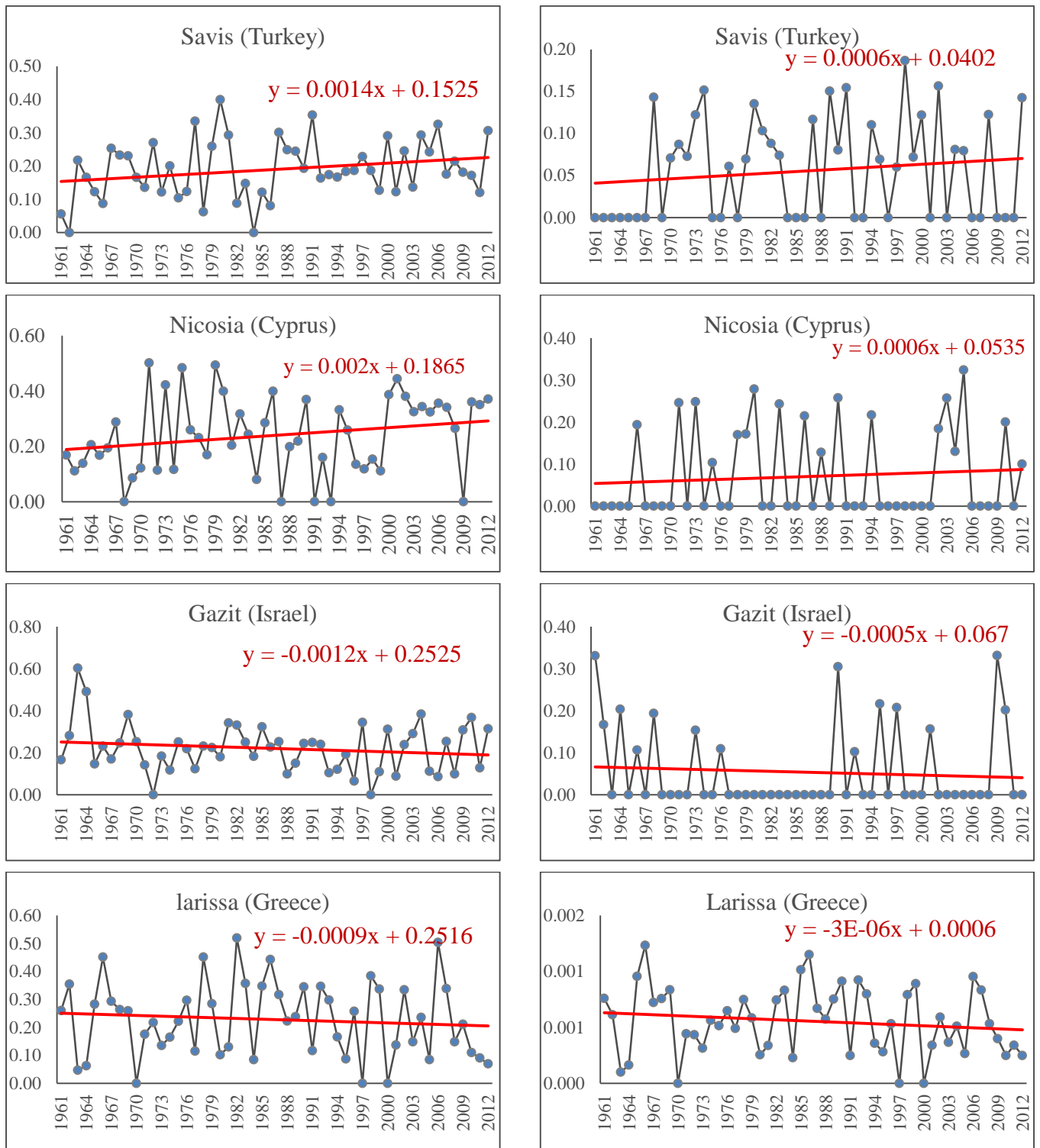


Figure 4.91 The average contribution of extreme and heavy wet days to total precipitation in some selected stations over 1961-2012.

(Left) very wet days (R95p) and (right) extremely wet days (R99p) in some selected stations
(The red line is the linear trend).

The Simple daily intensity index (SDII) is the index that takes into account not only the total amount of precipitation throughout the year but also reflects changes in daily rainfall. It combines the total amount of annual precipitation and the number of days when rainfall is greater than 0.1 mm. The mapping of the trends in the SDII is shown above with other maps of extreme precipitation indices trend (Fig 4.83). The lowest SDII values (<9.0 mm) occurred after 1990 especially in the years 1999, 2008 and 2010 (Fig 4.92), which were the driest on record, and these occurrences coincide temporally with the lowest PRCPTOT values (<300 mm) in Syria and (<150 mm) in Israel.

The highest values of SDII (>9.0 mm) were recorded in 1988, 1994, 1969 and 1974 (ordered from highest to lowest values), and of PRCPTOT (>600 mm) happened in 1988 and 1969 and exceeded 1000 mm in many stations in Turkey (Fig 4.91). More than 60% of the stations showed negative trends in this index that were statistically significant in 32.9% of the total stations (see also Table 4.13 above) whereas 38.5% of total stations showed increasing trends which were statistically significant in only 17.1% of the total stations.

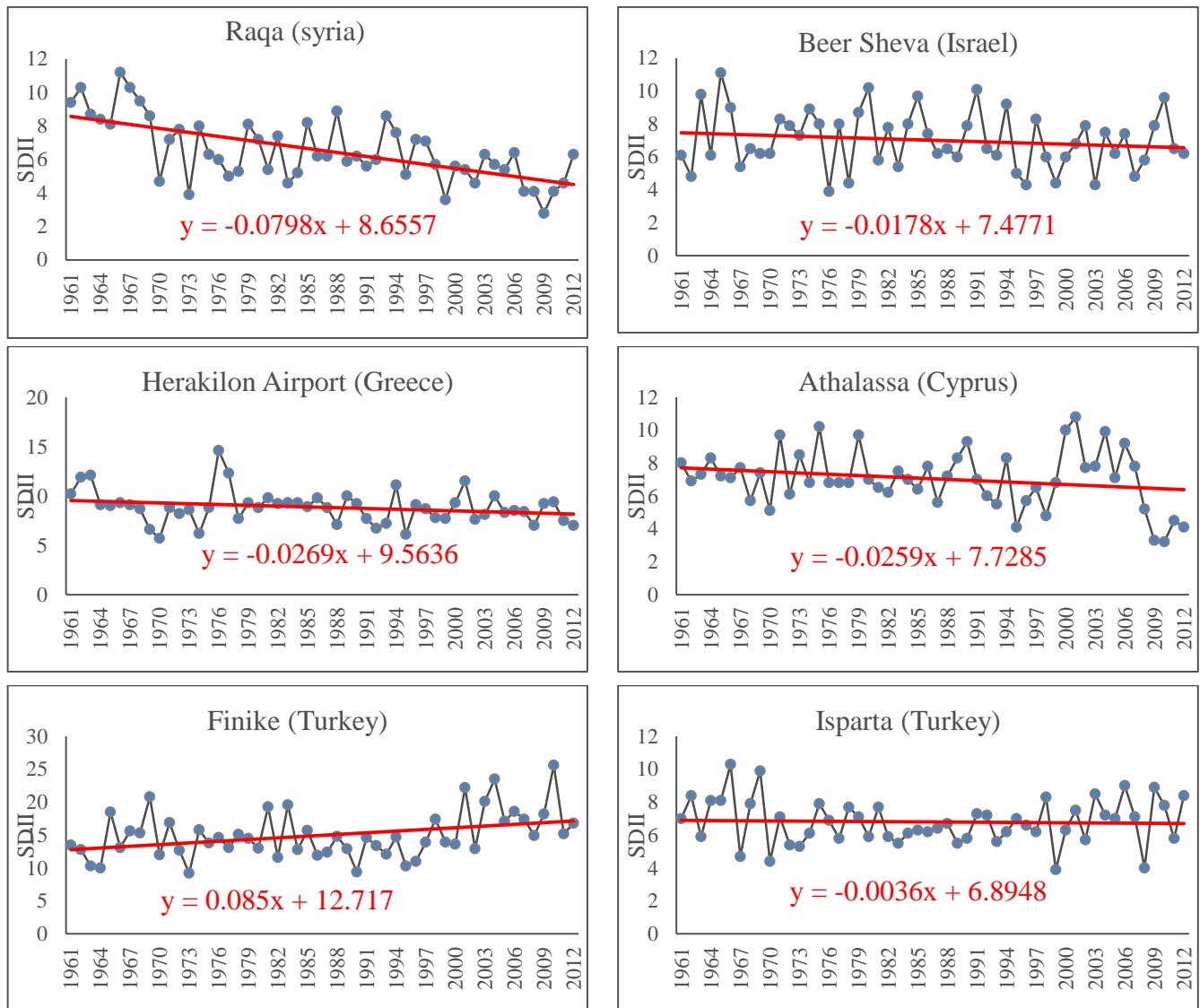


Figure 4.92 Interannual variability of SDII in some selected stations over 1961-2012

4.10.6 Correlations between extreme and mean precipitation indices

Analysis of correlations between precipitation indices was used here as an additional tool to inspect the data closely; the analysis was undertaken for mean conditions indices (wet-day total precipitation (PRCPTOT) and simple daily precipitation intensity (SDII)) and all the other indices listed in Table 4.14, which were calculated site-by-site, for all 70 daily precipitation stations. The correlations were calculated using the linear Pearson (product moment) correlation coefficient R , their statistical significance was assessed at the 0.05 level. The correlations

between extreme precipitation indices and total precipitation were listed in Table 4.14.

Table 4.14 Correlation coefficients between precipitation extremes indices over the 1961-2012

	PRCPTOT	SDII	RX1 day	RX5 days	R95	R99	R10	R20	CDD	CWD
PRCPTOT	1.00									
SDII	0.66^a	1.00								
RX1 day	0.53^a	0.63^a	1.00							
RX5 days	0.55^a	0.68^a	0.77^a	1.00						
R95	0.72^a	0.74^a	0.72^a	0.73^a	1.00					
R99	0.50^a	0.57^a	0.82^a	0.70^a	0.70^a	1.00				
R10	0.82^a	0.59^a	0.31^a	0.44^b	0.52^a	0.27	1.00			
R20	0.74^a	0.66^a	0.45^a	0.53^a	0.72^a	0.42^b	0.80^a	1.00		
CDD	-0.15	0.06	-0.05	-0.01	-0.06	-0.05	-0.12	-0.07	1.00	
CWD	0.51^a	0.04	0.08	0.20	0.15	0.07	0.50	0.18	-0.18	1.00

a Significant at the 0.01 level.

b Significant at the 0.05 level

Except for CDD (consecutive dry days), the other precipitation indices have positive correlations with annual total precipitation, and they are statistically significant at the 0.01 level. The total precipitation (PRCPTOT) and extreme precipitation indices are positively correlated and the correlation coefficients exceed 0.7, including very wet day precipitation (R95), heavy precipitation days (R10 mm), and very heavy precipitation days (R20 mm), others also exceed 0.5 which means that the indices selected in this study have good indicative functions

to the changes of annual total precipitation. These results agree with previous studies which reported that the majority of extreme precipitation indices are well correlated with the annual total precipitation (You *et al*, 2010; Wang *et al*; 2013).

It is also notable that the PRCPTOT correlations are strong for the number of heavy and very heavy precipitation days (R10 and R20) and moderate when we focus on the tail of the precipitation distribution (in particular, for the precipitation amount on extremely wet days, R99p). The correlation coefficients obtained between PRCPTOT and the RX1day and RX5days indices range, on average, between 0.53 and 0.55, with the highest values being in both Syria and Israel.

The correlations between PRCPTOT and R95p ($r=0.72$) are greater than PRCPTOT and R99p ($r=0.50$). This is certainly related to the character of the EM climate which has a long dry season in summer and the seasonal lowest precipitation occurs during this season. Only 2-3% of the annual precipitation and less than 0.5% in some areas can be received during summer, especially, in the southern parts and with a small number of wet days. As a consequence, the R99p index tends to be zero in many years while the PRCPTOT index varies from year to year with large inter-annual variability. These results are in line with the findings of Santo *et al* (2014) who proved the same tendency and correlations in western Mediterranean (mainly in Portugal).

In addition, there are statistically significant correlations among the precipitation indices. On average, the correlations between SDII and the extreme precipitation indices are in general strong and statistically significant at the 0.05 level (except CDD and CWD) ranging from 0.57 and 0.74. In regional scale, SDII did not show correlations with both CDD and CWD. The correlations between SDII and the RX1day, RX5days, R95p and R99p indices are, on average, stronger than the correlations between PRCPTOT and those same indices. For instance, the correlation coefficients between the SDII and both RX1day and RX5days indices range with an average between 0.50 and 0.85, with the highest values being found in Syria for RX1day, and in Syria, Cyprus and Israel for RX5days. Strong

correlations ($R > 0.7$) are found between the SDII and RX1day for 40 % of the stations, and between SDII and RX5D for 60 % of the stations.

The average correlation coefficients between SDII and the number of very heavy and extremely heavy precipitation days (R10 and R20 ,respectively) ranged between 0.59 and 0.66 and increased with the change from very heavy to extremely heavy precipitation days, this issue contrasts with the results obtained for the PRCPTOT index. Likewise, the correlation coefficients between SDII index and the percentile indices (R95p and R99p) at regional scale were stronger with R95p (0.74) than with R99p (0.57). For all 70 daily stations, the correlation coefficients between the SDII and the R95p fall in the interval 0.65–0.93 with very high values ($R > 0.8$) for more than 45% of the stations (Fig 4.93). Like the correlations between PRCPTOT and the indices for precipitation extremes, the correlations between SDII and those indices decrease as we approach closer to the tail of the precipitation distribution, in particular for precipitation on extremely wet days (R99p) (Fig 4.93).

Isabel *et al* (2014) found that the average correlations between SDII and R10 and R20 were strong ($R > 0.7$) in mainland Portugal. The same results obtained by Zhang *et al* (2015) who found a strong significant correlation between precipitation on wet days (SDII) and total precipitation (PRCPTOT) ($R = 0.84$). They have also detected strong correlation between SDII and other extreme indices such as R10 ($R = 0.85$), R20 ($R = 0.83$), R95P ($R = 0.83$) and R99P ($R = 0.68$). Several studies have reported that the majority of precipitation indices are correlated with the annual total precipitation, indicating a high correlation between annual total precipitation and extreme precipitation (Han and Gong, 2003; Wang *et al*, 2013).

SDII is considered one of the indices which describe moderate climate extremes; they are relevant for the management of water resources and land use, modelling of erosion, and other applications for ecosystem and hydrological impact modelling (Costa and Soares, 2009).

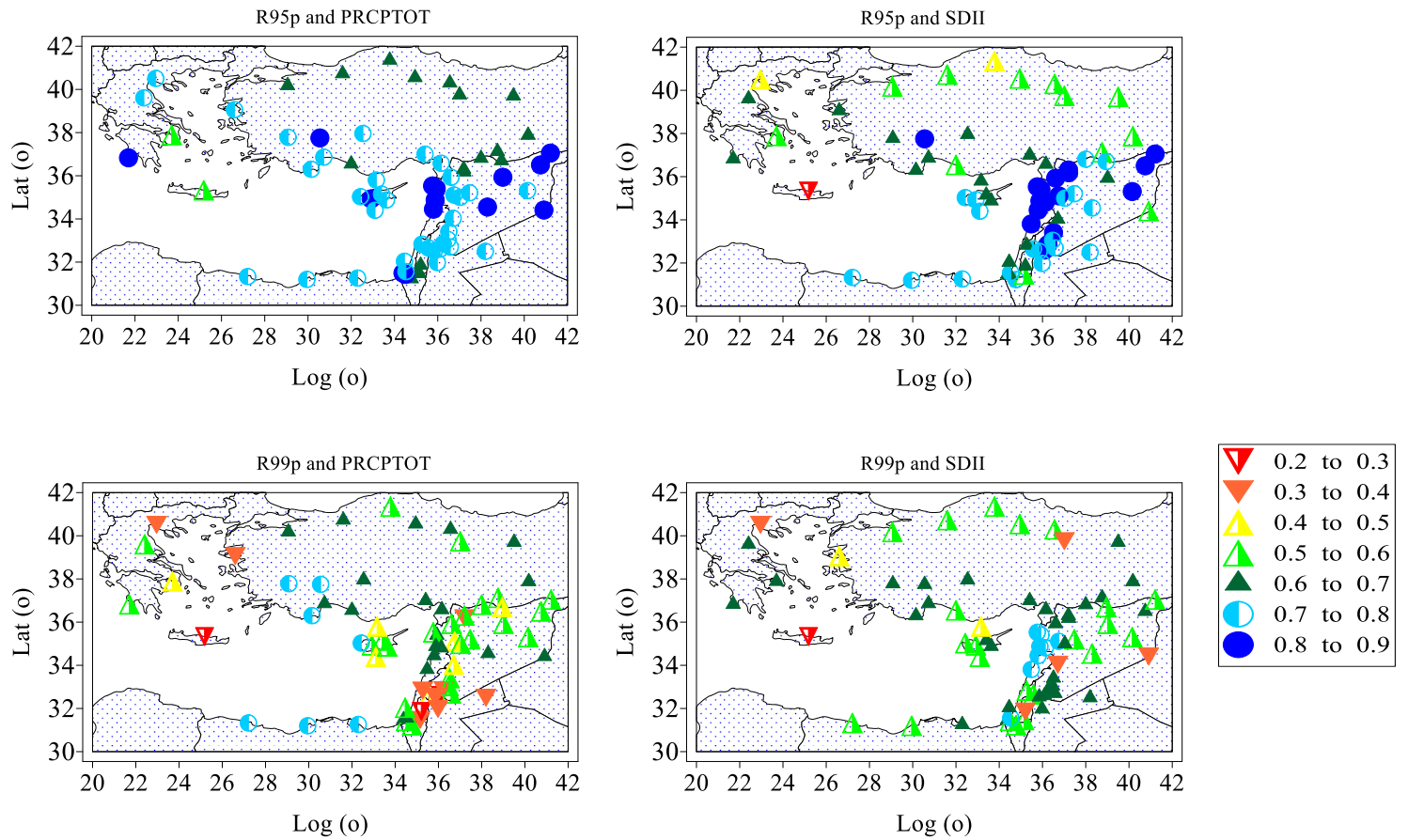


Figure 4.93 Spatial distributions of Pearson correlation coefficients between both R95p, R99p and PRCPTOT and SDII for the 1961-2012 in 70 stations with daily data over the EM.

All correlation coefficients between SDII and R99p are smaller than 0.7 except in some coastal stations in the southern parts of the EM like Lattakia in Syria (0.77) and in the northern parts such as Isparta in Turkey (0.71). 22 % of the stations show correlation coefficients smaller than 0.5. Among the stations, the spread of correlation coefficients between SDII and R99p indices is notably larger than R90p.

Both RX1, RX5 and R95p and R99p are highly and significantly correlated (R ranged between 0.70 and 0.82). The CWD index is moderately related to the PRCPTOT index with a correlation coefficient (0.51) which is statistically significant at 0.05.

Finally, the results showed that percent trends in precipitation extremes are, in general, highly and spatially correlated with the percent trend in PRCPTOT; moreover, all the correlations are statistically significant. This is particularly true

for the number of heavy to extremely heavy precipitation days (R10 to R20) and precipitation on wet and very wet days (R95p and R99p).

The absolute slope of the line of the best fit for both R95p and R99p is high (between 0.7 and 2.2) in the majority of stations indicating enhanced variability in the trends of precipitation extremes compared to the mean trends. Although extreme rainfall is generally not as spatially coherent as mean rainfall, we have shown that a spatial analysis of the interannual variability of indices of extremes can reveal interesting behaviour in the indices. Overall, it can be concluded that the EM tends to be drier in future and with reduced rainfall intensity.

Several studies discuss the relationship between extreme rainfall events and the presence of cyclones modulation local humidity advection (Duffourg and Ducrocq, 2011). The association of intense precipitation events with the intensity or position of cyclones can depend on the location of extreme event and its environment characteristics especially the orography (Reale and Lionello, 2013).

The employment of previous indices to study the behaviour of extreme precipitation events seems to be useful, since they represent persistent dry and wet spells and heavy and extreme rainfall days for each station without using different threshold values for each station. Moreover, this way can be transferable across many different climatic regimes and make the results in the EM comparable with those in other regions. Finally, the increases in extreme precipitation regimes (more intense rain events or severe drought) which are predicted for arid and semiarid regions (Easterling *et al*, 2000; IPCC, 2007, 2013) and increased inter-rainfall dry intervals can significantly impact grassland productivity even when precipitation event size is increased to maintain total rainfall amount (Fay *et al*, 2003; Heisler-White *et al*, 2008). Extreme climate events are often more important to natural and human systems than their mean values (Katz and Brown, 1992; Aguilar, 2009), for example, most social infrastructure is more sensitive to extreme events. They may have many impacts on the distribution of wild plants and animals, climate-induced extinctions, phenological changes, and both range and rates of the shifts of the species (Easterling *et al*, 2000).

Chapter Five

Conclusions

Main conclusions

The present thesis examines the spatial and temporal variability of annual, seasonal and daily precipitation amounts and the drought patterns for the Eastern Mediterranean (EM). It also explains the distribution of daily precipitation extremes for the EM. We can summarize the main conclusions by following:

1- The results of PCA applied to annual and seasonal precipitation and drought indices explained the general characteristics of precipitation and drought pattern over the EM and the influences of the major physical geographical features, such as the latitude and altitude, on the spatial and temporal variability of precipitation and drought.

2- The annual precipitation series during 1961-2012 displayed negative trends within the five decades over all the EM regions. This downward trend in precipitation was uniform in space and time. The southern parts of the EM showed the highest significant decrease due to the greatest decrease in precipitation in winter and spring. The highest decrease of annual mean precipitation occurred in the stations up to 250-500 m (-25 mm /decade), whereas the stations with high altitude (>1000m) detected non-significant trends near to zero, and the large part of this decreasing occurred after the 1990s in whole regions.

3- Both negative and positive trends were observed in seasonal precipitation. The trends in the spring and winter series were mostly negative and statistically significant. Trends in autumn were generally increasing, while the summer is almost dry season over the EM.

4- The gamma distribution has been found to provide the best model for describing monthly and annual precipitation over most of the EM. A parametric statistical analysis of annual rainfall distribution over a period of 52 years, covering two 26-yr periods, reveals some significant spatial and temporal changes in the shape and scale parameter patterns of the fitted gamma distribution. The detected increasing in the scale parameter (rate parameter) means that the distribution function covers events with extreme rainfall amounts. In the northern

parts of the EM (in Turkey), a clear decrease has been shown in the size parameter $1/\beta$ which can be interpreted as a tendency towards reduced probability of large annual rainfall amounts in the most recent years.

5- The rainfall seasonality \overline{ST} is a very accurately expression about interannual rainfall variability and gives an idea about the distribution of the rainfall among the months and divide the EM region in different rainfall regimes. A non-significant statistical trend of seasonality was indicate in most of the stations. 8% of total stations showed a statistically decreasing trends of seasonality whereas 5% of them showed a statistically increasing ones. Thus, it can be concluded that the observed rainfall regimes have not changed in the last five decades despite the observed negative trend in the annual rainfall amounts.

6- The daily analysis of precipitation confirms that high to moderate irregularity and rainfall concentration are the two very characteristic features of rainfall in the EM. Highest values of daily CI were detected in the southern parts of the EM. Distribution of annual precipitation CI trends indicated a significant increasing trend mainly occurring the northern and north western parts of the EM (Greece and Turkey) and some parts of southeastern parts (Syria and Israel) and a statistically decreasing trend at in 10% of total stations which are particularly located in south Syria and Israel.

7- Entropy theory is very effective in studying the spatio-temporal distribution of daily, monthly and annual rainfall and more efficient than CV for quantifying the complexity and variability of the changing climatic systems. The results showed that the entropy was linearly and positively related to the latitude, but it was not linearly correlated with the longitude.

8- Studying of spatiotemporal characteristics of meteorological drought events using different meteorological drought indices (DIs) showed that most areas of the EM suffered several extreme droughts, starting in the beginning of the 1970s, mid 1980s, 1990s, and end 2000s which enhance with the increasing of the time scale. In general, the north and northwestern parts of the EM have fewer drought events comparing with other parts of the EM. Abrupt changes of annual SPI and MCZI

detected two extreme droughts quite clear: one in the mid-1970s and the other in the beginning of the 1990s which was longer than the first one.

9- A comparative analysis of different drought indices (SPI, MCZI, Z-Score, Deciles and EDI) indicated that all these indices are highly correlated for same time steps and the correlation increases at higher time step with highest correlations at 6 and 9 month time scales. On the other hand, EDI is found to have high correlation with other DIs for all time scales.

10 - Comparisons showed that both SPI and EDI performed better in detecting the onset of drought, and these were recommended to the area drought monitoring system. However, EDI was more responsive to the initiation of a drought and more realistic than other DIs in studying the drought conditions due to its capability in detecting the exact time of drought onset and realistic quantification of severity of drought events in study area. This variety in responses of different DIs points to the need of using several indices for drought monitoring, thus it is recommended that at least EDI and SPI to be included into a drought monitoring system.

1- Analysis of climatic extreme indices recommended by the joint World Meteorological Organization (CCL/CLIVAR/JCOMM) and Expert Team on Climate Change Detection and Indices (ETCCDI) showed in general many regions of coherent change, with many stations showing statistically significant changes in most of these indices. The pattern of trends for the extremes was generally the same as that for total annual rainfall, with a change to drier conditions with a significant decreasing trend in the annual total precipitation amount (PRCPTOT) in 46% of total stations (3.1% per decade) in Syria, Israel, Jordan, north Libya and north Egypt. Significant increasing trend in the maximum number of consecutive days (CDD index) in 53% of total stations was also detected especially in north and northwest Turkey, Cyprus, Greece, north Libya and north Egypt.

2- The EM has experienced many and frequent drought events during last thirty years especially its southern parts. For example, four Syria consecutive droughts has affected since 2006, with the drought in 2007-2008 being particularly devastating. The losses from these frequent droughts had

significantly affected the population in the north and northeastern parts of Syria (Aleppo, Hasakah, Kamishli, Deir Ezzor and Raqa) because of the socioeconomic instability, Health problems, food insecurity, water resources shortage and crop failures. All these impacts led to the migration of 1.5 million farmers to the cities, and then to poverty and civil unrest (Gleick, 2014). These severe droughts, worsened by a warming climate, contributed to the outbreak of civil war and helped Spark Syrian War which has killed hundreds of thousands of people.

Limitations of the study and recommendations for further works:

The research team faced several limitations. Among them were the following:

- 1- The lack of stations in Jordan and Libya restricts our understanding of precipitation variability over these two areas and were not sufficient for spatial representation, which means that the determination of spatial rainfall distribution over large areas of these two countries needs more stations to be more represented. Besides, data of these stations is very expensive, which prevented us from obtaining more stations.
- 2- There are some limitations due to data inhomogeneities. Even if many of the ECA series were subjected to homogenization by the National Meteorological and Hydrological Services (NMHSs), there are certainly non-climatic influences and some artificial shifts in the time series that have to be corrected. Hence, with the information available in this research, there are some difficulties to know the accurate conclusions to what extent inhomogeneities affected the trends in the investigated extreme indices.
- 3- The comparison of drought indices was only undertaken between drought indices which are based on precipitation data. More comparisons are necessary between these indices and others which are designed to take into account both precipitation and potential evapotranspiration such like SPEI (Vicente-Serrano *et al.*, 2010) and RDI (Tsakiris, 2007). These comparisons are necessary to understand the impact of temperature on water demand and moisture availability, especially in regions where the temperature is more influential than precipitation such as arid lands in Syria and Israel. Although, the SPI has more popularity than any other DIs, it is not strong enough to define and explain the wider drought conditions since many other important hydro-meteorological variables which affect droughts (e.g., streamflow, soil moisture condition, evapotranspiration and reservoir storage volume) were not considered in SPI (Keyantash and Dracup, 2004; Smakhtin and Hughes, 2004). The characterization of droughts for different regions is difficult when only a single variable is used (Hisdal *et al.*, 2004)

4- The incomplete gamma distribution (Gamma with 2 parameters) was used for calculating the SPI at all locations so that they are comparable. This normalized gamma distribution causes problems in climates with low precipitation, or climates with a very distinct dry period of several months per year. Under these conditions the procedure is unable to give a good estimate of the two shape parameters (α and β) of the gamma distribution. However, the most suitable function may vary from location to location. For example, some studies have recommended using of the Pearson type III distribution within the calculation SPI algorithm in some regions (Kumar *et al.*, 2009; Blain, 2011).

5- There are many homogeneity tests that could be applied to the dataset used in this study in order to improve the consistency of precipitation data. Some new robust homogeneity software packages were developed during the last years. It will be interesting to test them together with the SNHT. This experiment would probably provide more reliability on drought results. Further, research using a wider set of drought indicators on a global scale, could provide more knowledge on the performance of drought indicators.

This study could be complemented analyzing various kinds of drought (agricultural and hydrological drought) because only the meteorological drought is considered and assessed here. This could be figured out using different time-scales on drought index computation. This experiment could provide more information about the behaviour of long-term and mid-term droughts over the region of interest. Furthermore, it would be interesting to analyse all main drought parameters (severity, duration and magnitude) together to get a real characterization of droughts. This multi-variate analysis could be achieved using Copulas Model to estimate the return periods for various categories of drought taking into account a given magnitude and/or duration using the severity-frequency-duration curves.

It will be good achieving to analyse the drought conditions over the EM across the 21st century, taking into account various IPCC climate change scenarios.

The temporal evolution of the main variables that explain drought could be analyzed using drought indices from different Regional Climate Models across the 21st century to give us a good idea about drought variability and change in the future.

We recommend that future studies should consider more climatic indices in order to investigate the possible impacts of some teleconnection patterns, such as NAO, which affect the interannual variation of the frequency of days with extreme precipitation over the EM. More specifically, correlation analysis can be explored between the teleconnection indices and monthly mean precipitation and frequencies of days with extreme values.

References

- Abou Zakhem, B, Hafez R. (2007). Chemical and isotopic composition of precipitations in Syria. AECS-GRSS no. 729, Atomic Energy Commission of Syria, Damascus.
- Abu-Taleb A, Alawneh A J, and Smadi M M (2007). Statistical analysis of recent changes in relative humidity in Jordan. *American Journal of Environmental Science* **3**, 75–77.
- Acero FJ, Gallego MC, García JA (2012). Multi-day rainfall trends over the Iberian Peninsula. *Journal of Theoretical Applied Climatology* **108**,411–423.
- Aguilar E, Auer I, Brunet M, Peterson T C and, Wieringa J (2003). Guidelines on Climate Metadata and Homogenization. WCDMP-No.53. WMO-TD No. 1186, 51pp.
- Aguilar E, Barry A A, Brunet M, Ekan L, Fernandes A, Massoukina M, Mbah J, Mhanda A, do Nascimento D J, Peterson TC, Umba O T, Tomou M and , Zhang X (2009). Changes in temperature and precipitation extremes in western central Africa, Guinea Conakry, and Zimbabwe, 1955–2006. *Journal of Geophysical Research: Atmosphere*. **114**, (D02115). doi: 10.1029/2008JD011010
- Aguilar E, Peterson TC, Ramirez Obando P, Frutos R, Retana JA, Solera M, Soley J, Gonzalez Garcia I, Araujo RM, Rosa Santos A, Valle VE Brunet M, Aguilar L, lvarez LA, Bautista M, Castañon C L. Herrera L, Ruano E, Sinay JJ, Sanchez E , Hernandez GI, Oviedo F, Obed F, Salgado JE,. Vazquez JL, Baca M, Gutierrez M, Centella C, Espinosa J. Martinez D, Olmedo B, Ojeda Espinoza CE, Nuñez R, Haylock M, H. Benavides H, Mayorga R (2005a). Changes in precipitation and temperature extremes in Central America and northern South America, 1961–2003. *Journal of Geophysical Research* **110**, D23107, doi: 10.1029/2005JD006119.

- Aguilar E., et al. (2005b), Changes in precipitation and temperature extremes in Central America and northern South America, 1961 – 2003, *J. Geophys. Res.* **110**, D23107, doi: 10.1029/2005JD006119.
- Akhtari R, Morid S, Mahdian M H , Smakhtin V(2009). Assessment of areal interpolation methods for spatial analysis of SPI and EDI drought indices. *International Journal of Climatology* **29**, 135–145.
- Al-Ahmadi K and Al-Ahmadi S (2013). Rainfall-Altitude Relationship in Saudi Arabia. *Journal of Advances in Meteorology Advanced*. 2013, doi:.org/10.1155/2013/363029.
- Alexander LV, Zhang X, Peterson T C, Caesar J, Gleason B, Klein Tank AMG, Haylock M, Collins D, Trewin B, Rahimzadeh F, Tagipour A, Kumar Kolli R, Revadekar J V, Griffiths G, Vincent L, Stephenson D B, Burn J, Aguilar E, Brunet M, Taylor M, New M, Zhai P, Rusticucci M and, Vazquez Aguirre J L (2006). Global observed changes in daily climate extremes of temperature and precipitation. *Journal of Geophysical Research-Atmospheres* **111**, doi: 10.1029/2005JD006290.
- Alexandersson H (1986). A homogeneity test applied to precipitation data. *Journal of Climatology* **6**:661–675.
- Alexandersson H, Moberg A (1997). Homogenization of Swedish temperature data. Part I: Homogeneity test for lineal trends. *International Journal of Climatology* **17**: 25–34.
- Allan RP, Soden BJ (2008). Atmospheric warming and the amplification of precipitation extremes. *Science* **321**, 1481–1494.
- Allan RP, Zveryaev II (2011). Variability in the summer season hydrological cycle over the Atlantic-Europe region 1979–2007. *International Journal of Climatology* **31**, 337–348.

- Alley RB, Marotzki J, Nordhaus WD, Overpeck JT, Peteet DM, Pielke RA, Pierrehumbert RT, Rhines PB, Stocker TF, Talley LD, Wallace JM (2003). Abrupt climate change. *Science* **299**, 2005– 2010.
- Alpert P, Ben-Gai T, Baharad A, Benjamini Y, Yekutieli D, Colacino M, Diodato L, Ramis C, Homar V, Romero R, Michaelides S and, Manes A (2002). The paradoxical increase of Mediterranean extreme daily rainfall in spite of decrease in total values. *Journal of Geophysical Research Letters* **29**, 311–314.
- Alpert P, Ben-Gai T, Baharad A, Benjamini Y, Yekutieli D, Colacino M, Diodato L, Ramis C, Homar V, Romero R, Michaelides S, Mases A (2002). The paradoxical increase of Mediterranean extreme daily rainfall in spite of decrease. *Journal of Geophysical Research Letters* **29** (10) doi: 10.1029/2001GL013554,
- Alpert P, Neeman BU, and Shay-El Y (1990). Climatological analysis of Mediterranean cyclones using ECMWF data. *Tellus Series A: Journal of Dynamic Meteorology and Oceanography* **42**, 65–77.
- ALREM report (2011). Link between desertification and climate change in the Mediterranean. European Union. doi: 10.2863/63777.
- Altin TB, Barak B, Altin BN (2012). Change in Precipitation and Temperature Amounts over Three Decades in Central Anatolia, Turkey. *Atmospheric and Climate Sciences* **2**, 107-125.
- Amanatidis GT, Paliatsos AG, Repapis CC, Bartzis JG (1993). Decreasing precipitation trend in the Marathon area, Greece. *International Journal of Climatology* **13**: 191–201
- American Meteorological Society (1997). Meteorological drought—Policy *Bulletin of the American Meteorological Society* **78**, 847–849.
- American Meteorological Society (2004). Statement on meteorological drought. In: *Bulletin of the American Meteorological Society* **85**, 771-773.

- Apaydin H, Erpul G, Bayramin I, and Gabriels D (2006). Evaluation of indices for characterizing the distribution and concentration of precipitation: A case for the region of South-eastern Anatolia Project, Turkey. *Journal of Hydrology*, **328**, 726–732.
- Arkadan A (2008). Climate changes in Lebanon, predicting uncertain precipitation events. Do climates cycles sexist? Climate Change and Water Resources in the Middle East, Springer, Pub, 2008, p. 552.
- Arnell NW (2004). Climate change and global water resources: SRES emissions and socio economic scenarios. *Global Environmental Chang* **14**, 31–52.
- Ashbel D (1938). Great floods in Sinai Peninsula, Palestine, Syria and the Syrian 10 desert, and the influence of the Red sea on their formation. *Quarterly Journal of the Royal Meteorological Society* **64**: 635-639.
- Australian Bureau of Metrology (2010). *Rainfall variability in Australia*. <http://www.bom.gov.au/climate/data/index.shtml>.
- Bacanli U G, Dikbas F and, Baran T (2011). Meteorological drought analysis case study: Central Anatolia. *Journal of Desalination and Water Treatment* **26(1–3)**, 14–23.
- Barbero R, MoronV (2011). Seasonal to decadal modulation of the impact of El Niño–Southern Oscillation on New Caledonia (SW Pacific) rainfall (1950–2010). *Journal of Geophysical Research* **116**, doi: 10.1029/2011JD016577
- Barnston A G, and Livezey R E (1987). Classification, seasonality, and persistence of low-frequency atmospheric circulation patterns. *Monthly Weather Review* **115**, 1083–1126.
- Barry R G, and Chorley R. (2003). Atmosphere, weather and climate. Eighth edition. Routledge: London.421pp.
- Barth H-J and, Steinkohl F (2004). Origin of winter precipitation in the central coastal lowlands of Saudi Arabia. *Journal of Arid Environment* **57**,101–115.

- Barua S, Ng AWM, and Perera B J C (2011). Comparative evaluation of drought indexes: case study on the Yarra River catchment in Australia. *Journal of Water Resources Planning and Management* **37**, 215-226.
- Behzadi J (2013). An Evaluation of Two Drought Indices, Standard Distribution and Deciles in Guilan, Iran. *Greener Journal of Social Sciences* 3(9), 472-478.
- Beirlant, J, Goegebeur Y, Segers J, and Teugels J (2004). *Statistics of Extremes*, Wiley, Chichester, England.
- Bello NJ (1998). Evidence of climate change based on rainfall records in Nigeria. *Journal of Weather* **53**, 412–418.
- Ben-Gai T, Bitan A, Manes A, Alpert P (1993). Long term change in October rainfall patterns in southern Israel. *Theoretical and Applied Climatology* **46**, 209–217.
- Ben-Gai T, Bitan A, Manes A, Alpert P, Rubin S (1998). Spatial and Temporal Changes in Rainfall Frequency Distribution Patterns in Israel. *Theoretical and Applied Climatology* **61**, 177–190.
- Benhamrouch A, Boucher D, Hamadache R, Martin-Vide J, Nery JT (2015). Spatial distribution of the daily precipitation concentration index in Algeria. *Journal of Natural Hazard and Earth System Sciences* **15**, 617-625.
- Benhamrouche A, Boucherf D, , Hamadache R, Bendahmane L, Martín-Vide, Teixeira Nery J (2015). Spatial distribution of the daily precipitation concentration index in Algeria. *Natural Hazards and Earth System Sciences* **15**, 617-625.
- Benhamrouche AY; Martin-Vide J (2011). Distribución Espacial de la Concentración Diaria de la Precipitación en la Provincia de Alicante. *Investigaciones Geográficas* **56**, 113-129.

- Benhamrouche AY; Martin-Vide J (2012). Avances metodológicos en el análisis de la concentración diaria de la precipitación en la España peninsular. *Anales de Geografía* **32(1)**, 11-27.
- Beniston M (2003). Climatic change in mountain regions: a review of possible impacts. *Journal of Climatic Change* **59**, 5–31.
- Beniston M, Stephenson DB, Christensen OB, Ferro CAT, Frei C, Goyette S, Halsnaes K, Holt T, Jylha K, Koffi B, Palutikof J, Scholl R, Semmler T, Woth K (2007). Future extreme events in European climate: an exploration of regional climate model projections. *Journal of Climate Change* **81**:71–95
- Beranova R, Huth R (2007). Time variations of the relationships between the North Atlantic Oscillation and European winter temperature and precipitation. *Journal of Studia Geophysica et Geodaetica* **51**, 575–590.
- Berger WH, Labeyrie LD (1985). Abrupt Climatic Change e Evidence and Implications. St. Hugues de Biviers, France, p. 8.
- Birsan MV, Molnar P, Burlamdo P and, Pfaundler M (2005). Streamflow trends in Switzerland. *Journal of Hydrology* **314**, 312–329.
- Bitan A, Saaroni H (1992). The horizontal and vertical extension of the Persian Gulf trough. *International Journal of Climatology* **12**, 733–747.
- Black E (2012). The influence of the North Atlantic Oscillation and European circulation regimes on the daily to interannual variability of winter precipitation in Israel. *International Journal of Climatology*, 32(11) 1654-1664.
- Black E, Brayshaw DJ and, Rambeau CMC (2010). Past, present and future precipitation in the Middle East: insights from models and observations. *Journal of Philosophical Transactions of the Royal Society* **368**, 5173–5184.
- Blain G C (2011). Modelling Extreme Minimum Air Temperature Series under Climate Change Conditions. *Ciência Rural*, **41**, 1877-1883.

- Blain GC (2011). Standardized precipitation index based on pearson type III distribution. *Brasileira de Meteorologia* **26(2)**, 167-180.
- Blunden J, Arndt D, Baringer M (2011). State of the Climate in 2010. *Bulletin of the American Meteorological Society* **92 (6)**, 27-76.
- Bonaccorso B, Bordi I, Cancelliere A, Rossi G, and Sutera A (2003). Spatial variability of drought: An analysis of the SPI in Sicily. *Journal of Water Resource Management* **17**, 273–296.
- Bordi I, Fraedrich K, Jiang J.M, and Sutera A (2004). Spatio-temporal variability of dry and wet periods in eastern China. *Journal of Theoretical and Applied Climatology* **79 (1–2)**, 81–91.
- Bordi I, Frigio S, Parenti P, Speranza A, and Sutera A (2001). The analysis of the Standardized Precipitation Index in the Mediterranean area: large-scale patterns. *Journal of Annali di Geofisica* **44 (5–6)**, 965–978.
- Brandt J, Thornes J.B (1996). Mediterranean Desertification and Land Use. Wiley, Chichester: pp. 554
- Camarasa-Belmonte M Bescós-Atín A, Sancho-Comíns J (1998). Evaluación del riesgo de erosión en relación con la dinámica ocupacional del suelo a partir de sistemas de información geográfica. In Gómez-Ortiz A and SalvadorFranch F (eds.) *Investigaciones Recientes de la Geomorfología Española*, Barcelona: pp. 579-592.
- Briffa KR, Jones PD, Hulme M (1994). Summer moisture variability across Europe, 1892–1991: an analysis based on the Palmer drought severity index. *International Journal of Climatology* **14**, 475–506.
- Briggs W (2008). On the Changes in the Number and Intensity of North Atlantic Tropical Cyclones. *Journal of Climate* **13**, 1387–1402.
- Broccoli A, and Manabe S (1992). The effects of orography on mid-latitude northern hemisphere climates. *Journal of Atmospheric Science* **5**, 1181– 1201.

- Brooks, C. and Carruthers, N (1953). Handbooks of statistical methods in meteorology, Meteorological Office, London, 412 pp, Great Britain Meteorological Office, Publication official 538.
- Brown B G, and Katz RW (1995). Regional analysis of temperature extremes: Spatial analog for climate change. *Journal of Climate* **8**,108–119.
- Brugnara Y, Brunetti M, Maugeri M, Nanni T, and Simolo C (2012). High-resolution analysis of daily precipitation trends in the central Alps over the last century. *International Journal of Climatology* **32**, 1406–1422.
- Brunet M, and F.G Kuglitsch (2008). Proceedings of the International Workshop on Rescue and Digitization of Climate records in the Mediterranean Basin. WCDMP, **67**, WMO-TD No.1432, XXII, 219pp.
- Brunetti M, Buffoni L, Mangianti F, Maugeri M, Nanni T (2004). Temperature, precipitation and extreme events during the last century in Italy. *Global and Planetary Change* **40**, 141–149.
- Brunetti M, Buffoni L, Maugeri M and, Nanni T (2000). Trends of minimum and maximum daily temperatures in Italy from 1865 to 1996. *Journal of Theoretical and Applied Climatology* **66**: 49–60.
- Brunetti M, Caloiero T, Coscarelli R, Gulla G, Nanni T, and Simolo C (2012). Precipitation variability and change in the Calabria region (Italy) from a high resolution daily dataset. *International Journal of Climatology* **32**, 57–73.
- Brunetti M, Maugeri M, Monti F, Nanni T (2006) Temperature and precipitation variability in Italy in the last two centuries from homogenised instrumental time series. *International Journal of Climatology* **26**, 345–381.
- Brunetti M, Maugeri M, Nanni T (2002). Atmospheric circulation and precipitation in Italy for the last 50 years. *International Journal of Climatology* **22**, 1455–1471.

- Budikova, D (2008). Effect of the Arctic Oscillation on precipitation in the Eastern USA during ENSO winters. *Journal of Climate Research* **37** (1), 3–16.
- Burgueño J (1993). La irregularitat de les precipitacions a Espanya. Aplicacions de l'index de disparitat consecutiva, Aportacions en homenatge al professor Luis Miguel Albentosa. Diputació de Tarragona, pp. 41-55.
- Buric D, Lukovic J, Bajat B, Kilibarda M, Ducic V (2015). Recent trends in daily rainfall extremes over Montenegro (1951–2010). *Journal of Natural Hazards and Earth System Science* **3**, 2347–2377.
- Burke EJ, Brown SJ (2010). Regional drought over the UK and changes in the future. *Journal of Hydrology* **394** (3–4):471–485.
- Burke EJ, Brown SJ, Christidis N (2006). Modelling the recent evolution of global drought and projections for the twenty-first century with the Hadley Centre climate model. *Journal of Hydrometeorology* **7** (5), 1113-125
- Buytaert W, Celleri R, Willems P (2006). Spatial and temporal rainfall variability in mountainous areas: a case study from the south Ecuadorian. Andes. *Journal of Hydrology* **329**, 413–421.
- Byun HR, Lee DK (2002). Defining three rainy seasons and the hydrological summer monsoon in Korea using available water resources index. *Journal of Meteorological Society in Japan* **80**, 33-44.
- Byun HR, Wilhite DA (1999). Objective quantification of drought severity and duration. *Journal of Climate* **12**, 2747–2756.
- Cannarozzo M, Noto LV, Viola F (2006). Spatial distribution of rainfall trends in Sicily (1921-2000). *Journal of Physics and Chemistry of the Earth* **31**, 1201-1211.
- Cattell RB (1966). The scree test for the number of factors. *Journal of Multivariate Behavioral Research* **1**, 245-276.

- Chapman, T.G (1986). Entropy as a measure of hydrologic data uncertainty and model performance. *Journal of Hydrology* **85**, 111–126.
- Chenoweth J, Hadjinicolaou P, Bruggeman A, Lelieveld J, Levin Z, Lange MA, Xoplaki E, Hadjikakou M (2011). The impact of climate change on the water resources of the eastern Mediterranean and Middle East region: modelled changes and socio-economic implications. *Journal of Water Resource Research*. **47**, W06506. doi: 10.1029/ 2010WR010269.
- Conrad V and Pollak, L.W (1950). *Methods in Climatology*. Harvard University Press, Cambridge.
- Klein Tank A.M.G (2002). Daily dataset of 20th century surface air temperature and precipitation series for European Climate Assessment (ECA). *International Journal of Climatology* **22**: 1441-1453.
- Corte-Real J, Zhang X, Wang X (1995). Large-scale circulation regimes and surface climatic anomalies over the Mediterranean. *International Journal of Climatology* **15**, 1135–1150.
- Cortesi N, Gonzalez-Hidalgo JC, Brunetti M, and Martin-Vide J (2012). Daily precipitation concentration across Europe 1971–2010. *Journal of Natural Hazards and Earth System Sciences* **12**, 2799-2810.
- Coscarelli R, Caloiero T (2012). Analysis of daily and monthly rainfall concentration in Southern Italy (Calabria region). *Journal of Hydrology* **416–417**, 145–156.
- Costa AC, and Soares A (2009). Trends in extreme precipitation indices derived from a daily rainfall database for the South of Portugal, *International Journal of Climatology* **29**, 1956-1975.
- Coughlan M J (1987). Monitoring drought in Australia. In *Planning for Drought: Toward a Reduction of Societal Vulnerability*, Wilhite DA, Easterling WE (eds). West View, Boulder, CO, PP 131–144.

- CRDE (2003). The Centre for Research on the Epidemiology of Disasters. Disasters Database. <http://www.cred.be/emdat/intro.htm>. Universite Catholique de Louvain – Brussels – Belgium.
- Cullen H, de Menocal PB (2000). North Atlantic influence on Tigris-Euphrates streamflow. *International Journal of Climatology* **20**, 853–863.
- Cullen HM, de Menocal PB (2000). North Atlantic influence on Tigris–Euphrates streamflow. *International Journal of Climatology* **20**, 853–863.
- Dai A (2011) Drought under global warming: a review. Wiley Interdisciplinary Reviews. *Journal of Climate Change* **2**, 45-65.
- Dai A, Fung I Y, and. Del Genio A D (1997). Surface observed global land Precipitation variations during 1900 – 1988, *Journal of Climate* **10**, 2943–2962.
- De Jong C; Lawler D, Essery R (2009). Mountain hydroclimatology and snow seasonality and hydrological change in mountain environments. *Journal of Hydrological Processes* **23**, 955–961.
- De Lima, MIP, Santo FE, Ramos AM, Trigo RM (2014). Trends and correlations in annual extreme precipitation indices for mainland Portugal, 1941–2007. *Journal of Theoretical and Applied Climatology* **119**(1-2), 55-75.
- De Luis M, Raventos J, Gonzalez-Hidalgo JC, Sanchez JR, Cortina J (2000). Spatial analysis of rainfall trends in the region of Valencia (East Spain). *International Journal of Climatology* **20**, 1451-1469.
- Delitala AMS, Cesari D, Chessa PA, and Ward MN (2000). Precipitation over Sardinia (Italy) during the 1946–1993 rainy seasons and associated large-scale climate variation. *International Journal of Climatology* **20**, 519–541.
- Delsole T, Tippet MK (2007). Predictability recent insights from information theory, *Reviews of Geophysics.*, **45**(4), RG4002, doi: 10.1029/2006RG000202,

- De-Luis M, González-Hidalgo JC, Brunetti M, Longares LA (2011). Precipitation concentration changes in Spain 1946-2005. *Journal of Natural Hazards and Earth Systems Sciences*, **11**, 1259-1265.
- De-Luis M, González-Hidalgo JC, Raventós J, Sánchez JR, Cortina J (1997). Distribución espacial de la concentración y agresividad de la lluvia en el territorio de la Comunidad Valenciana. *Cuaternario y Geomorfología* **11**, 33–44.
- De-Luis M, Raventós J, González-Hidalgo JC, Sánchez JR, Cortina J (2000). Spatial analysis of rainfall trends in the region of Valencia (East Spain). *International Journal of Climatology* **20**, 1451–1469.
- Denton G, Alley R, Comer GC, Broecker WS (2005). The role of seasonality in abrupt climate change. *Quaternary Science Reviews* **24**, 1159–1182.
- Diffenbaugh NS, Giorgi F (2012). Climate change hotspots in the CMIP5 global climate model ensemble. *Journal of Climate Chang* **114**, 813–822.
- Dogan S, Berktaş A, and Singh VP (2012). Comparison of multi monthly rainfall-based drought severity indices, with application to semi-arid Konya closed basin, Turkey. *Journal of Hydrology* **470–471**, 255–268.
- Dogdu MS, Sagnak C (2008). Climate change, drought and over pumping impacts on groundwaters: Two examples from Turkey. Paper submitted to the Third International BALWOIS Conference on the Balkan Water Observation and Information System, Ohrid, the Former Yugoslav Republic of Macedonia. May 2008.
- Donat M G, Durre I, Yang H, Alexander L V, Vose R and , Caesar J (2012). Global land-based datasets for monitoring climatic extremes, *Bulletin of the American Meteorological Society* **94**, 997-1006.
- Dormoy I, Peyron O, Combourieu-Nebout N, Goring S, Kotthoff U, Magny M, Pross G (2009). Terrestrial climate variability and seasonality changes in the

- Mediterranean region between 15000 and 4000 years deduced from marine pollen records. *Climate of the Past* **5**, 615–632.
- Dracup JA, Lee KS, Paulson EG (1980). On the definition of droughts, *Journal of Water Resources Research* **16** (2), 297-302.
- Dubrovsky M, Hayes M, Duce P, Trnka M, Svoboda M, Zara P (2014). Multi-GCM projections of future drought and climate variability indicators for the Mediterranean region. *Regional Environmental Change* **14**, 1907-1919.
- Duffourg F, Ducrocq V (2011). Origin of the moisture feeding the heavy precipitation systems over Southeastern France. *Journal of Natural Hazards and Earth System Sciences* **4**, 1163-1178.
- Dunkeloh A and Jakobeit J (2003). Circulation dynamics of Mediterranean precipitation variability 1948-98. *International Journal of Climatology* **23**, 1843–1866
- Durdu, OF (2010). Application of linear stochastic models for drought forecasting in the Buyuk Menderes river basin, western Turkey. *Journal of Stochastic Environmental Risk Assessment* **24**, 1145–1162.
- Easterling DR, Evans JL, Groisman PY, Karl TR, Kunkel KE and, Ambenje P (2000). Observed variability and trends in extreme climate events: a brief review. *Bulletin of the American Meteorological Society* **81**, 417–425.
- Easterling DR, Meehl GA, Parmesan C, Changnon SA, Karl TR, Mearns LO (2000). Climate extremes: observations, modeling, and impacts. *Science* **289**, 2068–2074.
- Ebrahimi N, Maasoumi E, Soofi ES (1999). Ordering Univariate Distributions by Entropy and Variance. *Journal of Econometrics* **90**, 317-336.
- ECSN (1995). Climate of Europe: Recent Variation, Present State and Future Prospects, National Meteorological Services First European Climate

Assessment, European Climate Support Network (ECSN), Nijkerk, the Netherlands, 72 pp.

Edossa D C, Babel M S, Gupta AD (2010). Drought analysis in the Awash River Basin, Ethiopia. *Journal of Water Resource Management* **24**, 1441–1460.

Ellis J (1995). Climate Variability and Complex Ecosystem Dynamics: Implications for Pastoral Development. 37-46 in Scoones 1. (ed.): *Living with Uncertainty: New Directions in Pastoral Development in Africa*. Exeter, Intermediate Technology Publications, London, UK.

Evans J P (2008). 21st century climate change in the Middle East. *Journal of Climatic Change* **92**, 417–432.

Evans J P (2010). Global warming impact on the dominant precipitation processes in the Middle East. *Journal of Theoretical and Applied Climatology* **99**, 389–402.

Evans J P, Smith R B and, Oglesby R J (2004). Middle East climate simulation and dominant precipitation processes. *International Journal of Climatology* **24**, 1671–1694.

Evans JP (2009). 21st century climate change in the Middle East. *Journal of Climate Chang* **92**, 417–432.

Ezemonye M. N, and Emeribe C.N (2011). Correlogram analysis of trends and cycles in rainfall over south-eastern Nigeria. *Pakistan Journal of Social Science* **8(6)**, 325-333.

Fay PA, Carlisle JD, Knapp AK, Blair JM and, Collins SL (2000). Altering rainfall timing and quantity in a mesic grassland ecosystem: design and performance of rainfall manipulation shelters. *Ecosystems* **3**,308–319.

- Fay PA, Carlisle JD, Knapp AK, Blair JM, Collins SL (2003). Productivity responses to altered rainfall patterns in a C4-dominated grassland. *Oecologia* **137**, 245–251.
- Feidas H, Nouloupoulou C h, Makrogiannis T and, Bora-Senta E (2007). Trend analysis of precipitation time series in Greece and their relationship with circulation using surface and satellite data: 1955–2001. *Journal of Theoretical and Applied Climatology* **87**, 155–177.
- Femia F, Werrell C (2012). Syria: Climate Change, Drought and Social Unrest. *Centre for Climate Security*, February 29.
- Femia F, Werrell C (2012). Syria: Climate Change, Drought and Social Unrest. The Centre for Climate and Security. (Accessed September 15, 2012).
- Feng LH and Zhang HC, 2005. Quantitative expression on drought magnitude and disaster intensity. *Journal of Natural Hazards and Earth System Sciences* **5**: 495–498.
- Edwards D C and McKee TB (1997). Characteristics of 20th Century Drought in the United States at Multiple Time Scales. *Atmospheric Science Paper* **634**: 1–30.
- Fernández J, Sáenz J, Zorita E. (2003). Analysis of wintertime atmospheric moisture transport and its variability over southern Europe in the NCEP-Reanalyses. *Journal of Climate Research* **23**, 195–215.
- Flocas HA, Hatzaki M, Asimakopoulos DN, Giannakopoulos C. (2008). Future changes in the occurrence of extreme precipitation. *Global Nest Journal* **10 (2)**, 255–262.
- Flocas HA, Simmonds I, Kouroutzoglou J, Keay K, Hatzaki M, Bricolas V, Asimakopoulos D. (2010) On cyclonic tracks over the Eastern Mediterranean. *Journal of Climate* **23**, 5243–5257.

- Fotopoulos S, Jandhyala V, Khapalova E (2010). Exact Asymptotic Distribution of the Change-point MLE for Change in the Mean of Gaussian Sequences. *Annals of Applied Statistics* **4**, 1081–1104.
- Fowler HJ, Ekstrom, M, Kilsby CG, and Jones PD (2005). New Estimates of future changes in extreme rainfall across the UK using regional climate model integrations. 1. Assessment of control climate. *Journal of Hydrology* **300**, 212–233.
- Frich P, Alexander L V, Della-Marta, P, Gleason B, Haylock M, Tank AMGK, Res C (2002). Observed coherent changes in climatic extremes during the second half of the twentieth century. *Journal of Climate Research* **19(3)**, 193–212.
- Friederichs P, Göber M, Bentzien S, Lenz A, and Krampitz R (2009). A Probabilistic Analysis of Wind Gusts Using Extreme Value Statistics. *Journal of Meteorologische Zeitschrift* **18 (6)**, 615-629.
- Friedman, D G (1957). The prediction of long-continuing drought in south and southwest Texas. Occasional Papers in Meteorology, No. 1, The Travelers Weather Research Center, Hartford, CT, 182 pp.
- García-Barrón L, Morales J, Sousa A (2013). Characterisation of the intraannual rainfall and its evolution (1837–2010) in the southwest of the Iberian Peninsula. *Journal of Theoretical Applied Climatology*. Doi: 10.1007/s00704-013-0855-7.
- Giannakopoulos C, Hadjinicolaou P, Kostopoulou E, Varotsos KV, Zerefos C (2010). Precipitation and temperature regime over Cyprus as a result of global climate change. *Journal of Advanced Geoscience* **23**, 17-24
- Gibbs W J and Maher J V (1967). Rainfall deciles as drought indicators. *Australian Bureau of Meteorology Bulletin* **48** (37 pp.)
- Giorgi F (2002). Variability and trends of sub-continental scale surface climate in the twentieth century. Part I: observations. *Journal of Climate Dynamics* **18**:675–691.

- Giorgi F and, Lionello P (2008). Climate change projections for the Mediterranean region. *Global Planet Change* **63**, 90–104.
- Gocic M, Trajkovic S (2013). Analysis of changes in meteorological variables using Mann-Kendall and Sen's slope estimator statistical tests in Serbia. *Journal of Global and Planetary Change* **100**, 172–182.
- Golodets C, Sternberg M, Kigel J, Boeken B, Henkin Z, Seligman NG, Ungar DE (2013). From desert to Mediterranean rangelands: will increasing drought and inter-annual rainfall variability affect herbaceous annual primary productivity? *Journal of Climatic Change* **119**, 785-798.
- González-Hidalgo JC, Brunetti M, De-Luis M (2011). A new tool for monthly precipitation analysis in Spain: MOPREDAS database (Monthly precipitation trends December 1945–November 2005). *International Journal of Climatology* **31**, 715–731.
- Goodess CM, Jones PD (2002). Links between circulation and changes in the characteristics of Iberian rainfall. *International Journal of Climatology* **22**, 1593-1615.
- Green TR, Bates BC, Charles SP, Fleming PM (2007). Physically based simulation of potential effects of carbon dioxide-altered climates on groundwater recharge. *Journal of Vadose Zone* **6(3)**, 597-609.
- Grimm AM, and Tedeschi R G (2009). ENSO and Extreme Rainfall Events in South America. *Journal of Climate* **22 (7)**, 1589-1609.
- Guan K, Good SP, Sato H, Wood EF, Li H (2014). Continental-scale impacts of intra-seasonal rainfall variability on simulated ecosystem responses in Africa. *Journal of Biogeosciences* **11**, 6939–6954.
- Guhathakurta P, Saji E (2013). Detecting changes in rainfall pattern and seasonality index vis-a-vis increasing water scarcity in Maharashtra. *Journal of Earth System Science* **122(3)**, 639-649.

- Gumble E J (1958). Statistics of extremes. Colombia University press, Newyork.
- Guttman, N. B (1999). Accepting the standardized precipitation index: a calculation algorithm. *Journal of the American Water Resources Association* **35**, 311–322.
- Han H, Gong DY (2003). Extreme climate events over northern China during the last 50 years. *Journal of Geographical Sciences* **13** (4), 469-479.
- Hare FK (1983). Climate and Desertification. Revised analysis (WMO-UNDP) WCP-44 pp 5-20. Geneva, Switzerland.
- Hatzaki M, Flocas HA, Asimakopoulos D N, Maheras P (2007).The Eastern Mediterranean teleconnection pattern: Identification and definition, *International Journal of Climatology* **27**, 727–737.
- Hatzianastassiou, N, Katsoulis, B, Pnevmatikos, J (2008). Spatial and Temporal Variation of Precipitation in Greece and Surrounding Regions Based on Global Precipitation Climatology Project Data. *Journal of Climate*, **21**, 1349-1370.
- Hausser J and Strimmer K, (2009). Entropy inference and the James-Stein estimator, with application to nonlinear gene association networks.” *Journal of Machine Learning Research* **10**, 1469-1484.
- Hayes MJ, Svoboda MD, Wall N, Widhalm M (2011). The Lincoln declaration on drought indices: universal meteorological drought index recommended. *Bulletin of the American Meteorological Society* **92** (4), 485–488.
- Hayes MJ, Svoboda MD, Wilhite A, Vanyarkho OV. (1999). Monitoring the 1996 drought using the standardized precipitation index. *Bulletin of the American Meteorological Society* **80**, 429–438.
- Haylock MR, Peterson TC, Alves LM, Ambrizzi T, Anunciacao YMT, Baez J, Barros VR, Berlato MA, Bidegain M, Coronel G, Corradi V, Garacia VJ, Grimm A M, Karoly D, Marengo J A, Marino M B, Moncunill DF, Nechet D, Quintan J, Rebello E, Rusticucci M, Santos J L, Trebejo I, Vincent LA (2005). Trends in

- Total and Extreme South American Rainfall in 1960–2000 and Links with Sea Surface Temperature. *Journal of Climate* **19**, 1490–1512.
- Heim R R (2002). A review of twentieth-century drought indices used in the United States. *Bulletin of the American Meteorological Society* **83**, 1149–1165, 2002.
- Heisler-White JL, Knapp AK, Kelly EF (2008). Increasing precipitation event size increases aboveground net primary production in a semi-arid grassland. *Oecologia* **158**, 129–140.
- Henderson KG and, Muller RA (1997). Extreme temperature days in the south-central United States. *Journal of Climate Research* **8**, 151–162.
- Hertig E, Paxian A, Vogt G, Seubert S, Paeth H, Jacobeit J (2012). Statistical and dynamical downscaling assessments of precipitation extremes in the Mediterranean area. *Meteorologische Zeitschrift* **21**, 61–77.
- Hertig E, Seubert S, Paxina A, Vogt G, Paeth H, Jacobeit J (2013). Changes of total versus extreme precipitation and dry periods until the end of the twenty-first century: statistical assessments for the Mediterranean area. *Journal of Theoretical and Applied Climatology* **111**, 1–20.
- Hirsch RM, Alexander RB and, Smith RA (1991). Selection of methods for the detection and estimation of trends in water quality. *Journal of Water Resource Research* **27**, 803–813.
- Hirsch RM, Slack JR (1984). Non-parametric trend test for seasonal data with serial dependence. *Journal of Water Resources Research* **20**(6), 727–732.
- Hisdal H, Tallaksen LM, Clausen B, Peters E, Gustard A (2004). Hydrological Drought Characteristics. 139 – 198 of: Tallaksen, LM, Lanen HAJ. (eds), *Hydrological Drought: Processes and estimation methods for streamflow and groundwater*. Development in Water Science **48**. Elsevier.

- Hoerling M, Eischeid J, Perlwitz J, Quan X, Zhang T, and Pegion P (2012). On the Increased Frequency of Mediterranean Drought. *Journal of Climate* **25**, 2146-2161.
- Holt T, Palutikof J (2004). *Precipitation extremes over the Mediterranean*. Climatic Research Unit, University of East Anglia, Norwich, UK.
- Hotelling H (1933). The most predictable criterion. *Journal of Educational Psychology* **26**, 139-142.
- Houze Jr RA (2012). Orographic Effects on precipitations Clouds. *Reviews of Geophysics* 50 ID: GR1001. doi: 10.1029/2011RG000365.
- Huang J, Sun S, Xue Y, Lin J, Zhang J (2014). Spatial and Temporal Variability of Precipitation and Dryness/Wetness during 1961–2008 in Sichuan Province, West China. *Journal of Water Resource Manage* **28**, 1655-1670.
- Hulme M, Barrow EM, Arnell NW, Harrison PA, Johns TC, Downing TE (1999). Relative impacts of human-induced climate change and natural climate variability. *Nature* **397**, 688– 691.
- Hurrell JW (1995). Decadal trends in the North Atlantic oscillation: regional temperature and precipitation. *Science* **269**, 676–679.
- Hurrell JW, Kushnir Y, Visbeck M (2001). The North Atlantic Oscillation. *Science* **291**, 603–605.
- Husak GJ, Joel M, Chris F (2007) Use of the gamma distribution to represent monthly rainfall in Africa for drought monitoring applications. *International Journal of Climatology* **27 (7)**, 935-944.
- Hutchinson P (1990). Frequency distribution of daily, monthly, seasonal and annual rainfalls in Somalia, and their use in the generation of rainfall distributions in data deficient areas. WMO Tropical Meteorology Research Program Report, Geneva, Switzerland **36**, 239-245.

- Huxman TE, Cable JM, Ignace DD, Eits JA, English NB, Weltzin J, Williams DG (2004). Response of net ecosystem gas exchange to a simulated precipitation pulse in a semiarid grassland: the role of native versus non-native grasses and soil texture. *Oecologia* **141**,295–305.
- International Food Policy Research Institute (IFPRI) (2009). Climate Change: Impact on Agriculture and Costs of Adaptation. Food Policy Report, Washington DC, September.
- IPCC (2001). The Scientific Basis. In: Contribution of Working Group I to the Third Assessment Report of the Intergovernmental Panel on Climate Change (Houghton JT, Ding Y, Griggs DJ, Noguer M, van der Linden PJ, Dai X, Maskell K, Johnson CA, eds). Cambridge and New York: Cambridge University Press, 881 pp.
- IPCC (2007). Technical summary. In: Solomon S, Qin D, Manning M, Chen Z, Marquis M, Averyt KB, Tignor M, Miller HL (eds) Climate Change: 2007, the physical science basis. Contribution of Working Group I to the 4th Assessment Report of the Intergovernmental Panel on Climate Change. Cambridge University Press, Cambridge. pp 91.
- IPCC (2012). Managing the Risks of Extreme Events and Disasters to Advance Climate Change Adaptation. A Special Report of Working Groups I and II of the Intergovernmental Panel on Climate Change. Field C B, Barros V, Stocker TF, Qin D, Dokken D J, Ebi K L, Mastrandrea M D, Mach K J, Plattner GK, Allen S K, Tignor M, and Midgley P M (eds.). Cambridge University Press, Cambridge, UK, and New York, NY, USA, 582 pp.
- IPCC (2013). Summary for Policymakers, in Climate Change. The Physical Science Basis. Contribution of Working Group I to the Fifth Assessment Report of the Intergovernmental Panel on Climate Change edited by Stocker TF, Qin D, Plattner GK, M Tignor M, Allen S K, Boschung J, Nauels A, Xia Y, Bex V, Midgley PM. Cambridge University Press, Cambridge, United Kingdom and New York, NY, USA. Jacobeit, J, Dünkelloh A, Hertig, E. (2007): Mediterranean

- rainfall changes and their causes, in *Global change: Enough water for all?*, edited by Lozán J L, Graß H, Hupfer P, Menzel L, Schönwiese CD, Wissenschaftliche Auswertungen, Hamburg, Germany, 195–199.
- Jacobeit J, Dünkeloh A, Hertig E (2007). Mediterranean rainfall changes and their causes, in *Global change: Enough water for all?*, edited by Lozán J. L, H. Graß, P. Hupfer, L. Menzel, and C.-D. Schönwiese, Wissenschaftliche Auswertungen, Hamburg, Germany, 195–199.
- Jacobeit J, Jönsson P, Barring L, Beck C, Ekström M (2001). Zonal indices for Europe 1780–1995 and running correlations with temperature. *Climatic Change* **48**, 219–241.
- Jandhyala V, Liu P, Fotopoulos S (2009). River Stream Flows in the Northern Québec Labrador Region: A Multivariate Change Point Analysis via Maximum Likelihood. *Journal of Water Resources Research* **45**. W02408, doi: 10.1029, 2007WR006499.
- Jaruskova (1996). Change-point Detection in Meteorological Measurement. *Journal of Monthly Weather Review* **124**, 1535–1543.
- Jiang YA, Chin Y, Zhau YZ, Chen PX, Yu XJ, Fan J, Bai SQ (2013). Analysis on changes of basic climatic elements and extreme events in Xinjiang, China during 1961–2010. *Advances in Climate Change Research* **4** (1), 20-29.
- Jin F, Kitoh A, Alpert P (2010). Water cycle changes over the Mediterranean: a comparison study of a super-high resolution global model with CMIP3. *Philosophical Transactions of the Royal Society* **68**, 5137-5149.
- Jolliffe IT (1987). Rotation of principal components: Some comments. *Journal of Climatology* **7**, 507–510.
- Jones P D, Leadbetter A, Osborn T J and Bloomfield J P (2006). The impact of climate change on severe droughts. River-flow reconstructions and implied

- groundwater levels. Science Report SC040068/SR2. Bristol: Environment Agency.
- Juras J (1994). Some common features of probability distributions for precipitation. *Journal of Theoretical and Applied Climatology* **49**, 69-76.
- Kafle HK, Bruins HJ (2009). Climatic trends in Israel 1970–2002: warmer and increasing aridity inland. *Journal of Climate Chang* 96, 63–77.
- Kahya E (2011). The impacts of NAO on hydrology of the East Mediterranean, in Hydrological, Socioeconomic and Ecological Impacts of the North Atlantic Oscillation in the Mediterranean Region, *Advances in Global Change Research*,. **46**, eds S. M. Vicente-Serrano and R. M. Trigo (Zaragoza: Springer). doi: 10.1007/978-94-007-1372-7_5
- Kahya E, Kalayci S (2004). Trend analysis of streamflow in Turkey. *Journal of Hydrology* **289**, 128–144.
- Kalamaras N, Michalopoulou H, Byun HR (2010). Detection of drought events in Greece using daily precipitation. *Journal of Hydrological Research* **41** (2), 126–133.
- Kanellopoulou E. A (2002). Spatial distribution of rainfall seasonality in *Greece Weather* **57**, 215- 219.
- Karl TR, Easterling DR (1999). Climate extremes: Selected review and future research directions. *Journal of Climate Change* **42**, 309–325.
- Karl TR, Knight RW (1998). Secular trends of precipitation amount, frequency, and intensity in the USA. *Bulletin American Meteorological Society* **79**, 231-241.
- Karl TR, Koscielny AJ (1982). Drought in the United States: 1895-1981. *Journal of Climatology* **2**, 313-329.
- Karpouzios DK, Kavalieratou S, Babajimopoulos C (2010) Trend analysis of precipitation data in Pieria Region (Greece). *European Water* **30**, 31-40.

- Katz RW (1991). *Towards a statistical paradigm for climate change*. Preprints, 7th Conference on Applied Climatology, American Meteorological Society, Boston.
- Katz RW (2010). Statistics of extremes in climate change. *Journal of Climatic Change* **100**, 71-76.
- Katz RW, Brown BG (1992). Extreme events in a changing climate variability is more important than averages. *Journal of Climate Change* **21**, 289–302.
- Katz RW, Glantz MH (1986). Anatomy of a rainfall index. *Monthly Weather Review* **114**, 764–771.
- Katz RW, Parlange MB, and Naveau P (2002). Statistics of extremes in hydrology. *Advances in Water Resources* **25**, 1287–1304.
- Kawachi T, Maruyama T, Singh V.P (2001). Rainfall entropy for delineation of water resources zones in Japan. *Journal of Hydrology* **246**, 36–44.
- Kendall M G (1975). Rank Correlation Methods. Griffin, London, UK.
- Douglas EM, Vogel RM and, Kroll CN (2000). Trends in floods and low flows in the United States: impact of spatial correlation. *Journal of Hydrology* **240**, 90–105.
- Kendall MG, Stuart A (1977). The Advanced Theory of Statistics. Charles Griffin and Company: London, High Wycombe. 400–401.
- Keskin ME, Terzi O, Taylan ED and, Kucukyaman D (2009). Meteorological drought analysis using data-driven models for the Lakes District, Turkey. *Journal of Hydrological Science* **54 (6)**, 1114–1124.
- Keyantash J, Dracup JA (2002). The quantification of drought: An evaluation of drought indices. *Bulletin of the American Meteorological Society* **83**, 1167–1180.
- Kim DW, Byun HR, and Choi KS (2009). Evaluation, modification, and application of the Effective Drought Index to 200-Year drought climatology of Seoul-Korea. *Journal of Hydrology* **378**, 1–12.

- Kioutsoukios I, Melas D, and Zerefos C (2010). Statistical assessment of changes in climate extremes over Greece (1955–2002). *International Journal of Climatology* **30**, 1723-1737.
- Kitoh A, Yatagai A, Alpert P (2008). First super-high-resolution model projection that the ancient “Fertile Crescent” will disappear in this century. *Journal of Hydrological Research Letters* **2**, 1–4.
- Klein B, Roether W, Manca BB, Bregant D, Beitzel V, Kovacevic V, Lucchetta A (1999). The large deep water transient in the eastern Mediterranean. *Journal of Deep Sea Research* **46**, 371 – 414.
- Klein Tank AMG, Konnen GP (2003). Trends in indices of daily temperature and precipitation extremes in Europe. *Journal of Climate* **16** (22), 3665-3680.
- Klein Tank AMG, Wijngaard JB, van Engelen A (2002). *Climate of Europe, Assessment of observed daily temperature and precipitation extremes*. KNMI, De Bilt, Netherlands.
- Knapp AK, Fay PA, Blair JM, Blair JM, Collins SL, Smith MD, Carlisle JD, Harper CW, Danner BT, Lett MS, McCarron JK (2002). Rainfall variability, carbon cycling, and plant species diversity in a mesic grassland. *Science* **298**, 2202–2205.
- Komuscu AU (1999). Using the SPI to analyse spatial and temporal patterns of drought in Turkey. *Drought Network News* **11** (1), 7–13.
- Komuscu AU (2001). An Analysis of Recent Drought Conditions in Turkey in Relation to Circulation Patterns. *Drought Network News* **13**, 2-3.
- Köppen W, Geiger R (1936). Das geographische system der klimate. In: Köppen W, Geiger R (eds) *Handbuch der klimatologie*. Bd 1, Teil C. Verlag Gebrüder Bornträger, Berlin, 44 p.

- Kostopoulou E, Jones P (2005). Assessment of climate extremes in Eastern Mediterranean. *Journal of Meteorology and Atmospheric Physics* **89**, 69–85.
- Koutsoyiannis D (2005). Uncertainty, entropy, scaling and hydrological stochastics.1. Marginal distributional properties of hydrological processes and state scaling. *Journal of Hydrological Science* **50(3)**, 381–404.
- Kraus EB (1977). Subtropical droughts and cross-equatorial energy transports. *Monthly Weather Review* **105**, 1009–1018.
- Krichak SO, Alpert P (1998). Role of large-scale moist dynamics in the November 1-5, 1994 hazardous Mediterranean weather. *Journal of Geophysical Research: Atmospheres* **103 (D16)**, 19453–19468.
- Krichak SO, Alpert P (2005). Decadal trends in the East Atlantic-West Russia pattern and Mediterranean precipitation. *International Journal of Climatology* **25**, 183–192.
- Krichak SO, Alpert P, and Krishnamurti TN (1997a). Interaction of topography and 14 tropospheric flow - a possible generator for the Red sea trough. *Journal of Meteorology and 15 Atmospheric Physics* **63**, 149-158.
- Krichak SO, Alpert P, and Krishnamurti TN (1997b). Red Sea Trough/cyclone 18 development \pm numerical investigation. *Journal of Meteorology and Atmospheric Physics* **63**, 19 159-170.
- Krichak SO, Kishcha P, Alpert P (2002). Decadal trends of main Eurasian oscillations and the Eastern Mediterranean precipitation. *Journal of Theoretical and Applied Climatology* **72**, 209–220.
- Kucharski F, Polzin D, Hastenrath S (2008). Teleconnection Mechanisms of Northeast Brazil Droughts: Modelling and Empirical Evidence. *Revista Brasileira de Meteorologia* **23 (2)**, 115-125.

- Kumar MN; Muthly CS; Sai MVRS; Roy PS (2009). On the use of Standardized Precipitation Index (SPI) for drought intensity assessment. *Journal of Meteorological applications* **16**, 381-389.
- Kutiel H (1991). Recent spatial and temporal variations in mean sea level pressure over Europe and the Middle East, and their influence on the rainfall regime in the Galilee, Israel. *Journal of Theoretical and Applied* **44**, 151-166.
- Kutiel H, Maheras P, Guika S (1996). Circulation and extreme rainfall conditions in the eastern Mediterranean during the last century. *International Journal of Climatology* **16**, 73–92.
- Kutiel H, Maheras P, Guika S (1996). Circulation indices over the Mediterranean and Europe and their relationship with rainfall conditions across the Mediterranean. *Journal of Theoretical and Applied Climatology* **54**, 125–138.
- Kutiel H, Maheras P, Türkes M, Paz S (2002). North Sea-Caspian Pattern—an upper level atmospheric teleconnection affecting the Eastern Mediterranean – Implications on the regional climate. *Journal of Theoretical and Applied Climatology* **72**, 173–192.
- Kutiel, H (1985). The multimodality of the rainfall course in Israel as reflected by the distribution of dry spells. *Journal of Meteorology and Atmospheric Physics* **39**, 15–27.
- Lagi M, Bertrand KZ, Bar-Yam Y (2012). The Food Crises and Political Instability in North Africa and the Middle East. ARXIV: 1108.2455. (Accessed September 15, 2012).
- Lana X, Burgueño A, Martínez MD, Serra C (2009). A review of Statistica analyses on monthly and daily rainfall in Catalonia. *Journal of Weather and Climate of the Western Mediterranean* **6**, 15–29.
- Lana X, Burgueño A, Martínez MD, Serra C (2015). Complexity and predictability of the monthly Western Mediterranean Oscillation index *International Journal*

of *Climatology*, Article first published online: 22 SEP 2015. doi: 10.1002/joc.4503

- Lana X, Serra C, Burgueno A (2001). Patterns of monthly rainfall shortage and excess in terms of the standardized precipitation index for Catalonia (NE Spain). *International Journal of Climatology* **21**, 1669–1691.
- Lau K, Wu H (2007). Detecting Trends in Tropical Rainfall Characteristics, 1979–2003. *International Journal of Climatology* **27**, 979–988.
- Lavell A, Oppenheimer M, Diop C, Hess J, Lempert RLI, Muir-Wood R, Myeong S (2012). Climate change: new dimensions in disaster risk, exposure, vulnerability, and resilience. In: Managing the Risks of Extreme Events and Disasters to Advance Climate Change Adaptation [Field CB, Barros V, Stocker T F, Qin D, Dokken D J, Ebi K L, Mastrandrea M D, Mach K J, Plattner G K, Allen S K, Tignor M, and Midgley P M (Eds.)]. A Special Report of Working Groups I and II of the Intergovernmental Panel on Climate Change (IPCC). Cambridge University Press, Cambridge, UK, and New York, NY, USA, pp.25–64.
- Lawrimore JH, Halpert MS, Bell GD, Menne MJ, Lyon B, Schnell RC, Gleason KL, Easterling DR, Thiaw W, Wright WJ, Heim RR, Robinson DA, Alexander L (2001). Climate assessment for 2000. *Bulletin of the American Meteorological Society* **82**, 1–39.
- Le Houérou HN, Bingham RL, Skerbek W (1988). Relationship between the variability of primary production and the variability of annual precipitation in world arid lands. *Journal of Arid Environments* **15**, 1–18.
- Lelieveld J, Hadjinicolaou P, Kostopoulou E, Chenoweth J, El Maayar M, Giannakopoulos C, Hannides C, Lange M, Tanarhte M, Tyrlis E and , Xoplaki E (2012). Climate change and impacts in the eastern mediterranean and the Middle East. *Journal of Climatic Change* **114** (3), 667–687.

- Levin N, Saaroni H (1999). Fire weather in Israel—synoptic climatological analysis. *Geo Journal* **47**,523–538.
- Li X, Jiang F, Li L, Wang G (2011). Spatial and temporal variability of precipitation concentration index, concentration degree and concentration period in Xinjiang, China. *International Journal of Climatology* **31** (11), 1679–1693.
- Li Y, Cai W, Campbell E P (2005). Statistical Modeling of Extreme Rainfall in Southwest Western Australia. *Journal of Climate* **18**, 852-863.
- Linacre E, Hobbs J (1977). The Australian climatic environment. Wiley, Brisbane Australia
- Lionello P (2012). The climate of the Mediterranean region in future climate projections. In Mediterranean Climate: from past to future. Planton S, Lionello P, Artale V, Aznar R, Carillo A, Colin J, Congedi L, Dubois C, Elizalde A, Gualdi S, Hertig E, Jacobeit D, Jordà G, Li L, Mariotti A, Piani C, Ruti P, Sanchez-Gomez E, Sannino G: Sevault F, Somot S, Tsimplis M N. pp.
- Lionello P, Bhend J, Buzzi A, Della-Marta PM, Krichak S, Jansá A, Maheras P, Sanna A, Trigo IF, Trigo R (2006). Cyclones in the Mediterranean region: climatology and effects on the environment. In: Lionello P, Malanotte-Rizzoli P, Boscolo R (eds) Mediterranean Climate Variability, Developments in Earth and Environmental Sciences 4. Elsevier: New York, 324–372.
- Lionello P, Giorgi F (2007). Winter precipitation and cyclones in the Mediterranean region: future climate scenarios in a regional simulation. *Advances in Geoscience*. **12**, 153–8.
- Liu B, Chen X, Lian Y, Wu L (2013). Entropy-based assessment and zoning of rainfall distribution. *Journal of Hydrology* **490**, 32-40.
- Livada I, Asimakopoulos DN (2005). Individual seasonality index of rainfall regimes in Greece. *Journal of Climate Research* **28**,155-161.

- Lloyd-Hughes B, Saunders AM (2002). A drought climatology for Europe. *International journal of climatology* **22**, 1571 – 1592.
- Lloyd-Hughes, B and M. A. Saunder (2002). A drought climatology for Europe. *International Journal of Climatology* **22**, 1571–1592.
- Longobardi A, Villani P (2009). Trend analysis of annual and seasonal rainfall time series in the Mediterranean area. *International Journal of Climate Change* **30**, 1538- 1546.
- López-Bustins JA, Martin-Vide J, Sanchez-Lorenzo A (2008). Iberia winter rainfall trends based upon changes in teleconnection and circulation patterns. *Global and Planetary Change* **63**, 171–176.
- López-Bustins JA, Pascual D, Pla E, Retana J (2013). Future variability of droughts in three Mediterranean catchments. *Journal of Natural Hazards* **69(3)**, 1405-1421.
- López-Bustins JA, Serrano E, Ayarzagüena B, Sanchez-Lorenzo A (2015). Spatial and temporal temperature trends in the lower stratosphere during the extended boreal winter from reanalyses. *International Journal of Climatology*, doi:10.1002/joc.4253.
- López-Franca N, Sánchez E, Romera R, Domínguez, M (2013) Dry spells analysis over the Mediterranean basin for present and climate change conditions using ENSEMBLES regional climate models. *Física de Tierra* **25**, 123-136.
- López-Moreno JI, Vicente S, Gimeno L, Nieto R (2009). Stability of the seasonal distribution of precipitation in the Mediterranean region: observations since 1950 and projections for the 21st century. *Geophysics Research Letter* **36**:L10703.
- López-Moreno JI, Vicente-Serrano SM, Morán-Tejeda E, Lorenzo-Lacruz J, Kenawy A, Beniston M (2011). Effects of the North Atlantic Oscillation (NAO) on combined temperature and precipitation winter modes in the Mediterranean

- mountains: Observed relationships and projections for the 21th century. *Journal of Global and Planetary Change* **77**, 62–76.
- Lorenzo-Lacruz J, Vicente-Serrano SM, López-Moreno JI, Beguería S, García-Ruiz JM, Cuadrat JM (2010). The impact of droughts and water management on various hydrological systems in the headwaters of the Tagus River (central Spain). *Journal of Hydrology* **386**, 13–26.
- Lu AG, Kang SC, Pang DQ (2008). Altitude effect of precipitation and the influence of global warming on it in China. (In Chinese). *Frontiers in Ecology and the Environment* **17**(5), 1875–1878.
- Lund R, Reeves J (2002). Detection of Undocumented Changepoints: A Revision of the Two-phase Regression Model. *Journal of Climate*, **15**, 2547–2554.
- Luterbacher J, Xoplaki E, Casty C, Wanner H, Pauling A, Küttel M, Rutishauser T, Brönnimann S, Fischer E, Fleitmann D, Gonzalez -Rouco, Garcia- FJ ,Herrera R, Barriendos M, Rodrigo F, Gonzalez-Hidalgo JC, Saz MA, Gimeno L, Ribera P, Brunet M, Paeth H, Rimbu N, Felis T, Jacobeit J, Dünkeloh A, Zorita E, Guiot J, Türkeş M, Alcoforado MJ, Trigo R, Wheeler D, Tett S, Mann ME, Touchan R, Shindell DT, Silenzi S, Montagna P, Camuffo D, Mariotti A, Nanni T, Brunetti M, Maugeri M, Zerefos C, De Zolt S, Lionello P, Rath V, and Beltrami H (2006). Mediterranean climate variability over the last centuries: A review, in: The Mediterranean Climate: an overview of the main characteristics and issues, In: Lionello, P, Malanotte-Rizzoli, P, and Boscolo R. (Eds.), Amsterdam, Elsevier, pp. 27-148.
- MacDonald GM (2007). Severe and sustained drought in southern California and the West: present conditions and insights from the past on causes and impacts. *Quaternary International* **173**, 87-100.

- Maheras P, Flocas HA, Patrikas I, Anagnostopoulou C (2001). A 40 year objective climatology of surface cyclones in the Mediterranean region: spatial and temporal distribution. *International Journal of Climatology* **21**(1), 109–130.
- Maheras P, Xoplaki E and, Kutiel H (1999). Wet and dry, monthly anomalies across the Mediterranean basin and their relationship with circulation 1860–1990. *Journal of Theoretical Applied Climatology* **64**,189–199.
- Malanotte-Rizzoli P, Manca BB, d’Alcala MR, Theocharis A, Brenner S, Budillon G, Ozsoy E (1999). The eastern Mediterranean in the 80^s and in the 90^s: the big transition in the intermediate and deep circulations. *Journal of Dynamics of Atmospheres and Oceans* **29**, 365–395.
- Mann HB (1945). Non-parametric tests against trend. *Econometrica Journal* **13**, 245–259.
- Mann ME (2002). Large-scale climate variability and connections with the Middle East in the past. *Journal of Climatic Change* **55**, 287–314.
- MAP (2007). Mediterranean Action Plan. Water demand management, progress and policies. Proceedings of the 3rd Regional Workshop on Water and Sustainable Development in the Mediterranean. Zaragoza, Spain, 19–21 March 2007. MAP Technical Reports Series No. 168.
- Mariotti A (2010). Recent Changes in the Mediterranean Water Cycle: A Pathway toward Long-Term Regional Hydroclimatic Change. *Journal of Climate* **23**, 1513-1525.
- Mariotti A, Struglia MV, Zeng N, and Lau KM (2002). The hydrological cycle in the Mediterranean region and implications for the water budget of the Mediterranean Sea. *Journal of Climate* **15**, 1674–1690
- Martin ML, Luna M Y, Morata A, and Valero F (2004). North Atlantic teleconnection patterns of low frequency variability and their links with

- springtime precipitation in the Western Mediterranean. *International Journal of Climatology* **24**, 2004, 213–230.
- Martin–Vide, J (2011): Estructura temporal fina y patrones espaciales de la precipitación en la España peninsular. *Memorias de la Real Academia de Ciencias y Artes de Barcelona* **LXV 3**, 119-158.
- Martin-Vide J (2004). Spatial distribution of a daily precipitation concentration index in Peninsular Spain. *International Journal of Climatology* **24**, 959–971.
- Martín-Vide J, and Gómez L (1999). Regionalization of Peninsular Spain based on the length of dry spells. *International Journal of Climatology* **19**, 537–555.
- Martin-Vide J, Lopez-Bustins JA (2006). The Western Mediterranean Oscillation and rainfall in the Iberian Peninsula. *International Journal of Climatology* **26**, 1455–1475.
- Martin-Vide J, Olcina J (2001). Climas y tiempos de España Madrid Alianza Editorial. 258 pp.
- Martín-Vide, X (1987). Propiedades y aplicaciones de un índice de disparidad en pluviometría. X Congreso Nacional de Geografía. *Comunicaciones* **11**, 267-276.
- MathWave Technologies (2011). EasyFit Software Version 5.5, USA. <http://www.mathwave.com/help/easyfit/index.html>.
- Mavromatis T (2007). Drought index evaluation for assessing future wheat production in Greece. *International Journal of Climatology* **27**, 911–924.
- McKee TB, Doesken NJ, Kleist J (1993). The relationship of drought frequency and duration to time scales. In: *Preprints, 8th Conference on Applied Climatology*, 17–22 January 1993, Anaheim, CA, 179–184.
- McKee TB, Doesken NJ, Kleist J (1995). Drought monitoring with multiple time scales. Preprints, Ninth Conference on Applied Climatology, Dallas, TX, *Bulletin of the American Meteorological Society* 233–236.

- Mehta AV and, Yang S (2008). Precipitation climatology over Mediterranean Basin from ten years of TRMM measurements. *Advances in Geosciences* **17**, 87–91.
- Mestas-Nuñez AM (2000). Orthogonality properties of rotated empirical modes. *International Journal of Climatology* **20**, 1509–1516.
- Metaxas D A, Bartzokas A, Repapis C C and, Dalezios NR (1993). Atmospheric circulation anomalies in dry and wet winters in Greece. *Meteorologische Zeitschrift* **2(3)**, 127–131.
- Michaelides S. C, Tymvios F. S, and Michaelidou T (2009). Spatial and temporal characteristics of the yearly rainfall frequency distribution in Cyprus. *Journal of Atmospheric Research* **94**, 606–615.
- Millán MM, Estrela MJ, Miró J (2005). Rainfall components: variability and spatial distribution in a Mediterranean area. *Journal of Climate* **18(14)**, 2682–2705.
- Milly P, Betancourt J, Falkenmark M, Hirsch R, Kundzewicz Z, Lettenmaier D , and Stouffer R (2008). Stationarity Is Dead: Whither Water Management. *Science* **319**, 573-574.
- Miranda JD, Armas C, Padilla FM, Pugnaire FI (2011). Climatic change and rainfall patterns: effects on semiarid plant communities of the Iberian southeast. *Journal of Arid Environment* **75**, 1302–1309.
- Mishra AK, Ozger M, Singh VP (2009). An entropy-based investigation into the variability of precipitation. *Journal of Hydrology*. **370**, 139–157.
- Mishra AK, Singh, VP (2010). A review of drought concepts. *Journal of Hydrology*. **354 (1–2)**, 202–216.
- Moberg A and Bergstrom H (1997). Homogenization of Swedish temperature data. Part III: The long temperature records from Uppsala and Stockholm. *International Journal of Climatology* **17**: 667–699.
- Mohtadi S (2012). Climate Change and the Syrian Uprising. *Bulletin of the Atomic Scientists*, August 16.

- Mooley D. A (1973). Gamma-distribution probability model for Asian summer monsoon monthly rainfall. *Monthly Weather Review* **101**, 160-176.
- Morid S, Smakhtin V, Moghaddasi M (2006). Comparison of seven meteorological indices for drought monitoring in Iran. *International Journal of Climatology* **26**, 971–985.
- Morin E (2011). To know what we cannot know: global mapping of minimal detectable absolute trends in annual precipitation. *Journal of Water Resource Research* 47:W07505. doi: 10.1029/2010WR009798.
- Nandintsetseg B and, Shinoda M (2012). Assessment of drought frequency, duration, and severity and its impact on pasture production in Mongolia. *Journal of National Hazards* **66(2)**, 995–1008.
- Narisma GT, Foley JA, Licker R, Ramankutty N (2007). Abrupt changes in rainfall during the twentieth century. *Journal of Geophysical Research Letters* **34**:L06710.:doi:10.1029/2006GL028628.
- Nastos P T and, Zerefos C S (2009). Spatial and temporal variability of consecutive dry and wet days in Greece. *Journal of Atmospheric Research* **94**, 616– 628.
- Nastos PT, Zerefos CS (2010). Climate Change and precipitation in Greece. *Hellenic Journal of Geosciences* **45**, 185-192.
- Neves JA (2012). Documentation reproduced from package spi, version 1.1. License: GPL-2. <http://cran.r-project.org/web/packages/spi/spi.pdf>
- New M, Todd M, Hulme M, Jones P (2001). Precipitation measurements and trends in the twentieth century. *International Journal of Climatology* **21**, 1899–1922.
- Ngongondo C, Xu C.Y, Gottschalk L, and Alemaw B (2011). Evaluation of spatial and temporal characteristics of rainfall in Malawi: a case of data scarce region. *Theoretical and Applied Climatology*, **106**, 79-93.
- Niemeyer, S (2008). New drought indices. *Options Méditerranéennes, Série A: Séminaires Méditerranéens*, **80**, 267–274.

- Nohara D, Kitoh A, Hosaka M, Oki T (2006). Impact of climate change on river discharge projected by multi-model ensemble. *Journal of Hydrometeorology* **7**, 1076–1089.
- Norrant C, Douguédroti A (2006). Monthly and daily precipitation trends in the Mediterranean (1950-2000). *Journal of Theoretical and Applied Climatology* **20**, 565-475.
- Noy-Meir I (1973). Desert ecosystems: environment and producers. *Annual Review of Ecology, Evolution and Systematics*. **4**, 25–51.
- Obasi GOP (1994) .WMO's role in the international decade for natural disaster reduction. *Bulletin of the American Meteorological Society* **75**, 1655–1661
- Oikonomou Ch, Flocas HA, Hatzaki M, Asimakopoulos DN, Giannakopoulos C (2008). Future changes in the occurrence of extreme precipitation events in eastern Mediterranean. *Glob NEST Journal* **10(2)**, 255–262.
- Olascoaga M.J (1950). Some aspects of Argentine rainfall. *Tellus* **2 (4)**, 312–318.
- Oliver J E (1980). Monthly precipitation distribution: a comparative index. *The Professional Geographer* **32**:300–309.
- Olukayode Oladipo E (1985). A comparative performance analysis of three meteorological drought indices. *Journal of Climatology* **5(6)**, 655–664
- Önol B and, Semazzi F H M (2009). Regionalization of climate change simulations over the eastern Mediterranean. *Journal of Climate* **22**:1944–1961.
- Önol B, Unal YS (2014) Assessment of climate change simulations over climate zones of Turkey. *Journal of Regional Environmental Change*. doi: 10.1007/s10113-012-0335-0
- Palmieri S, Siani AM, D'Agostino A (1991). Climate fluctuations and trends in Italy within the last hundred years. *Annales Geophysicae* **9**, 769–776.

- Palutikof JP, Goodess CM, Guo X (1994). Climate change, potential evapotranspiration and moisture availability in the Mediterranean basin, *International Journal of Climatology* **14**, 853-869.
- Pandey R P, Dash B B, Mishra S K, and Singh R (2008). Study of indices for drought characterization in KBK districts in Orissa (India). *Journal of Hydrological Process* **22**, 1895–1907.
- Paredes D, Trigo RM, Garcia-Herrera R, Franco-Trigo I (2006). Understanding precipitation changes in Iberia in early spring: weather typing and storm-tracking approaches. *Journal of Hydrometeorology* **7**, 101–113.
- Park J H, Kim K B and Change H Y (2014). Statistical properties of effective drought Index (EDI) for Seoul, Busan, Daegu, Mokpo in South Korea. *Asia-Pacific Journal of Atmospheric Sciences*. doi:10.1007/s13143-014-0035-4.
- Parry M L (ed) (2000). Assessment of potential effects and adaptations for climate change in Europe: The Europe ACACIA Project. Norwich: Jackson Environment Institute, University of East Anglia, 320 pp.
- Partal T and Kahya E (2006). Trend analysis in Turkish precipitation data. *Journal of Hydrological Processes*. **20**, 2011-2026.
- Paulo AA, Pereira LS, Matias PG (2003). Analysis of local and regional droughts in southern Portugal using the theory of runs and the standardized precipitation index. In: Rossi G, Cancelliere A, Pereira LS, Oweis T, Shatanawi M, Zairi A (eds) tools for drought mitigation in Mediterranean regions. Kluwer, Dordrecht, pp 55–78.
- Paulo AA, Rosa RD, Pereira LS (2012). Climate trends and behaviour of drought indices based on precipitation and evapotranspiration in Portugal. *Journal of Natural Hazards and Earth Systems Sciences* **12 (5)**, 1481–1491.
- Pausas, JG (2004). Changes in fire and climate in the eastern Iberian Peninsula (Mediterranean basin). *Climatic Change* **63 (3)**, 337-350.

- Pearson K (1901). On lines and planes of closest fit to systems of points in space. *Philosophical Magazine B* 2,559-572.
- Pereira LS (2011). Challenges on water resources management when searching for sustainable adaptation to climate change focusing agriculture. *Journal of European Water* **34**, 41–54
- Pereira LS, Cordery I and Iacovides I (2002). Coping with water scarcity, UNESCO IHP VI, technical documents in hydrology, No. 58. UNESCO, Paris.
- Pereira LS, Cordery I and, Iacovides I (2009). Coping with water scarcity: Addressing the challenges. Springer, Dordrecht, 382 pp.
- Pérez-Palazón¹ MJ, Pimentel R, Herrero J, Aguilar C, Perales JM, J. Polo MJ (2015). Extreme values of snow-related variables in Mediterranean regions: trends and long-term forecasting in Sierra Nevada (Spain). *International Association of hydrological Science* **369**, 157–162.
- Peterson T C and Vose R S (1997). An overview of the Global Historical Climatology Network temperature database. *Bulletin of the American Meteorological Society* **78**, 2837-2849.
- Petrosa G, Mantzavelas Antonis M, Marianthia T (2011). Development of an adapted empirical drought index to the Mediterranean conditions for use in forestry. *Agricultural and Forest Meteorology* **151**, 241–250.
- Petterssen S (1956). Weather Analysis and forecasting (2nd edn), vol. 1. McGraw-Hill Book Company: New York.428pp.
- Pham MT, Vanhaute WJ, Vandenberghe S ,De Baets B, Verhoest NEC (2013). An assessment of the ability of Bartlett–Lewis type of rainfall models to reproduce drought statistics. *Hydrology and Earth System Science* **17**, 5167–5183.
- Philandras CM, Nastos PT, Kapsomenakis J, Douvis KC, Tselioudis G, Zerefos CS (2011). Long term precipitation trends and variability within the Mediterranean

- region. *Journal of Natural Hazards Earth System* **11**, 3235-3250.
- Piervitali E, Colacino M and, Conte M (1998). Signals of climatic change in the central–western Mediterranean Basin. *Journal of Theoretical and Applied Climatology* **58**, 211–219.
- Polade S D, Pierce D W, Cayan D R, Gershunov A and Dettinger M D (2014). The key role of dry days in changing regional climate and precipitation regimes. *Scientific Reports* **4**. doi: 10.1038/srep04364.
- Price C, Stone L, Huppert A, Rajagopalan B, and Alpert P (1998). A possible link between El-Nino and precipitation in Israel, *Journal of Geophysical Research Letters* **25**, 3963– 3966.
- Pross J, Kotthoff U, Muller UC, Peyron O, Dormoy I, Schmiedl G, Kalaitzidis S, Smith AM (2009). Massive perturbation in terrestrial ecosystems of the Eastern Mediterranean region associated with the 8.2 ka climatic event. *Journal of Geology* **37**, 887–890.
- Pryor S. C. and Schoof J. T (2008). Changes in the seasonality of precipitation over the contiguous USA. *Journal of Geophysical Research* **113**: D21108, doi: 10.1029/2008JD01025.
- Quadrelli R, Lazzeri M, Cacciamani C, and Tibaldi S (2001). Observed winter alpine precipitation variability and links with large-scale circulation pattern. *Journal of Climate Research* **17**, 275–284.
- Quiring S M and Papakyriakou T N (2003). An evaluation of agricultural drought indices for the Canadian prairies. *Journal of Agricultural and Forest Meteorology* **118**, 49–62.
- Quiring SM and, Ganesh S (2010). Evaluating the utility of the vegetation condition index (VCI) for monitoring meteorological drought in Texas. *Journal of Agriculture and Forest Meteorology* **150** (3), 330–339.

- R Development Core Team (2011). *R: a language and environment for statistical computing*. Vienna, Austria: R Foundation for Statistical Computing.
- Ramos MC (2001). Rainfall distribution patterns and their change over time in a Mediterranean area. *Journal of Theoretical and Applied Climatology* **3**, 163-170.
- Ramos MC, Martínez-Casasnovas J (2006). Erosion rates and nutrient losses affected by composted cattle manure application in vineyard soils of NE Spain. *Catena*, **68**, 177–185.
- Raziei T, Bordi I, and Pereira, L. S (2008). A precipitation-based regionalization for Western Iran and regional drought variability. *Journal of Hydrology and Earth System Sciences* **12**, 1309–1321.
- Raziei T, Daryabar J, Bordi I, Pereira LS (2014). Spatial patterns and temporal trends of precipitation in Iran. *Journal of Theoretical and Applied Climatology* **115**, 531-540.
- Raziei T, Saghafian B, Paulo A A, Pereira L S, and Bordi I (2009). Spatial patterns and temporal variability of drought in Western Iran, *Journal of Water Resource Management* **29**, 439–455.
- Reale, M, Lionello, P (2013). Synoptic climatology of winter intense precipitation events along the Mediterranean coasts. *Journal of Natural Hazards and Earth System Sciences* **13**, 1707–1722.
- Rencher A C (1998), *Multivariate Statistical Inference and Applications*, New York: Wiley.
- Revfeim, K. J. A (1985). A note on the comparison of theoretical and empirical quantiles for monthly rainfall totals. *Journal of Atmosphere Ocean* **23**, 414/419.
- Rey JC, Rodriguez M F, Cortez A, Lobo D, Ovalles F, Gabriels D, Parra RM. 2012. Analysis of precipitation aggressiveness and concentration in Venezuela. Los Andes Region. *Bioagro* **24** (2), 115-120.

- Ribera P, Garcia R, Diaz HF, Gimeno L, Hernandez E. (2000). Trends and interannual oscillations in the main sea-level surface pressure patterns over the Mediterranean, 1955–1990. *Journal of Geophysical Research Letters* **27**(8), 1143–1146.
- Richman MB (1986). Rotation of principal components. *Journal of Climatology* **6**, 293-335.
- Richman MB, Gong X (1999). Relationships between the definitions of the hyperplane width in the fidelity of principal component loading patterns. *Journal of Climatology* **12**, 1557–1576.
- Rodionov S N A (2004). Sequential algorithm for testing climate regime shifts. *Journal of Geophysical Research Letters* **31**, L09204, doi: 10.1029/2004GL019448.
- Rodionov, S N A (2005). Brief overview of the regime shift detection methods Large-Scale Disturbances (Regime Shifts) and Recovery in Aquatic Ecosystems: Challenges for Management toward Sustainability, edited by: Velikova V and Chipev, N.
- Rodó X, Baert E, and Comin F A (1997). Variations in seasonal rainfall in Southern Europe during the present century: relationships with the North Atlantic Oscillation and the El Nino-Southern Oscillation. *Journal of Climate Dynamics* **13**, 275 – 284.
- Roether W, Manca BB, Klein B, Bregant D, Georgopoulos D, Beitzel V, Kovacevic V, Lucchetta A (1996). Recent changes in eastern Mediterranean deep waters. *Science* **271**, 333 – 335.
- Rojas M, Li L Z, Kanakidou M, Hatzianastassiou N, Seze G and Le Treut H (2013). Winter weather regimes over the Mediterranean region: their role for the regional climate and projected changes in the twenty-first century *Journal of Climate Dynamics* **41**, 551–71.

- Ropelewski CF, Halpert MC (1996). Quantifying Southern Oscillation Precipitation Relationships. *Journal of Climate* **9**, 1043-1059.
- Roudier P and Mahe G (2010). Study of water stress and droughts with indicators using daily data on the Bani River (Niger basin, Mali). *International Journal of Climatology* **30**, 1689–1705.
- Saaroni H, Ziv B (2000). Summer rain episodes in Mediterranean climate, the case of Israel>climatological- dynamical analysis. *International Journal of Climatology* **20**, 191–209.
- Saaroni H, Bitan A, Alpert P, Ziv B (1996). Continental polar outbreaks into the eastern Mediterranean. *International Journal of Climatology* **16**, 1175–1191.
- Saaroni H, Halfon N, Ziv B, Alperth P, Kutielb H (2010). Links between the rainfall regime in Israel and location and intensity of Cyprus lows. *International Journal of Climatology* **30**, 1014–1025.
- Salinger J (1995). Conditions leading to drought in New Zealand. *Journal of Water Atmosphere* **3 (1)**, 11-12.
- Salmi T, Määttä A, Anttila P, Ruoho-Airola T, and Amnell T (2002). Detecting trends of annual values of atmospheric pollutants by the Mann– Kendall test and Sen’s slope estimates – the Excel template application Makesens. Finnish Meteorological Institute, Helsinki, Finland, 35 pp.
- Salvati L, Venezian- Scarascia ME and, Zitti M (2009). Monitoring drought severity in agriculture through a synthetic index based on dry periods: a case study in the Mediterranean basin. *Journal of Irrigation and Drainage Engineering* **58**, 596–606.
- Sang YF, Wang Z, Liu C (2012). Spatial and temporal variability of daily temperature during 1961e2010 in the Yangtze River Basin, China. *Quaternary International* **304**, 33-42.

- Santo FE, Ramos AM, Lima MIP, Trigo RM R (2014). Seasonal changes in daily precipitation extremes in mainland Portugal from 1941 to 2007. *Journal of Regional Environment Chang***17**, 1765-1788.
- Santos J F, Pulido-Calvo I, and Portela M M (2010). Spatial and temporal variability of droughts in Portugal. *Journal of Climate Research* **46**, W03503, doi: 10.1029/2009WR008071.
- Saris F, Hannah DM, Eastwood WJ (2010). Spatial variability of precipitation regimes over Turkey. *Journal of Hydrological Sciences* **55**, 234-249.
- Scheffer M Carpenter S, Foley JA, Folke C, Walker B (2001). Catastrophic shifts in ecosystems. *Nature* **413**, 591– 596.
- Schonwiese CD, Rapp J (1997). Climate Trend Atlas of Europe — Based on Observations 1891–1990. Kluwer Academic Publishers: Dordrecht
- Schonwiese CD, Rapp J, Fuchs T, Denhard M (1994). Observed climate trends in Europe 1891–1990. *Meteorologische Zeitschrift* **3**, 22–28.
- Schuttemeyer D (2005). The Surface Energy Balance over Drying Semi-Arid Terrain in West Africa, PhD Thesis, ISBN 90-8504-192-9, Meteorology and Air Quality Group, Wageningen University, The Netherlands.
- Seager R, Liu H, Henderson N, Simpson I, Kelley C, Shaw T, Kushnir Y and Ting M (2014). Causes of increasing aridification of the Mediterranean region in response to rising greenhouse gases. *Journal of Climate* **27**, 4655–76.
- Sen P K (1968). Estimates of regression coefficient based on Kendall's tau. *Journal of American Statistical Association* **63**, 1379–1389.
- Sen PK (1968). Estimates of the regression coefficient based on Kendall's tau. *Journal of the American Statistical Association* **63**, 1379-1389.

- Serra C, Burguen A, Martinez MD and , Lana X (2006) Trends in dry spells across Catalonia NE Spain during the second half of the 20th century. *Journal of Theoretical Applied Climatology* **85**,165–183.
- Serrano A, Mateos V L and, García, J A (1999). Trend analysis of monthly precipitation over the Iberian Peninsula for the period 1921–1995. *Physics and Chemistry of the Earth Journal* **24 (B)**, 85–90.
- Sevruk B, Matokova-Sadlonova K, Toskano L (1998). Topography effects on small-scale precipitation variability in the Swiss pre-Alps. IAHS-AISH Publication, **248**, 51–58.
- Shafran-Nathan R, Svoray T, Perevolotsky A (2012). The resilience of annual vegetation primary production subjected to different climate change scenarios. *Journal of Climate Chang* **118**,227-243.
- Shahabfar A and Eitzinger J (2013).Spatio-Temporal Analysis of Droughts in Semi-Arid Regions by Using Meteorological Drought Indices. *Atmosphere* **4**, 94-112.
- Shaltout M, Omstedt A (2014). Recent precipitation trends and future scenarios over the Mediterranean Sea. *Giofizika* **31**, 127-150.
- Shaltout M, Omstedt, A (2012).Calculating the water and heat balances of the Eastern Mediterranean Basin using ocean modelling and available meteorological, hydrological and ocean data. *Oceanologia* **54**, 199–232.
- Shannon CE. The mathematical theory of communication (1948). *Journal of Bell System Technical* **27**:379–423.
- Sharma MA, Singh JB (2010). Use of Probability Distribution in Rainfall Analysis. *New York Science Journal* **3(9)**, 40-49.
- Shaw G, Wheeler, D. (Eds.) (1994). Statistical Techniques in Geographical Analysis .Halsted Press, New York.
- Shay-El Y, Alpert P, and DaSilva A (2000). Preliminary estimation of horizontal fluxes of cloud liquid water in relation to subtropical moisture budget studies

- employing ISCCP, SSMI and GEOS-1/DAS datasets, *Journal of Geophysical Research* **105**18067- 18088.
- Shay-El Y, and Alpert P (1991). A diagnostic study of winter diabatic heating in the Mediterranean in relation to cyclones. *Journal of Royal Meteorological Society* **117**, 715-747.
- Shehadeh N and Ananbeh S (2013).The impact of climate change upon winter rainfall. *American Journal of Environmental Science* **9** (1), 73-81.
- Shi Peng, Qiao Xueyuan, Chen Xi, Zhou Mi, Qu Simin, Ma Xinxin, and Zhang Zhicai (2014). Spatial distribution and temporal trends in daily and monthly precipitation concentration indices in the upper reaches of the Huai River, China. *Stochastic Environmental Research and Risk Assessment* **28** (2), 201-212.
- Shlomi Y, Ginat H (2009). Rainfall in the Arava 1950-2008, Preliminary report. Scientific report submitted to the water and the Arava drainage authorities, Dead Sea and Arava Science Center, 23 pp. (in Hebrew).
- Sillmann J and, Roeckner E (2008). Indices of extreme events in projections of anthropogenic climate change. *Journal of Climate Change* **86**, 83–104.
- Silva GAM, and Mendes D (2013). Comparison Results for the CFSv2 Hindcasts and Statistical Downscaling over the Northeast of Brazil. *Advances in Geosciences Journal* **35**, 79-88.
- Sims AP, Dutta D, Niyogi S, Raman S (2002). Adopting indices for estimating soil moisture: A North Carolina case study. *Journal of Geophysical Research Letters* **29**.doi:10.1029/2001GL013343.
- Sirdas S, Sahin AD (2008). Relationship between drought and solar irradiation variables. *Journal of Hydrological processes* **22**, 1460-1472.
- Sirdas S, Sahin, AD (2008). Relationship between drought and solar irradiation variables. *Journal of Hydrology Process* **22**, 1460–1472.

- Skaf M, Mathbout S (2010). Precipitation Changes in al Jazeera region and their potential effects on vegetation (In Arabic). *The Arab Journal of Arid Environments* **3** (2), 71-78.
- Smadi MM (2006). Observed abrupt changes in minimum and maximum temperatures in Jordan in the 20th century. *American Journal of Environmental Science* **2** (3) 114-120.
- Smakhtin VU and Hughes DA (2007). Automated estimation and analyses of meteorological drought characteristics from monthly rainfall data. *Environmental Modelling Software* **22**, 880–890.
- Sonmez F K, Komuscu AU, Erkan A and, Turgu E (2005). An analysis of spatial and temporal dimension of drought vulnerability in Turkey using the standardized precipitation index. *Journal of National Hazards* **35**, 243–264.
- SPSS for Windows. 2007. Version 17.0. Chicago, Illinois. SPSS, Incorporated.
- Stanhill G, Rapaport C (1988). Temporal and spatial variation in the volume of rain falling annually in Israel. *Israel Journal of Earth Sciences* **37**, 211–221.
- Steinberger EH, Gazit-Yaari N (1996). Recent changes in the spatial distribution of annual precipitation in Israel. *Journal of Climate* **9**, 3328-3336.
- Štěpánek P (2007). *AnClim—software for time series analysis (for Windows)*. Department of Geography, Faculty of Natural Sciences, Masaryk University, Brno (1.47 MB).
- Štěpánek P, Zahradníček P, Skalák P (2009). Data quality control and homogenization of air temperature and precipitation series in the area of the Czech Republic in the period 1961–2007. *Journal of Advanced Research* **3**: 23–26.

- Stričević R, Đurović N, Đurović, Ž (2011). Drought classification in Northern Serbia based on SPI and statistical pattern recognition. *Meteorological Applications Journal* **18**, 60–69.
- Subak S, Palutikof J P, Agnew M D, Watson S J, Bentham C G, Cannell M G R, Hulme M, McNally S, Thornes J E, Waughray D, Woods J C (2000). The impact of the anomalous weather of 1995 on the UK economy. *Journal of Climate Change* **44**, 1–26.
- Sumner G, Homar V, Ramis C (2001). Precipitation seasonality in eastern southern costal Spain. *International Journal of Climatology* **21**, 219–247.
- Sun H, Chen Y, Li W, Li F, Chen Y, Hao X, Yang Y (2010). Variation and abrupt change of climate in Ili River Basin, Xinjiang. *Journal of Geographical Science* **20** (5) 652–666.
- Tabari H, Hosseinzadeh Talaee P (2011). Temporal variability of precipitation over Iran: 1966–2005. *Journal of Hydrology* **396** (3–4), 313–320.
- Tannehill I. R (1947). *Drought: Its Causes and Effects*. Princeton University Press, 264 pp.
- Tarawneh1 Q Kadiglou M (2002). An analysis of precipitation climatology in Jordan. *Journal of Theoretical and Applied Climatology* doi 10.1007/s00704-002-0705-5
- Tatli H, Dalfes N, Montes S (2004). A statistical downscaling method for monthly total precipitation over Turkey. *International Journal of Climatology* **24**, 161–188.
- Tayanc M, İm U, Doğruel M Karaca M (2009). Climate change in Turkey for the last half century. *Journal of Climatic Change* **94**(3–4), 483–502.
- Taylor, WA (2000a). Change-point Analyser. A powerful new tool for detecting changes, preprint, available at:

- <http://www.variation.com/%20cpa/tech/changepoint.html>. Last access: 10 March 2011.
- Taylor, WA (2000b). Change-Point Analyzer 2.3 software package, Taylor Enterprises, Libertyville, Illinois, available at: <http://www.variation.com/cpa/index.html>. Last access: 10 March 2011.
- Tebaldi C, Hayhoe K, Arblaster J, Meehl G (2006). Going to the extremes: an intercomparison of model-simulated historical and future changes in extreme events. *Journal of Climate Chang* **79**,185–211.
- Tielborger K, Fleischer A, Menzel L, Metz J, Sternberg M (2010). The aesthetics of water and land: a promising concept for managing scarce water resources under climate change. *Journal of Philosophical Transition of the Royal Society* **368**, 5323-5337.
- Tolika K, Anagnostopoulou C, Maheras P (2004). Trends in extreme events across Greece in the 2nd half of the 20th century (part APrecipitation), 7th Panhellenic (International) Conference of Meteorology, Lefkosia.
- Tolika K, Anagnostopoulou CHR, Maheras P, Kutiel H (2007). Extreme precipitation related to circulation types for four case studies over the Eastern Mediterranean. *Journal of advances of Geosciences* **12**, 87-93.
- Toreti A, Xoplaki E, Maraun D, Kuglitsch F G, Wanner H, Luterbacher J (2010). Characterisation of extreme winter precipitation in Mediterranean coastal sites and associated anomalous atmospheric circulation patterns. *Journal of Natural Hazards and Earth System Science*, **10(5)**, 1037–1050.
- Toros H (1993). Trend analysis of climatologic series in Turkey. MSc thesis, Institute of Science Technology, Istanbul Technical University.

- Trenberth KE, Dai A, Rasmussen RM, Person DB (2003). The Changing character of precipitation. *Bulletin American Meteorological Society* **84**, 1205-1217.
- Trenberth KE (2011). Changes in precipitation with climate change. *Journal of Climate Research*, **47**: 123-138.
- Trigo I F, Davies T D, Bigg G R (1999). Objective climatology of cyclones in the Mediterranean region. *Journal of Climate* **2**, 1685–1696.
- Trigo R M, Davies T D, Bigg G R (2000). Decline in Mediterranean rainfall caused by weakening of Mediterranean cyclones. *Journal of Geophysical Research Letters* **27**, 2913–2916.
- Trigo R, Pereira J, Pereira M, Mota B, Calado M, Da Camara C, Santo F (2006). The exceptional fire season of summer 2003 in Portugal. *International Journal of Climatology* **26(13)**, 1741–1757.
- Trigo RM, Palutikof JP (2001). Precipitation scenarios over Iberia: a comparison between GCM output and different downscaling techniques. *Journal of Climate* **14**, 4422–4446.
- Tsakiris G, Pangalou D Vangelis H (2007) Regional drought assessment based on the Reconnaissance Drought Index (RDI). *Journal of Water Resource Management* **21**:821–833.
- Tsakiris G, Vangelis H (2004). Towards a drought watch system based on spatial SPI. *Water Resource Management* **18**, 1–12.
- Tsonis A A (1996). Widespread increases in low-frequency variability of precipitation over the past century. *Nature* **382**, 700–702.
- Türkeş M (1996). Spatial and temporal analysis of annual rainfall variations in Turkey. *International Journal of Climatology* **16**, 1057–1076.

- Türkeş M, Erlat E (2003). Precipitation changes and variability in Turkey linked to the North Atlantic oscillation during. *International Journal of Climatology* **23**, 1771–1796.
- Türkeş M, Erlat E (2006). Influences of the North Atlantic Oscillation on precipitation variability and changes in Turkey. *Nuovo Cimento Della Societa Italiana Di Fisica C-Geophysics and Space Physics* **29**, 117–135.
- Türkeş M, Koc T, Saris F (2009). Spatiotemporal variability of precipitation total series over Turkey. *International Journal of Climatology. International Journal of Climatology* **29**, 1056–1074.
- Türkeş M, Tatlı H (2009). Use of the standardized precipitation index (SPI) and a modified SPI for shaping the drought probabilities over Turkey. *International Journal of Climatology* **29**, 2270–2282.
- Türkeş, M (1998). Influence of geopotential heights, cyclone frequency and Southern Oscillation on rainfall variations in Turkey. *International Journal of Climatology* **18**, 649-680.
- UKMO (1995). *Modelling Climate Change 1860–2050*. United Kingdom Meteorological Office (UKMO), The Hadley Centre for Climate Prediction and Research, 12 pp.
- Ulbrich U, Lionello P, Belusć D, Jacobeit J, Knippertz P, Kuglitsch FG, Leckebusch GC, Luterbacher J, Maugeri M, Maheras P, Nissen KM, Pavan V, Pinto JG, Saaroni H, Seubert S, Toreti A, Xoplaki E and Ziv B (2012). Climate of the Mediterranean: synoptic patterns, temperature, precipitation, winds, and their extremes. In: Lionello P et al. (eds) *The climate of the Mediterranean region: from the past to the future*. Elsevier, pp 301–346. doi:10.1016/B978-0-12-416042-2.00005-7. ISBN 9780124160422.
- Valero F, Luna MY, Martín ML, Morata A, González-Rouco F (2004). Coupled modes of large-scale climatic variables and regional precipitation in the Western Mediterranean in autumn. *Journal of Climate Dynamics* **22**, 307–323.

- Vasiliades L, Loukas A, Liberis N (2011). A water balance derived drought index for Pinios River basin, Greece. *Water Resource Manager* **25**, 1087–1101.
- Vicente-Serrano S M, Gonzalez-Hidalgo J C, De Luis M, Raventos J. (2004). Drought patterns in the Mediterranean area: the Valencia region (eastern Spain). *Journal of Climate Research* **26** (1), 5–15.
- Vicente-Serrano S., Beguería S, López-Moreno JJ, El Kenawy AM, Angulo M (2009). Daily atmospheric circulation events and extreme precipitation risk in Northeast Spain: the role of the North Atlantic Oscillation, Western Mediterranean Oscillation and Mediterranean Oscillation. *Journal of Geophysical Research* **114**, D08106. doi: 10.1029/2008 JD011492.
- Vicente-Serrano SM, Beguería S, Lopez-Moreno JJ, Garcia-Vera MA, Stepanek P (2010). A complete daily precipitation database for northeast Spain: reconstruction, quality control, and homogeneity. *International Journal of Climatology* **30**: 1146–1163.
- Vicente-Serrano SM, BegueríaS, Lorenzo-Lacruz J, Camarero JJ, López-Moreno JJ, Azorin-Molina C, Revuelto J, Morán-Tejeda E, Sanchez-Lorenzo A (2012). Performance of drought indices for ecological, agricultural, and hydrological applications *Journal of Earth Interact* **16**, 1–27.
- Vicente-Serrano SM, López-Moreno JJ (2008). The nonstationary influence of the North Atlantic Oscillation on European precipitation. *Journal of Geophysical Research-Atmosphere* **113**, D20120.
- Vicente-Serrano, S. M (2006). Differences in Spatial Patterns of Drought on Different Time Scales: An Analysis of the Iberian Peninsula. *Journal of Water Resource Management* **20**, 37–60.
- Vinnikov K Ya, Groisman P Ya and Lugina, K. M (1990). Empirical data on contemporary global climate changes (temperature and precipitation). *Journal of Climate* **3**, 662-677.

- Voudouris, K, Panagopoulos A, Koumantakis J (2000). Multivariate statistical analysis in the assessment of hydrochemistry of the northern Korinthia prefecture alluvial aquifer system, Peloponnese, Greece. *Journal of Natural Resources Research* **9**(2), 135–143.
- Walsh R. P. D. Lawer, D. M (1981). Rainfall seasonality: Description, spatial patterns and change through time. *Weather* **36**, 201 – 208.
- Wang Q, Wu J, Lei T, He B, Wu Z, Liu M (2014). Temporal-spatial characteristics of severe drought events and their impact on agriculture on a global scale. *Quaternary International* **349**, 10-21.
- Wang SJ, Zhang MJ, Sun MP, Wang BL, Li (2013). Changes in precipitation extremes in alpine areas of the Chinese Tianshan Mountains, central Asia, 1961e2011. *Journal of Quaternary International* **311** (17), 97-107.
- Wang W, Xing W, Yang T, Shao Q, Peng S, Yu Z Yong B (2013). Characterizing the changing behaviours of precipitation concentration in the Yangtze River Basin, China. *Journal of Hydrological Process* **27**:3375–3393.
- Wang XL and Feng Y (2010). RHtestsV3 User Manual. Climate Research Division, Atmospheric Science and Technology Directorate, Science and Technology Branch, Environment Canada.
- Wei M, Flrke M, Menzel L, Alcamo J (2007) Model-based scenarios of Mediterranean droughts. *Journal of Advances in Geoscience* **12**,145–151.
- Weltzin JF, Loik ME, Schwinning S, Williams DG, Fay PA, Haddad BM, Harte J, Huxman TE, Knapp AK, Lin G, Pockman WT, Shaw R, Small EE, Smith MD, Smith SD, Tissue DT, Zak JC (2003). Assessing the response of terrestrial ecosystems to potential changes in precipitation. *Bioscience* **53**,941–952.
- Weltzin JF, Loik ME, Schwinning S, Williams DG, Fay PA, Haddad BM, Harte J, Huxman TE, Knapp AK, Lin G, Pockman WT, Shaw MR, Small EE, Smith MD,

- Smith SD, Tissue DT, Zak JC (2003). Assessing the response of terrestrial ecosystems to potential changes in precipitation. *BioScience* **53**,941–952.
- Wettstein J J, Mearns LO December (2002). The influence of the North Atlantic-Arctic Oscillation on mean, variance and extremes of temperature in the north eastern United States and Canada. *Journal of Climate* **15**, 3586–3600.
- White D, Richman H, Yarnal B (1991). Climate regionalization and rotation of principal components. *International Journal of Climatology* **11**, 1-25.
- White DH, Walcott J J (2009). The role of seasonal indices in monitoring and assessing agricultural and other droughts. *Journal of Crop and Pasture Science* **60**, 599–616.
- Whitmore JS (1968).The relationship between mean annual rainfall and locality and site factors. *South Africa Journal of Science* **64**, 423-427.
- Wigley T M L (1985). Impact of extreme events. *Nature* **316**, 106–107.
- Wigley T M L (1988). The effect of changing climate on the frequency of absolute extreme events. *Climate Monitoring* **17**, 44–55. (Reprinted in *Climatic Change* (2009) **97**, 67–76.
- Wilby RL L, Wigley TML (2000). Precipitation predictors for downscaling: observed and general circulation model relationships, *International Journal of Climatology* **20**, 641–661.
- Wilhite DA (1997). Responding to drought: common threads from the past, visions for the future. *Journal of the American Water Resources Association* **33**, 951–959.
- Wilhite DA (2000). Drought as a natural hazard: concepts and definitions. In: Wilhite, D.A. (Ed.), *Drought: a Global Assessment*. Routledge, London, pp. 3-18.

- Wilhite DA, Glantz M H (1985). Understanding the drought phenomenon: The role of definitions. *Water International* **10**, 111–120.
- Wilhite DA, Svoboda M, Hayes M (2007). Understanding the complex impacts of drought: a key to enhancing drought mitigation and preparedness. *Water Resource Management* **21**, 763–774.
- Wilks DS (1989). Rainfall intensity, the Weibull distribution, and estimation of daily surface run off. *Journal of Applied Meteorology* **28**, 52-58.
- Wilks DS (1990). Maximum likelihood estimation for gamma distribution using data containing zeros. *Journal of Climate* **3**, 1495-1501.
- Willems P, Arnbjerg-Nielsen K, Olsson J, Nguyen V T V (2012). Climate Change Impact Assessment on Urban Rainfall Extremes and Urban Drainage: Methods and Shortcomings. *Journal of Atmospheric Research* **103**, 106-118.
- Williams CJR, Kniveton DR, Layberry R (2010). Assessment of a climate model to reproduce rainfall variability and extremes over Southern Africa. *Journal of Theoretical and Applied Climatology* **99**, 9-27.
- World Meteorological Congress (2011). *Abridged final report with resolutions*. WMO- NO.1077, Geneva, Switzerland.
- World Meteorological Organization (1975). *Drought and agriculture*. WMO Note 138, Publ. WMO-NO. 392, Geneva, Switzerland, 127 pp.
- World Meteorological Organization (1992). *International Meteorological Vocabulary*. 2^d ed. WMO- No. 182, Geneva, Switzerland.
- World Meteorological Organization (2012). *Standardized Precipitation Index User Guide*. WMO-No.1090, Geneva, Switzerland.
- Wu H, Svoboda MD, Hayes MJ, Wilhite DA, Wen F (2007). Appropriate application of the Standardized Precipitation Index in arid locations and dry seasons. *International Journal of Climatology* **27**, 65–79.

- Wu H, Hayes J T, Wilhite D A, Svoboda M D (2005). The effect of the length of record on the Standardized Precipitation Index. *International Journal of Climatology* **25**, 505–520.
- Wu H, Hayes M J, Weiss A, Hu Q (2001). An evaluation of the standardized precipitation index, the China-Z Index and the statistical Z-Score. *International Journal of Climatology* **21**, 745–758.
- Xenos DI, Passios S, Georgiades E, Parlís E, Koutsoyiannis D (2002). Water demand management and the Athens water supply. Proceedings of the 7th BNAWQ Scientific and Practical Conference 'Water Quality Technologies and Management in Bulgaria', Sofia, 44–50, Bulgarian National Association on Water Quality.
- Xoplaki E (2002) Climate variability over the Mediterranean, PhD Thesis, University of Bern, Switzerland. Available at: http://sinus.unibe.ch/klimet/docs/phd_xoplaki.pdf
- Xoplaki E, Gonzalez-Rouco J F, Luterbacher J, Wanner H (2004). Wet season Mediterranean precipitation variability: influence of largescale dynamics and trends. *Journal of Climate Dynamics* **23**, 63–78.
- Xoplaki E, Luterbacher J, Burkard R, Patrikas I, Maheras P (2000). Connection between the large-scale 500-hPa geopotential height fields and precipitations over Greece during wintertime. *Journal of Climate Research* **14**, 129-146.
- Xoplaki E, Trigo RM, García-Herrera RF, Barriopedro D, D'Andrea F, Fischer EM, Gimeno L, Gouveia C, Herná'ndez E, Kuglitsch FG, MDOIariotti A, Nieto R, Pinto JG, Pozo-Va'zquez D, Saaroni H, Toreti A, Trigo IF, Vicente-Serrano SM, Yiou P, Ziv B (2012). Large-scale atmospheric circulation driving extreme climate events in the mediterranean and its related impacts. In: Lionello P et al. (eds) The climate of the Mediterranean region: from the past to the future. Elsevier, pp 347–417. doi:10.1016/B978-0-12-416042-2.00006-9. ISBN 9780124160422

- Yaakov A, Haim K, Hanoch L (2013). Empirical models of rain-spells characteristics – A case study of a Mediterranean-arid climatic transect. *Journal of Arid Environments* **97**, 84-91.
- Yavuz H, Erdoğan S (2012). Spatial analysis of monthly and annual precipitation trends in Turkey. *Journal of Water Resources Management* **26** (3), 609–621.
- Yevjevich, V (1967). An Objective Approach to Definition and Investigations of Continental Hydrologic Droughts. *Hydrology Papers* **23**, Colorado State University, Fort Collins, USA.
- You Q, Kang S, Aguilar E, Nick Pepin N, Flugel WA, Yan Y, Xu Y, Zhang Y, Huang J (2010). Changes in daily climate extremes in China and their connection to the large scale atmospheric circulation during 1961–2003. *Journal of Climate Dynamics*. doi: 10.1007/s00382-009-0735-0
- Yue S, Pilon P, Cavadias G (2002). Power of the Mann–Kendall and Searman’s rho test for detecting monotonic trend in hydrological series. *Journal of Hydrology* **259**, 254–271.
- Zangvil A, Karas S, Sasson A (2003). Connection between Eastern Mediterranean seasonal mean 500 hPa height and sea-level pressure patterns and the spatial rainfall distribution over Israel. *International Journal of Climatology* **23**, 1567–1576.
- Zappa G, Hawcroft M K, Shaffrey L, Black E and Brayshaw D J (2015). Extratropical cyclones and the projected decline of winter Mediterranean precipitation in the CMIP5 models. *Journal of Climate Dynamics*. In press (doi: 10.1007/s00382-014-2426-8).
- Zarga A, Sadiq R, Naser B, Khan FI .A review of drought indices (2011). *Journal of Environmental Reviews* **19**, 333-349.

- Zhai J, Su B, Krysanova V, Vetter T, Gao C, Jiang T (2010). Spatial variation and trends in PDSI and SPI indices and their relation to streamflow in 10 large regions of China. *Journal of Climate* **23**, 649–663.
- Zhai L, Feng Q (2008). Spatial and temporal pattern of precipitation and drought in Gansu Province Northwest China. *Journal of National Hazards* **49** (1), 1–24.
- Zhai PM, Zhang XP, Wan H, Pan XH (2005). Trends in total precipitation and frequency of daily precipitation extremes over China. *Journal of Climate* **18**, 1096–1108.
- Zhang J, Shen X, Wang B (2015). Changes in precipitation extremes in Southeastern Tibet, China. *Journal of Quaternary International*. doi.org/10.1016/j.quaint.2015.02.009
- Zhang Q, Sun P, Singh V.P, hen X (2012). Spatial–temporal precipitation changes (1956–2000) and their implications for agriculture in China. *Journal of Global and Planetary Change* **82–83**, 86–95.
- Zhang X, Aquilar E, Sensoy S, Melkonyan H, Tagiyeva U, Ahmed N (2005a). Trends in Middle East climate extreme indices from 1950–2003. *Journal of Geophysical Research* **11**, D22104, doi: 10.2029/2005JD006181.
- Zhang X, Hegerl G, Zwiers FW, Kenyon J (2005b). Avoiding inhomogeneity in percentile-based indices of temperature extremes. *Journal of Climate* **18**, 1641–1651.
- Zhang X, Yang F. (2004). RClimDex (1.0) User Guide. Climate Research Branch Environment Canada. Downsview, Ontario, Canada, 22p.
- Zhang ZG, Liu XR (2000). Information entropy analysis on non- uniformity of precipitation distribution in time-space (1): basic concept and data analysis (In Chinese). *Journal of Advances in Water Resources* **2**, 133–137.

- Zhao CH, Deng X, Yuan Y, Yan H, Lian H (2013) Prediction of drought risk based on the WRF model in Yunnan Province of China. *Journal of Advances in Meteorology* **2013**, 1–9.
- Zhao C, Ding Y, Ye B, Yao S, Zhao Q, Wang Z, Wang Y (2011). An analyses of long-term precipitation variability based on entropy over Xinjiang, northwestern China. *Journal of Hydrology and Earth System Sciences Discussions* **8**, 2975–2999.
- Zheng H, Zhang L, Liu C, Shao Q, Yoshihiro F (2007). Changes in stream flow regime headwater catchments of the Yellow River basin since the 1950s. *Journal of Hydrological Process* **21**, 886–893.
- Ziv B, Dayan U, Kushnir Y, Roth C, Enzel Y (2006). Regional and global atmospheric patterns governing rainfall in the southern Levant. *International Journal of Climatology* **26** (1), 55–73.
- Ziv B, Saaroni H, Alpert P (2004). The factors governing the summer regime of the eastern Mediterranean. *International Journal of Climatology* **24**, 1859–1871.
- Ziv B, Saaroni H, Pargament R, Harpaz T , Alpert P (2013). Trends in Rainfall Regime over Israel, 1975-2010, and their relationship to large Scale variability. *Journal of Regional Environmental Changes Journal* doi: 10.1007/s10113-013-0414-x
- Ziv B, Saaroni H, Romem M, Heifetz E, Harnik N, Baharad A (2010). Analysis of conveyor belts in winter Mediterranean cyclones. *Journal of Theoretical and Applied Climatology* **99**,441–455.
- Zveryaev II (2004). Seasonality in precipitation variability over Europe. *Journal of Geophysical Research* **109**, D05103, doi: 10.1029/2003JD00 3668.

Zveryaev II, Allan RP (2010). Summertime precipitation variability over Europe and its links to atmospheric dynamics and evaporation. *Journal of Geophysical Research* **115**, D12102, doi: 10.1029/2008JD011213.

Zwiers F W, Kharin V V (1998). Changes in the extremes of the climate simulated by CCC GCM2 under CO₂ doubling. *Journal of Climate* **11**, 2200–2222.